Partners in UK offshore wind

MORGAN OFFSHORE WIND PROJECT GENERATION ASSETS

Preliminary Environmental Information Report

Volume 6, annex 6.1: Physical processes technical report

Image of an offshore wind farm

April 2023
Final

Document status

Version	Purpose of document	Authored by	Reviewed by	Approved by	Review date
Rev01	Draft for Client review	RPS	bpEnBW		12/09/2022
Rev02	Addressing client comments	RPS	bpEnBW		17/10/2022
Rev03	Final	RPS	bpEnBW	bpEnBW	01/12/2022

Prepared by:	Prepared for:
RPS	**Morgan Offshore Wind Ltd**

Contents

Tables

Figures

Glossary

Term	Meaning
Bathymetry	The measurement of depth of water in oceans, seas, or lakes.
Bed resistance coefficient	Represents the roughness or friction applied to the flow by the seabed
Ebb tide	The tidal phase during which the water level is falling
Erosion	Depletion of sediment in the intertidal region
Fetch	Length in the wind direction of the marine area where water waves are generated by wind.
Flood tide	The tidal phase during which the water level is rising
High Water Mark	The level reached by the sea at high tide
Highest Astronomical Tide	The highest tidal height predicted to occur under average meteorological conditions and any combination of astronomical conditions
Hydrodynamic boundary conditions	The conditions used in a model boundary which can included surface elevation and velocity which will affect the rest of the model domain. The boundary condition can vary with time and along the boundary.
Intertidal region	An area of a shoreline that is covered at high tide and uncovered at low tide
Lee	Shelter from wind or weather given by an object
Littoral currents	Flow derived from tide and wave climate
Low Water Mark	The level reached by the sea at low tide
Lowest Astronomical Tide	The lowest tidal height predicted to occur under average meteorological conditions and any combination of astronomical conditions.
Mean High Water	The highest water level reached during and average tide
Mean High Water Spring	The most inshore level location reached by the sea at high tide during mean high water spring tide. This is defined as the average throughout the year, of two successive high waters, during a 24-hour period in each month when the range of the tide is at its greatest.
Mean Low Water Spring	The most offshore location reached by the sea at low tide during low water spring tide. This is defined as the average throughout the year, of two successive low waters, during a 24-hour period in each month when the range of the tide is at its greatest.
Mean Sea Level	The average tidal height over a long period of time
Metocean	Refers to the syllabic abbreviation of meteorology and (physical) oceanography
Neap tide	Tide that occurs when the sun and moon are at right angles to each other and the gravitational pull of the sun partially cancels out the pull of the moon on the ocean
Refraction	The change in direction of a wave passing from one medium to another caused by its change in speed
Residual current	The net flow over the course of the tidal cycle. This is effectively the driving force of the sediment transport.
Sandwave	A lower regime sedimentary structure that forms across from tidal currents
Scour protection	Measures to prevent loss of seabed sediment around any structure placed in or on the seabed (e.g. by use of protective aprons, mattresses, rock and gravel placement)
Sedimentation	The process of settling or being deposited as a sediment
Significant wave height	Mean wave height (trough to crest) of the highest third of the waves
Slack tide	Tidal phase at which the current turns from flood to ebb (high-water slack tide) or from ebb to flood (low-water slack tide)
Spectral waves	Describes the distribution of wave energy with frequency (1/ period) and direction
Spring tide	Tide that occurs when the sun and moon are directly in line with the Earth and their gravitational pulls on the ocean reinforce each other
Suspended Particulate Matter	Particles that are suspended in the water column
Turbidity	The quality of being cloudy, opaque, or thick with suspended matter
Wave height	The distance from trough to crest of a wave
Wave period	The time it takes for two successive crests (one wavelength) to pass a specified point

Acronyms

Acronym	Description
2D UHRS	2D Ultra High Resolution Seismic
ASG	Aanderaa Seaguard
BEIS	Department for Business, Energy and Industrial Strategy
BERR	Department for Business Enterprise and Regulatory Reform
BGS	British Geological Survey
BODC	British Oceanographic Data Centre
CCO	Coastal Channel Observatory
CD	Chart Datum (generally defined as LAT)
CEFAS	Centre for Environment, Fisheries and Aquaculture Science
ClV	Cleveleys
CPT	Cone Penetration Test
DA	Depth Averaged
DHI	Danish Hydraulic Institute
DSV	Digital Sound Velocity
ECMWF	European Centre for Medium-range Weather Forecast
EMODnet	European Marine Observation and Data Network
GyM	Gwynt y Môr
HAT	Highest Astronomical Tide
HWM	High Water Mark
INFOMAR	Integrated Mapping for the Sustainable Developments of Ireland’s Marine Resource

Acronym	Description
LAT	Lowest Astronomical Tide
MBES	Multi-Beam Echo Sounder
LWM	Low Water Mark
MDS	Maximum Design Scenario
MEDIN	Marine Environmental Data and Information Network
MHW	Mean High Water
MHWN	Mean High Water Neaps
MHWS	Mean High Water Springs
MLWN	Mean Low Water Neaps
MLWS	Mean Low Water Springs
MSL	Mean Sea Level
MT	Mud Transport
NOAA	National Oceanic and Atmospheric Administration
OSP	Offshore Substation Platform
PEIR	Preliminary Environmental Information Report
PT	Particle Tracking
RhF	Rhyl Flats
SBP	Sub-Bottom Profiler
SIG	Nortek Signature
SPM	Suspended Particulate Matter
SSC	Suspended Sediment Concentration
SSS	Side Scan Sonar
ST	Sand Transport
TSSF	Tide and Storm Surge Forecast
UKCS	United Kingdom Continental Shelf
UKCP	UK Climate Projections
UKHO	United Kingdom Hydrographic Office

Units

Unit	Description
º	Degrees
cm/s	Centimetre per second
mm	Millimetre
m	Metre
m^3	Cubic metres
m^3/h	Cubic metres per hour
km	Kilometre
$m^3/d/m$	Cubic metres transported per day per metre width of transport path (i.e. perpendicular to direction of transport)
m/s	Metres per second
mg/l	Milligrams per litre (Suspended Sediment Concentration)

1 PHYSICAL PROCESSES TECHNICAL REPORT

1.1 Introduction

1.1.1.1 This physical processes technical report provides information relating to the physical environment and processes for the Morgan Offshore Wind Project Generation Assets (hereafter referred to as the Morgan Generation Assets). The purpose of the technical report is to provide details of the supporting study undertaken by means of numerical modelling. It describes the current baseline conditions and quantifies the potential changes due to the installation and presence of the Morgan Generation Assets.

1.1.1.2 The preparation of a Preliminary Environmental Information Report (PEIR) and subsequent application is a live process with refinements being made to the project description throughout this period, as information is acquired from the range of studies and assessments undertaken. For this reason, the modelled scenarios presented in this technical report will, inevitably, vary by a small degree from those ultimately assessed. However, due to the limited nature of these refinements, the technical report would remain a legitimate resource for supporting information. When disparities occur, they will be cited within the assessment with reference to the applicability of the modelled data presented in this report and used to support the assessment.

1.1.1.3 This report is divided into three main sections:

- Baseline conditions – describing current hydrography and sedimentology
- Environmental variations – describing changes to baseline arising from the installation and presence of the Morgan Generation Assets
- Construction phase changes – describing the dispersion and fate of sediment mobilised during construction phase activities.

1.1.1.4 For the purposes of this physical processes technical report, physical processes are defined as encompassing the following elements:

- Tidal elevations and currents
- Waves
- Bathymetry
- Seabed sediments
- Suspended sediments
- Sediment transport.

1.2 Study area

1.2.1.1 The Morgan physical processes study area is illustrated in Figure 1.1 and defined as the:

- Morgan Array Area (the area within which the wind turbines, foundations, inter-array cables, interconnector cables and Offshore Substation Platforms (OSPs) forming part of the Morgan Generation Assets will be located)
- Seabed and coastal areas that may be influenced by changes to physical processes due to the Morgan Generation Assets defined as one spring tidal excursion which is the distance suspended sediment is transported prior to being carried back on the returning tide.

1.2.1.2 It is however noted that the physical processes study area forms the focus for the assessment and that the numerical model extent is not limited to this region. The modelling study therefore also identifies any potential impacts beyond the physical processes study area.

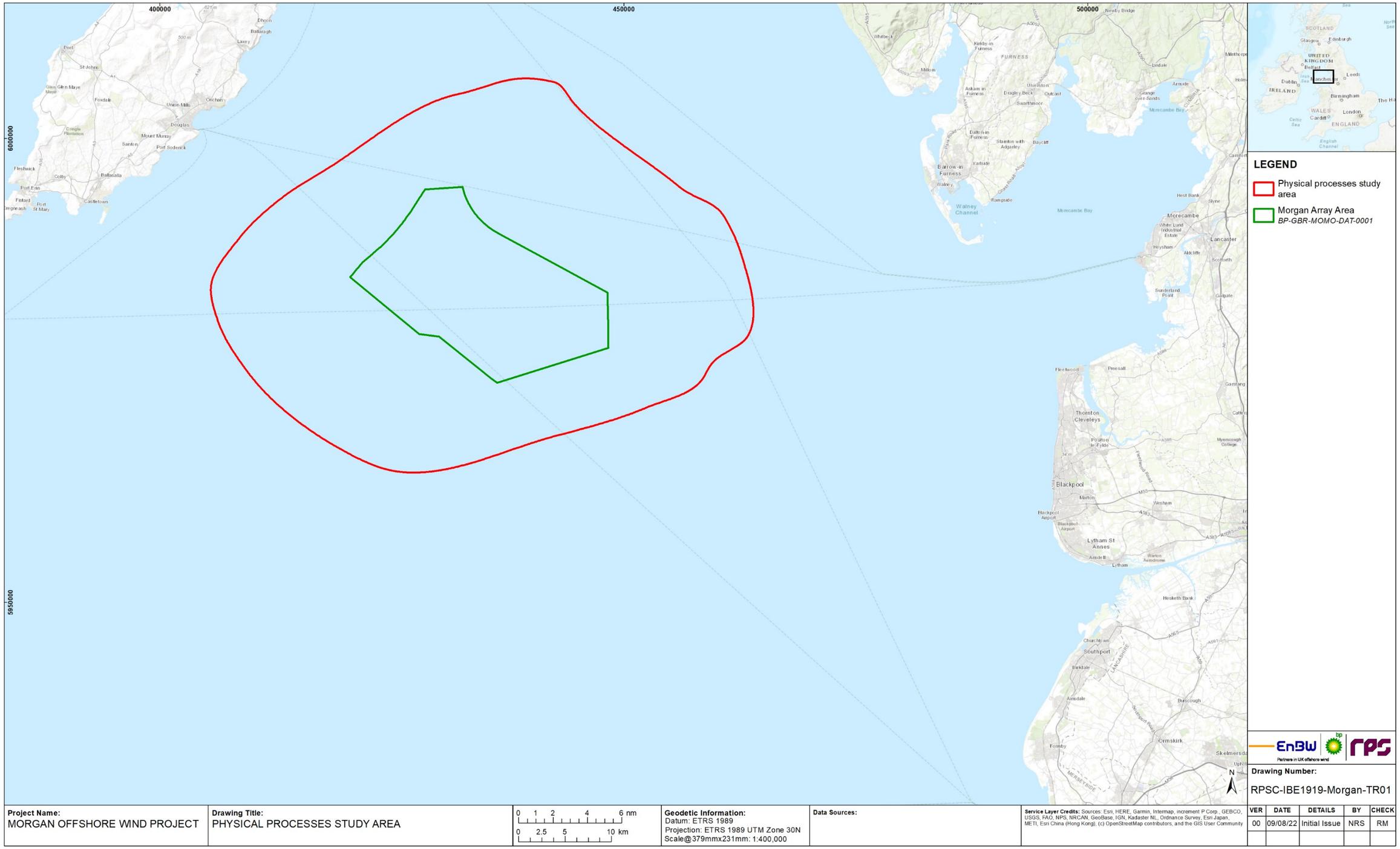

Figure 1.1: Physical processes study area.

1.3 Methodology

1.3.1.1 The physical processes study was undertaken to provide information of potential changes to physical processes and the fate of mobilised sediment during the construction phase by means of numerical modelling. Numerical models were developed and calibrated using a combination of publicly available datasets and those collected specifically for the Morgan Generation Assets.

1.3.1.2 These models were then implemented in comparative studies to determine the potential impact of the infrastructure on tidal flow, wave climate and sediment transport patterns for a representative project design scenario It is noted that this method investigates the influence on the drivers of physical processes rather than instigating detailed morphological studies. In the event that significant potential impacts were identified more detailed studies may be required.

1.3.1.3 The models were also used to undertake simulations of site preparation, cable trenching and pile installation activities to quantify potential increases in Suspended Sediment Concentration (SSC) and subsequent deposition. This information was then applied in the context of the physical processes environmental impact assessment and those of related disciplines.

Numerical modelling

1.3.1.4 Numerical modelling techniques were used to describe tide, wave and sediment transport regimes. The MIKE suite of software was employed, as a single model mesh could be used to simulate these processes both individually and in combination. The model domain is shown in Figure 1.2. The MIKE suite of models is a widely used industry standard modelling suite developed by the Danish Hydraulic Institute (DHI). It has been approved for use by industry and government bodies including Natural Resources Wales. The MIKE suite is a modular system that contains a number of different but complementary modules encompassing different physical processes: these are summarised in Table 1.1 and described in further detail within the relevant sections. A summary of the modelled environmental scenarios is provided in Table 1.2.

Table 1.1: MIKE suite of models.

Simulation	Model	Description
Baseline and post-construction tidal flow	MIKE21 Flexible Mesh (FM) modelling system	The FM Module is a 2-dimensional, Depth Averaged (DA) hydrodynamic model which simulates the water level variations and flows in response to a variety of forcing functions in lakes, estuaries and coastal areas. The water levels and flows are resolved on a mesh covering the area of interest when provided with bathymetry, bed resistance coefficient, wind field, hydrodynamic boundary conditions, etc.
Baseline and post-construction wave climate	MIKE21 Spectral Wave (SW)	The wave modelling was undertaken using the spectral wave model, MIKE21 SW. The waves were computed on the same grid as the tidal flows. The model resolves the wave field by simulating wind generation of waves within the model domain and the propagation of externally generated swell waves through the domain. The model setup ensured that the detail of both locally generated wind waves and swell conditions from further afield were captured.
Baseline and post-construction littoral currents	MIKE21 FM and SW	The MIKE suite facilitates the coupling of models. The DA hydrodynamic model, used for the tidal modelling, coupled with a spectral wave model, provides a full wave climate incorporating the impact of water levels and currents on waves and wave breaking. Using this, the littoral currents (i.e. those currents driven by tidal, wave and meteorological forces) were examined.
Baseline and post-construction sediment transport	MIKE21 Sand Transport (ST)	This module enables assessment of bed sediment transport rates and initial rates of bed level change for non-cohesive sediment resulting from currents or combined wave-current flows. The model combines inputs from both the hydrodynamic model and, if required, the wave propagation model. It uses sediment size and gradation to determine the bed level changes and sediment transport rates.
Foundation installation	MIKE21 Mud Transport (MT)	A sample of four representative Pile Installation Scenarios were simulated to cover the range of conditions across the Morgan Generation Assets array area both in terms of tidal currents and sediment type. The MIKE MT module allows the modelling of erosion, transport and deposition of cohesive and cohesive/granular sediments. This model is suited to sediment releases in the water column and allows sediment sources which may vary spatially and temporally.
Cable installation	MIKE21 Particle Tracking (PT)	The PT module was implemented for cable installation as it has the advantage that it could be used to describe the transport of material released in a specific part of the water column. In this way, the dispersion would not be over-estimated, or the corresponding sedimentation underestimated.

Table 1.2: Summary of Modelled Environmental Variation Scenarios.

Variation/ operation	Description	Parameter modelled
Hydrography Section 0	Models updated to take account of the installation of the Morgan Generation Assets and associated features to quantify: • Changes to tidal currents • Changes to wave climate • Changes to littoral currents.	• Wind turbines: 68 installations with four-legged suction bucket foundations, each jacket leg with a diameter of 5m, spaced 48m apart, and each bucket with a diameter of 16m. Scour protection to a height of 2.5m. Total footprint of 10,816m^2 per wind turbine • OSPs: four installations with three-legged suction bucket foundations, each jacket leg with a diameter of 3m, spaced 30m apart, and each bucket with a diameter of 14m. Scour protection to a height of 2.5m. Total footprint of 3,277m^2 footprint per OSP • Inter-array cables: cable protection with a height of 3m and 5m width. Cable crossings, each crossing with a height of 4m, a width of 32m and a length of 60m • Interconnector cables: cable protection with a height of 3m and 10m width. Cable crossings, each crossing with a height of 3m, a width of 20m and a length of 50m
Sedimentology Section 1.7.3	Models updated to take account of the installation of the Morgan Generation Assets and associated features to quantify changes to sediment transport characteristics.	As above with the addition of: • Scour protection simulated using an area of fixed bed around each structure.
Seabed features clearance Section 1.8.2	Dispersion modelling relating to sandwave clearance. Dredging of sandwave crest and disposal at troughs is undertaken in a cycle along cable routes.	• Clearance is undertaken at 100m/h along 5.6km sample cable routes of a width of 104m with dredging undertaken at 10,000m^3/h with a spill rate of 3% • Inter-array cable clearance is undertaken to an average depth of 5.1m • With sediment released through water column.
Augured pile installation Section 1.8.3	Dispersion modelling of suspended sediment arising from augured pile installation. Under a range of tidal conditions.	Four sample scenarios are presented, in each case: • Piles are 16m in diameter and 60m deep • Two adjacent operations occur simultaneously • Drilling undertaken at 0.89m/h • 13,460m^3 of material mobilised per pile • Released throughout water column.
Cable installation Section 1.8.4	Dispersion modelling of suspended sediment arising from cable installation via trenching. Relating to: • Inter-array cable • Interconnector cable.	For inter-array cables sample trenching operations are presented. • Trench 3m wide at seabed and 3m deep with triangular cross section • Trenching is undertaken at 450m/h.

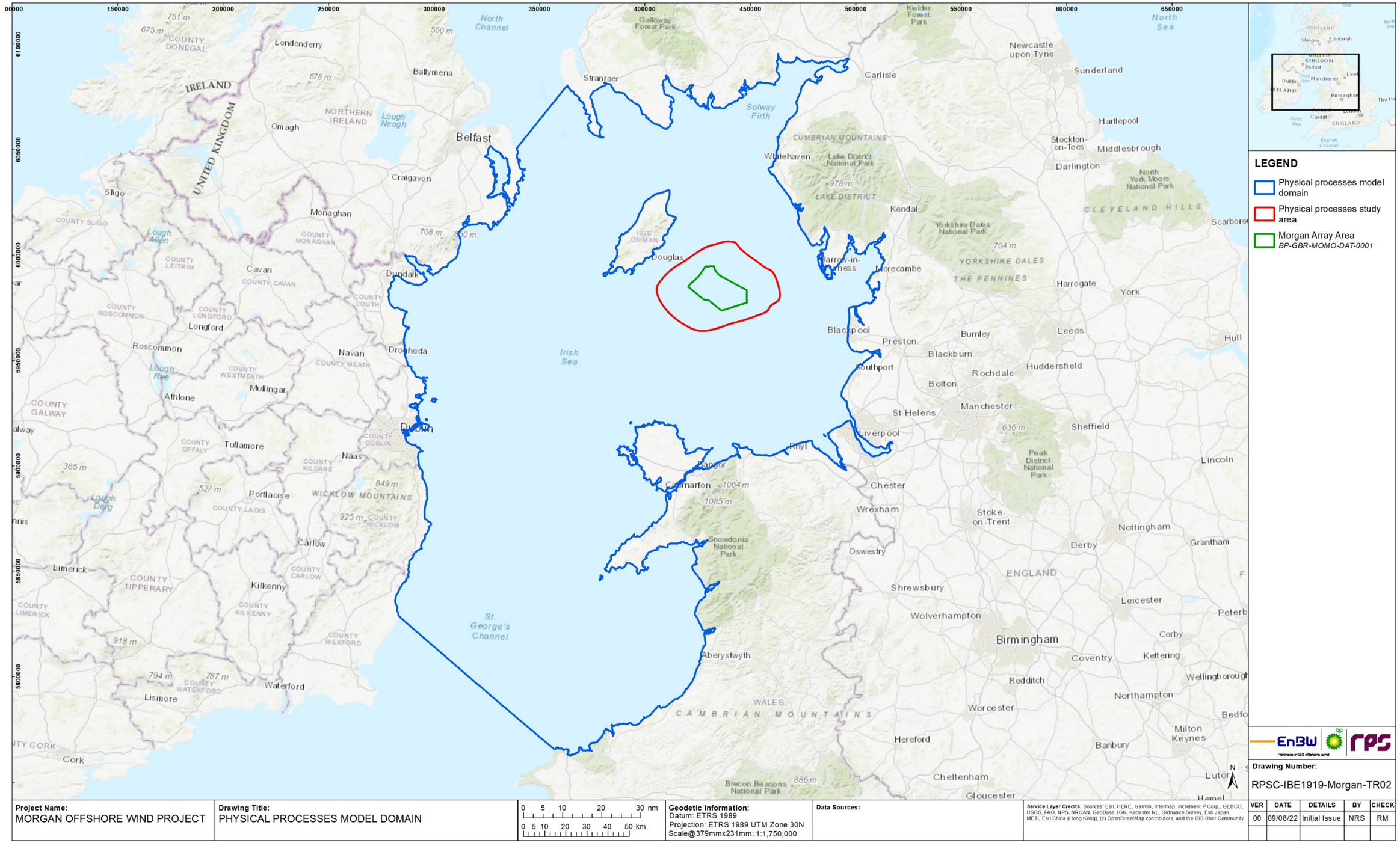

Figure 1.2: Model domain (blue outline).

1.4 Desktop study

1.4.1.1 Information on the physical environment within the physical processes study area and beyond to the model domain was collected through a detailed desktop review of existing studies and datasets. These are summarised in Table 1.3.

Table 1.3: Summary of Key Resources.

Title	Source	Year	Author
European Marine Observation and Data Network (EMODnet) – Seabed classification	https://www.emodnet-geology.eu/	2022	EMODnet
EMODnet – Bathymetry data	https://www.emodnet-bathymetry.eu/	2022	EMODnet
EMODnet – Metocean data	https://map.emodnet-physics.eu/	2022	EMODnet
Department for Environment Food and Rural Affairs – Bathymetry data	https://environment.data.gov.uk/DefraDataDownload	2022	DEFRA
National Oceanic and Atmospheric Administration (NOAA) –Atmospheric data	DHI Metocean Data Portal	2022	NOAA
National Network of Regional Coastal Monitoring Programmes	https://coastalmonitoring.org/cco/	2022	Coastal Channel Observatory (CCO)
Centre for Environment, Fisheries and Aquaculture Science (CEFAS) – wave data	https://wavenet.cefas.co.uk/map	2022	CEFAS
ABPmer Data exporer	https://www.seastates.net/explore-data/	2022	ABPmer
Hydrography of the Irish Sea, SEA6 Technical Report	UK Government	2005	Howarth M.J.
Atlas of UK Marine Renewable Energy Resources	https://www.renewables-atlas.info/	2022	ABPmer
Geology of the seabed and shallow subsurface: The Irish Sea.	British Geological Survey (BGS)	2015	Mellett *et al*.
BGS – sediment sample data	https://mapapps2.bgs.ac.uk/geoindex_offshore	2022	BGS
Suspended Sediment Climatologies around the UK.	Department for Business, Energy and Industrial Strategy (BEIS)	2016	Cefas
Metocean Data collection for the Ormonde offshore wind project.	Marine Data Exchange	2011	Geotechnical Engineering and Marine Surveys (GEMS)
Irish Sea Zone Hydrodynamic measurment campaign	Marine Data Exchange	2010 to 2013	EMU Ltd (now Fugro Ltd)
Admiralty Tide Tables	United Kingdom Hydrographic Office (UKHO)	2022	UKHO
Marine Environmental Data Information Network (MEDIN) Seabed Mapping Programme	Admiralty Marine Data Portal	2022	MEDIN
Integrated Mapping for the Sustainable Developments of Ireland's Marine Resource (INFOMAR) Seabed Mapping Programme	Geological Survey Ireland (GSI) and Marine Institute	2022	INFOMAR
Long term wind and wave datasets	European Centre for Medium-range Weather Forecast (ECMWF)	2022	ECMWF
UK tide gauge network and database of current observation	British Oceanographic Data Centre (BODC)	2021	BODC
UK Climate Projections (UKCP)	Met Office	2018	Met Office
A user-friendly database of coastal flooding in the UK from 1915-2014	Scientific Data (journal)	2015	Haigh *et al.*
BODC	National Oceanography Centre	various	National Oceanography Centre
Review of aggregate dredging off the Welsh coast	HR Wallingford	2016	HR Wallingford

1.5 Site-specific surveys

A summary of the surveys undertaken of relevance to physical processes is outlined in Table 1.4.

Table 1.4: Summary of survey undertaken to inform physical processes.

Title	Extent of survey	Overview of survey	Survey contractor	Date	Reference to further information
Environmental Baseline Surveys and Habitat Assessments	Morgan Offshore Wind Project Survey Area	Geophysical survey to determine characteristics of seabed sediment, characterise benthic communities (infauna and epifauna) and identification of any environmentally significant habitats (e.g. potential Habitats Directive Annex I and priority marine features). Deployment included multi-beam echo sounder (MBES), digital sound velocity (DSV) sensor, side scan sonar system (SSS), Sub-Bottom Profiler (SBP) & 2D Ultra High Resolution Seismic (2D	Gardline Ltd	June to September 2021	Gardline (2022)

Title	Extent of survey	Overview of survey	Survey contractor	Date	Reference to further information
		UHRS) sensor. Additionally, seabed imagery was collected along with grab samples and core penetration testing (CPT).			
Geophysical survey	Morgan Array Area	Geophysical survey to establish bathymetry, seabed sediment and identify seabed features. Deployment included MBES with multibeam backscatter.	XOCEAN Ltd	June 2021 to March 2022	XOCEAN (2022)
Metocean survey	Morgan and Mona Array Area	Metocean and FLidar deployments to ascertain wind, wave, and tidal currents.	Fugro	November 2021 to November 2022	Fugro (2022)

1.6 Baseline environment

1.6.1 Bathymetry

1.6.1.1 The model domain had full bathymetry data coverage and was populated using a combination of data sources. The site-specific geophysical survey undertaken for both the Morgan and Mona Array Areas and the resulting bathymetry data, as detailed in Table 1.4, was used to populate the model. The extent of this survey data is shown in Figure 1.4, Gardline (2022) and XOcean (2022). The survey data provided to Lowest Astronomical Tide (LAT) vertical datum was converted to model mean sea level datum using reference values published by Admiralty.

1.6.1.2 Where additional data was required for the model extent beyond the survey area, bathymetry data was sourced from the MEDIN Seabed Mapping Programme via the Admiralty Marine Data Portal as shown in Figure 1.3. Each of the datasets for the east Irish Sea area was combined into a single set giving priority to the most recent survey data. For areas within region which did not have coverage from the MEDIN dataset further data was sourced from the DEFRA Survey Data Download site. This was undertaken for specific bays such as Conwy Bay and the Dee Estuary.

1.6.1.3 For the remaining model domain, the EMODnet 100m resolution tiled data was utilised. This database is available under the European Inspire Directive and provides access to data in a variety of formats, datums and resolutions based on a combination of survey datasets. All data was converted, where necessary, to mean sea level datum generally with a resolution of at least three times the mesh resolution to ensure that coastal features were represented within the numerical modelling, as illustrated in Figure 1.5.

1.6.1.4 The resolution of the model bathymetry was designed to reflect variations in water depth and bed forms for the accurate simulation of tidal currents. Additional model resolution was also included to incorporate the installation of the Morgan Generation Assets. This enabled the same cell arrangement to be used for the baseline and post-construction assessment, thereby avoiding the introduction of any numerical mesh effects into the assessment. Across the Morgan Generation Assets, the resolution varied between circa 50m down to 10m in order that the influence of scour protection on the tidal flow and sediment transport for the Morgan Generation Assets could be quantified. With increasing distance from the physical processes study area, the cell size was increased but maintained at a level which retained model accuracy. Figure 1.6 illustrates the mesh resolution with an inset of the mesh within the Morgan Array Area.

1.6.1.5 The extent of the domain, Figure 1.2, was designed to provide the basis for a model which could be utilised for tide, wave and sediment transport modelling. The focus of the study is a tidal excursion from the Morgan Generation Assets to quantify any changes due to the installation however a larger domain is required to develop wave fields and ensure that tidal currents are simulated with the benefit of identifying any potential effects beyond the physical processes study area.

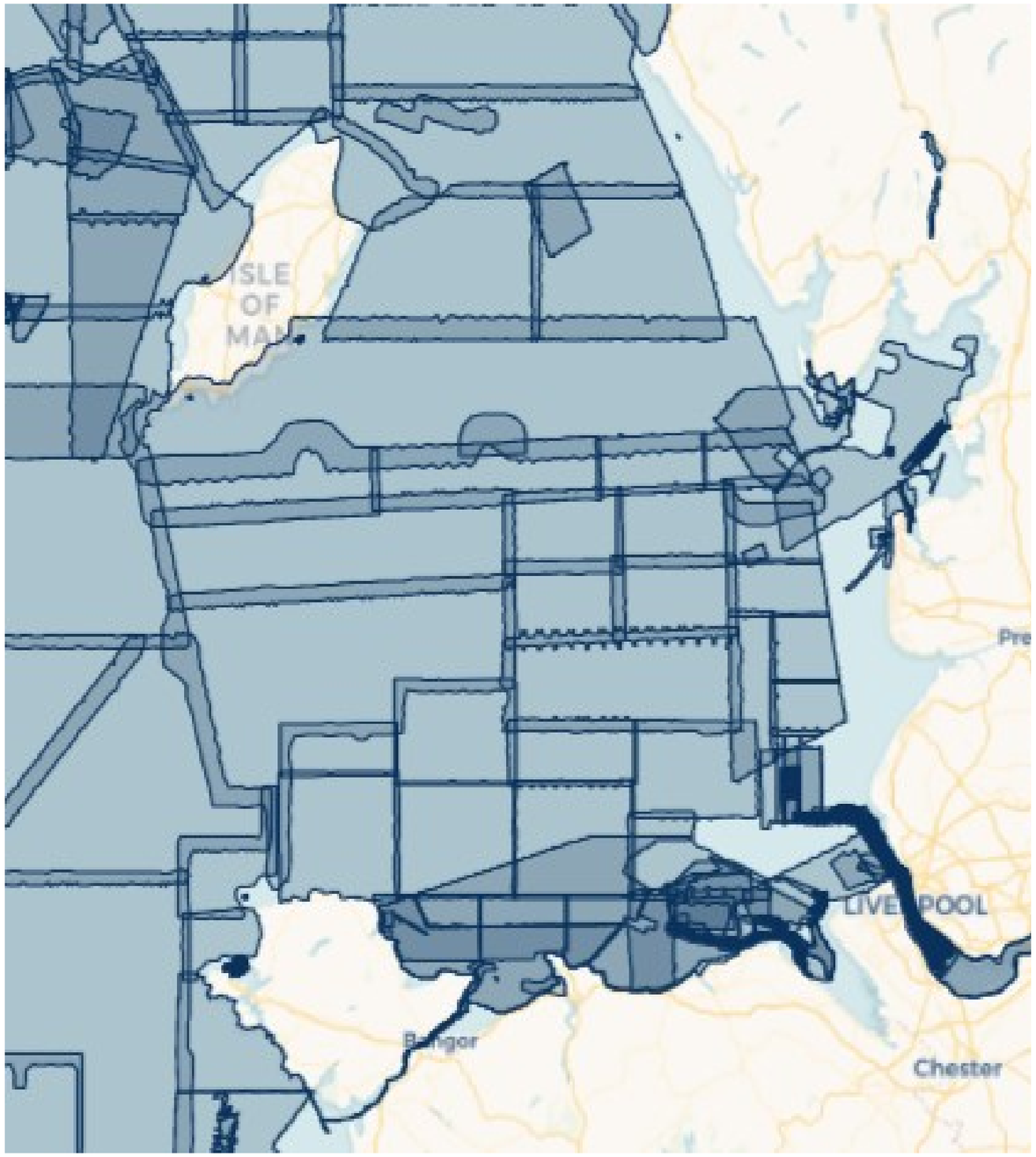

Figure 1.3: MEDIN bathymetric data coverage.

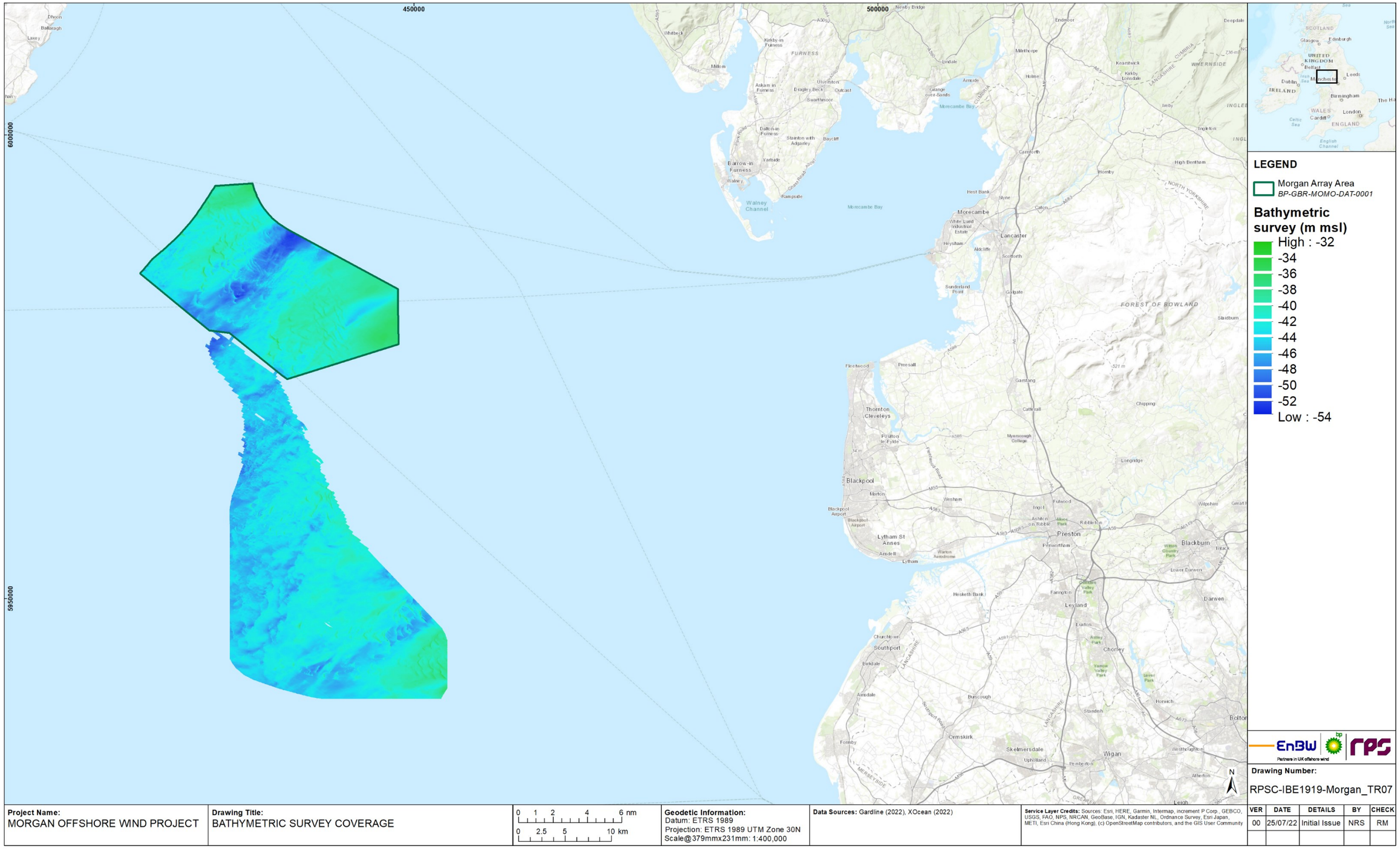

Figure 1.4: Morgan and Mona Scoping Array bathymetric survey data coverage – Source: Gardline (2022) and XOcean (2022).

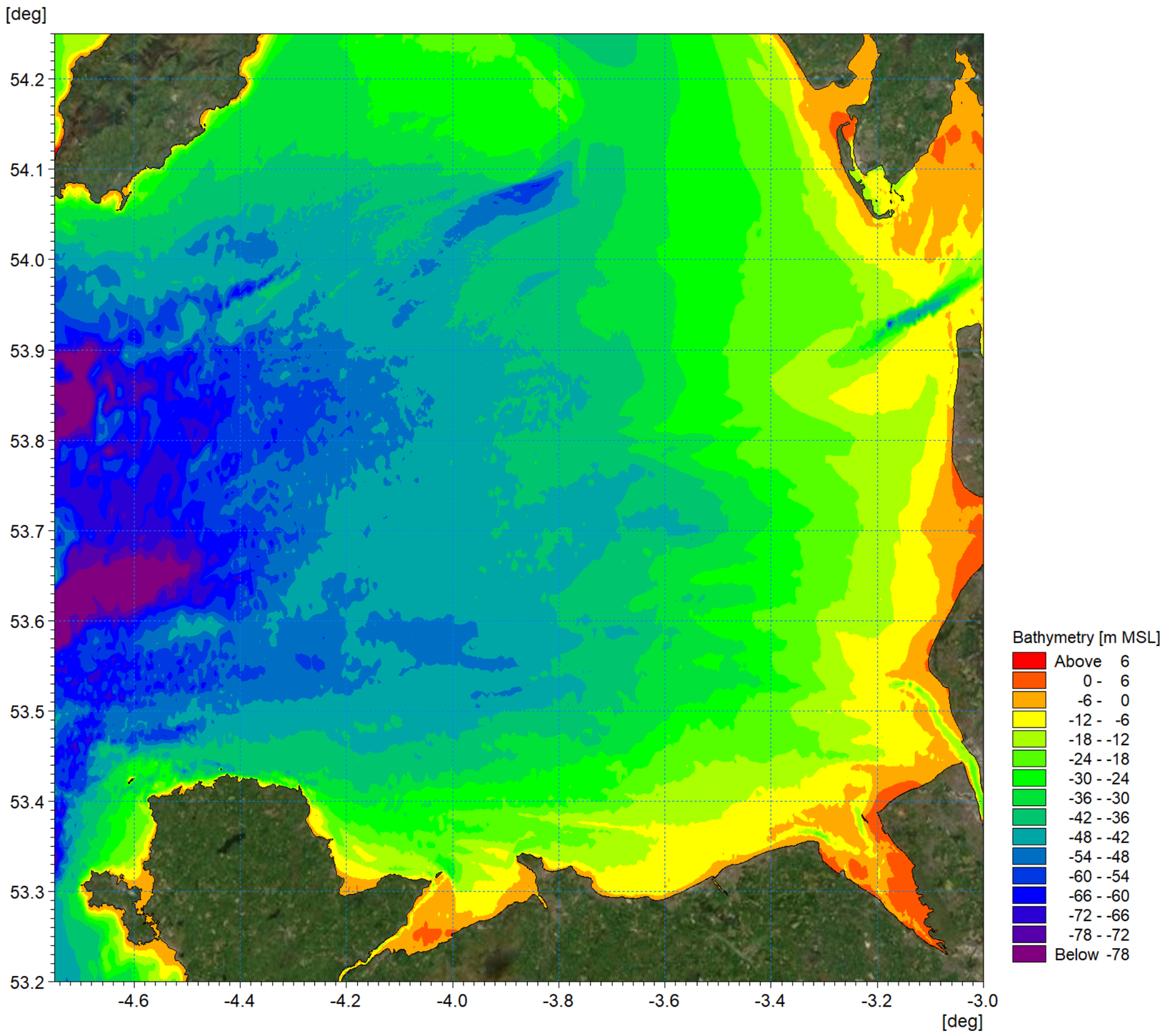

Figure 1.5: Model bathymetry within the east Irish Sea.

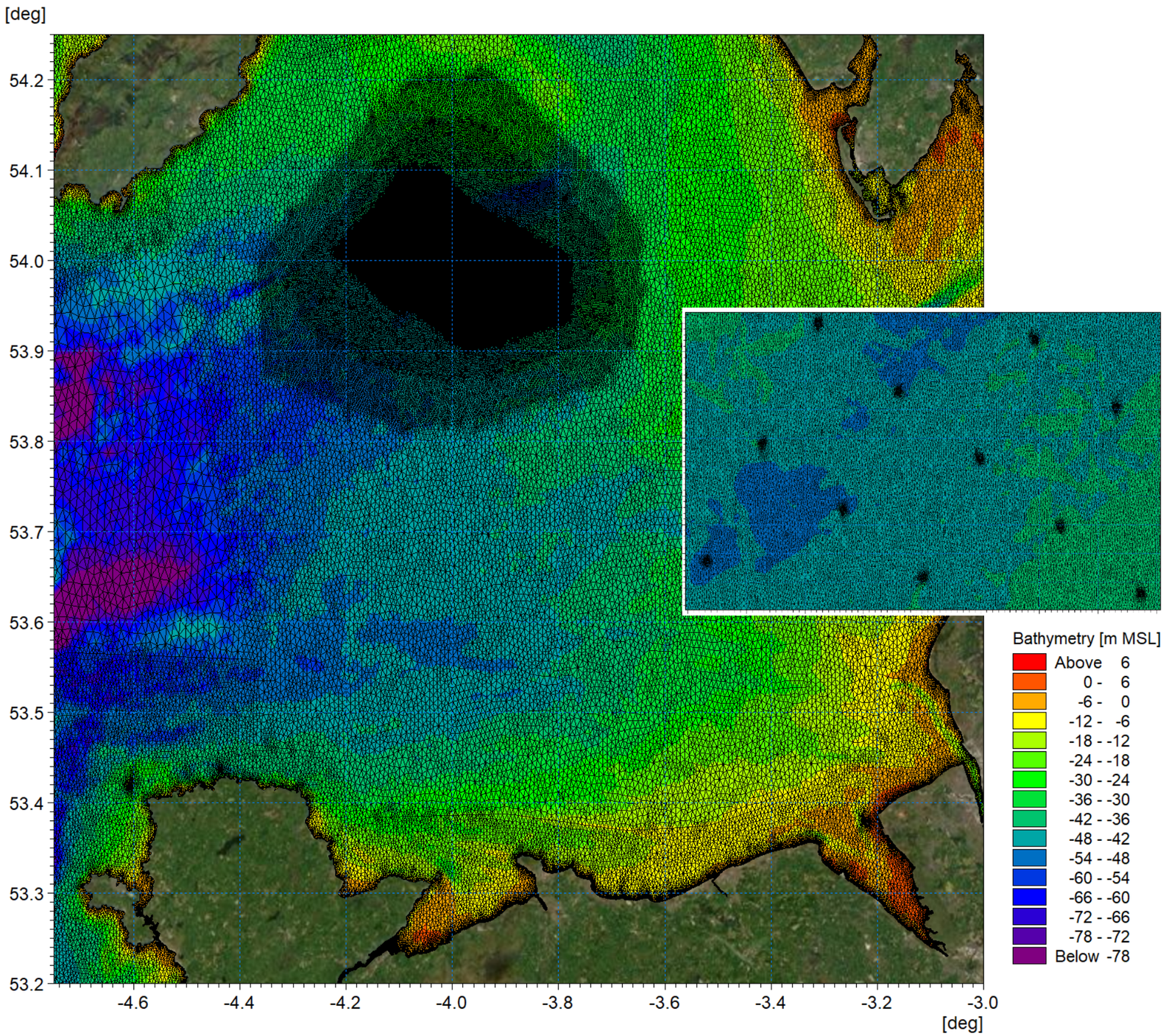

Figure 1.6: Model mesh with section of Morgan Array Area inset.

1.6.2 Hydrography

1.6.2.1 The UKHO states that the mean tidal range at the Standard Port of Holyhead is approximately 3.65m whilst at Douglas it is 4.55m. The tidal characteristics shown in Table 1.5 in metres referenced to Chart Datum (CD):

Table 1.5: Tidal Levels at Standard Ports.

Tidal level (m CD)	Holyhead	Douglas
LAT	0.0	-0.3
Mean Low Water Springs (MLWS)	0.7	0.8
Mean Low Water Neaps (MLWN)	2.0	2.4
Mean Sea Level (MSL)	3.3	3.8
Mean High Water Neaps (MHWN)	4.4	5.4
Mean High Water Springs (MHWS)	5.6	6.9
Highest Astronomical Tide (HAT):	6.3	7.9

1.6.2.2 The semi-diurnal tides are the dominant physical process in the Irish Sea moving into the Irish Sea from the Atlantic Ocean through both the North Channel and St. George's Channel. The tidal range in the Irish Sea is highly variable with the range in Liverpool Bay exceeding 10m on the largest spring tides, the second largest in Britain.

1.6.2.3 The tidal flow simulations which form the basis of the study were undertaken using the MIKE21 FM flexible mesh modelling system. The FM Module is a two-dimensional, DA hydrodynamic model which simulates the water level variations and flows in response to a variety of forcing functions in lakes, estuaries and coastal areas. The water levels and flows are resolved on a mesh covering the area of interest when provided with bathymetry, bed resistance coefficient, hydrodynamic boundary conditions, etc.

1.6.2.4 The tidal model was driven using boundary conditions extracted from RPS' Tide and Storm Surge Forecast (TSSF) model of Irish coastal waters (RPS, 2018), the extent and bathymetry of which is illustrated in Figure 1.7. This model was also developed using flexible mesh technology with the mesh size (model resolution) varying from circa 24km along the offshore Atlantic boundary to circa 200m around the Irish coastline. These boundaries were fully defined 'flather' boundaries for which both surface elevation and current vectors are specified.

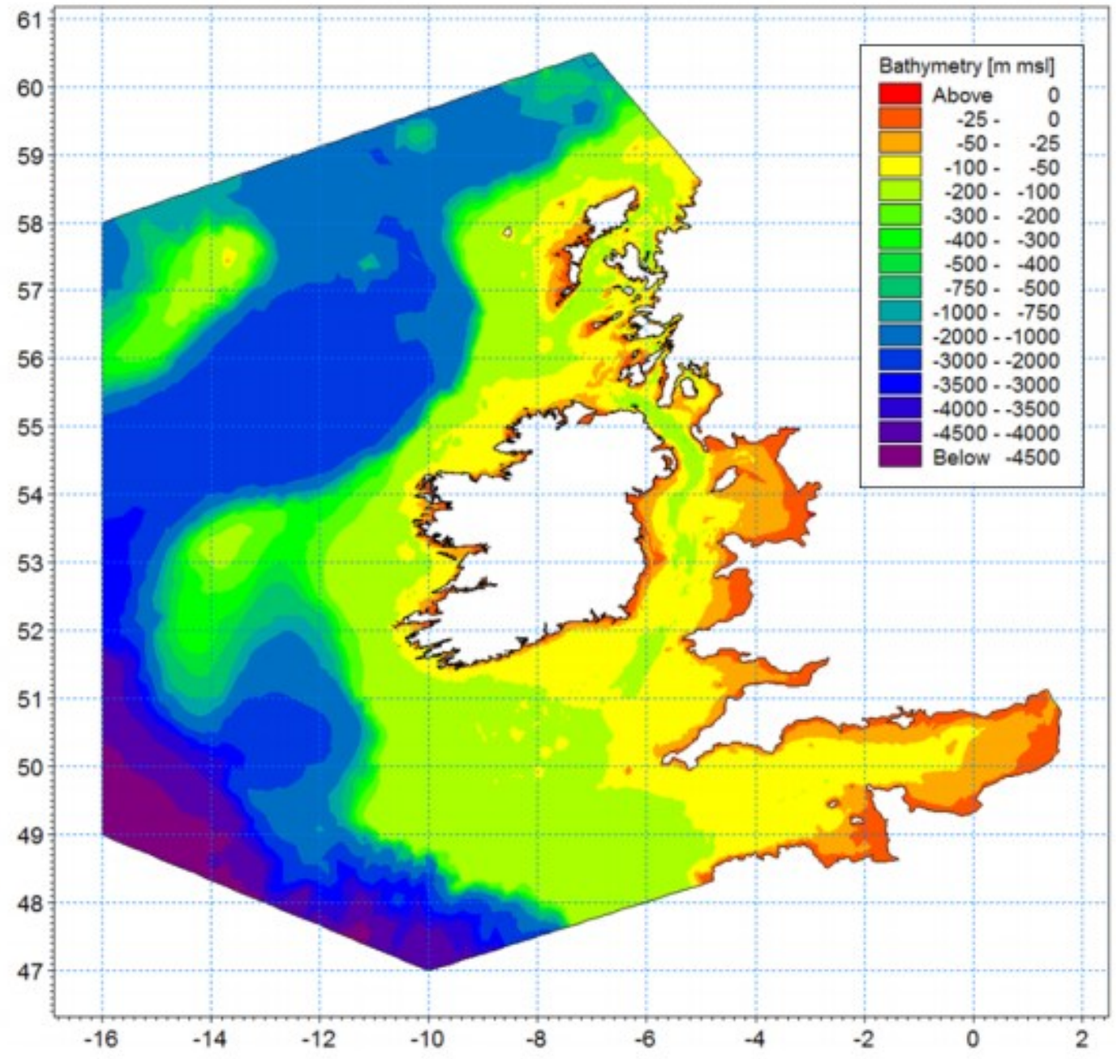

Figure 1.7: Extent and bathymetry of Irish Seas TSSF model.

1.6.2.5 A large amount of hydrometric data was available across the model domain as detailed in Table 1.3. A selection of the principal resources such as Admiralty tidal harmonics, BODC and CCO are illustrated in Figure 1.8. The selection of calibration data presented in this is shown in Figure 1.9.

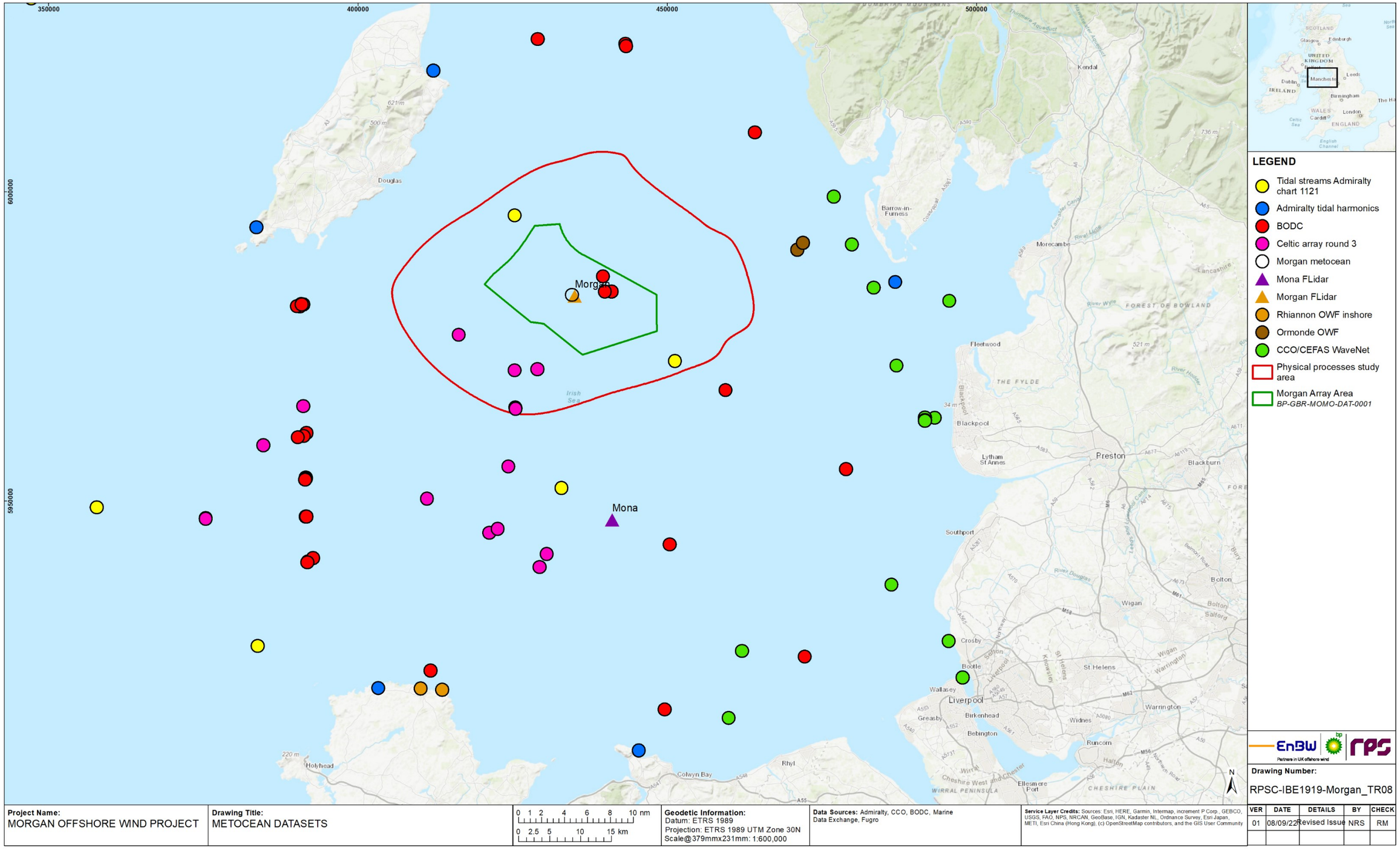

Figure 1.8: Availability of metocean datasets across the east Irish Sea.

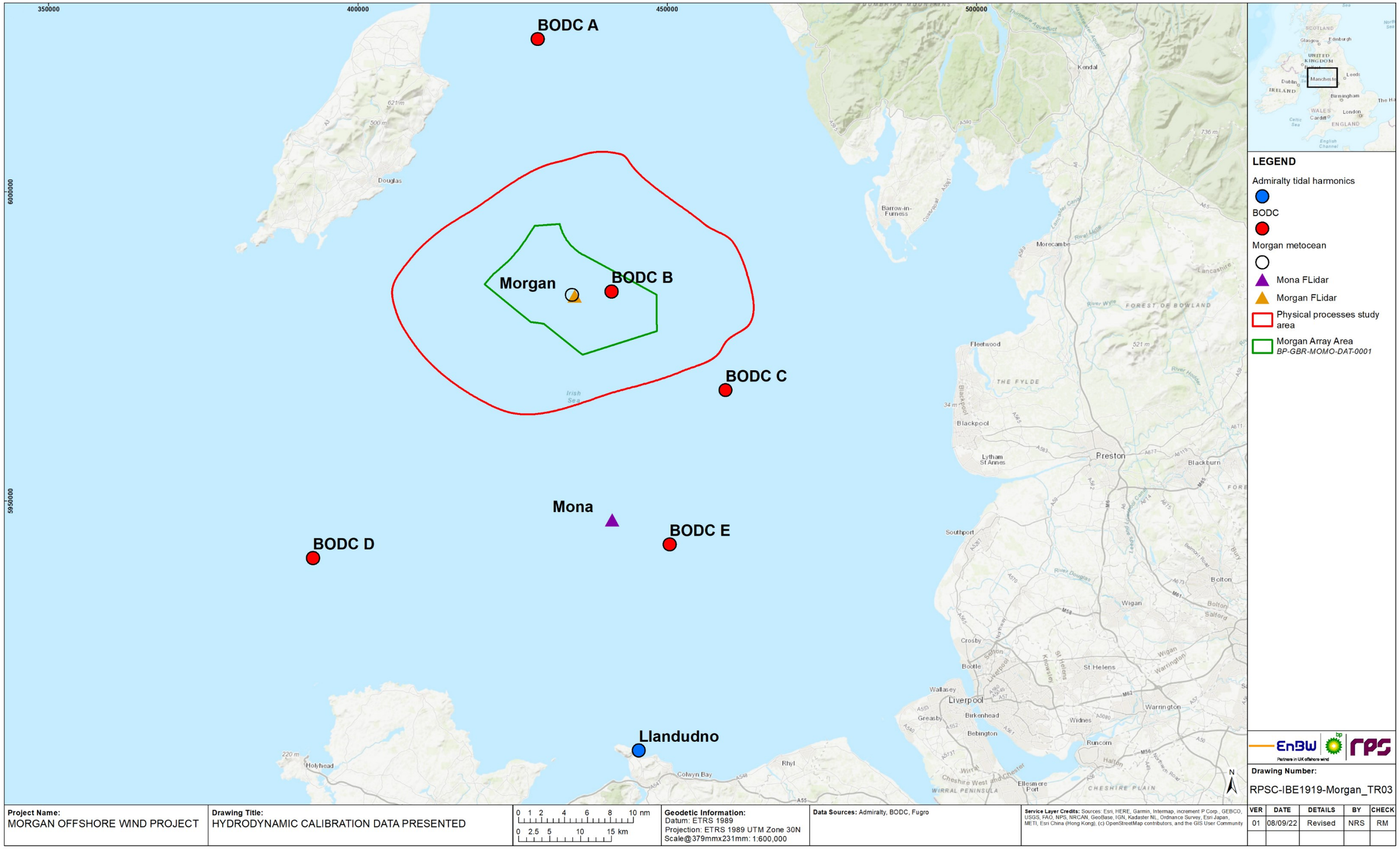

Figure 1.9: Location of calibration data presented.

1.6.2.6 Figure 1.10 shows the comparison of the modelled (red) and Admiralty tidal levels predicted from harmonic analysis (blue) at Llandudno. The model correlated well through both spring and neap tidal phases. The comparative study undertaken to quantify the potential changes in tidal currents was undertaken during both and neap spring tides to ensure a wide range of tidal conditions were applied in the modelling. The validation data presented therefore includes both tidal phases for each location of calibration data available is illustrated in Figure 1.9.

1.6.2.7 For site specific calibration data, Morgan floating lidar plots (FLidar) are presented first illustrating spring and neap tides within the Morgan Array Area. Each plot displays the current speed data on the left axis and the current direction on the right axis. The modelled depth average current speed is shown by a red trace and current direction by an orange trace. The measured data was collected at various water depths noted within the legend.

1.6.2.8 The Morgan FLidar and Mona FLidar tidal current data are presented in Figure 1.13 to Figure 1.12 and show similar trends in that that current speeds during neap tides are half of the speed during spring tides. As well as the flood tide approaching from an easterly direction with the ebb tide being slightly weaker. The modelled data fits within the range of the Mona and Morgan measured data following similar tidal flow patterns

1.6.2.9 Figure 1.15 to Figure 1.17 show the comparison between the Aanderaa Seaguard (ASG) and Nortek Signature (SIG) measuring devices against modelled metocean data during different tidal phases. The two devices were deployed at the Morgan site and the DA current speed and direction are reported. The model current directionality correlates between both the ASG and SIG devices however current speeds between the model and ASG are more correlated than with the SIG device during the spring tide. In the neap tidal phase, the device speed and direction are within the range of the modelled data however the correlation is weaker than during the spring tidal phase. Comparisons of surface elevation between the ASG and modelled data are illustrated for both spring and neap tidal phases in Figure 1.16 and Figure 1.18.

1.6.2.10 For each location of BODC data, a pair of plots are presented firstly relating to spring tides and secondly neap tides. In each plot the current speed data is presented on the left axis whilst the current direction is presented to the right. The modelled depth average current speed is shown by a red trace and current direction by an orange trace. The measured data was collected at various water depths noted within the legend.

1.6.2.11 Site A presented in Figure 1.20 indicated that the flood tide which approaches the Morgan Generation Assets from the northeast direction and is more dominant than the ebb tide. Peak neap tidal current speeds are typically half of those experienced during spring tide. The modelled data largely lie within the range of the measured data and replicates the asymmetric tidal flows patterns.

1.6.2.12 This is also the case for site C shown in Figure 1.23 and Figure 1.24 for spring and neap respectively. Current directions and the dominance of flood tides are replicated with the model domain. Tidal currents at site D are more strongly bi-directional as flow is accelerated around Anglesey as illustrated in Figure 1.25 and Figure 1.26. It is noted that there is a wide variation in the measured tidal currents with respect to depth and 70m at this location would represent near bed conditions. The model does however correlate in terms of current directionality and the dominance of flood tide currents.

1.6.2.13 Finally, at the Morgan Array Area, site B, the tidal current speeds and directions are well represented by the model. This is the case for both neap, Figure 1.21, and spring, Figure 1.22, tidal flows. The calibration data demonstrates that the numerical model simulates the tidal currents in the region. This includes the representation of the dominant flood tide.

1.6.2.14 To provide a representation of tidal flows across the domain Figure 1.29 and Figure 1.30 illustrates tidal patterns during peak ebb and flood on a neap tide whilst Figure 1.31 and Figure 1.32 illustrates the spring tide. These points in the tidal cycle are used as reference for the assessment of potential impacts and changes to tidal flows due to the Morgan Generation Assets. The period selected for the comparative study represents a spring tide on the upper end of the range experienced in the region; this was to ensure the study included the greatest variation in tidal conditions, (i.e. water depth and current speed). Residual tidal flows and how they drive sediment transport regimes are examined in section 1.6.6.

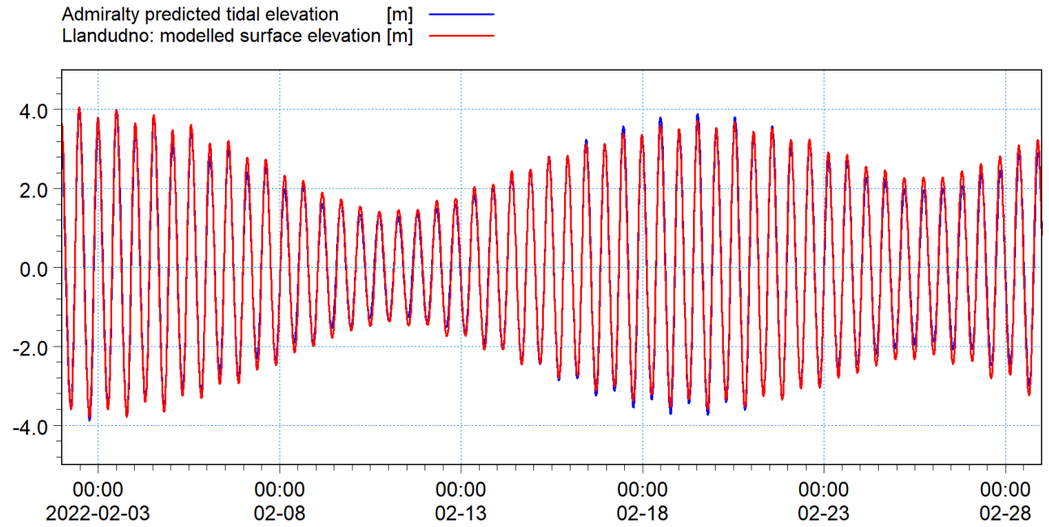

Figure 1.10: Comparison of model and admiralty harmonic tide data for Llandudno.

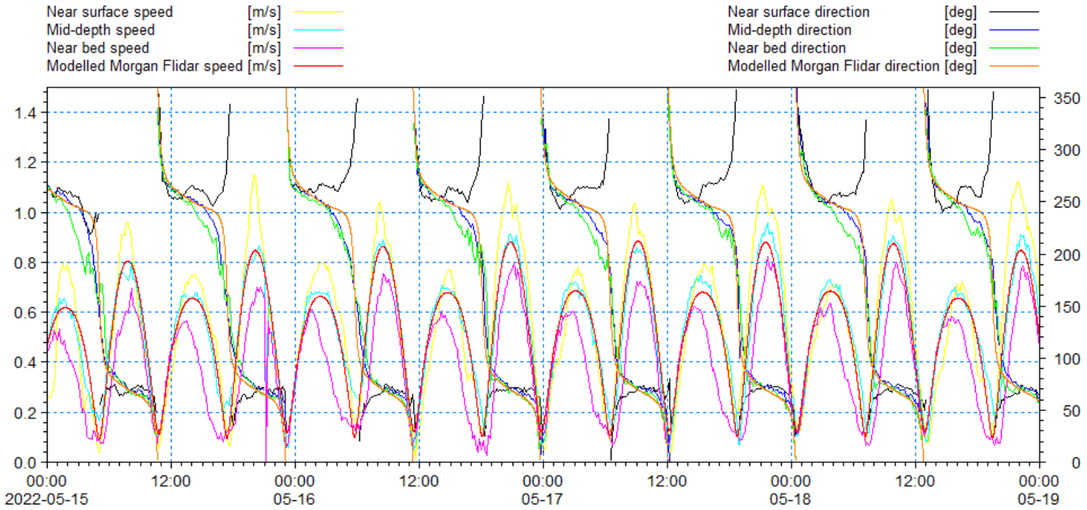

Figure 1.11: Comparison of model and recorded Morgan FLidar – current speed and direction spring.

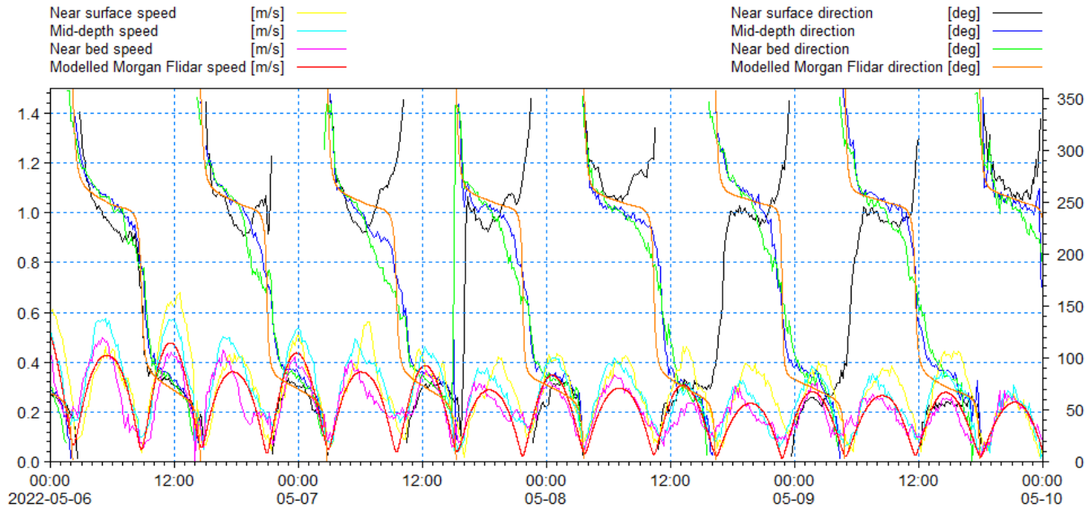

Figure 1.12: Comparison of model and recorded Morgan FLidar – current speed and direction neap.

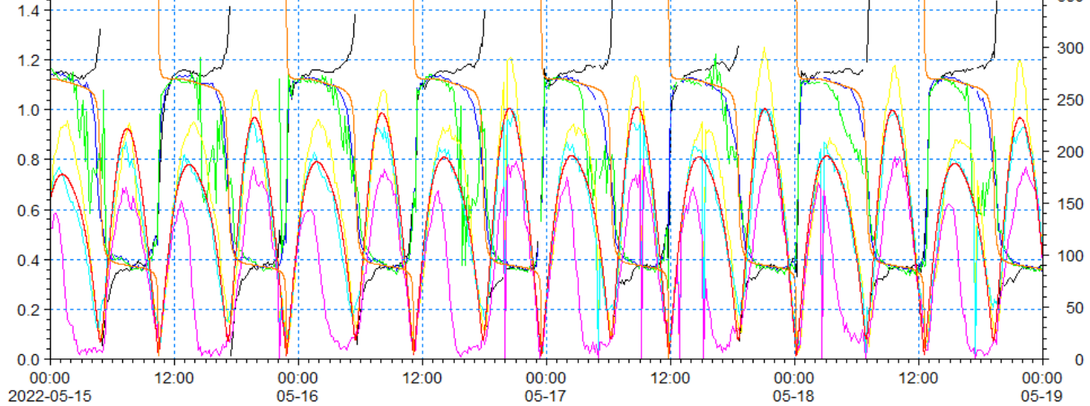

Figure 1.13: Comparison of model and recorded Mona FLidar – current speed and direction spring.

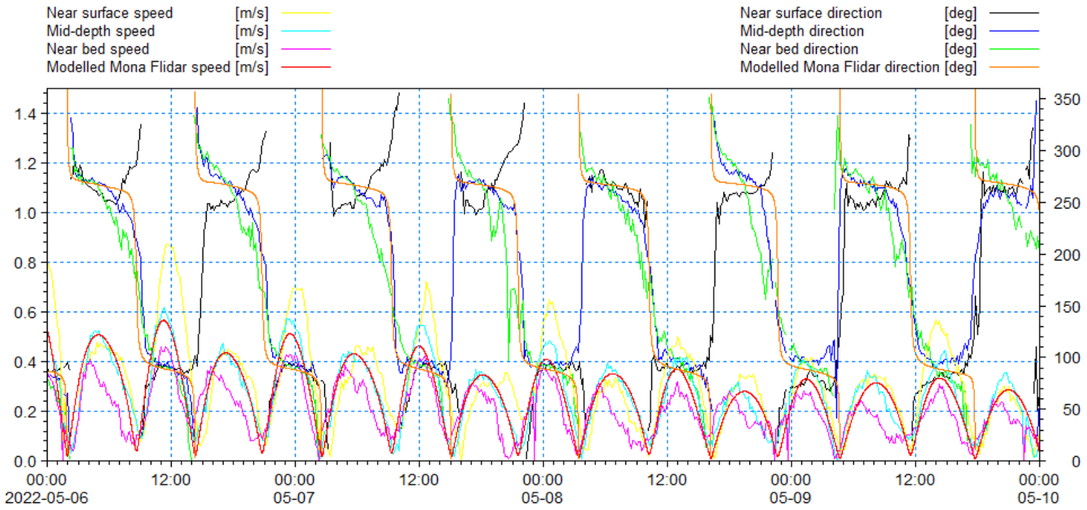

Figure 1.14: Comparison of model and recorded Mona FLidar – current speed and direction neap.

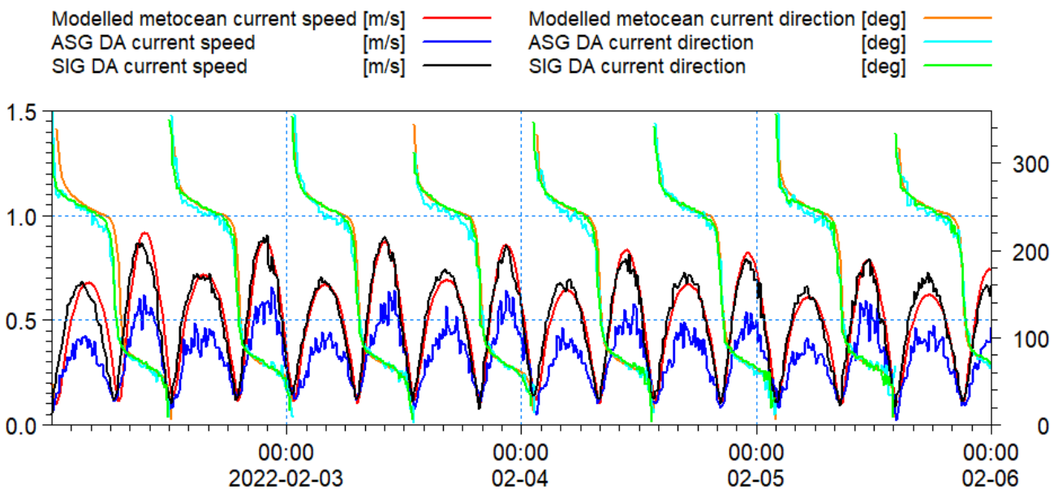

Figure 1.15: Comparison of modelled metocean and recorded DA ASG and SIG – current speed and direction spring.

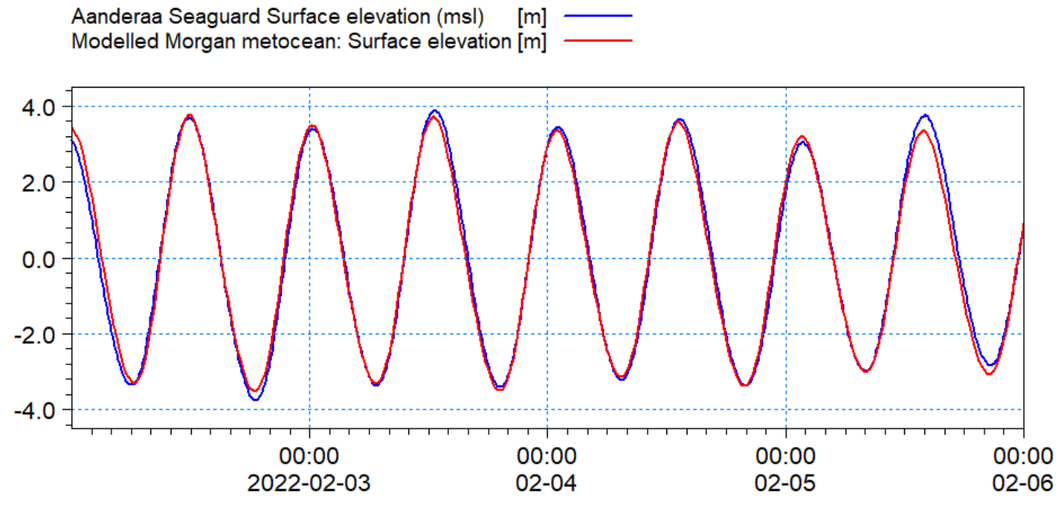

Figure 1.16: Comparison of modelled Morgan metocean and recorded ASG – spring surface elevation.

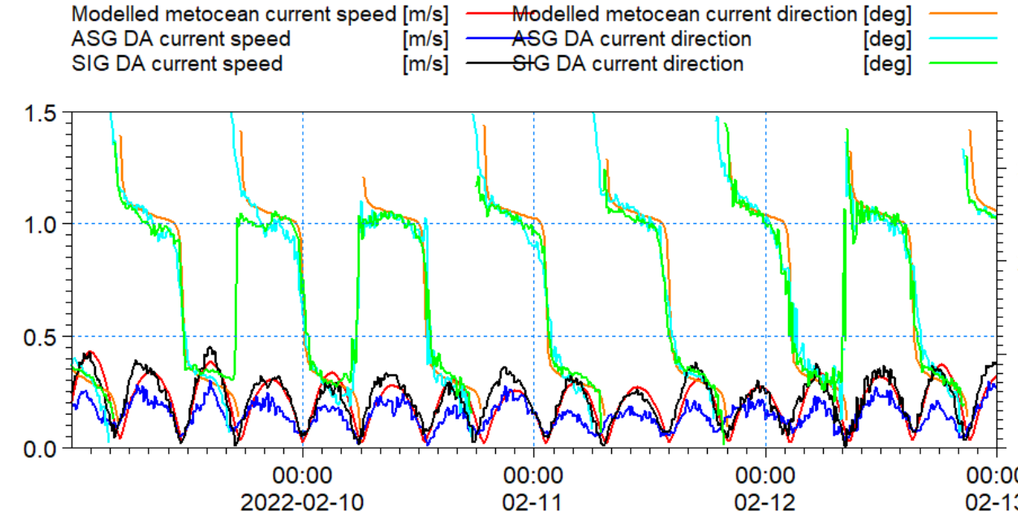

Figure 1.17: Comparison of modelled metocean and recorded DA ASG and SIG DA – current speed and direction neap.

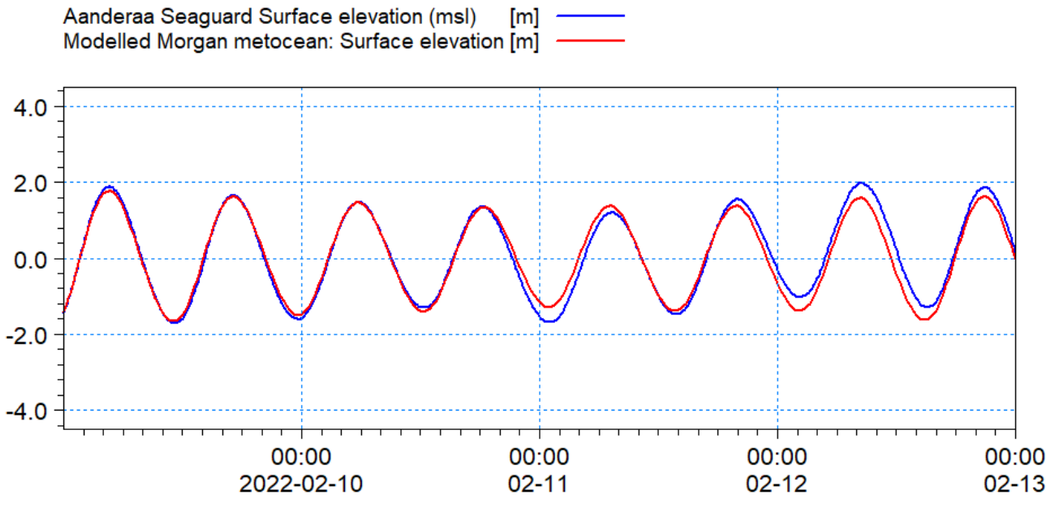

Figure 1.18: Comparison of modelled Morgan metocean and recorded ASG – neap surface elevation.

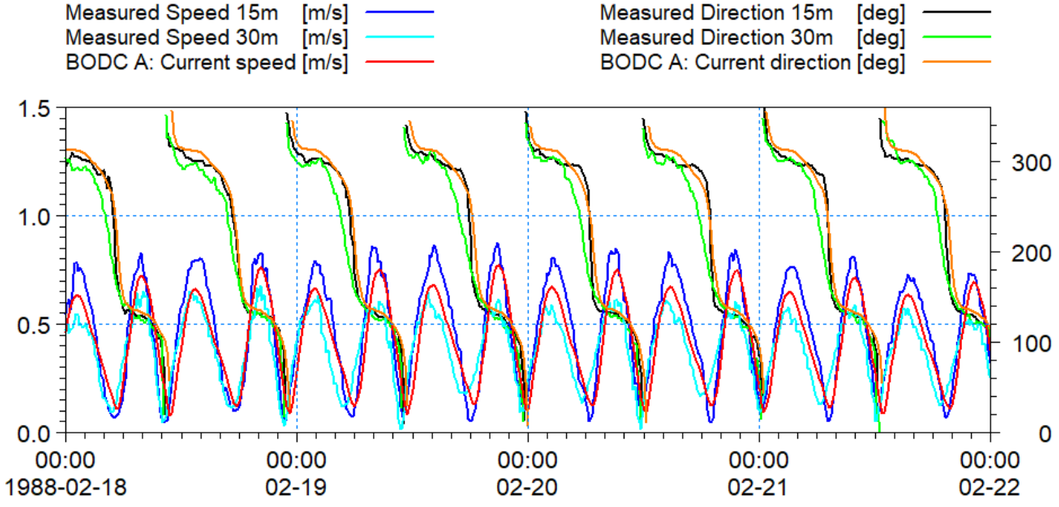

Figure 1.19: Comparison of model and recorded data BODC Location A – current speed and direction spring.

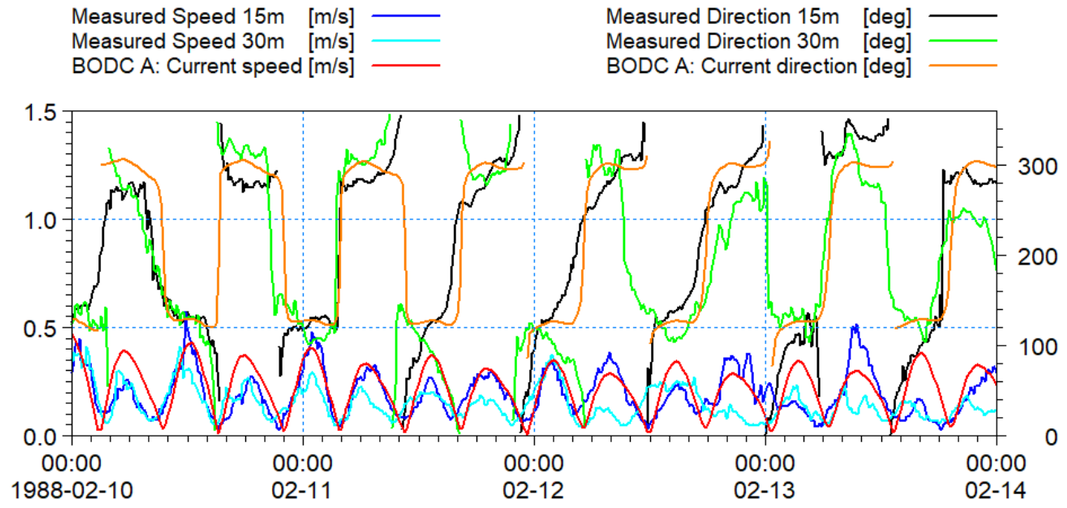

Figure 1.20: Comparison of model and recorded data BODC Location A – current speed and direction neap.

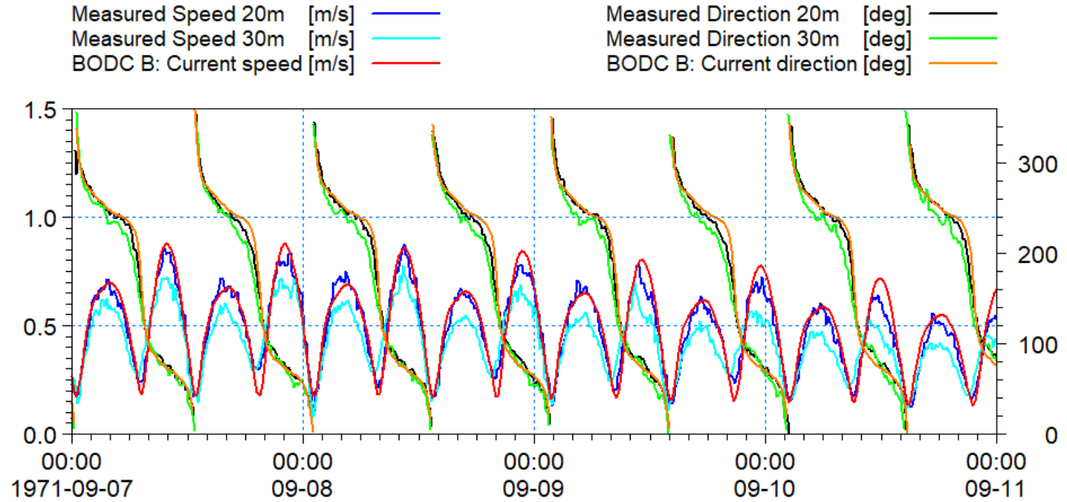

Figure 1.21: Comparison of model and recorded data BODC Location B – current speed and direction spring.

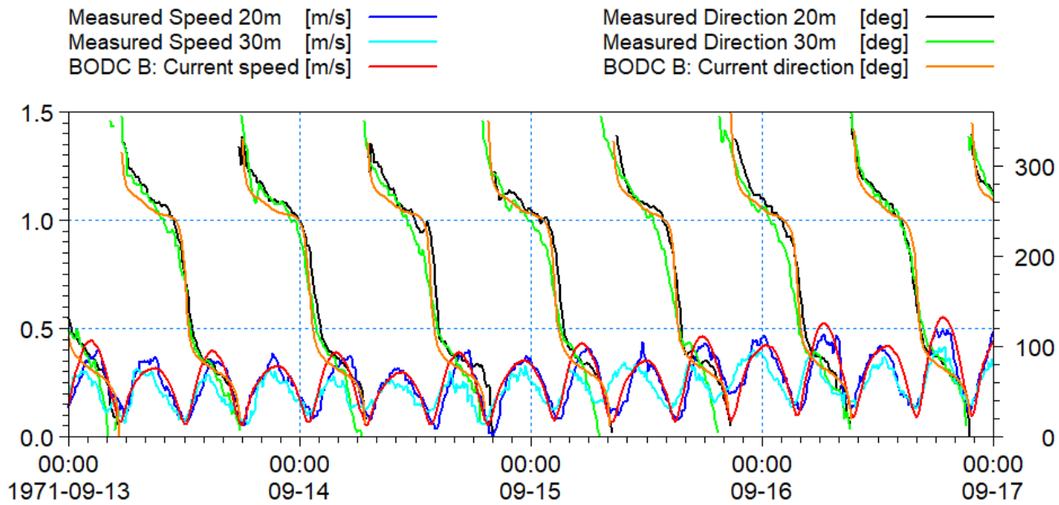

Figure 1.22: Comparison of model and recorded data BODC Location B – current speed and direction neap.

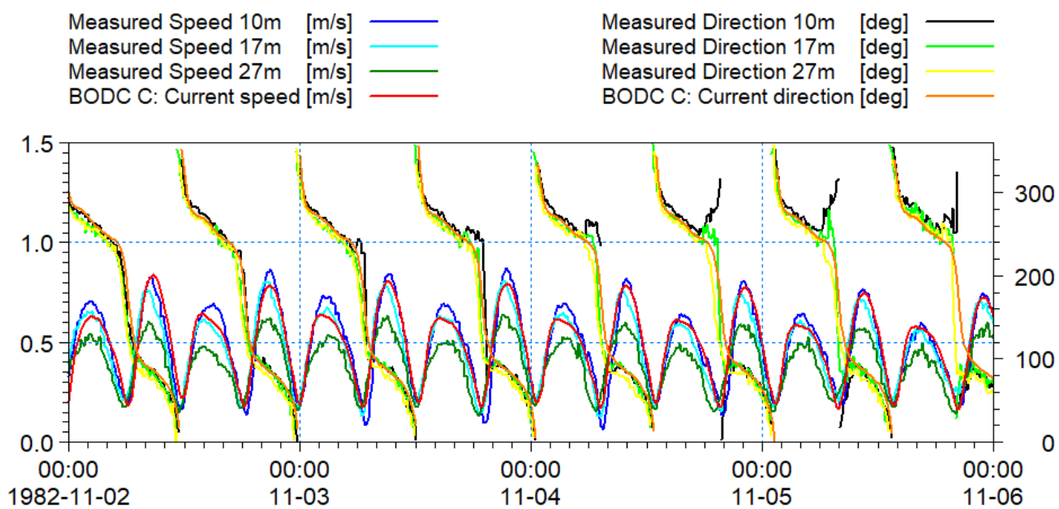

Figure 1.23: Comparison of model and recorded data BODC Location C – current speed and direction spring.

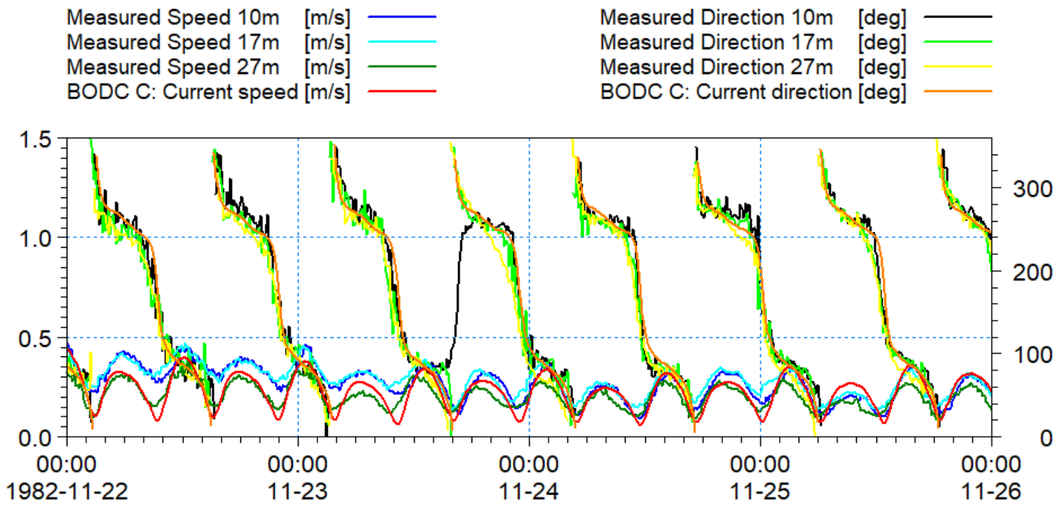

Figure 1.24: Comparison of model and recorded data BODC Location C – current speed and direction neap.

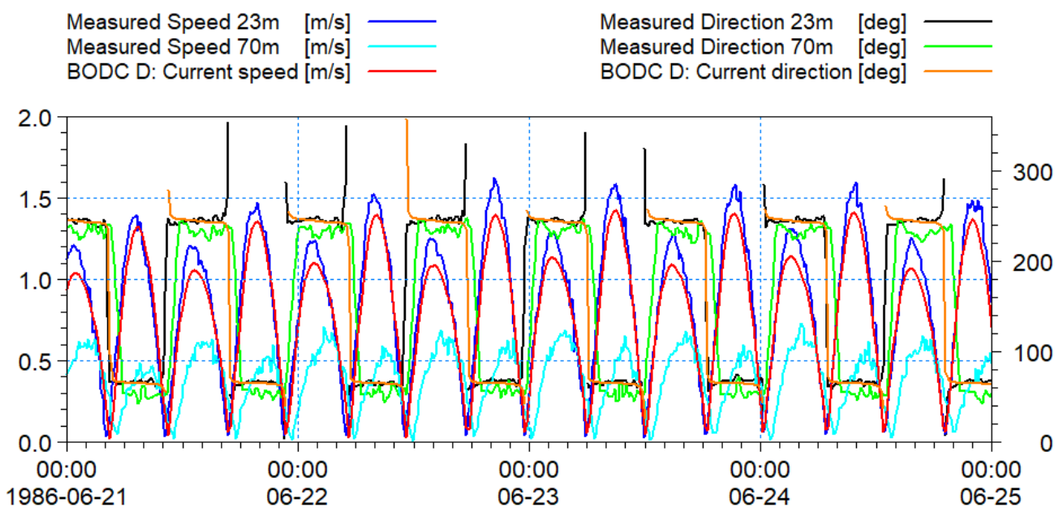

Figure 1.25: Comparison of model and recorded data BODC Location D – current speed and direction spring.

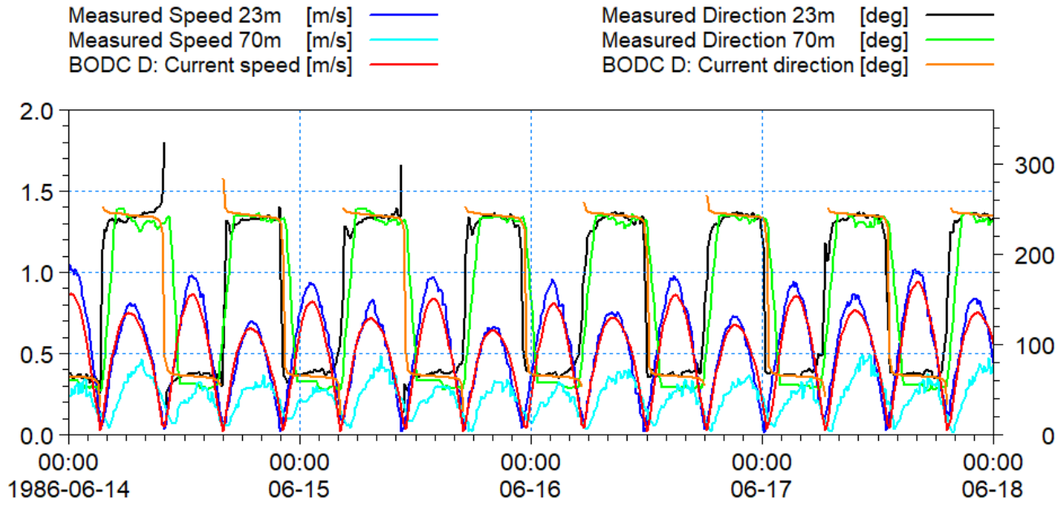

Figure 1.26: Comparison of model and recorded data BODC Location D – current speed and direction neap.

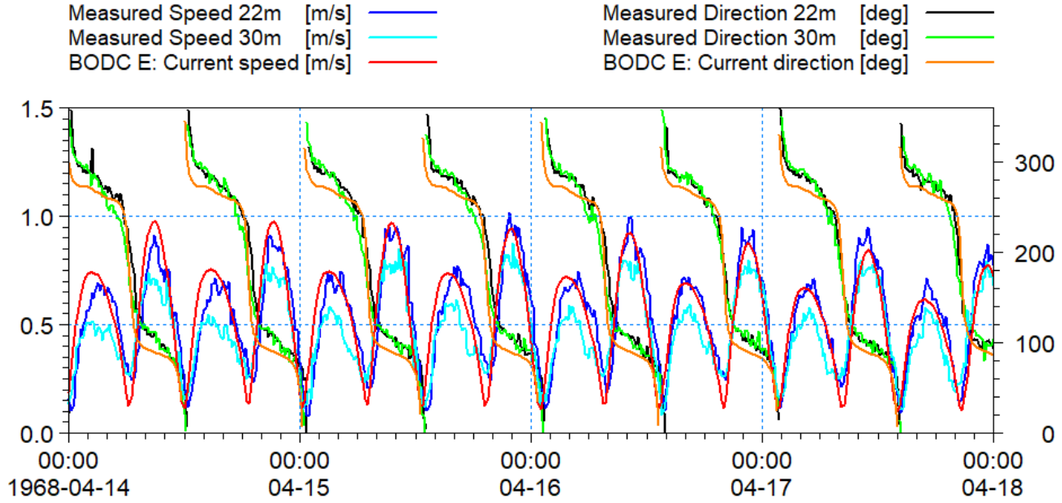

Figure 1.27: Comparison of model and recorded data BODC Location E – current speed and direction spring.

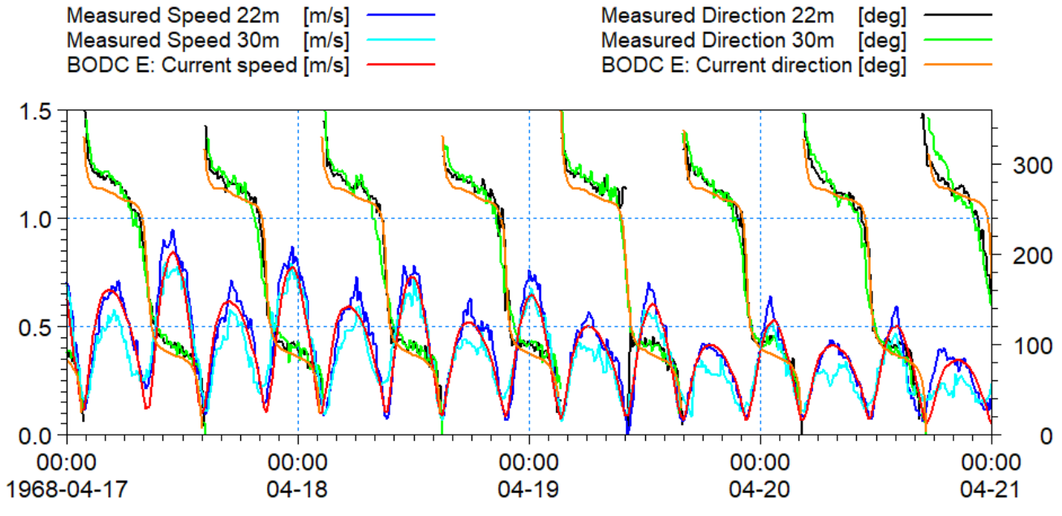

Figure 1.28: Comparison of model and recorded data BODC Location E – current speed and direction neap.

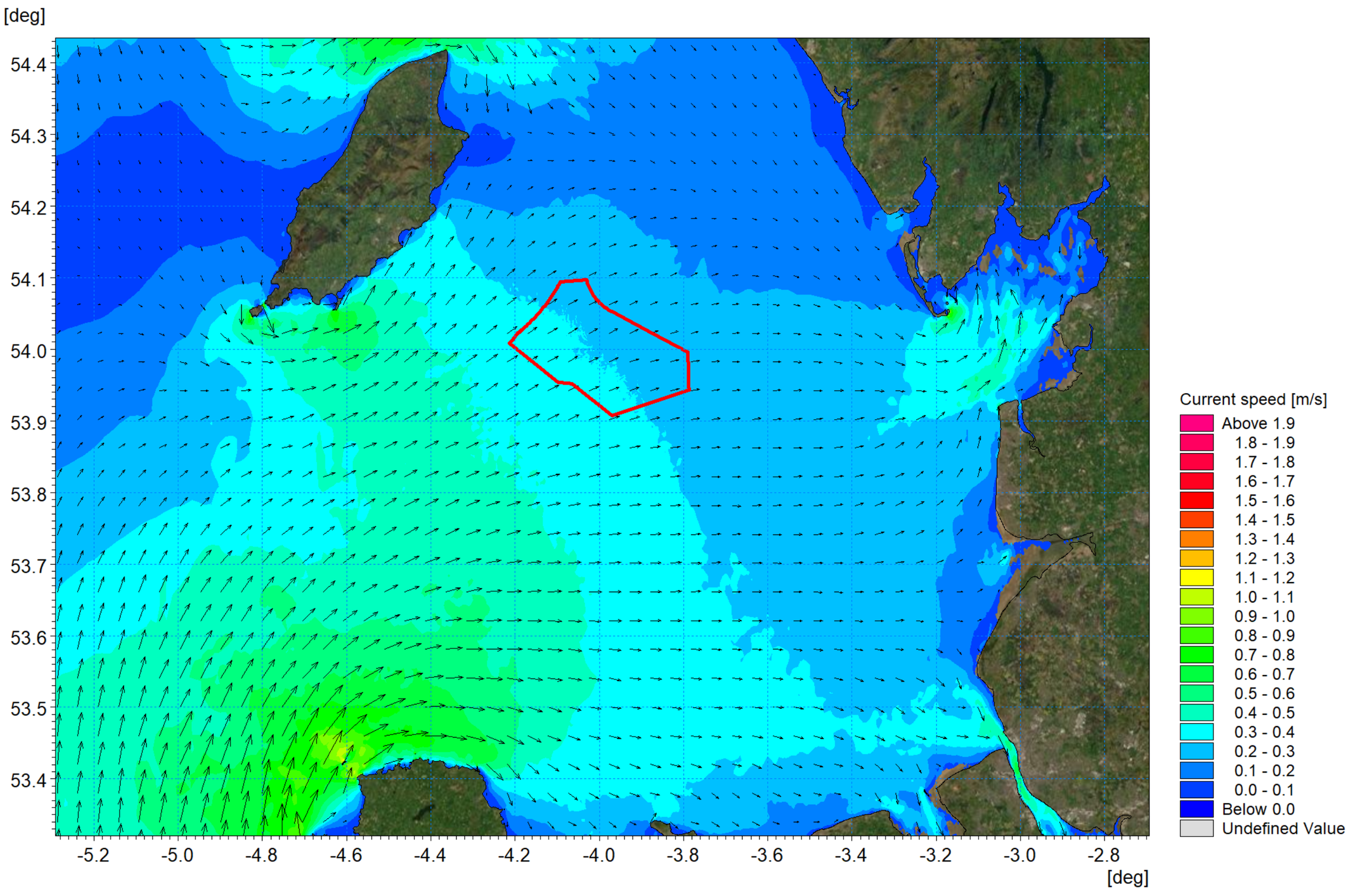

Figure 1.29: Tidal flow patterns – neap tide flood.

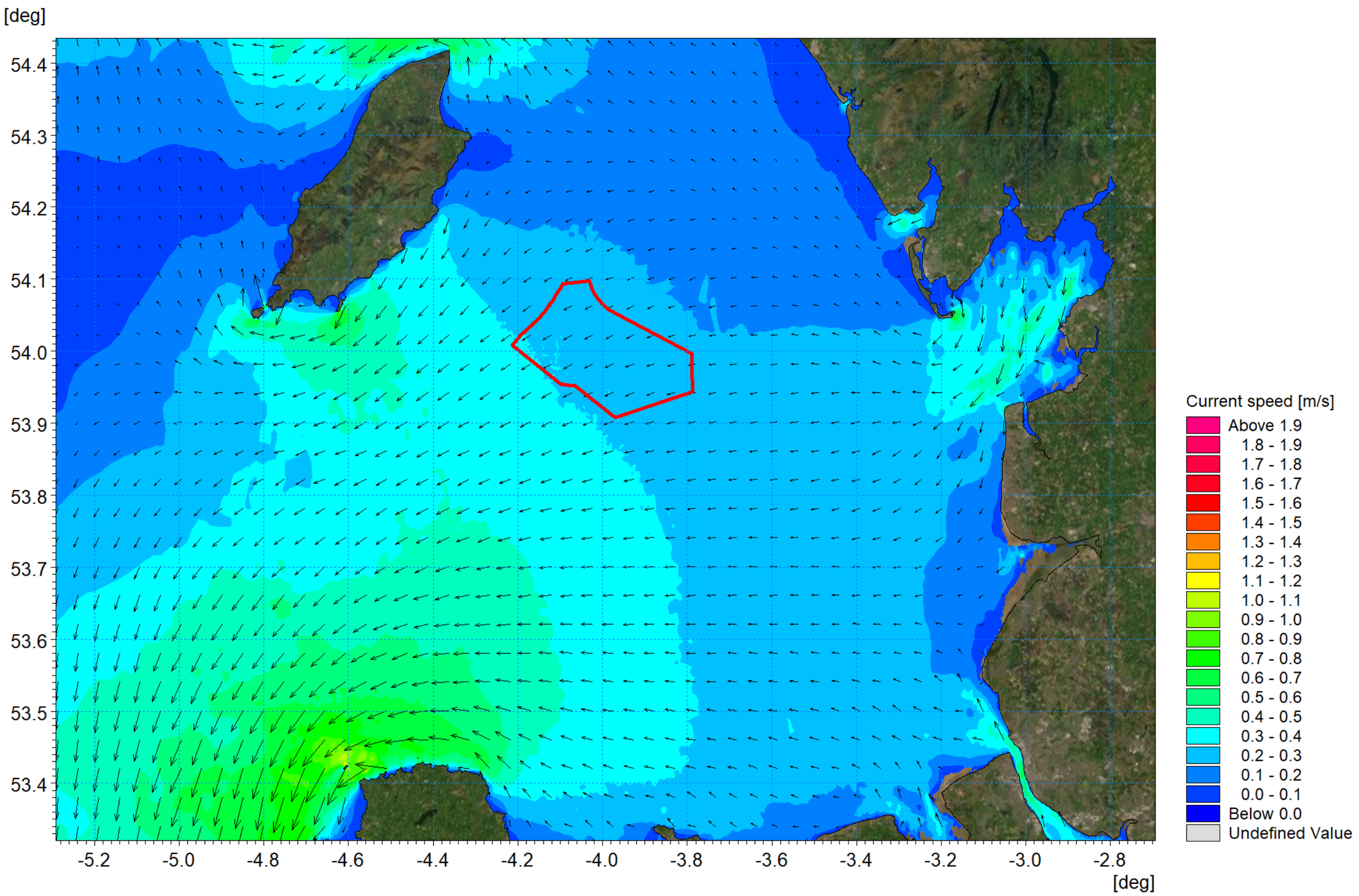

Figure 1.30: Tidal flow patterns – neap tide ebb.

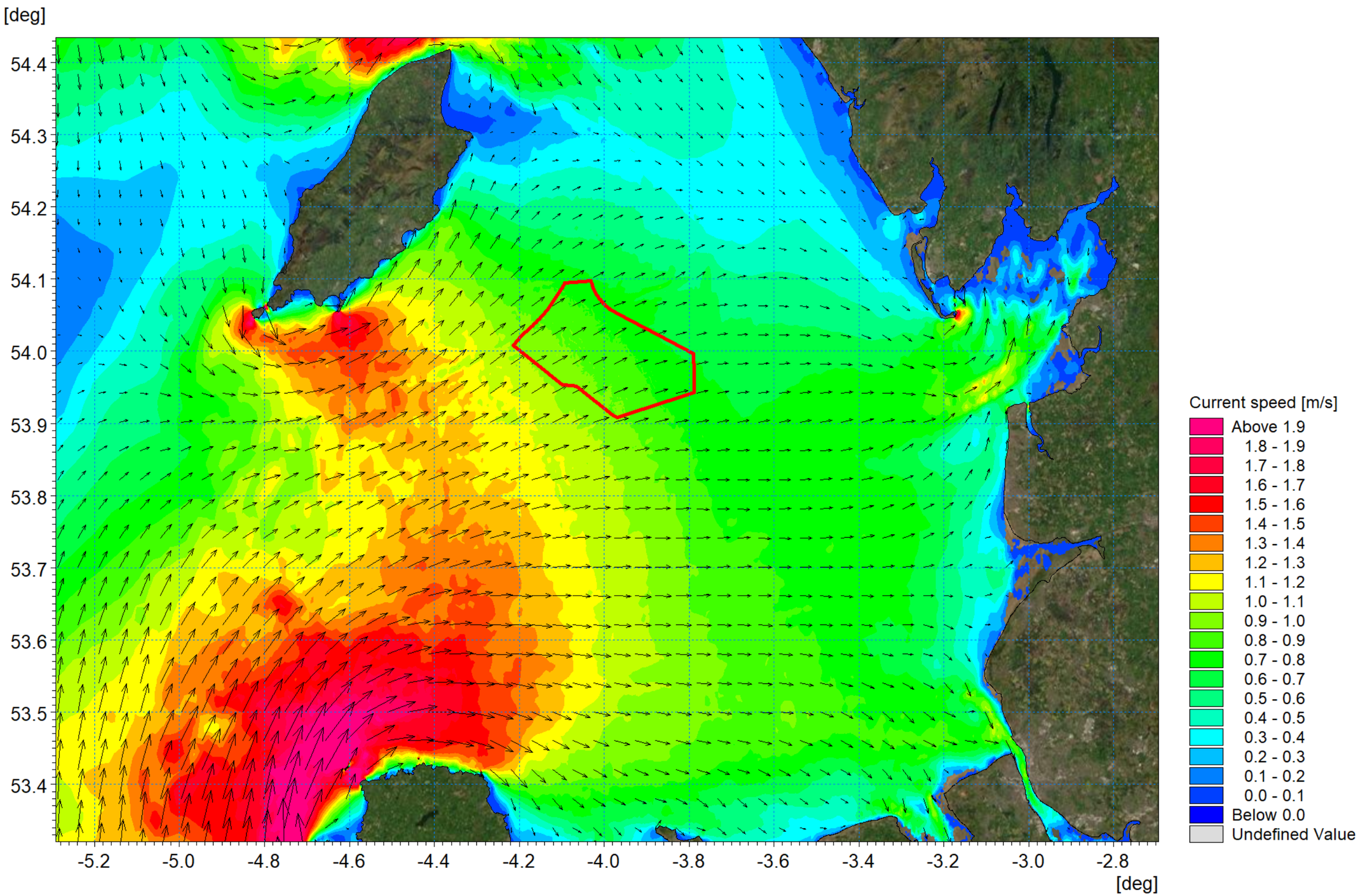

Figure 1.31: Tidal flow patterns – spring tide flood.

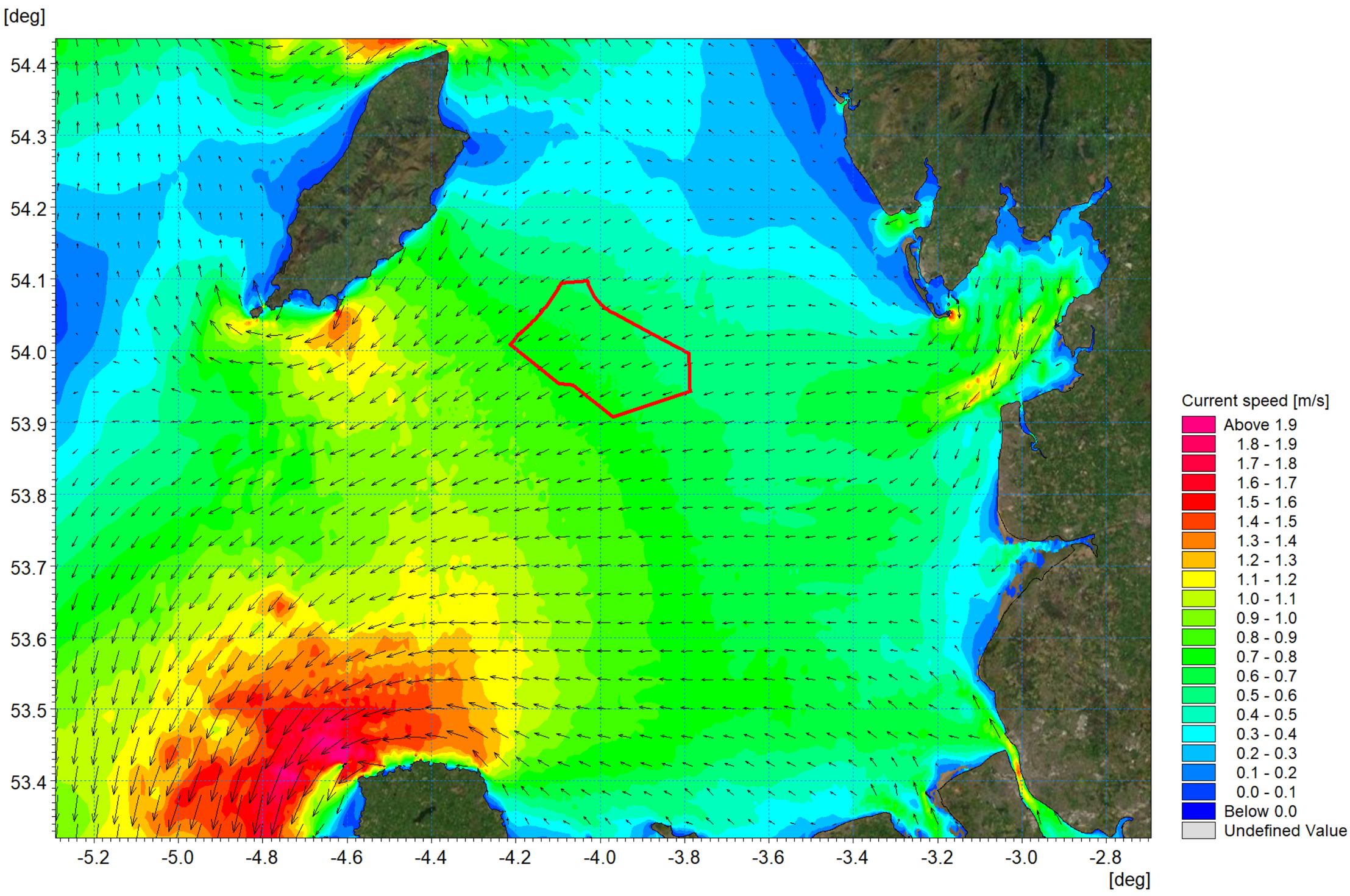

Figure 1.32: Tidal flow patterns – spring tide ebb.

1.6.3 Wave climate

1.6.3.1 Waves in the east Irish Sea are highest to the southwest of the Isle of Man with the highest mean annual significant wave height of 1.39m recorded between the Isle of Man and Anglesey. Significant wave height is reduced closer to the coast with the lowest significant wave height of 0.73m recorded to the west of the Dee Estuary (ABPmer, 2008). In the Morgan physical processes study area mean annual wave height ranges from 1.1m to 1.3m. Over 40% of the waves arise from the southwest with all significant wave heights (>4m) arriving from the southwest or west (ABPmer, 2018). This is illustrated in Figure 1.33 which shows the wave rose for a point located within this area. Similarly, the corresponding wind rose presented in Figure 1.34 which illustrates the predominant winds are from the southwest with the site being located in the lee of the Isle of Man.

1.6.3.2 As offshore waves transfer from the deep offshore water to shallower coastal areas, a number of important modifications may result due to interactions of offshore deep-water waves with the seabed, with the resultant modifications producing shallow water waves. These physical 'wave transformation' interactions include:

- Shoaling and refraction (due to both depth and current interactions with the wave)
- Energy loss due to breaking
- Energy loss due to bottom friction
- Momentum and mass transport effect.

1.6.3.3 The wave model developed for the assessment was calibrated using data collected during storm Christoph which occurred during January 2021. The model simulated water levels using boundary data extracted from the RPS TSSF model and applied meteorological conditions from the ECMWF operational dataset. Wave conditions at the model boundary were also provided from the ECMWF operational dataset.

1.6.3.4 The model output data was then compared with measured data obtained from the National Network of Regional Coastal Monitoring Programmes held by the CCO at the locations shown in Figure 1.35. For each of the three location three parameters are presented relating to mean wave direction, significant wave height and peak wave period.

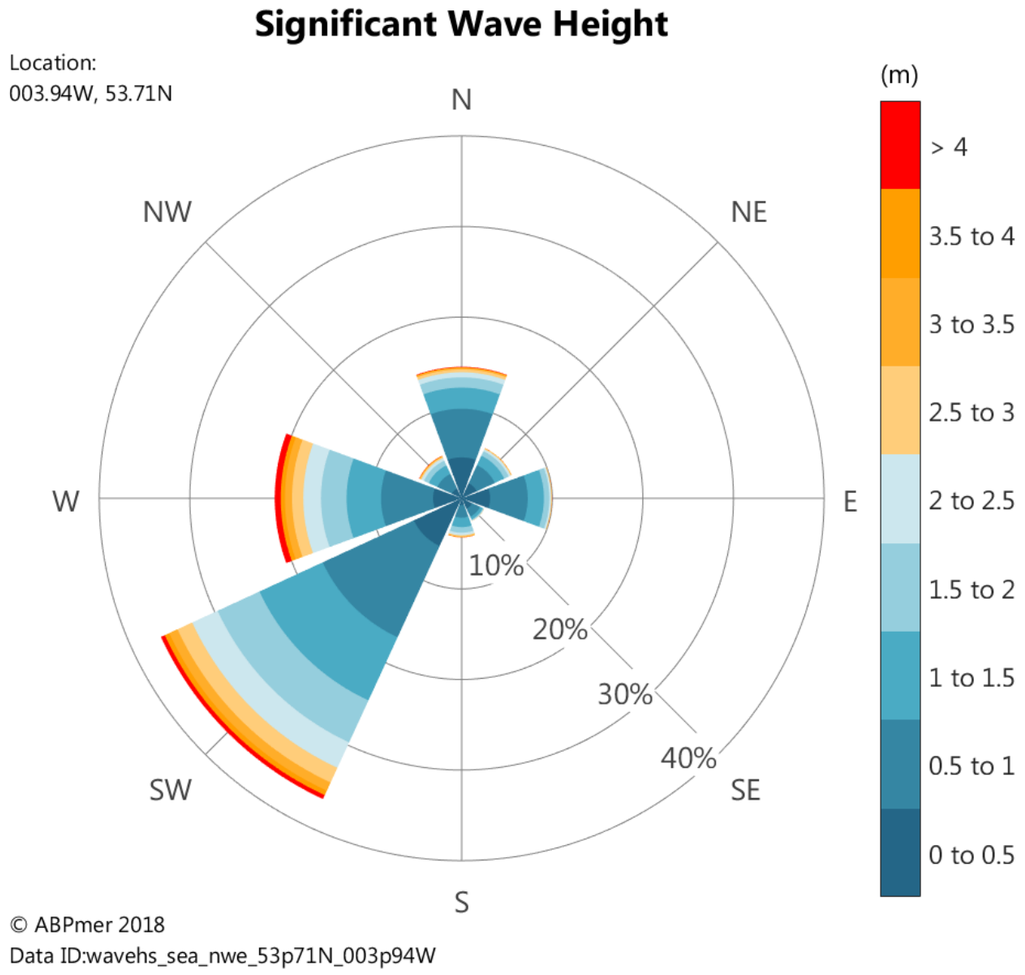

Figure 1.33: Wave rose for Morgan Array Area.

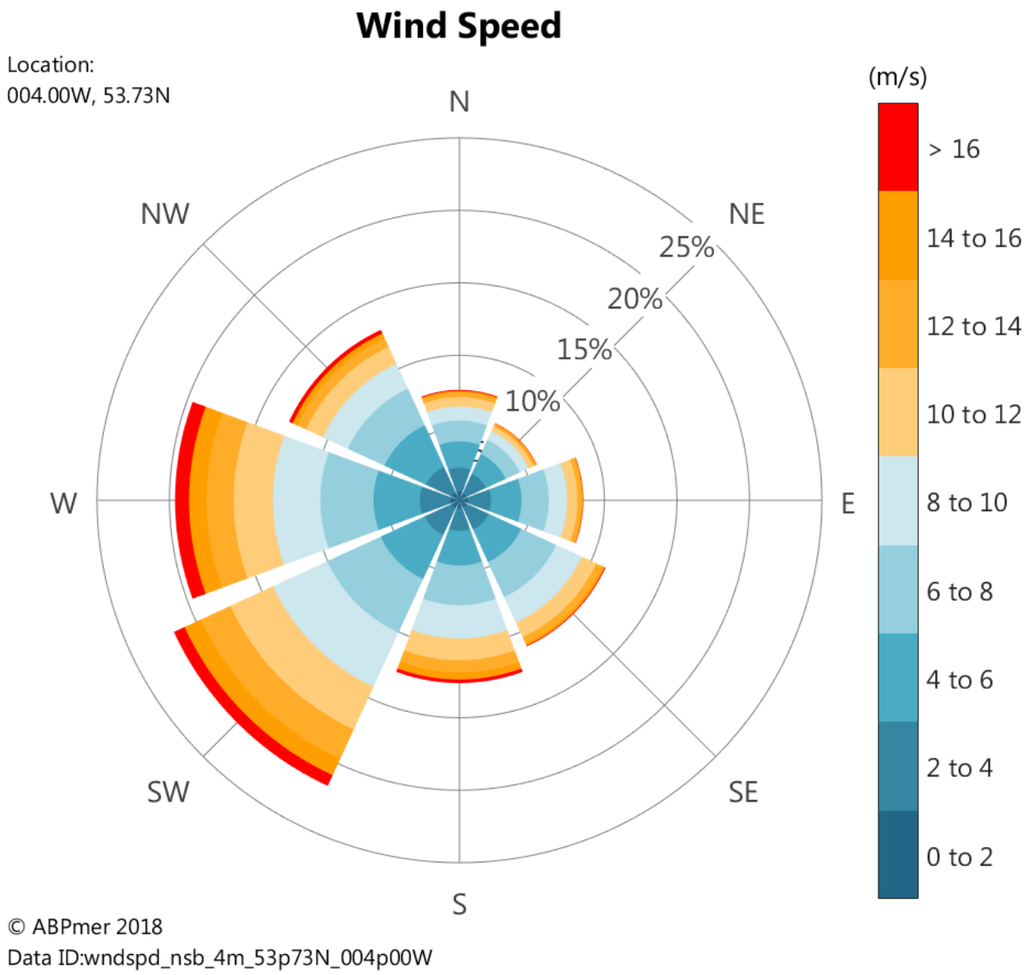

Figure 1.34: Wind rose for Morgan Array Area.

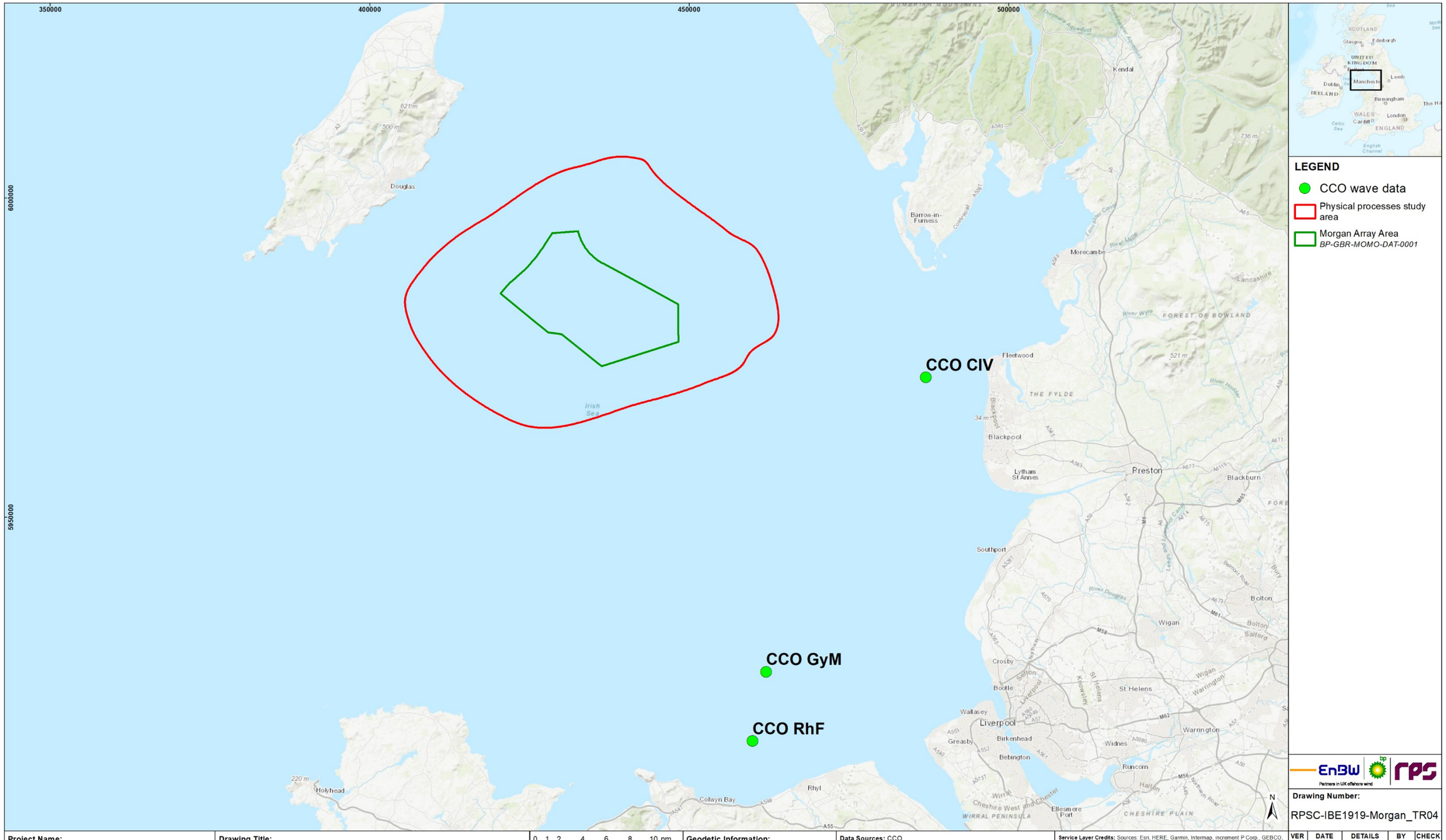

Figure 1.35: Location of wave calibration data presented.

1.6.3.5 Storm Christoph approached the east Irish Sea from an easterly direction and therefore the calibration site located to the east of the physical processes study area provide a good indicator as to how well the wave model transforms wave through the physical processes study area. Model and measured data for site Cleveleys (CIV) located at the mouth of Morecambe Bay are presented in Figure 1.36 to Figure 1.38. In each case it can be seen that the hourly interval model data tracks the progress of the storm. It is noted that the model is less 'peaky', but this is to be expected given that the ECMWF data is at three hourly intervals and linear interpolation was applied.

1.6.3.6 For the two southerly sites Gwynt y Môr (GyM) (Figure 1.39 to Figure 1.41) and Rhyl Flats (RhF) (Figure 1.42 to Figure 1.44) located on the southeast extent of the physical processes study area there is also a good correlation between modelled and monitored data. This indicated that the wave model was suitable for use in the comparative study of the potential impacts of the Morgan Generation Assets infrastructure on wave climate.

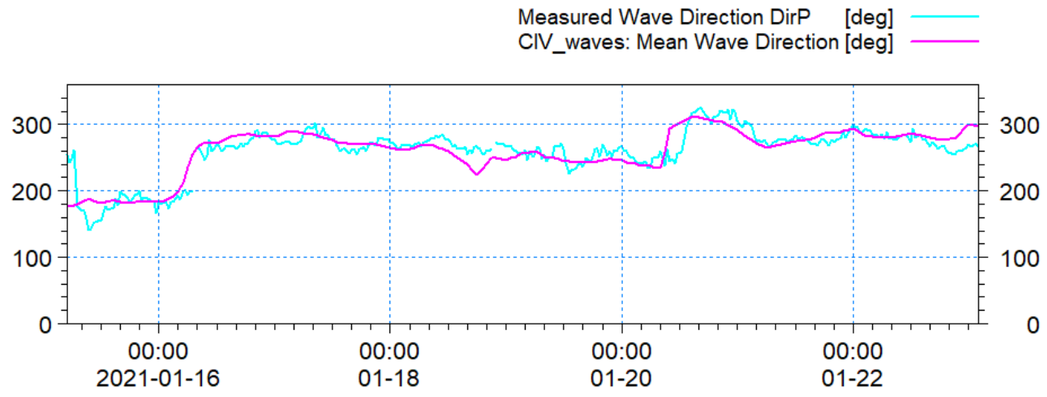

Figure 1.36: Validation of modelled mean wave direction with measured data at CIV.

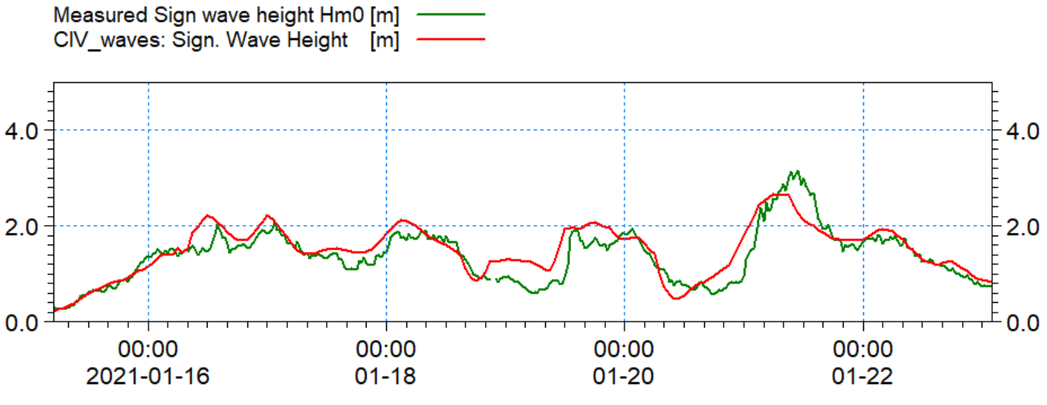

Figure 1.37: Validation of modelled significant wave height with measured data at CIV.

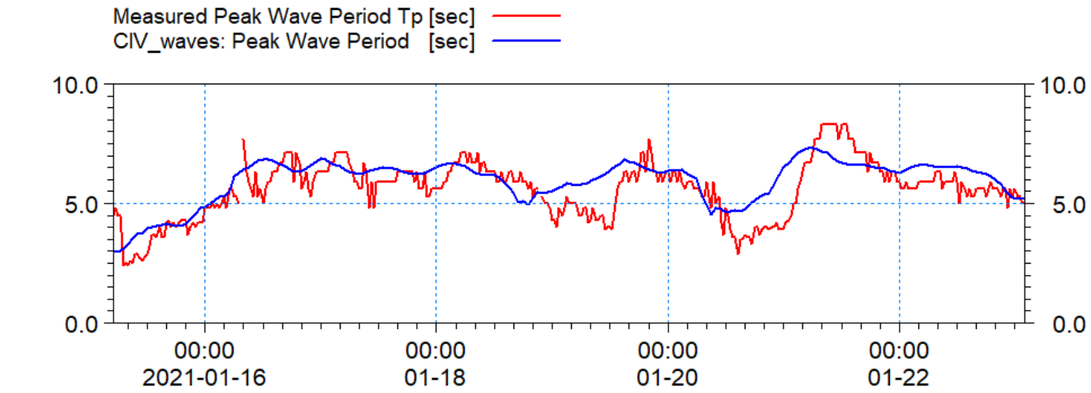

Figure 1.38: Validation of Modelled Peak Wave Period with Measured Data at CIV.

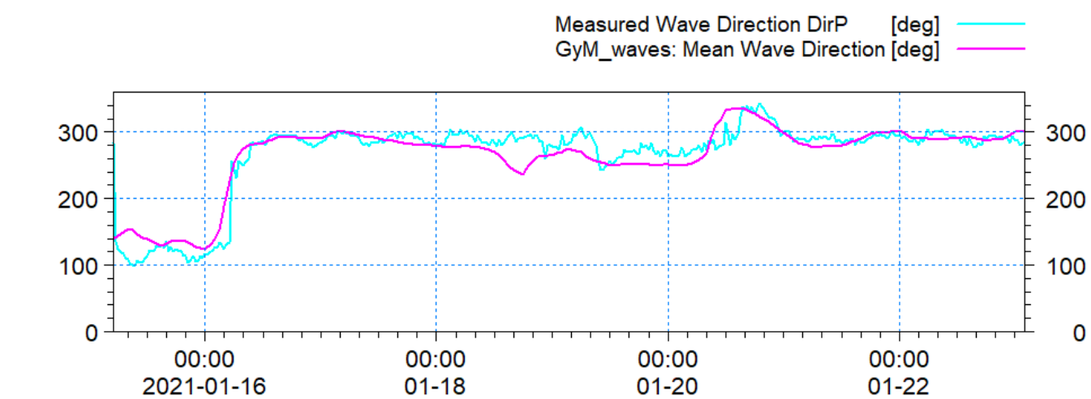

Figure 1.39: Validation of modelled mean wave direction with measured data at GyM.

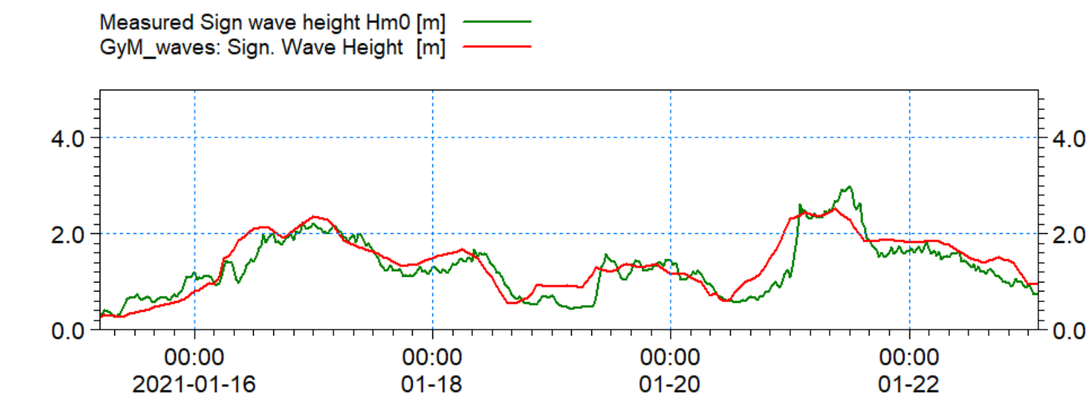

Figure 1.40: Validation of modelled significant wave height with measured data at GyM.

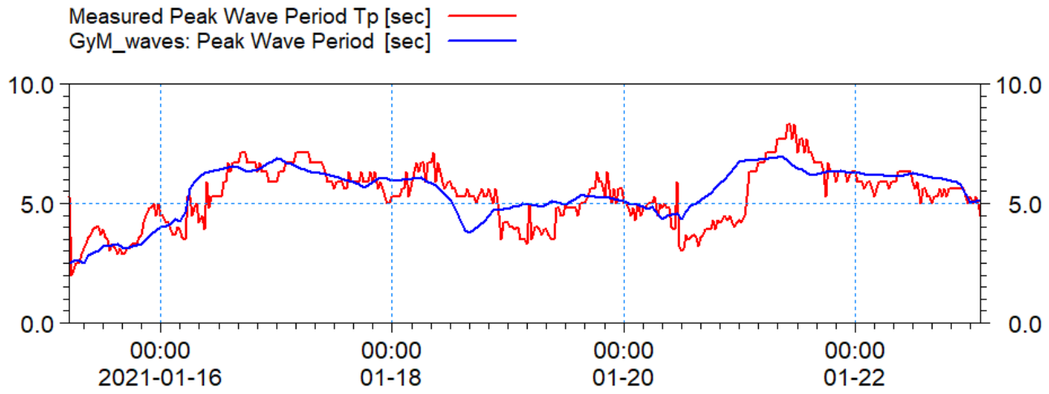

Figure 1.41: Validation of modelled peak wave period with measured data at GyM.

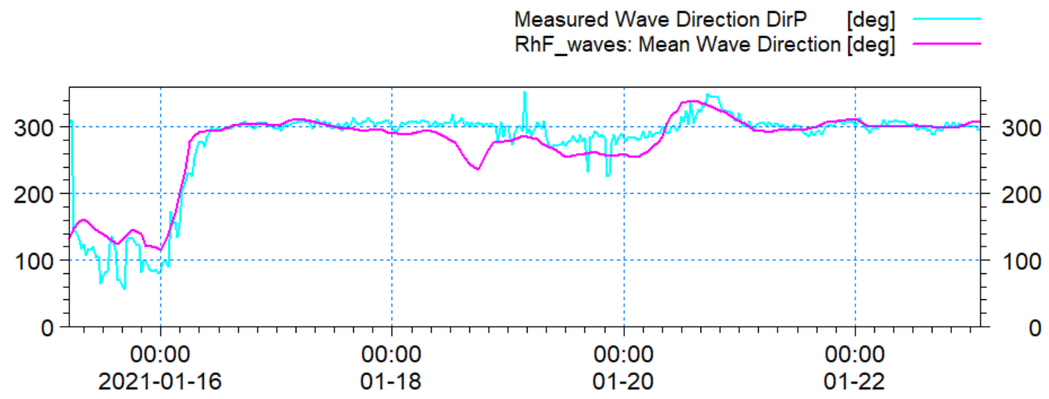

Figure 1.42: Validation of modelled mean wave direction with measured data at RhF.

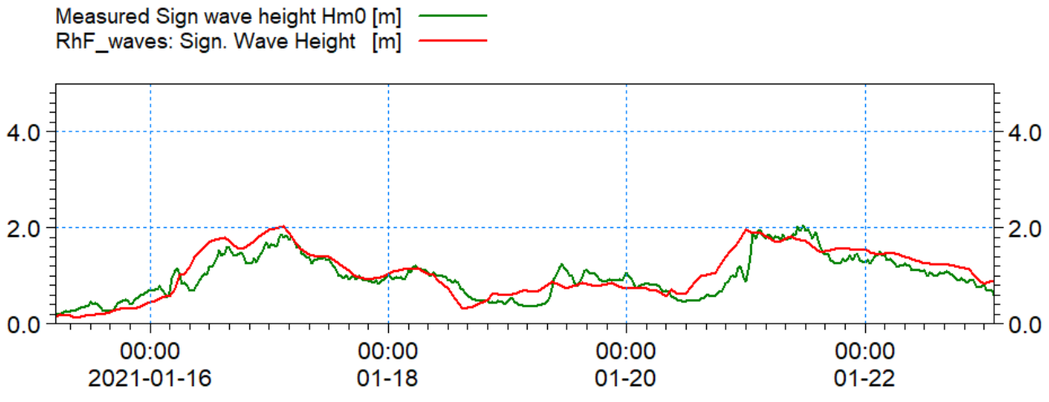

Figure 1.43: Validation of modelled significant wave height with measured data at RhF.

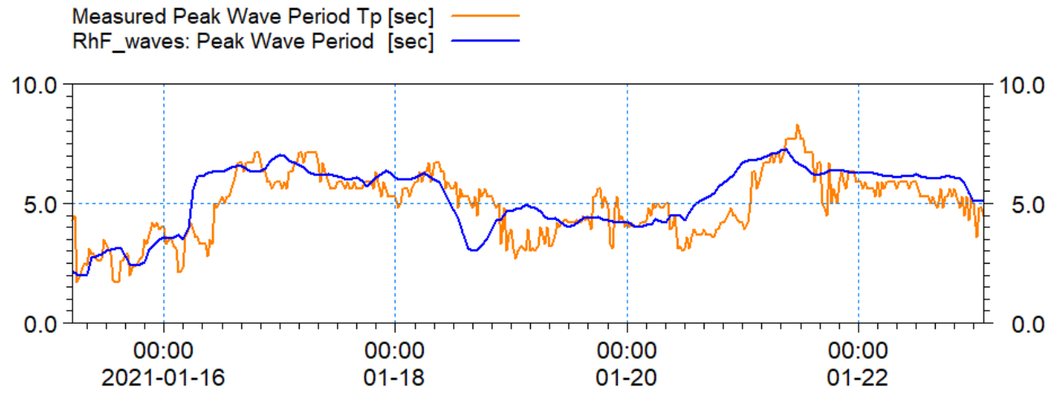

Figure 1.44: Validation of modelled peak wave period with measured data at RhF.

1.6.3.1 In order to evaluate the potential changes in wave climate due to the Morgan Generation Assets, a comparative study was carried out. This meant that baseline wave climate was required; due to the comparative nature of the assessment, a full metocean study was not essential however representative sea-states were required.

1.6.3.2 An analysis was undertaken to determine the offshore conditions for which waves reach the site from all directions. Twenty-two years of data were obtained from the ECMWF operational dataset for locations on the north and south boundaries of the model domain. Extreme value analysis using peak over threshold was undertaken for each 30º sector to determine the 1in1 and 1in20 year offshore wave climate. These were then used as boundary conditions within the wave modelling to determine the resultant wave climate at the site and across the physical processes study area.

1.6.3.3 In addition to boundary wave data, it was necessary to analyse the wind field to include the contribution of local wind seas. For this, for a representative point for each of the key directions, was identified and utilised from the NOAA 40-year dataset. This was analysed on the same sectoral basis as the wave data to give an indication of the return period wind speed. Figure 1.45 shows the model domain with wind and wave roses relating to the forcing data.

1.6.3.4 The wave modelling was undertaken using the spectral wave model, MIKE21 SW, to provide a full wave climate and wave breaking across the physical processes study area. The model used a quasi-stationary formulation which meant that for each event the wave field fully established over a number of numerical iterations until convergence was reached. The model resolves the wave field by simulating wind generation of waves within the model domain and the propagation of externally generated swell waves through the domain. The model setup ensured that the detail of both locally generated wind waves and swell conditions from further afield were captured.

1.6.3.5 The following set of figures (Figure 1.46 to Figure 1.49) show the wave climate for four 1in1 year return period events from the principal directions; north (000°), northeast (030°), southwest (210º) and southwest (240°) direction respectively. These sectors were selected to be representative of the characteristics of the wave climate and also for sectors for which the Morgan Generation Assets may potentially affect marine processes along the coastline. The wave modelling was undertaken at Mean High

Water (MHW) being the high water level on an average tide. Figure 1.49 shows the waves approaching from the west and demonstrates, as anticipated, the largest waves approach from this sector.

1.6.3.6 A second set of figures are presented relating to the 1in20 year return period; Figure 1.50 to Figure 1.53. These show data for the principal directions of 000°,030°, 240° and 270° and tidal height as the 1in1 year return period. They have been introduced to ensure that the baseline for a more arduous conditions is established for assessment of the potential effect of the Morgan Generation Assets on wave climate.

.

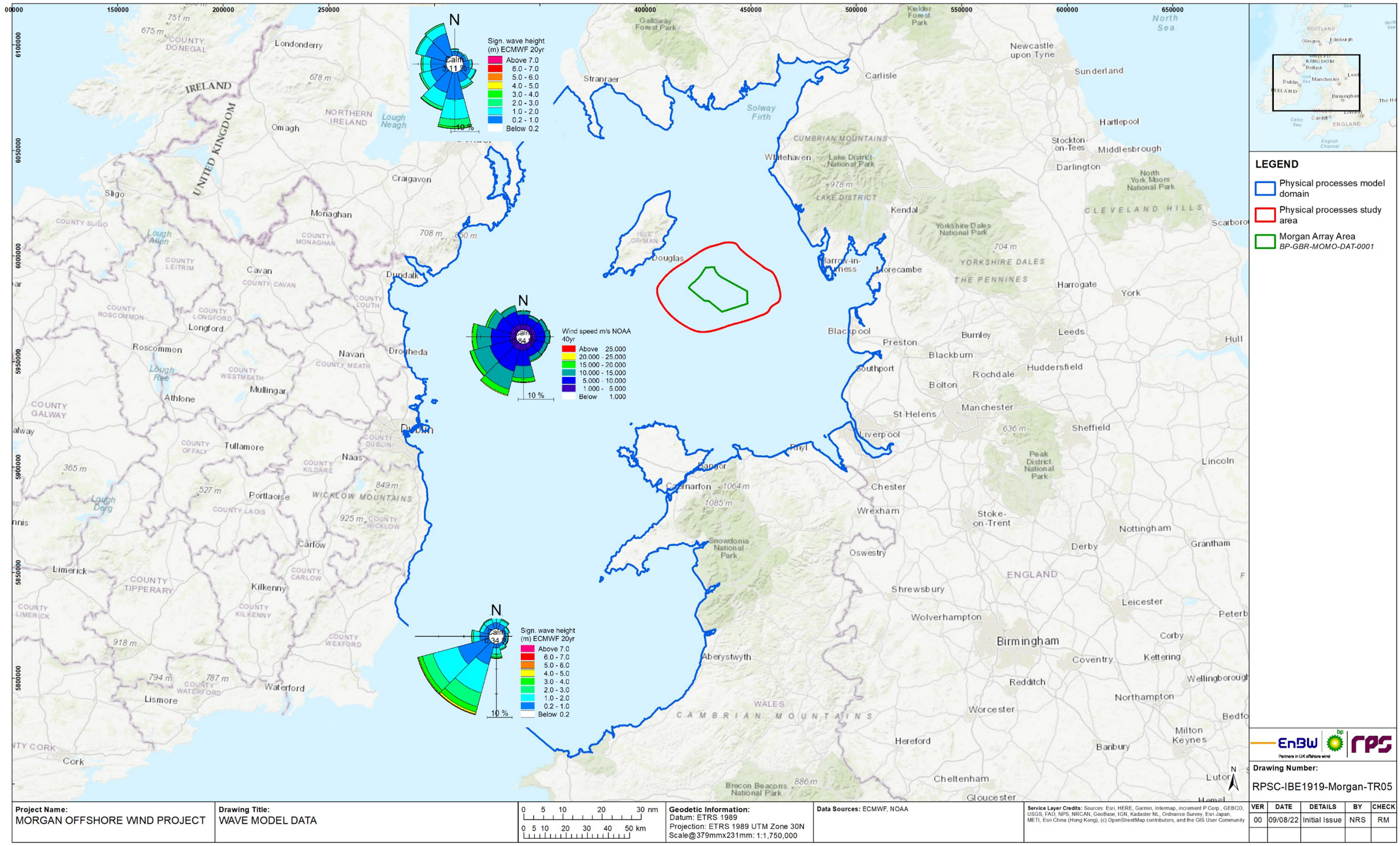

Figure 1.45: Wave roses for model boundaries- 22 year ECMWF Dataset and wind rose for 40 year NOAA dataset.

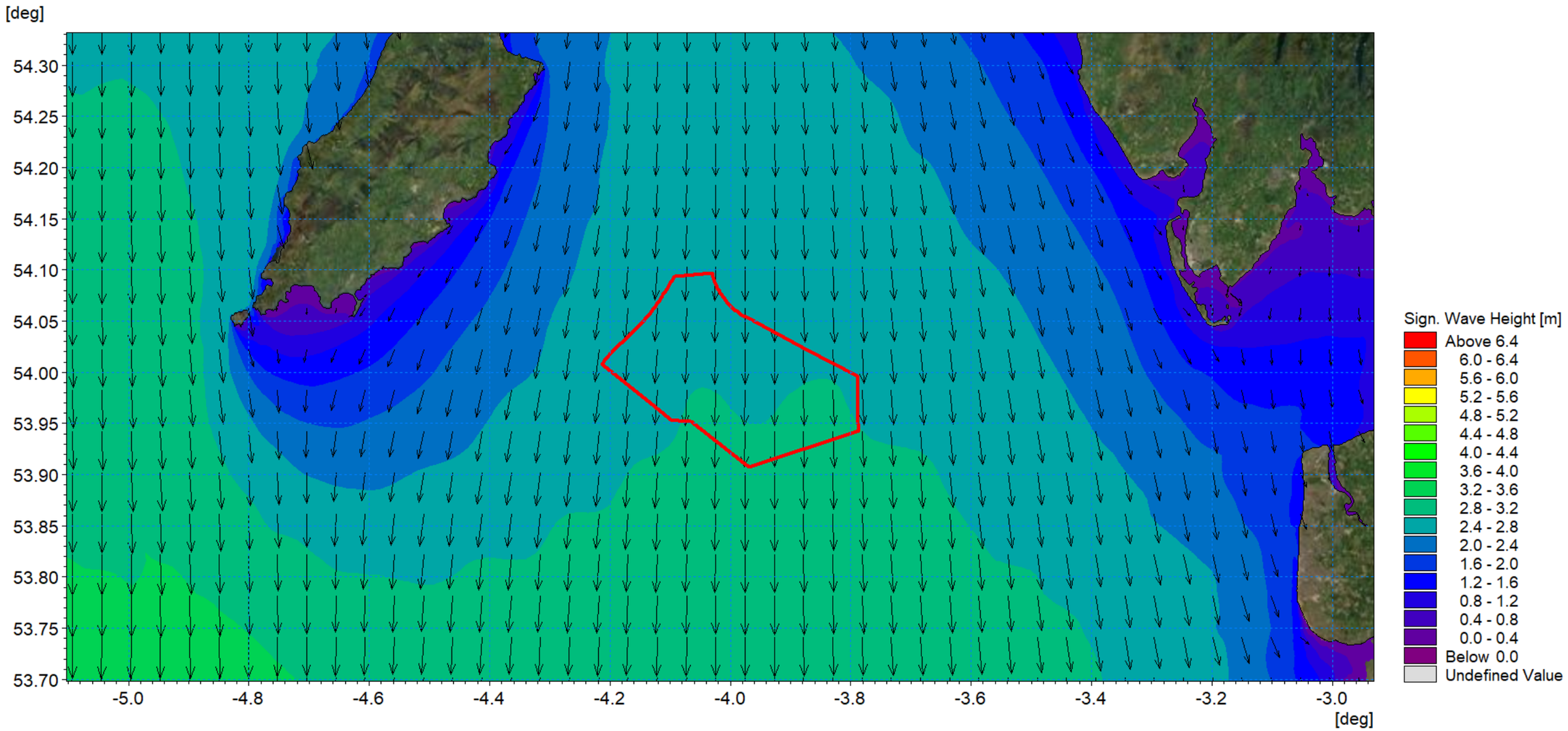

Figure 1.46: Wave climate 1:1 year storm from 000° MHW.

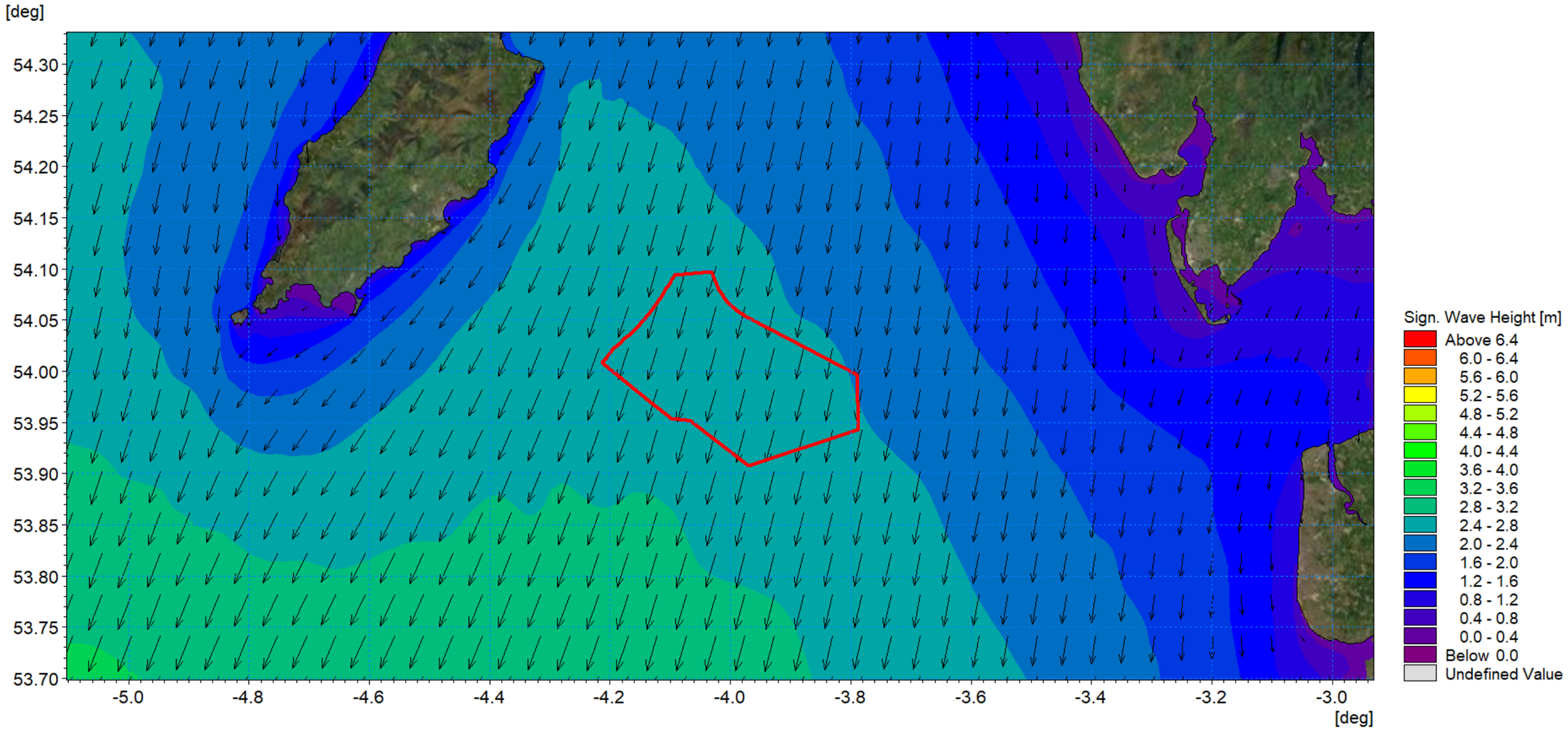

Figure 1.47: Wave climate 1:1 year storm from 030° MHW.

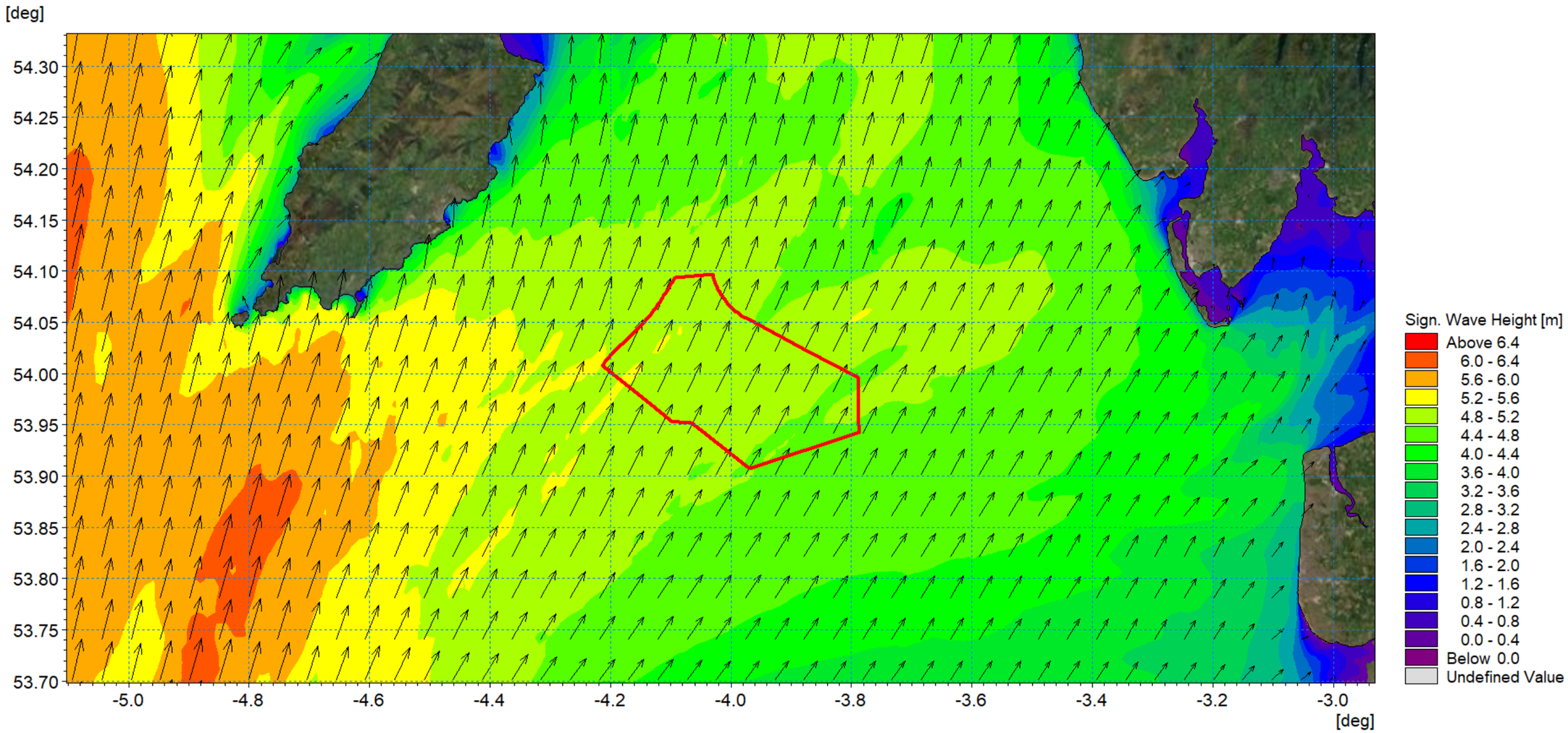

Figure 1.48: Wave climate 1:1 year storm from 210° MHW.

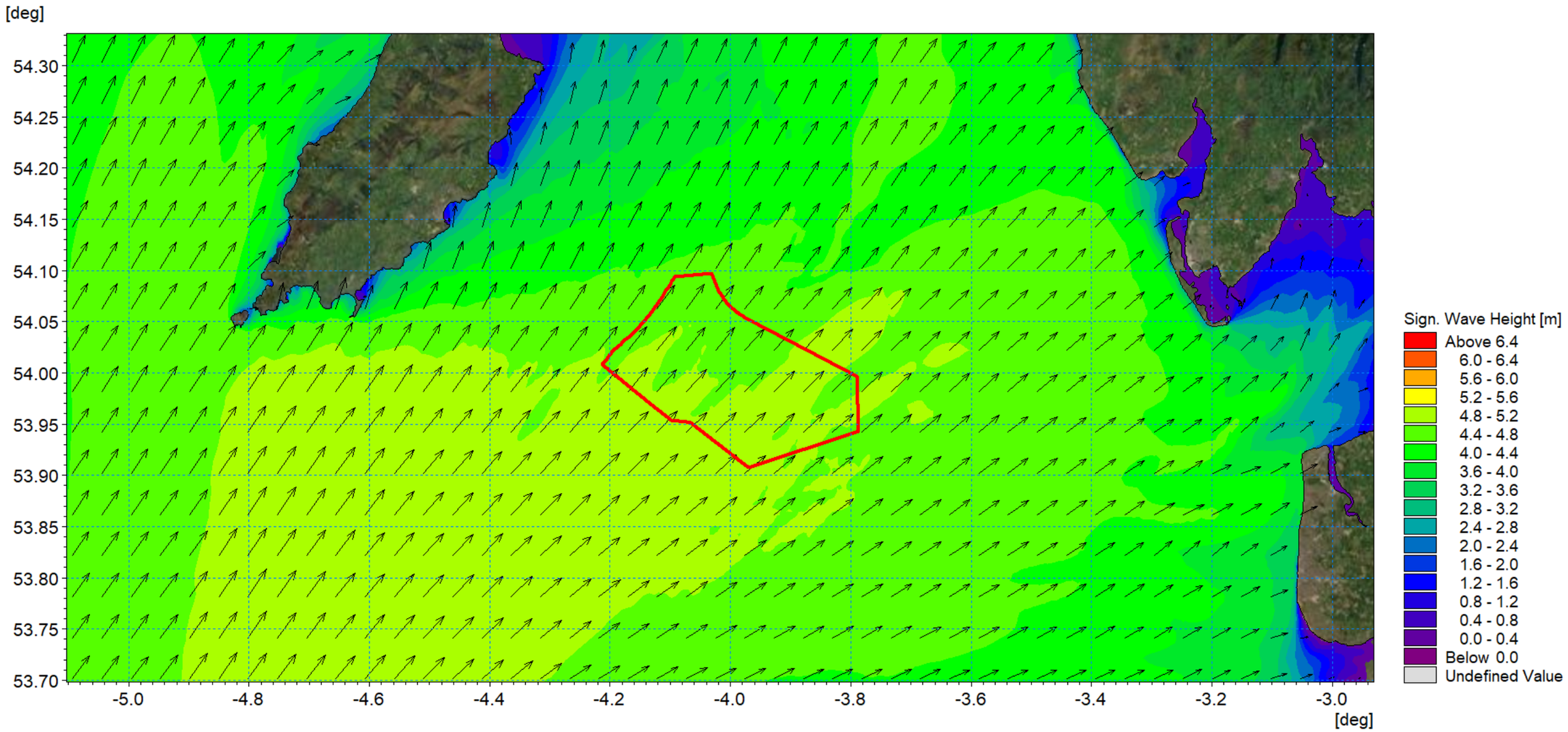

Figure 1.49: Wave climate 1:1 year storm from 240° MHW.

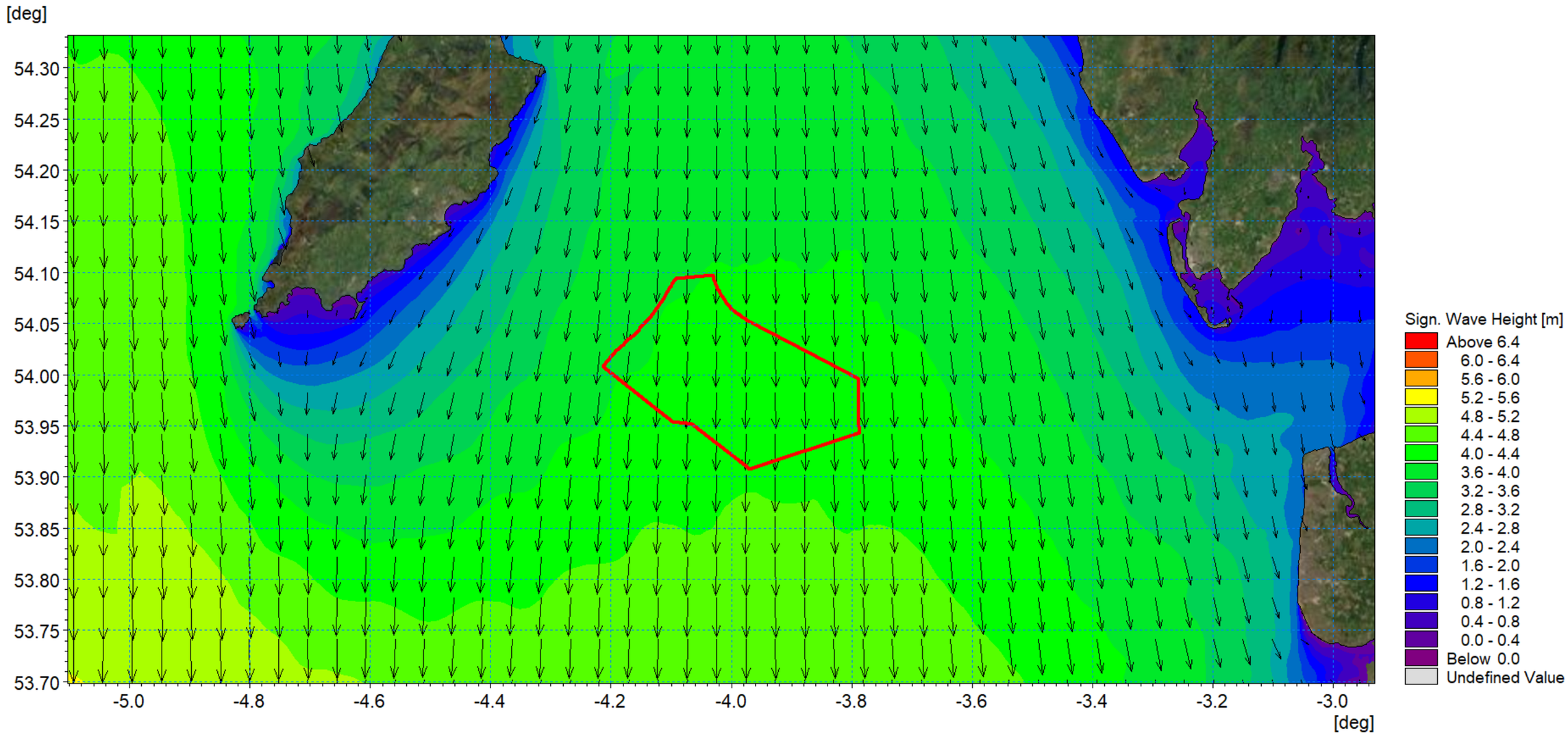

Figure 1.50: Wave climate 1:20 year storm from 000° MHW.

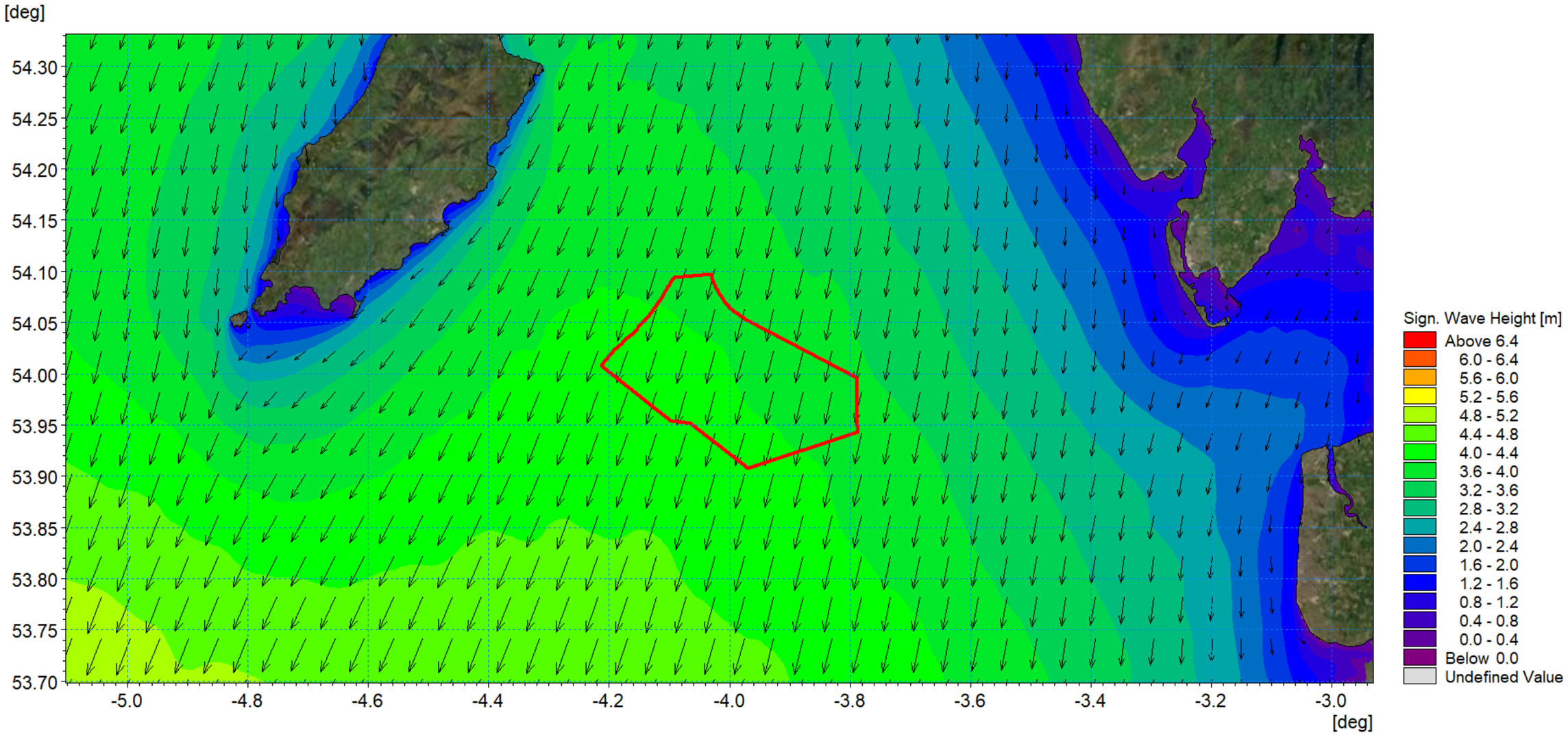

Figure 1.51: Wave climate 1:20 year storm from 030° MHW.

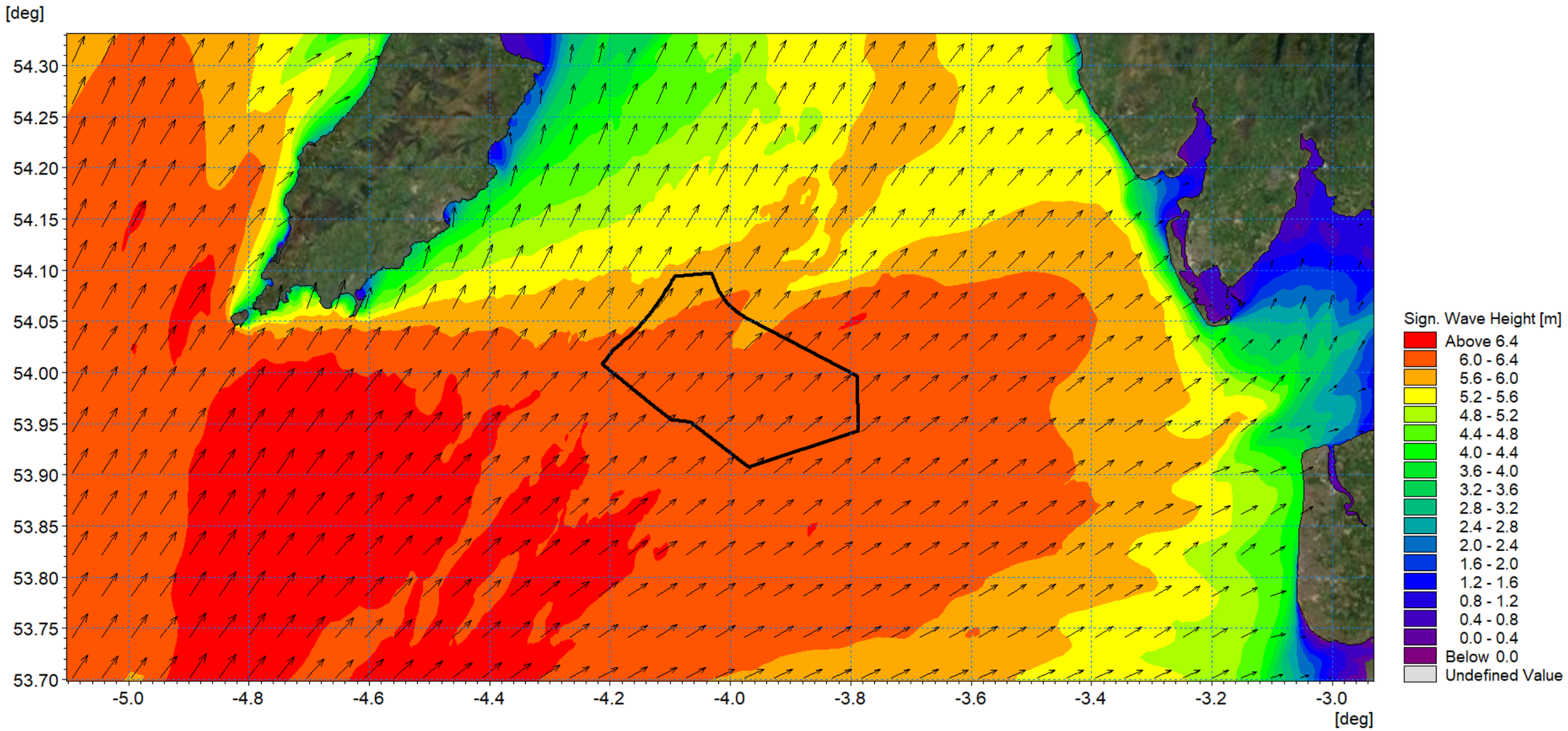

Figure 1.52: Wave climate 1:20 year storm from 240° MHW.

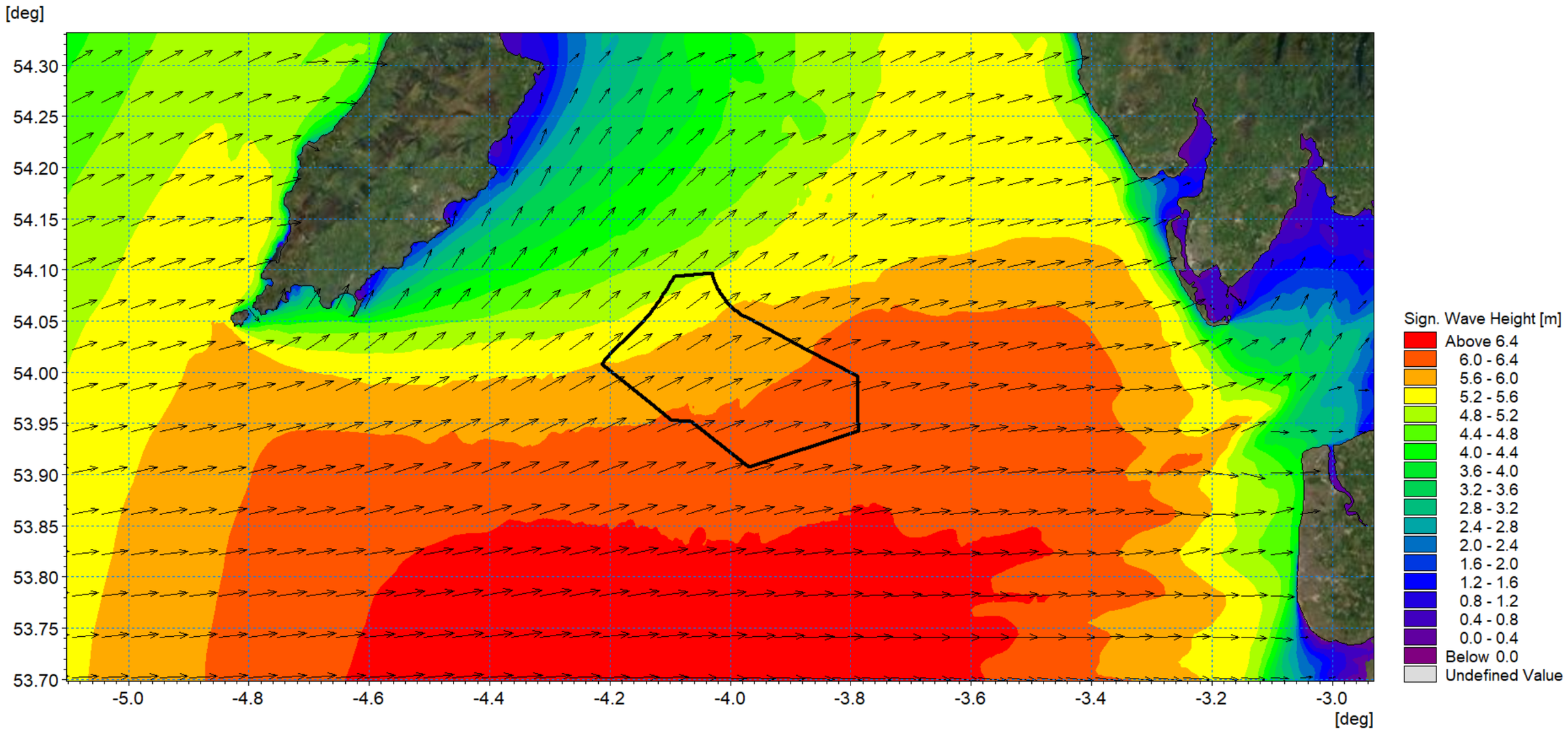

Figure 1.53: Wave climate 1:20 year storm from 270° MHW.

1.6.4 Littoral currents

1.6.4.1 The MIKE suite facilitates the coupling of models. The DA hydrodynamic model, used for the tidal modelling, coupled with the spectral wave model, provides a full wave climate incorporating the impact of water levels and currents on waves and wave breaking. Using this, the littoral currents (i.e. those currents driven by tidal, wave and meteorological forces) were examined.

1.6.4.2 The 1in1 year storm from 210° sector was simulated with the inclusion of spring tides to encompass a wide range of tidal conditions and the resulting flood and ebb currents are presented in Figure 1.54 and Figure 1.55 respectively. These correspond with the (calm) tidal plots presented in Figure 1.31 and Figure 1.32. As expected, the presence of the northeast going waves increase the currents on the flood tide whilst reducing them on the ebb.

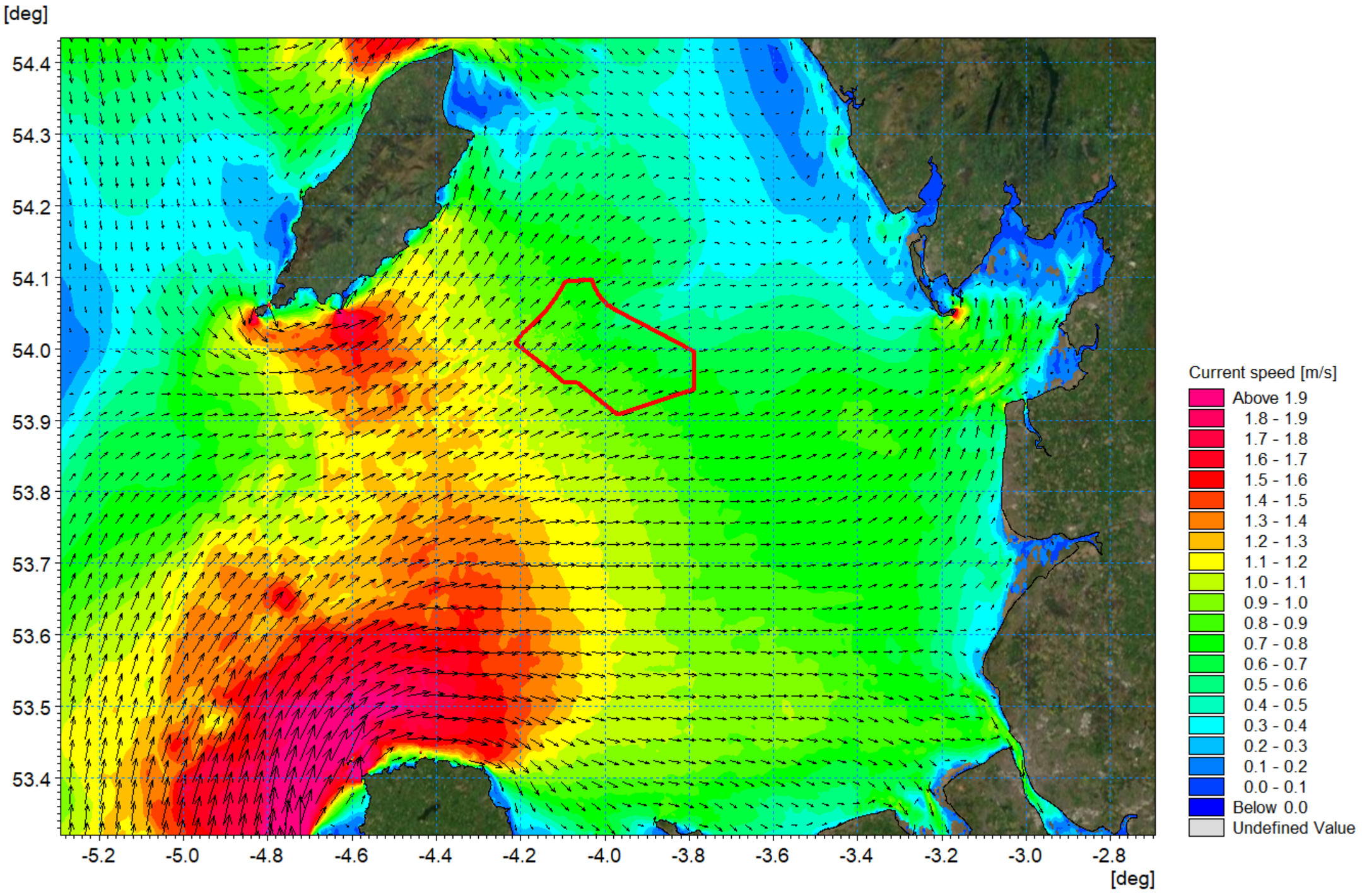

Figure 1.54: Littoral current 1:1 year storm from 210° - Flood Tide.

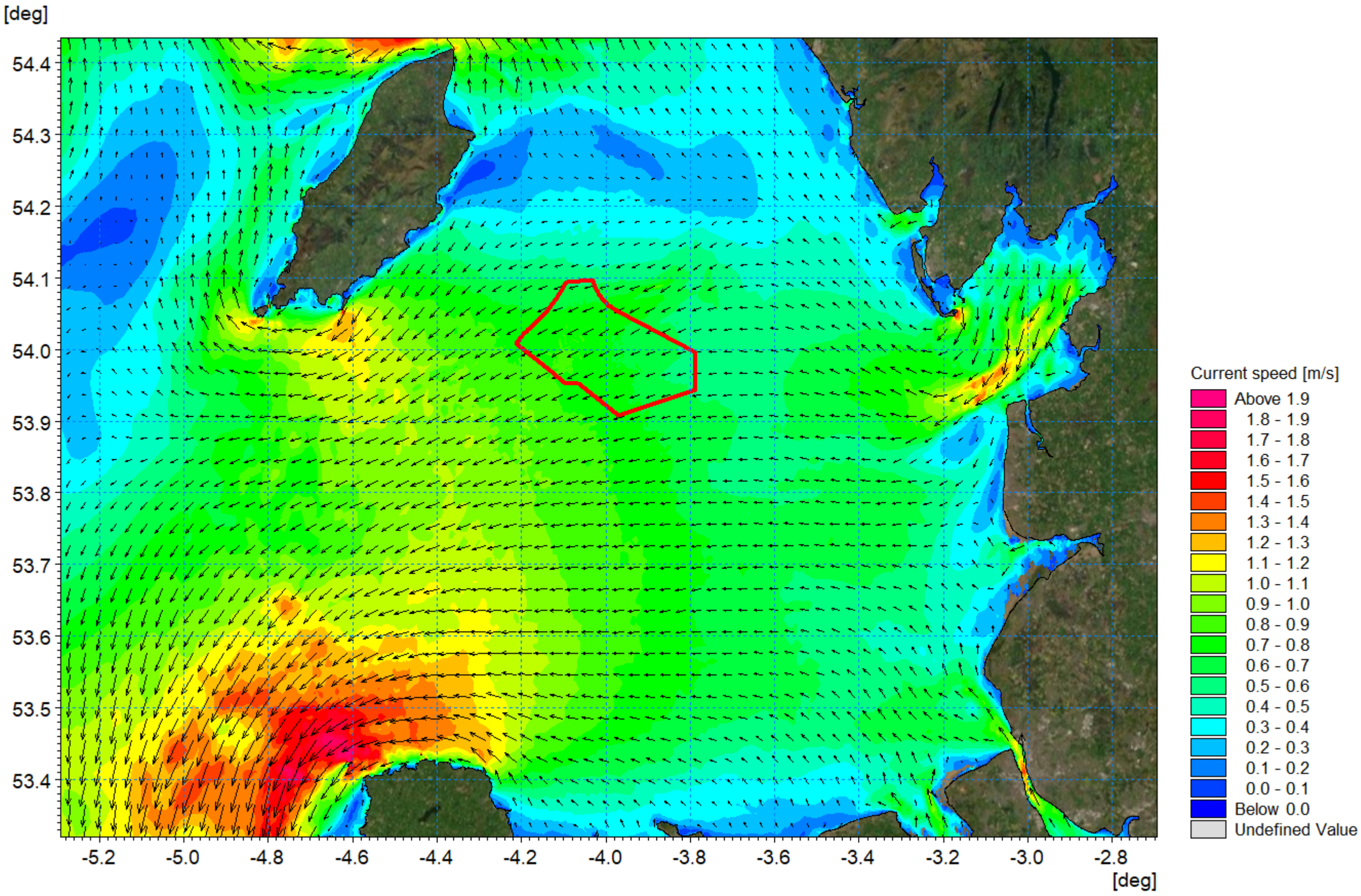

Figure 1.55: Littoral current 1:1 year storm from 210° - Ebb Tide.

1.6.5 Sedimentology and seabed substrate

1.6.5.1 An overview of surficial sediment geology and the seabed features data is presented in this section, based on a range of data sources including both publicly available datasets and interpretation undertaken of the SSS data collected during the recent geophysical surveys (Table 1.4). An understanding of seabed substrate types is required to assess the potential impacts which may arise due to the installation of wind turbines, offshore platform foundations and array cables.

1.6.5.2 The sediment grading properties applied within the modelling for both sediment transport assessment and characterisation of mobilised material during seabed preparation and installation operations was derived from BGS datasets as illustrated in Figure 1.56. These datasets included both generalised Folk classification from borehole logs and detailed particle analysis data.

1.6.5.3 The SSS interpretation defined a range of sediment types within the Morgan Array Area comprising gravelly sand, sand, and gravel. Sandwaves and megaripples are associated with these sediment types. To inform the modelling study seabed sediment information was required beyond the extent of the survey data and the EMODnet Geology database was utilised. The seabed classification shown in Figure 1.57 shows both the datasets.

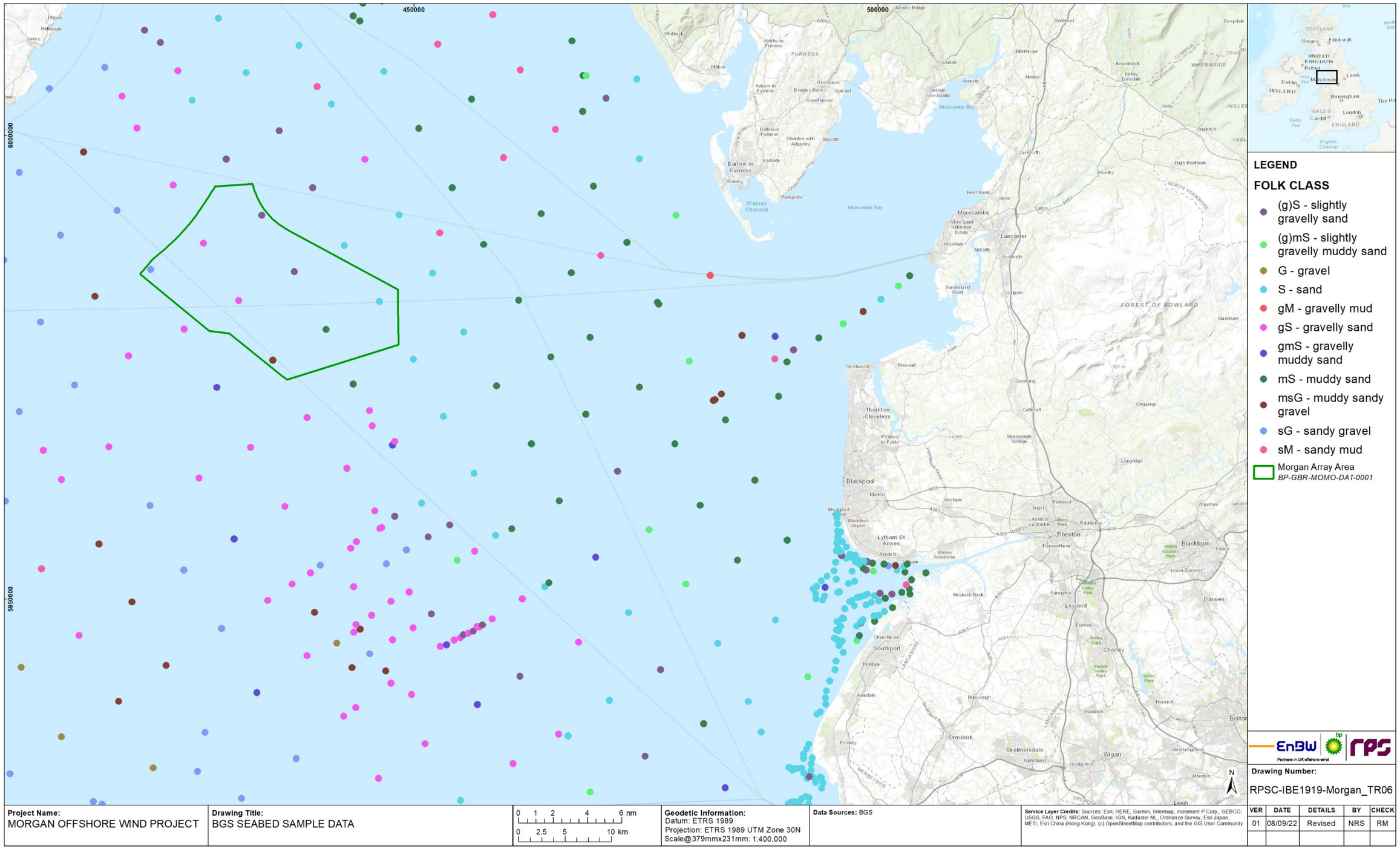

Figure 1.56: Seabed classification BGS.

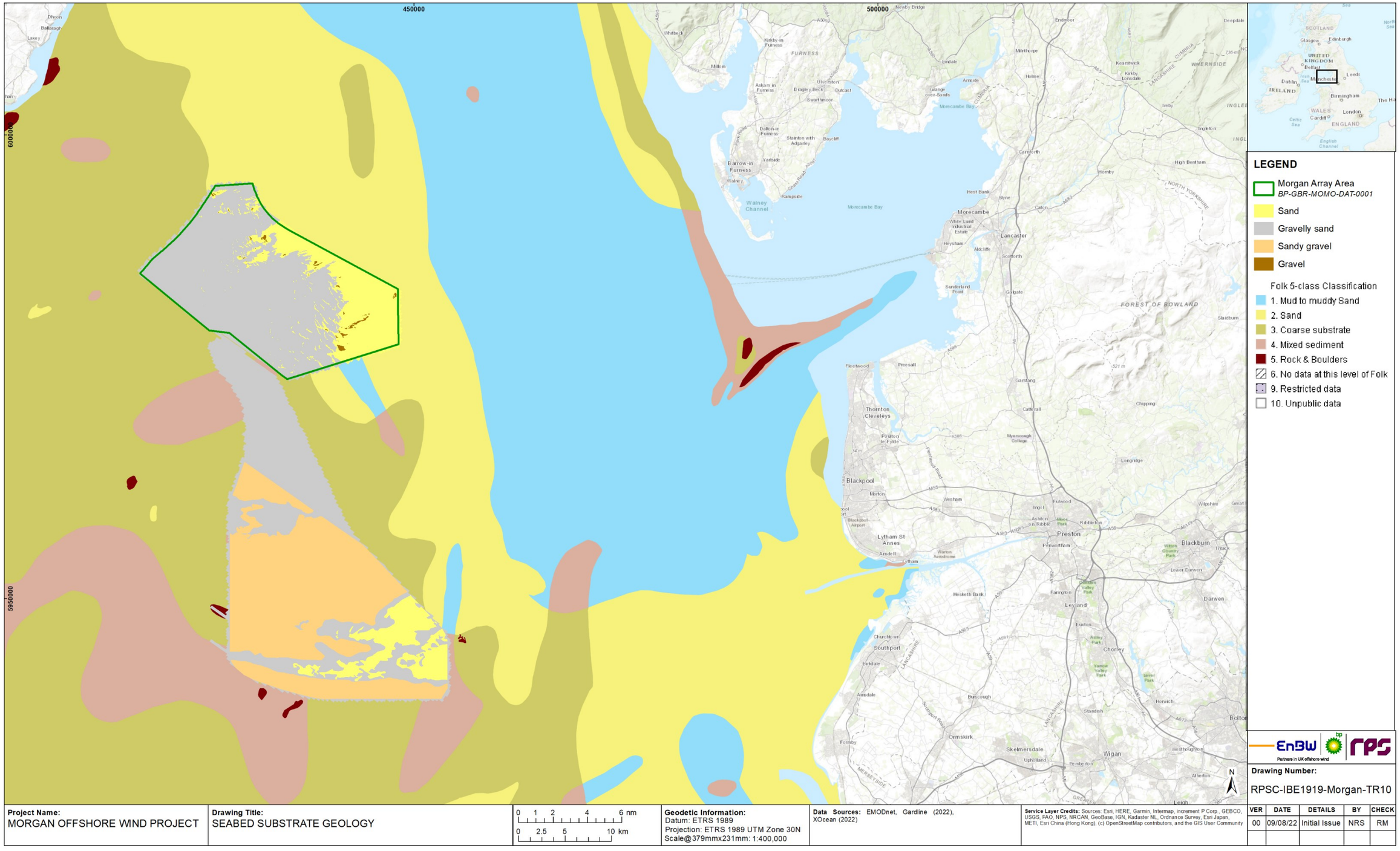

Figure 1.57: Seabed substrate geology EMODnet and SSS.

1.6.6 Sediment transport

1.6.6.1 The MIKE21 ST module enables assessment of bed sediment transport rates for non-cohesive sediment resulting from currents or combined wave-current flows. It was used to determine the sediment transport pattern within the model domain. The model combines inputs from both the hydrodynamic model and, if required, the wave propagation model. It used sediment characterisation provided by the recent survey and EMODnet data as presented in the previous section to determine the sediment transport characteristics. For each region a representative sample from the BGS was used to define the bed sediment and grading.

1.6.6.2 It is noted that for a detailed sediment transport study greater detail of sediment characteristics across the model domain and along the coastline would be required. In the context of a comparative study to identify the impact of the Morgan Generation Assets infrastructure on sediment transport patterns the sediment characteristics identified within the survey and sampling were interpolated to those areas in the EMODnet data with similar sediment classifications.

1.6.6.3 The model domain was set up with a layer of mobile bed sediment. In areas where sediment is present an initial layer depth was set to 3m and tapered to zero in the areas of rocky outcrops to ensure that sediment was not exhausted during the simulated events. Sediment transport was examined relating to spring tidal conditions over the course of two tidal cycles (one day) to provide a ‘snap-shot’ for comparison. The simulation included a period for the hydrodynamics to stabilise and develop across the domain prior to sediment transport being enabled (i.e. a “warm-up” period).

1.6.6.4 Three aspects were examined:

- Residual current, which is the net flow over the course of the tidal cycle. This is effectively the driving force of the sediment transport
- Potential sediment transport over this period
- Potential sediment transport during flood and ebb tides. This provides information for a ‘snap-shot’ in time to enable the process to be illustrated.

1.6.6.5 The residual current is presented in Figure 1.58 and it should be noted that a log scale has been used to cover the range of residual current speeds encountered. The current vectors indicate residual flow into the east Irish Sea from the north and west which correlates with this region being a sediment sink. There are strong circulatory currents where tidal flows interact with headlands and embayments.

1.6.6.6 An indication of transport rate is shown in Figure 1.59, again using a log scale palette as the values within the offshore regions are several orders of magnitude smaller than those along the coastline. The greatest transport rates are seen in areas where finer sand fractions are present and in estuaries and at headland where tidal currents are strongest. The mechanism is more clearly illustrated in Figure 1.60 and Figure 1.61 for flood and ebb tides respectively. It is evident that transport rates are highest during the dominant flood tide and the region is a sediment sink.

1.6.6.7 By way of completeness, and for use in the comparative study, residual currents relating to the 1in1 year return period storm approaching from 210º are also presented, Figure 1.62. As anticipated, the littoral currents and dominant flood tide significantly increase easterly residual currents particularly along the Welsh coastline. This in turn would result in increased sediment transport rates during storm conditions.

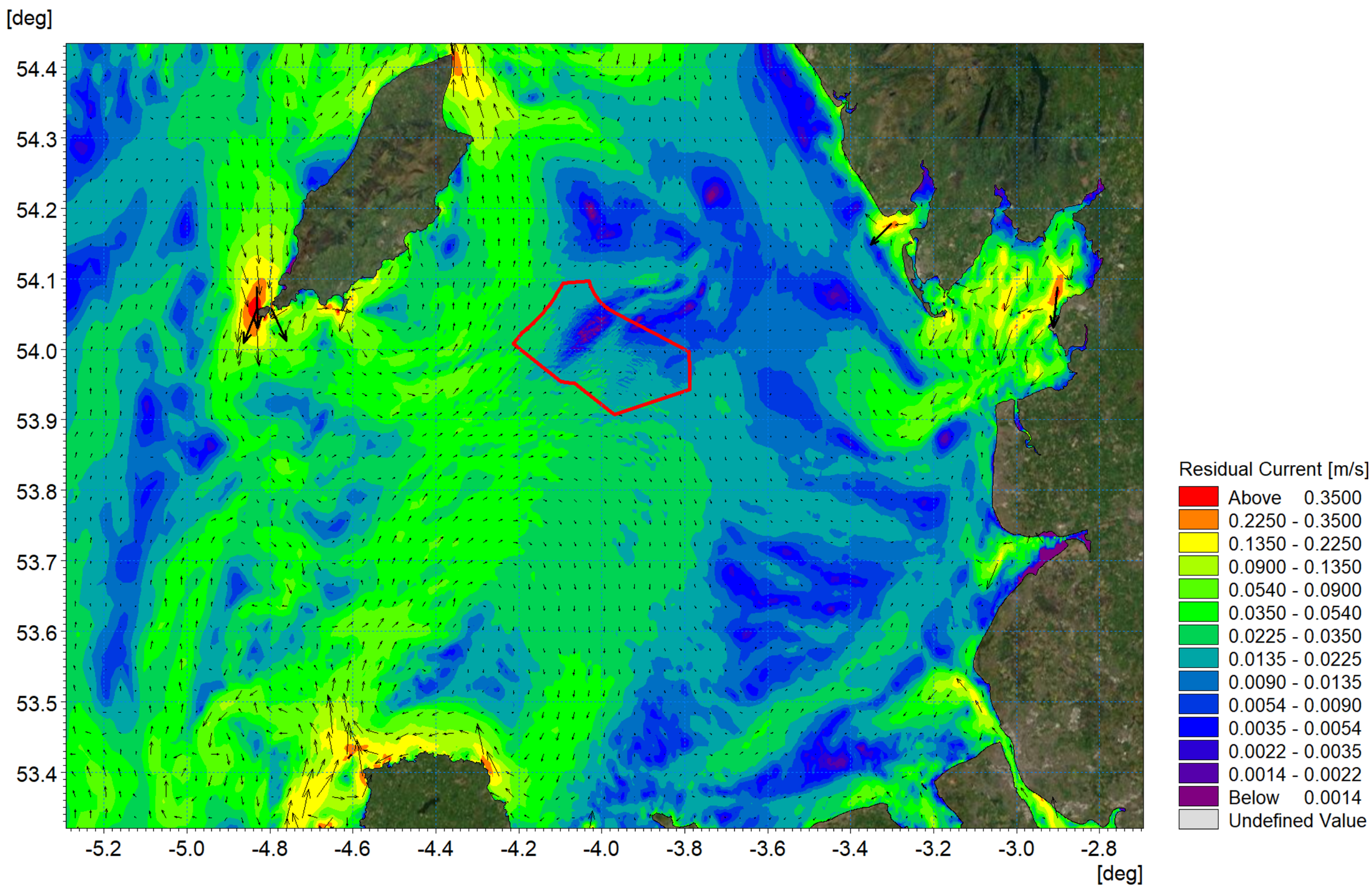

Figure 1.58: Residual current spring tide.

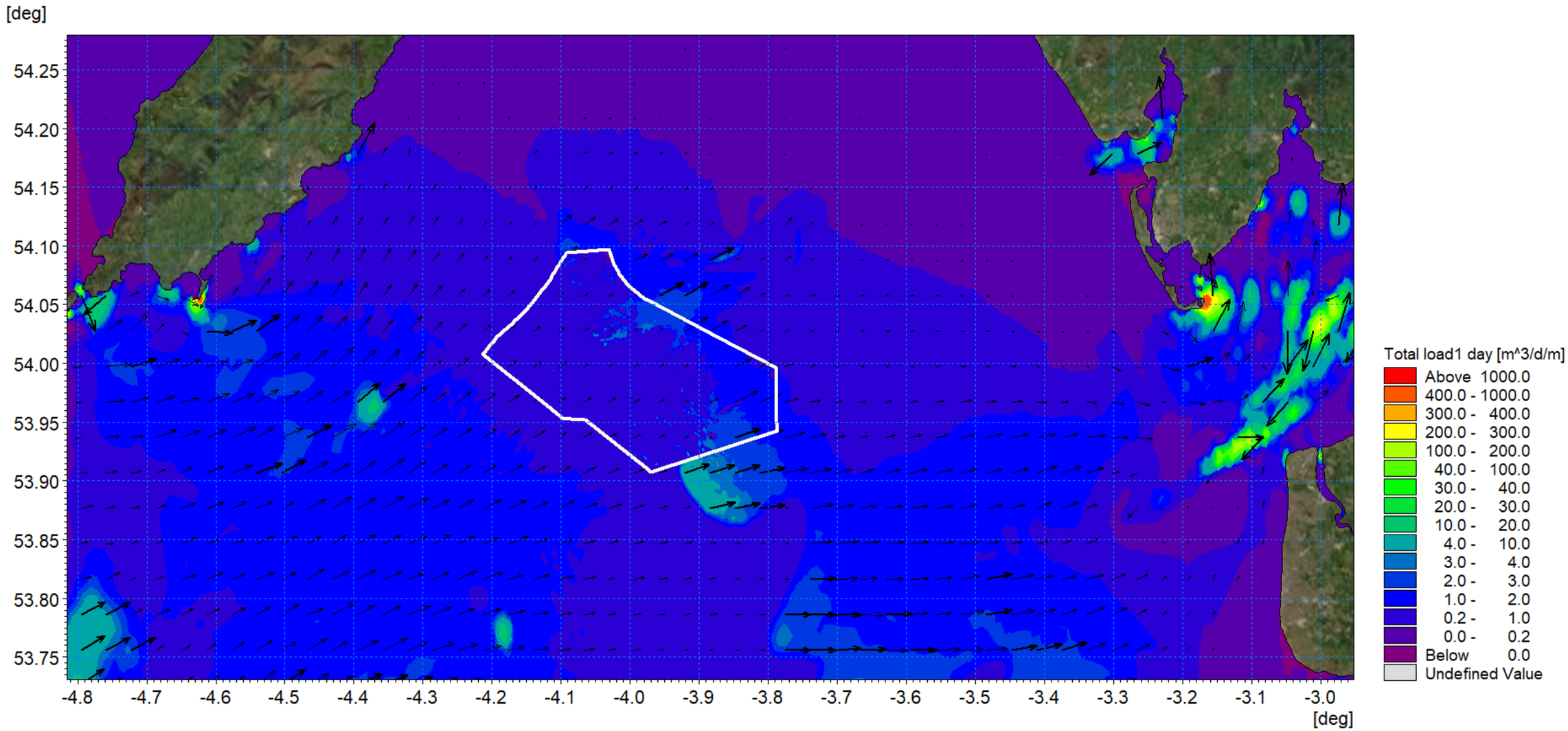

Figure 1.59: Potential sediment transport over the course of 1 day (two tide cycles).

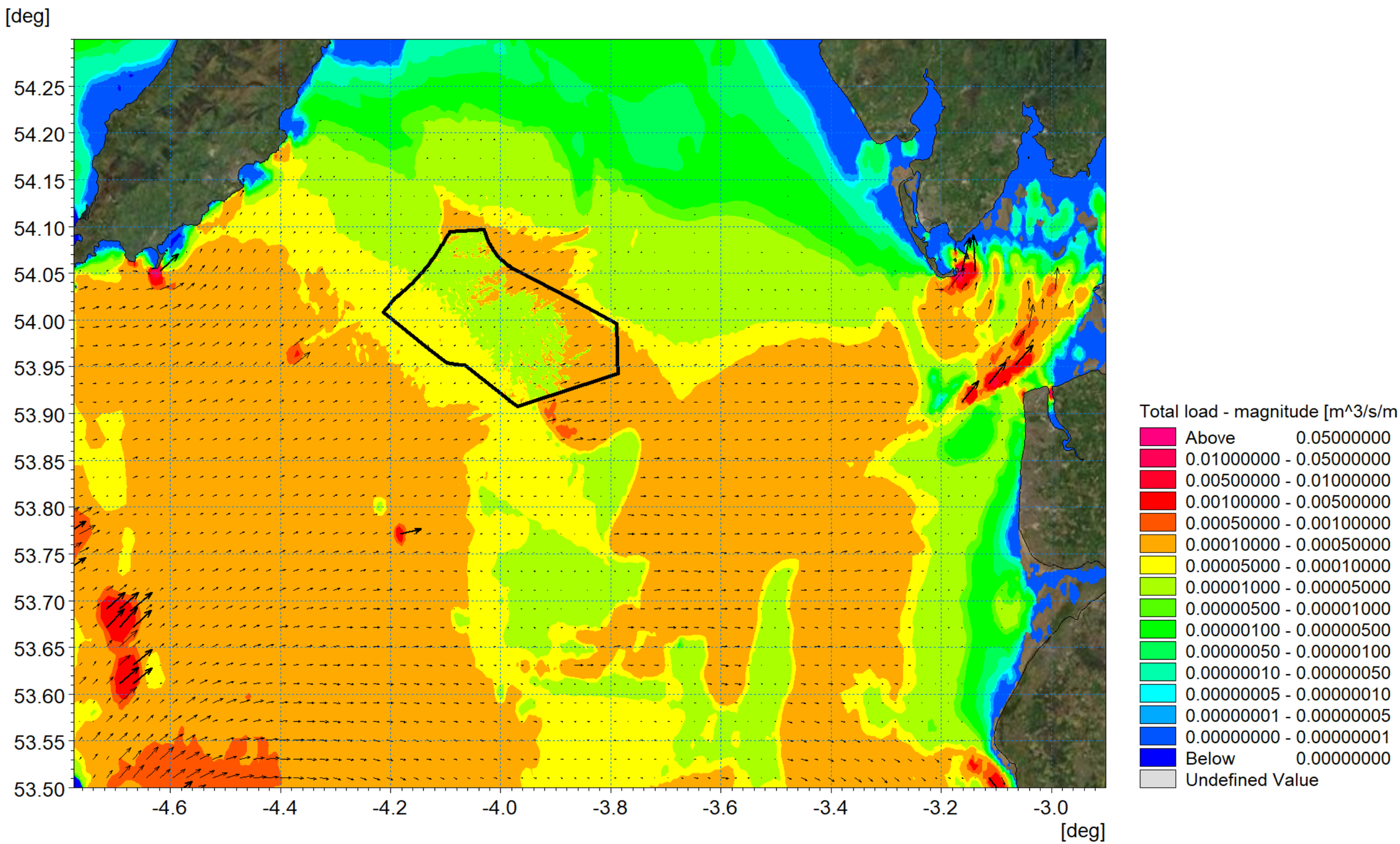

Figure 1.60: Sediment transport – flood tide.

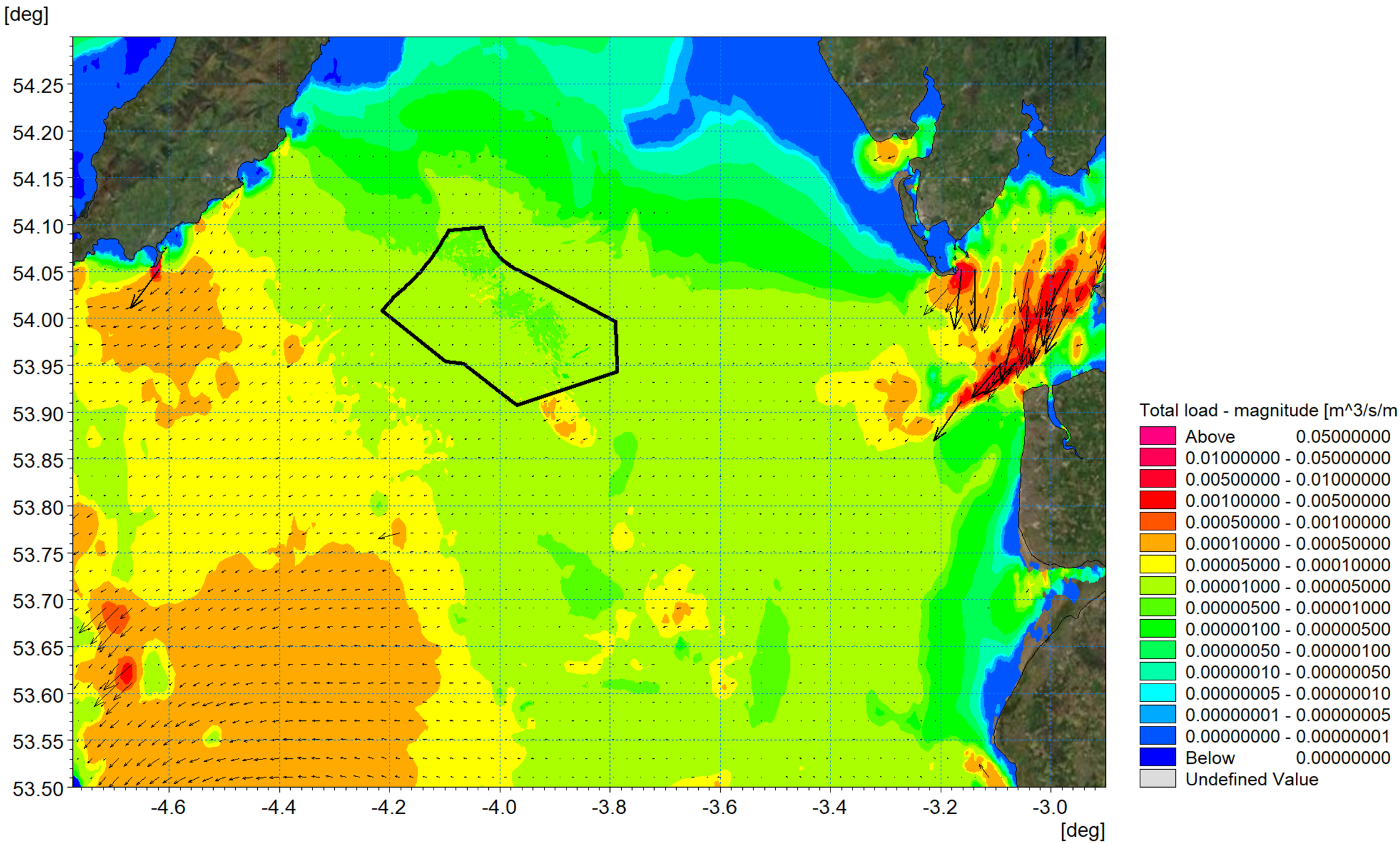

Figure 1.61: Sediment transport – ebb tide.

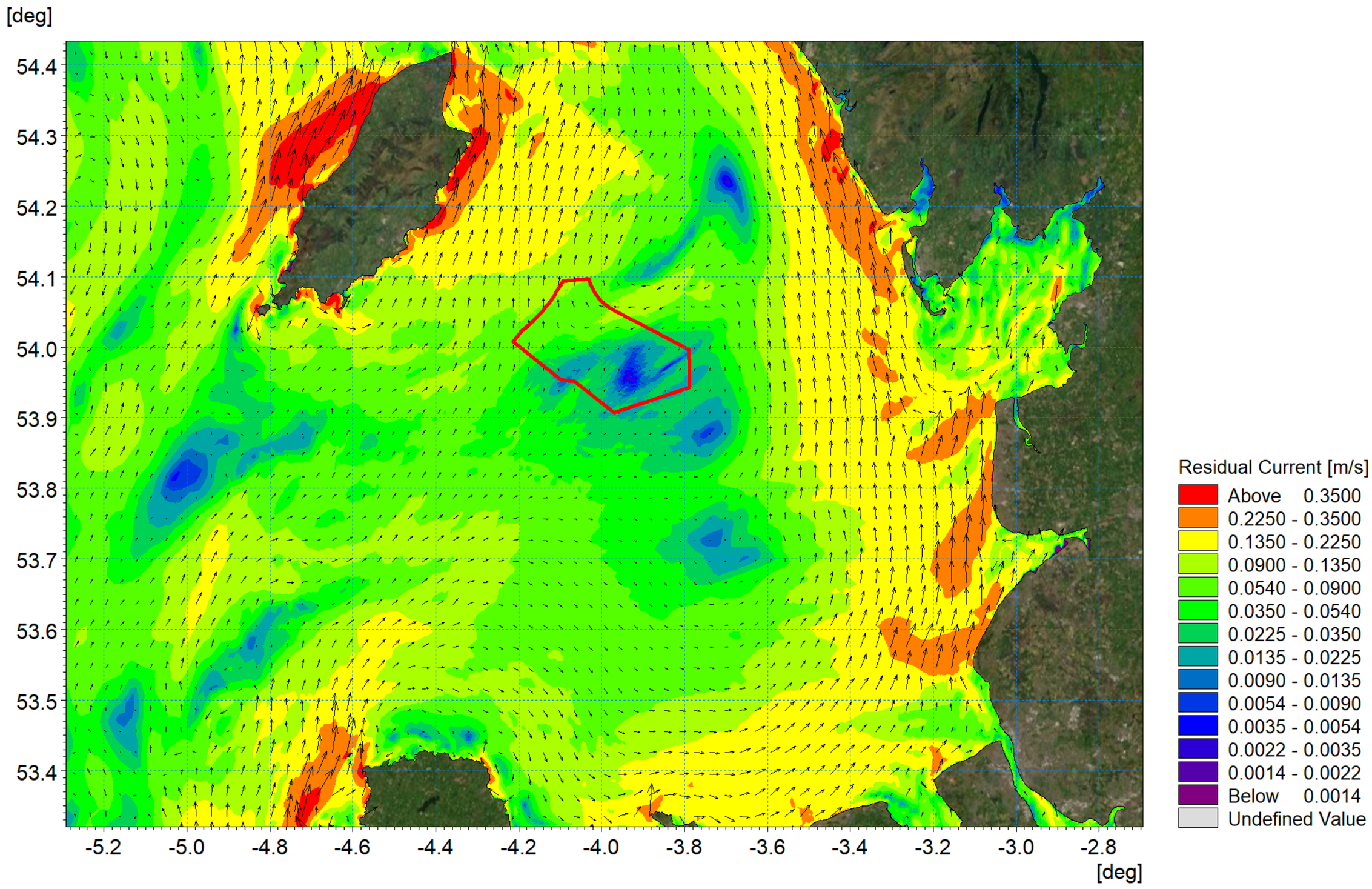

Figure 1.62: Residual current spring tide with 1:1 year storm from 210º.

1.6.7 Suspended sediments

1.6.7.1 The principal mechanisms governing SSC in the water column are tidal currents, with fluctuations observed across the spring-neap cycle and across the different tidal stages (high water, peak ebb, low water, peak flood) observed throughout both datasets. It is key to note that SSCs can also be temporarily elevated by wave-driven currents during storm events. During high-energy storm events, levels of SSC can rise significantly, both near bed and extending into the water column. Following storm events, SSC levels will gradually decrease to baseline conditions, regulated by the ambient regional tidal regimes. The seasonal nature and frequency of storm events supports a broadly seasonal pattern for SSC levels.

1.6.7.2 Based on the data recorded within the Morgan metocean study site, the average near bed turbidity associated is circa 2mg/l. As shown in Figure 1.63, spikes in near surface turbidity correspond with increases in the significant wave height during storm conditions. The data is presented for the November 2021 to March 2022 period with peaks reaching circa 20mg/l.

1.6.7.3 For more generalised conditions the Cefas Climatology Report 2016 (Cefas, 2016) and associated dataset provides the spatial distribution of average non-algal Suspended Particulate Matter (SPM) for the majority of the UK Continental Shelf (UKCS). Between 1998 and 2005, the greatest plumes are associated with large rivers such as those that discharge into the Thames Estuary, The Wash and Liverpool Bay, which show mean values of SPM above 30mg/l. Based on the data provided within the Morgan metocean site, the average near bed SPM associated with close proximity to the Morgan Generation Assets has been estimated as circa 2mg/l from November 2021 to March 2022 period as illustrated in Figure 1.63. The levels of SPM reported by CEFAS between 1998 to 2005 of approximately 0.9mg/l to 3mg/l are similar to the values recorded at Morgan. Higher levels of SPM are experienced more commonly in the winter months; however, due to the tidal influence, even during summer months the levels may become elevated. As shown in Figure 1.63 spikes in near surface turbidity correspond with increases in the significant wave height.

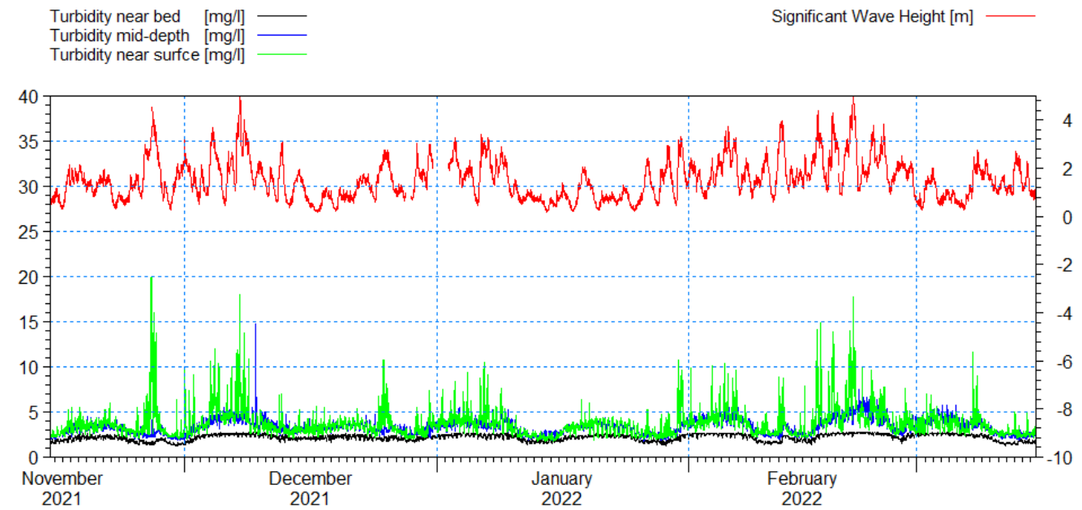

Figure 1.63: Turbidity levels from the Morgan metocean site.

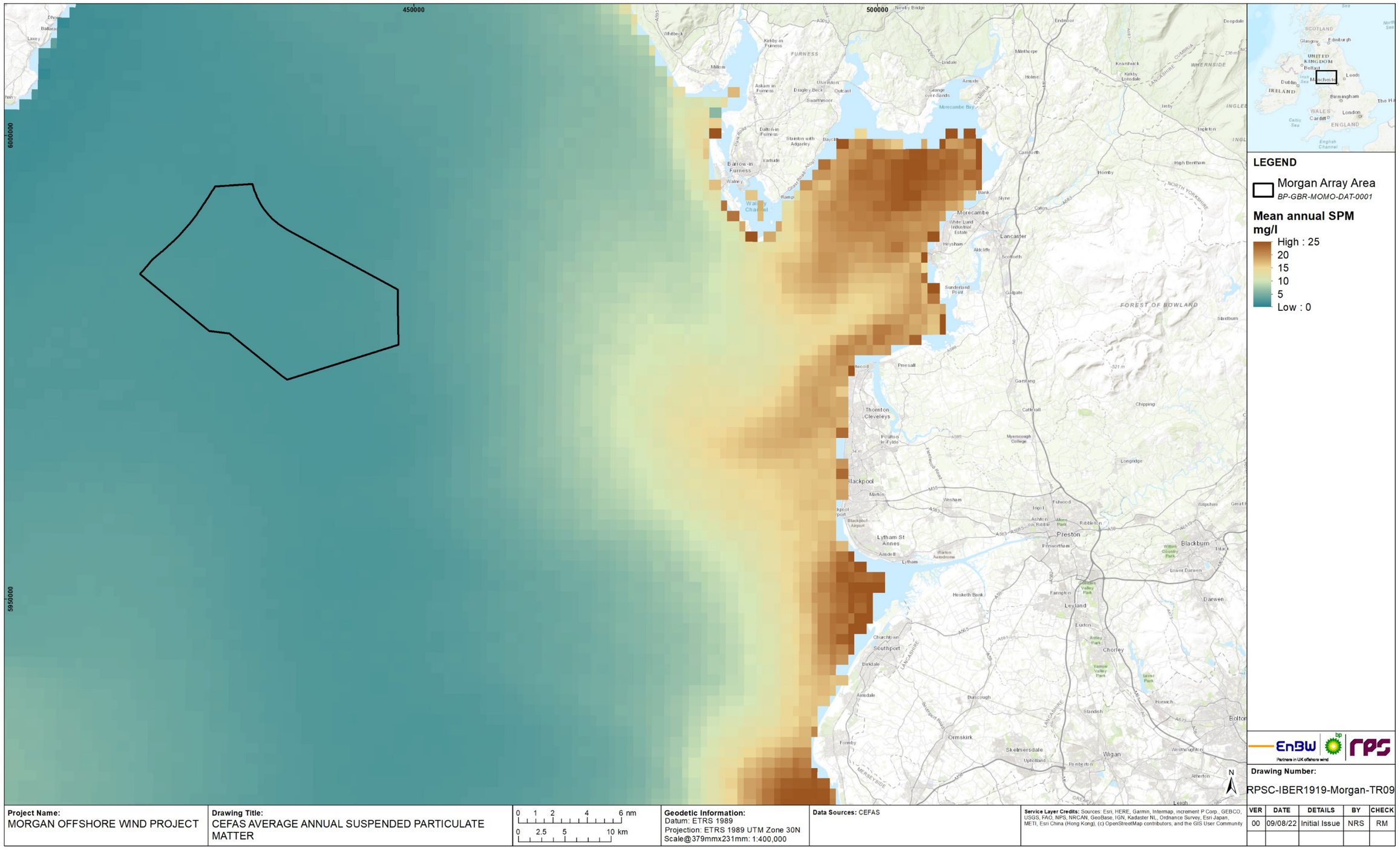

Figure 1.64: Distribution of average non-algal SPM – CEFAS.

1.7 Potential environmental changes

1.7.1 Overview

1.7.1.1 The potential changes to the baseline hydrographic conditions as a result of the installation and presence of the Morgan Generation Assets are quantified in the following sections. These changes relate to the presence of the infrastructure within the water column and seabed and are therefore associated with wind turbine legs along with cable and scour protection. The potential changes to sea state and sediment transport regimes were established by repeating the modelling undertaken in the previous section with the inclusion of the Morgan Generation Assets. The modelling was undertaken using an indicative layout which included the following changes in line with the indicative Maximum Design Scenario (MDS) for physical processes:

- Leg structures 5m in diameter relating to 68 wind turbines each comprising four legs
- Scour protection 56m diameter and 2.5m in height associated with 16m suction bucket foundations for each wind turbine leg
- Leg structures 3m in diameter relating to 4 OSPs each comprising three legs
- Scour protection 49m diameter and 2.5m in height associated with 14m suction bucket foundations for each OSP leg
- Inter-array cable protection to a height of 3m and 5m width with cable crossings 4m in height, 32m width and 60m length
- Interconnector cable protection to a height of 3m and 10m width with cable crossings 3m in height, 20m width and 50m length.

1.7.1.2 It should be noted that the scale of the model mesh meant that the general flow and sediment patterns around the structures could be observed on the wider scale. The detailed impact of secondary scour is localised, site and design specific in nature. The modelling included the provision of scour protection as defined in the project description presented in volume 1, chapter 3: Project description of the Preliminary Environmental Information Report (PEIR) and a detailed assessment of the effectiveness of the scour protection proposed at each foundation location was not undertaken as this was not the purpose of the computational modelling. The scour protection does not have implications on the global scale and is restricted to reducing sediment erosion in the vicinity of the foundations; there would be larger implications if scour protection were not provided (Whitehouse *et al.*, 2006).

1.7.1.3 The methodology implemented for the modelling used parameters selected from the project description outlined in volume 1, chapter 3: Project description of the PEIR, to ascertain the most influential and likely scenario for each physical process aspect under examination. The indicative layout used within the modelling study is presented in Figure 1.65. The layout applied cable protection in regions where trenching to 3m depth was unlikely (i.e. in the vicinity of rocky outcrops) and where inter-array cable connect with generating assets.

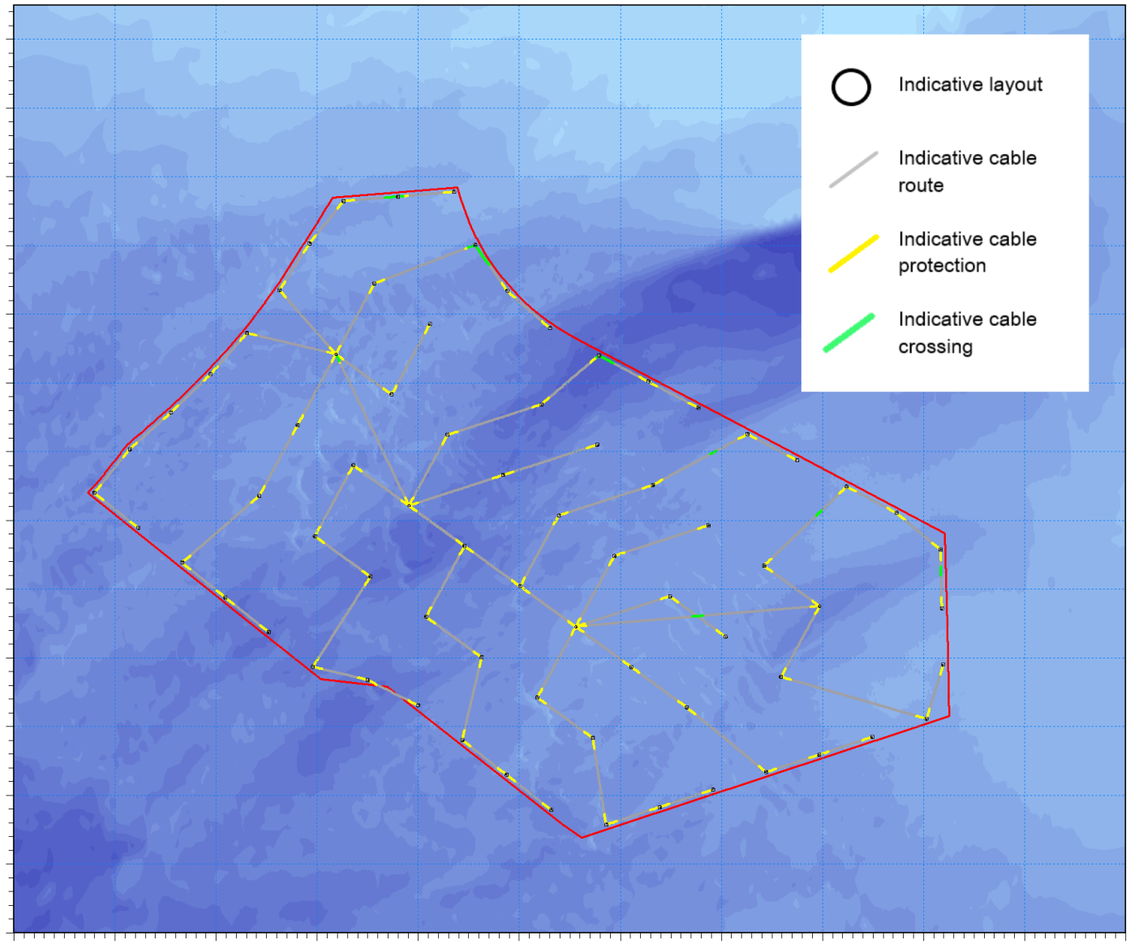

Figure 1.65: Modelled array and trenching route indicative layout.

1.7.2 Post-construction hydrography

Tidal flow

1.7.2.1 The hydrodynamic simulations were repeated with the addition of infrastructure as outlined in the previous section. The bathymetry was also amended to take account the scour and cable protection. The following figures show the same mid flood and mid ebb steps from the simulation as were presented in Figure 1.31 and Figure 1.32 respectively, but with the Morgan Generation Assets foundation and structures in place. Due to the limited magnitude of the changes, difference plots have also been provided. These are the proposed minus the baseline condition, therefore increases in current speed will be positive. The same procedure for calculating differences and plotting figures has been implemented throughout this report.

1.7.2.2 Figure 1.66 shows the post-construction flood tide flow patterns with Figure 1.67 showing the changes, and as the changes are limited to the vicinity of the development

a more focused plot is provided in Figure 1.68. In the difference figures a log scale has been introduced to accentuate the values for clarity. Similarly, Figure 1.69, Figure 1.70 and Figure 1.71 show the same information for the ebb tide. During peak current speed the flow is redirected in the immediate vicinity of the structures and cable protection. The variation is a maximum of 4cm/s in the immediate vicinity of the structure which constitutes less than 3% of the peak flows. This reduces significantly with increased distance from each structure with changes being significantly smaller in the areas where cable protection is present, within 500m of the installation changes are <2mm/s which would be indiscernible for baseline conditions.

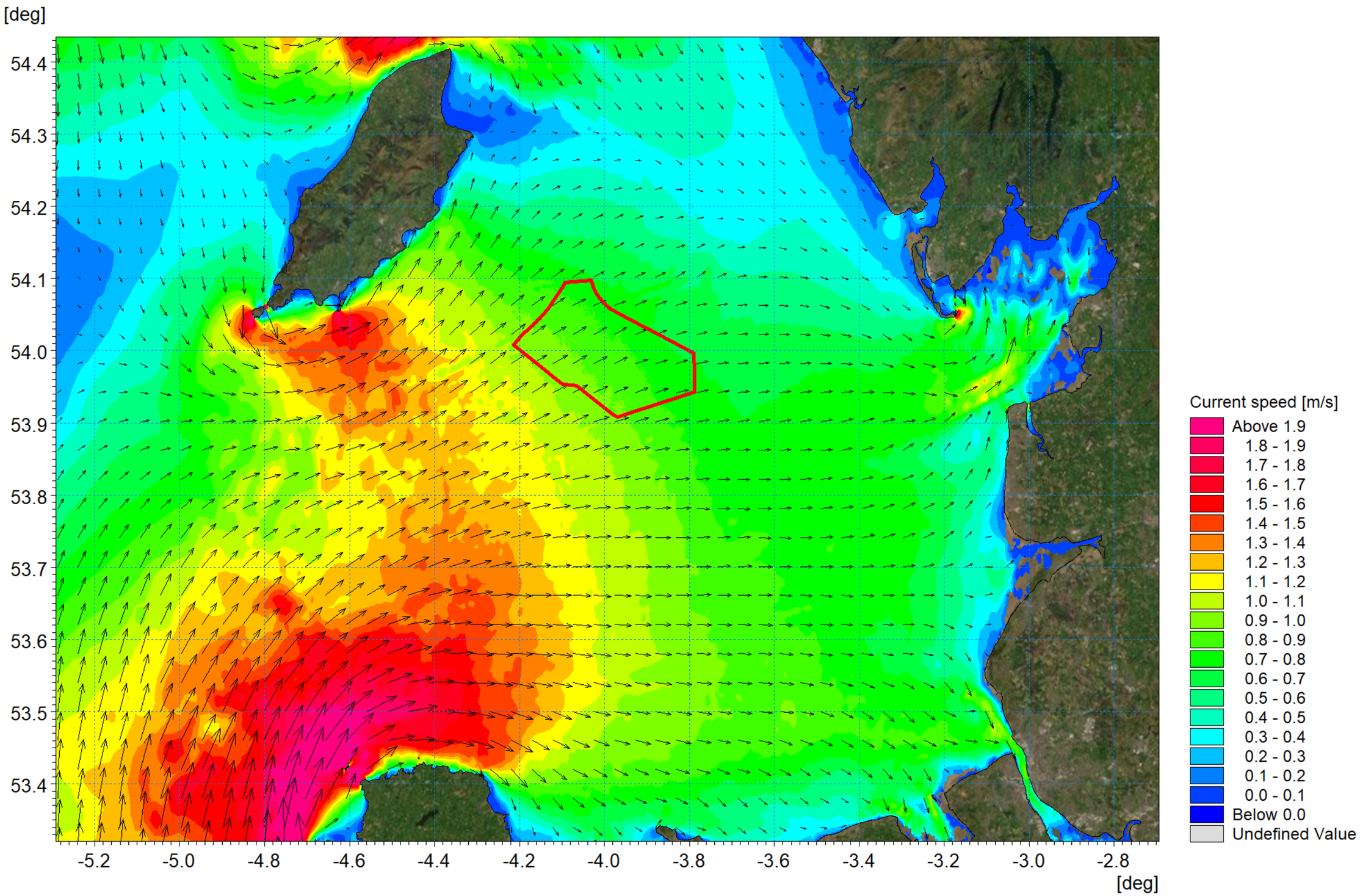

Figure 1.66: Post-construction tidal flow pattern – flood tide.

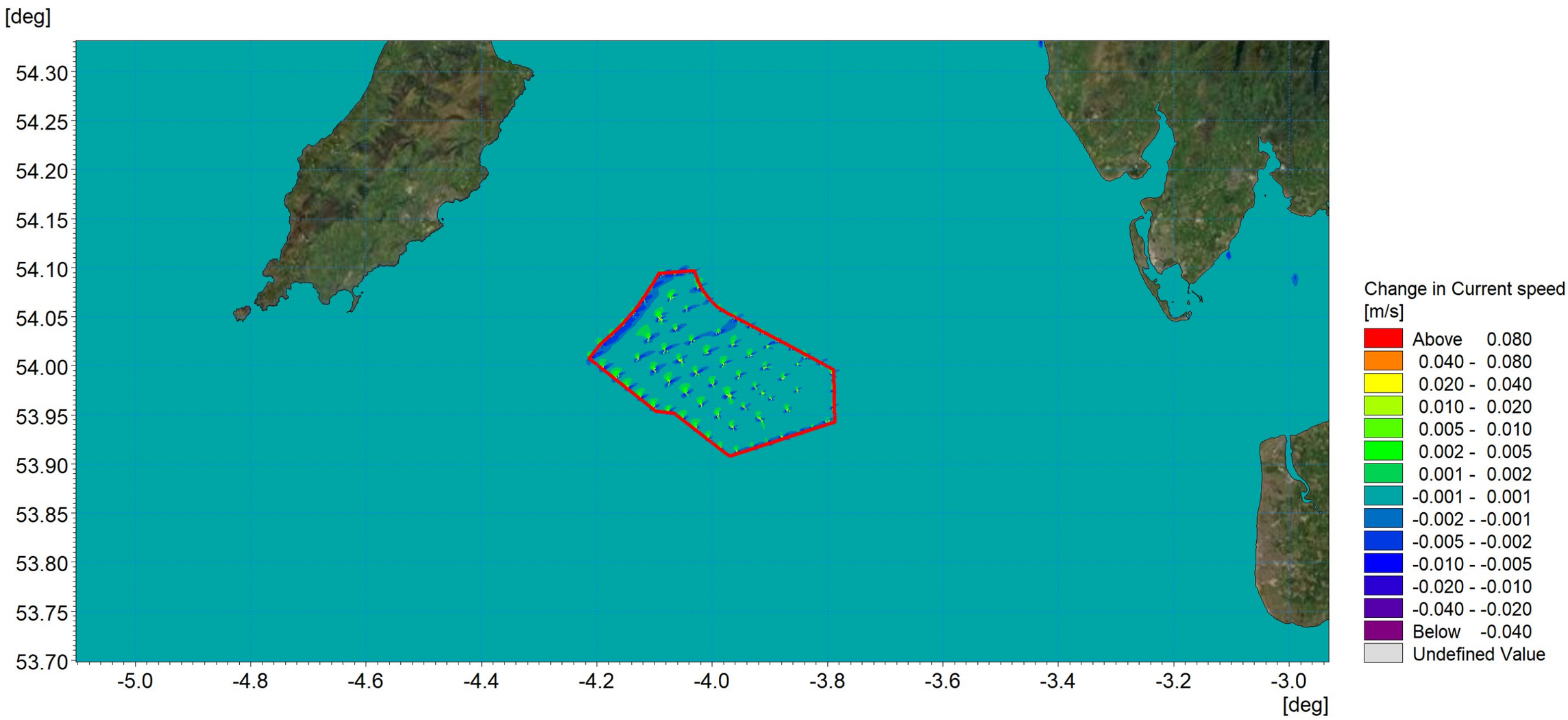

Figure 1.67: Change in tidal flow (post-construction minus baseline) – flood tide.

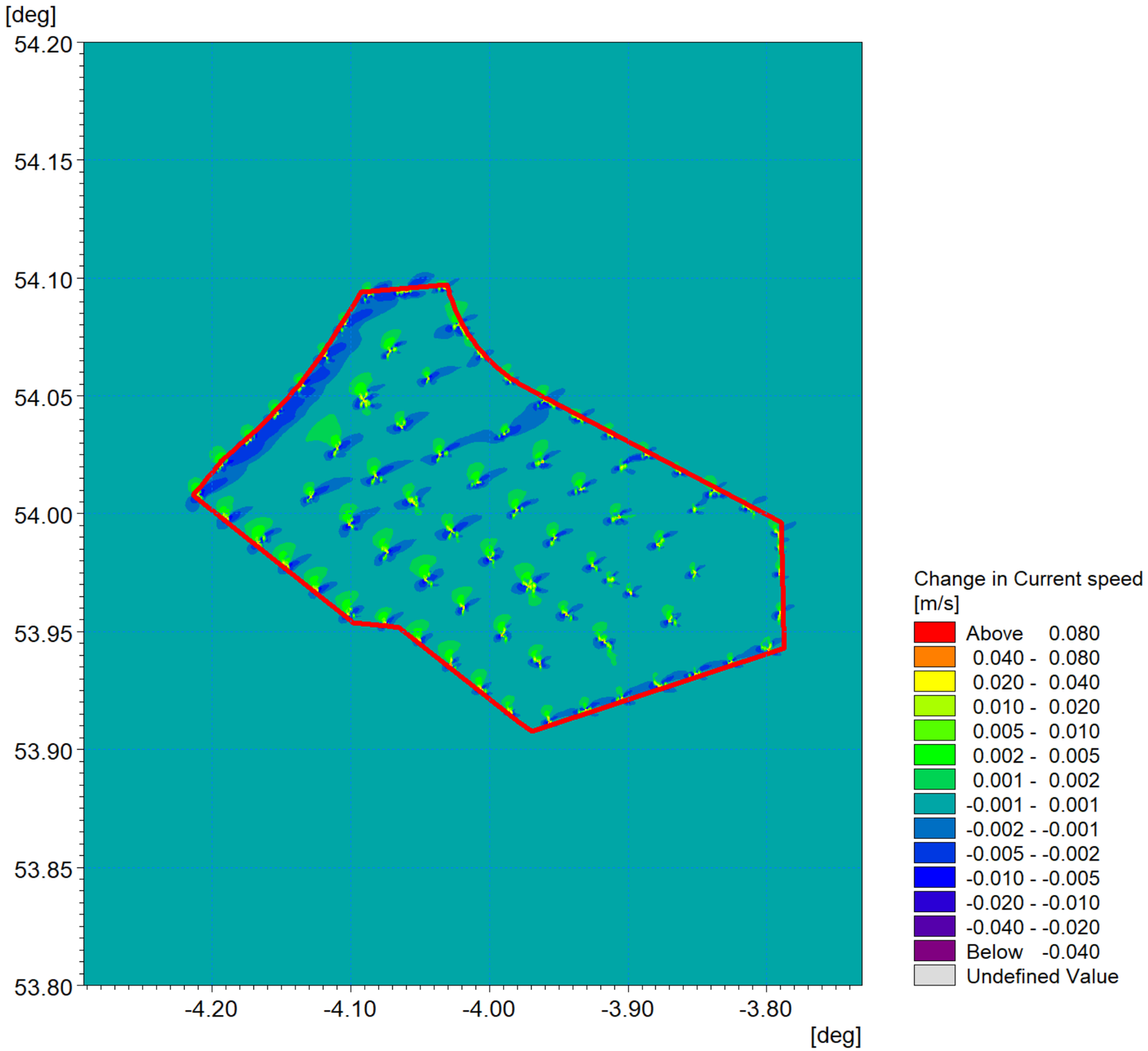

Figure 1.68: Change in tidal flow (post-construction minus baseline) Morgan Array Area – flood tide detail view.

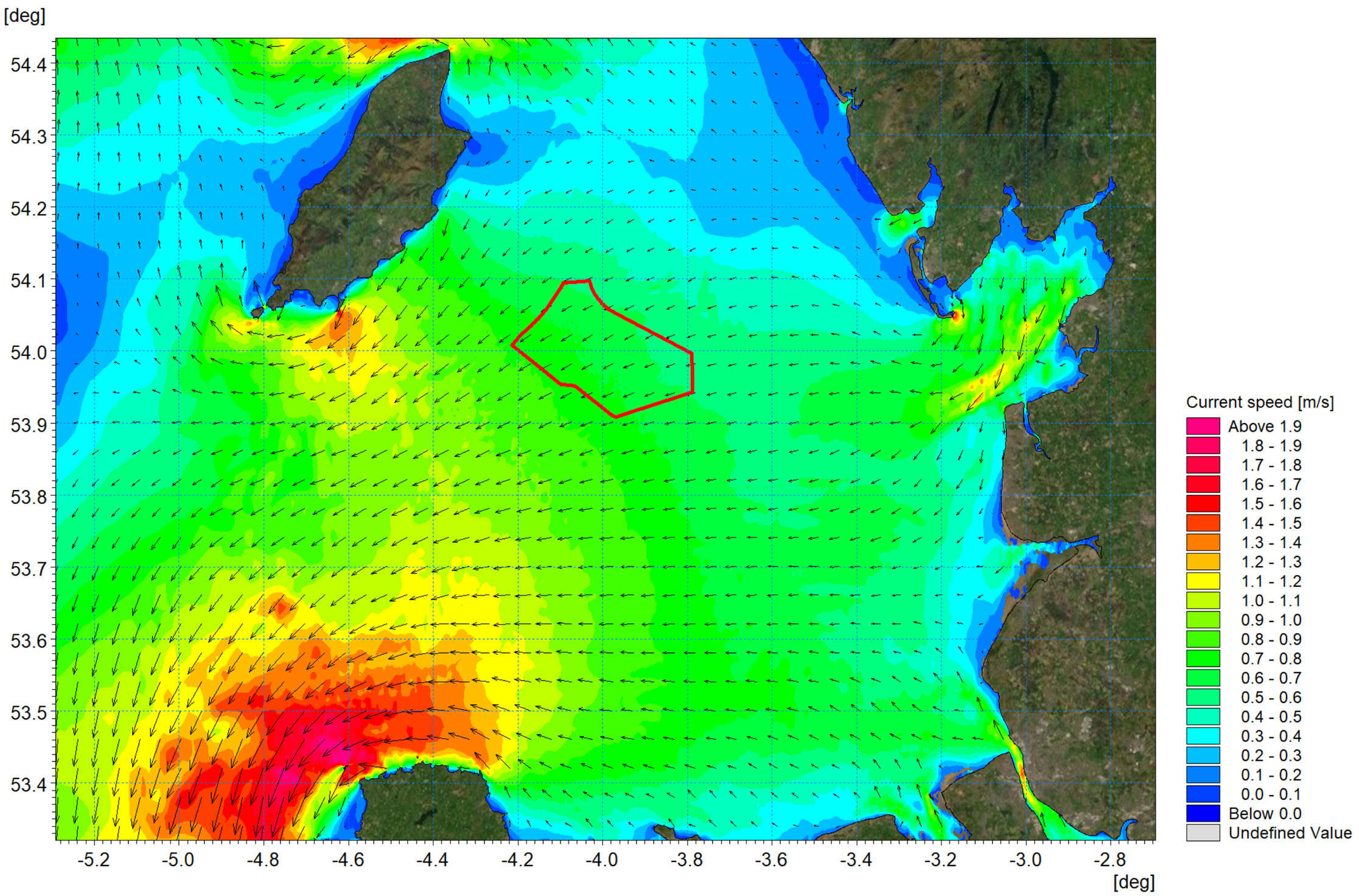

Figure 1.69: Post-construction tidal flow pattern – ebb tide.

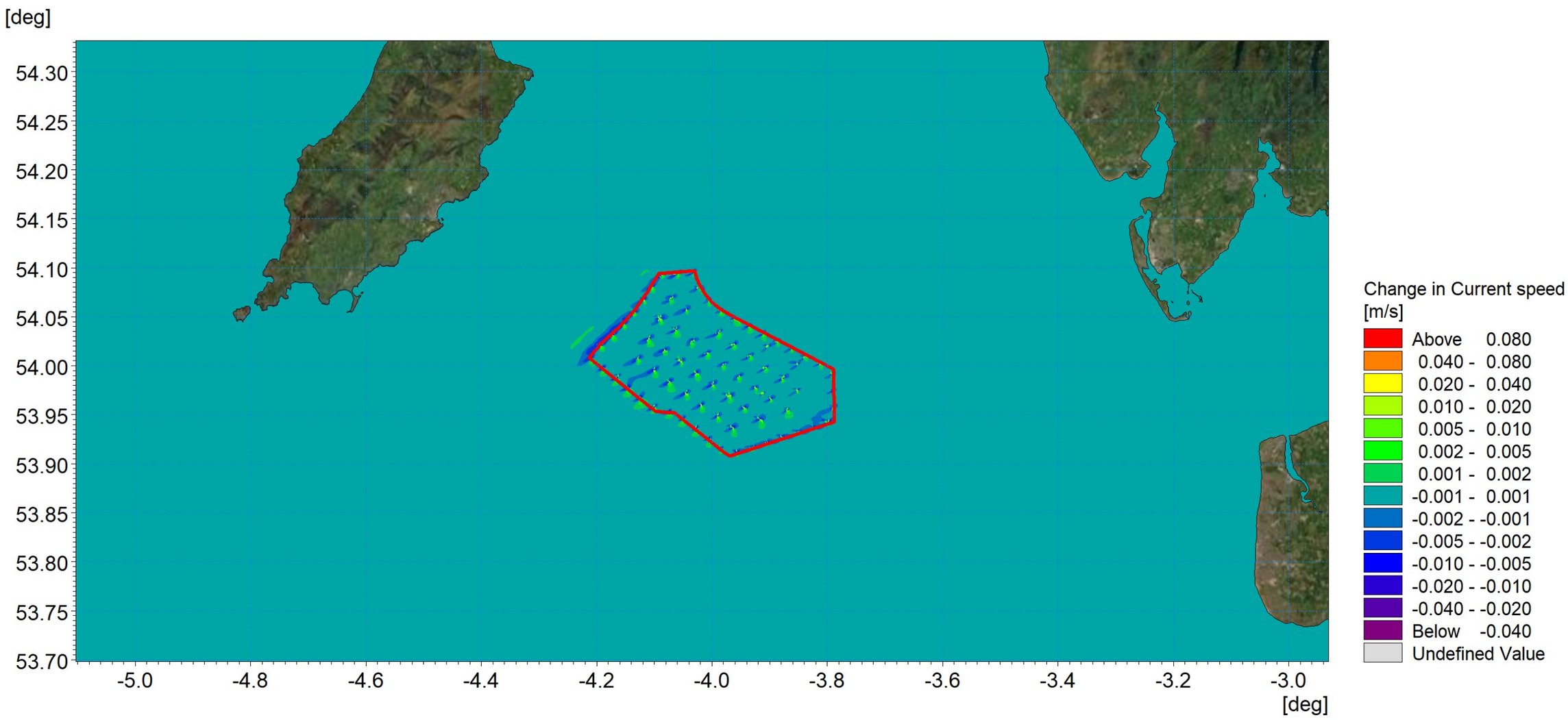

Figure 1.70: Change in tidal flow (post-construction minus baseline) – ebb tide.

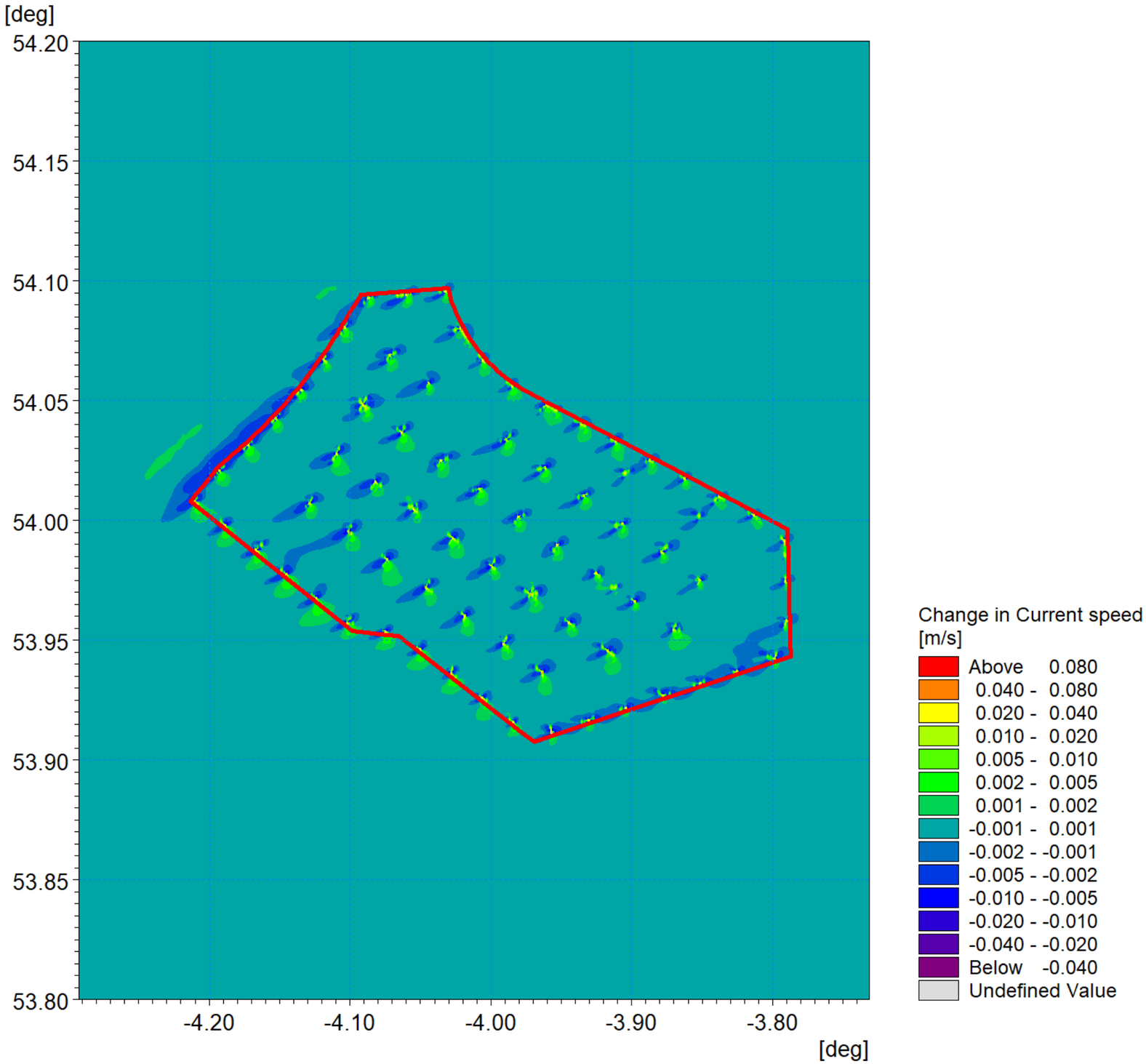

Figure 1.71: Change in tidal flow (post-construction minus baseline) Morgan Array Area – ebb tide detailed view.

Wave climate

1.7.2.3 Using the same principle as for the tidal modelling, the wave climate modelling was repeated with the inclusion of the Morgan Generation Assets structures, foundations and cable protection. Again, changes were found to be indiscernible from the baseline scenario by visual inspection therefore difference plots have been provided and using the same scale for all scenarios. The same principal directions are presented for the 1in1 year storm and 1in20 year storm as presented for the baseline in section 1.6.3.

1.7.2.4 The post construction phase 000º storm is presented for the 1in1 year in Figure 1.72 with the difference shown in Figure 1.73. Similarly, the 1in20 year storm from this direction is presented in Figure 1.74 and Figure 1.75. The changes are seen as reductions in the lee of the structures. The maximum changes are in the order of 3cm for the annual event and 3.5cm for the more extreme storm event which represents less than 1% of the baseline significant wave height. The wave shadow is typically less than one half of this value. These changes would be indiscernible from the baseline wave climate and would not impact on the shoreline or nearshore banks.

1.7.2.5 The potential change in wave climate relative to baseline conditions for annual and more extreme storms are of similar proportions so, for brevity, only the 1in20 year results are presented for the remain directions. Figure 1.76 depicts the 030º post construction scenario with Figure 1.77 showing the change from baseline conditions. The magnitude of the changes at the location of the structures is a reduction in wave height of 3cm whilst, once again the shadow if typical less 2cm which is less than 1% of the baseline condition.

1.7.2.6 For the westerly storms from 240º and 270º the incident wave heights are typically twice that of the fetch limited directions. For these scenarios the effect of the presence of the infrastructure is much smaller with changes in wave height typically less than 0.25% as presented in Figure 1.78 to Figure 1.81.

1.7.2.7 In summary, the presence of the Morgan Generation Assets was seen to have the greatest influence when storms approached from the north sectors where baseline wave height were smallest. In all cases the changes in wave climate would be imperceptible and would not interact with the shoreline or nearshore banks and morphology.

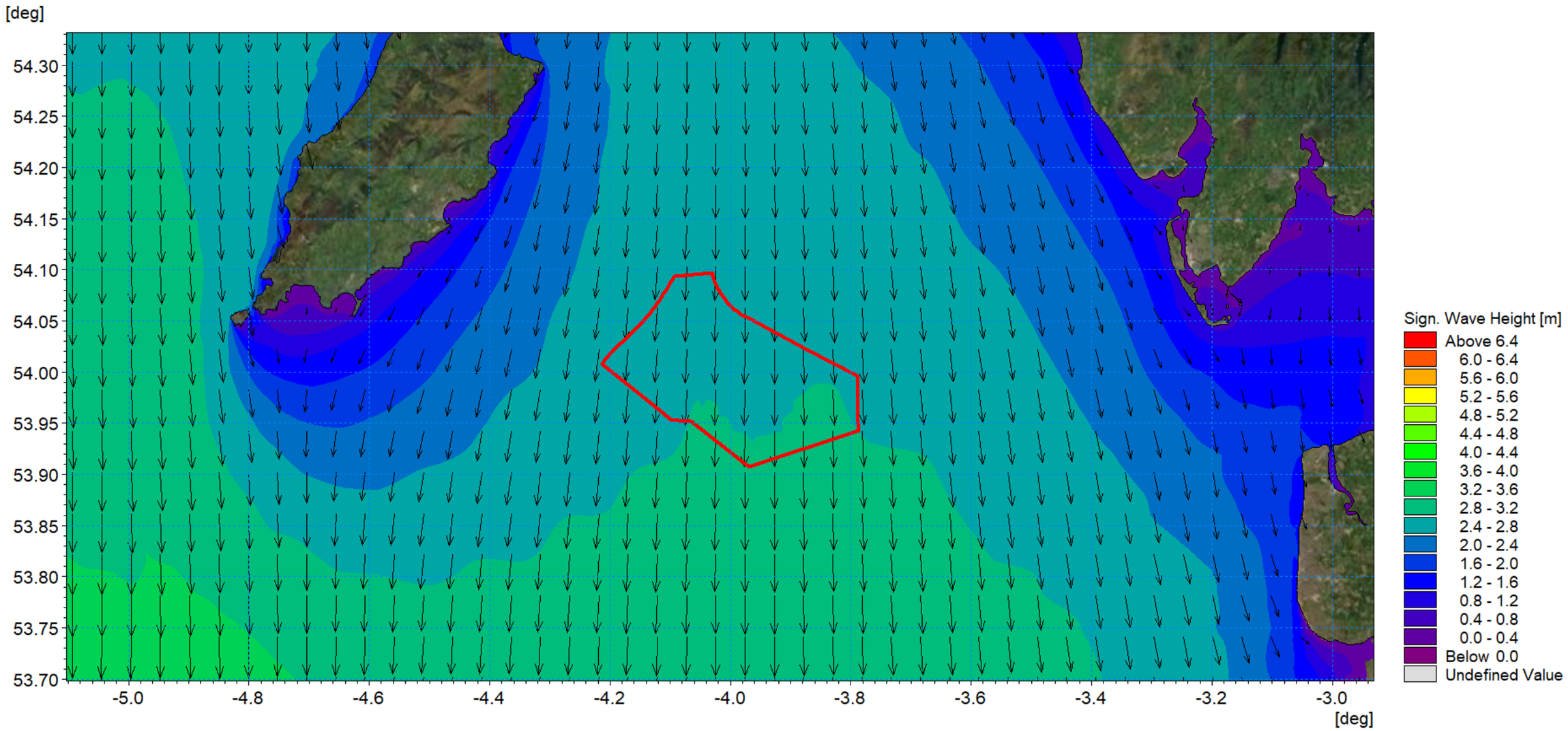

Figure 1.72: Post-construction wave climate 1in1 year storm 000° MHW.

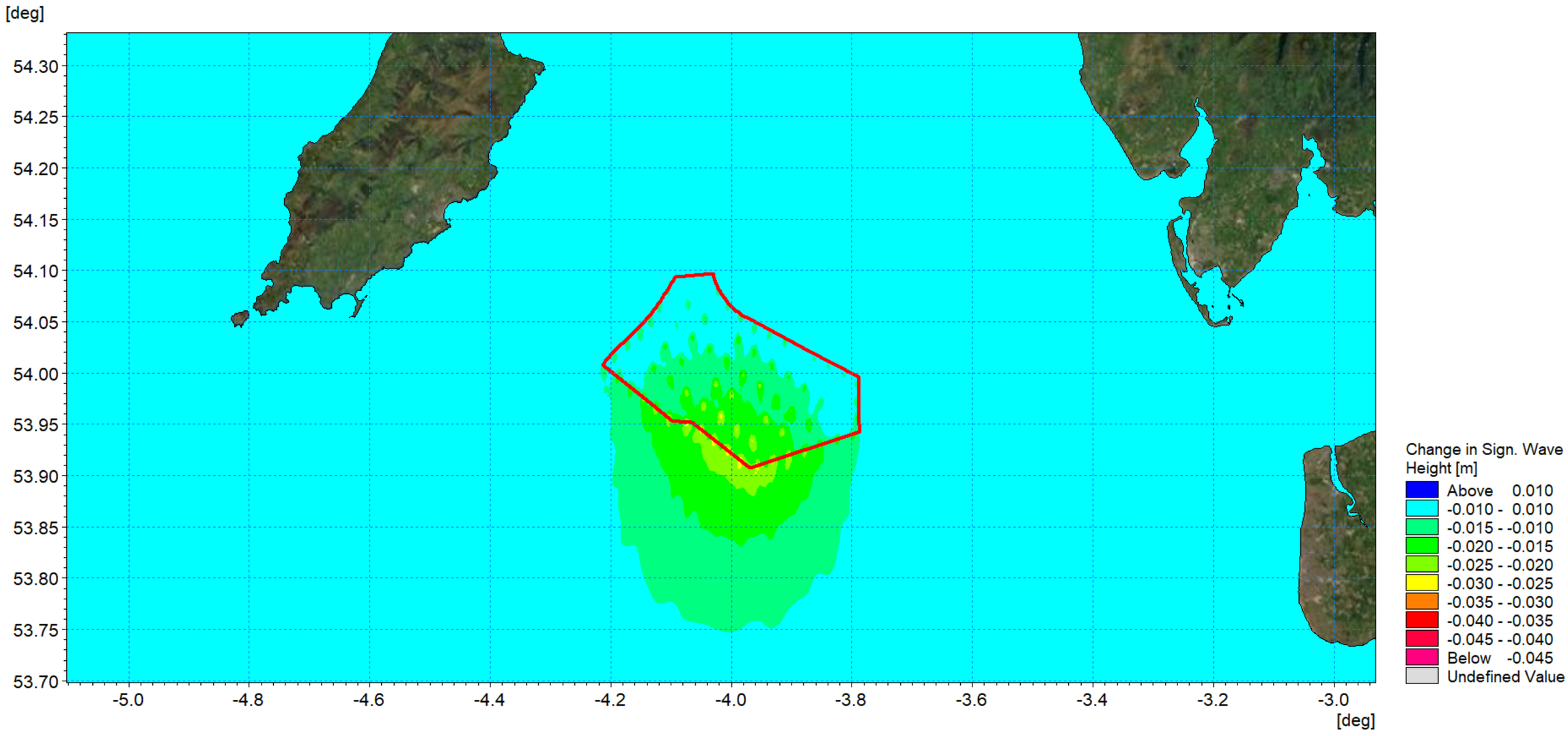

Figure 1.73: Change in wave climate 1in1 year storm 000° MHW (post-construction minus baseline).

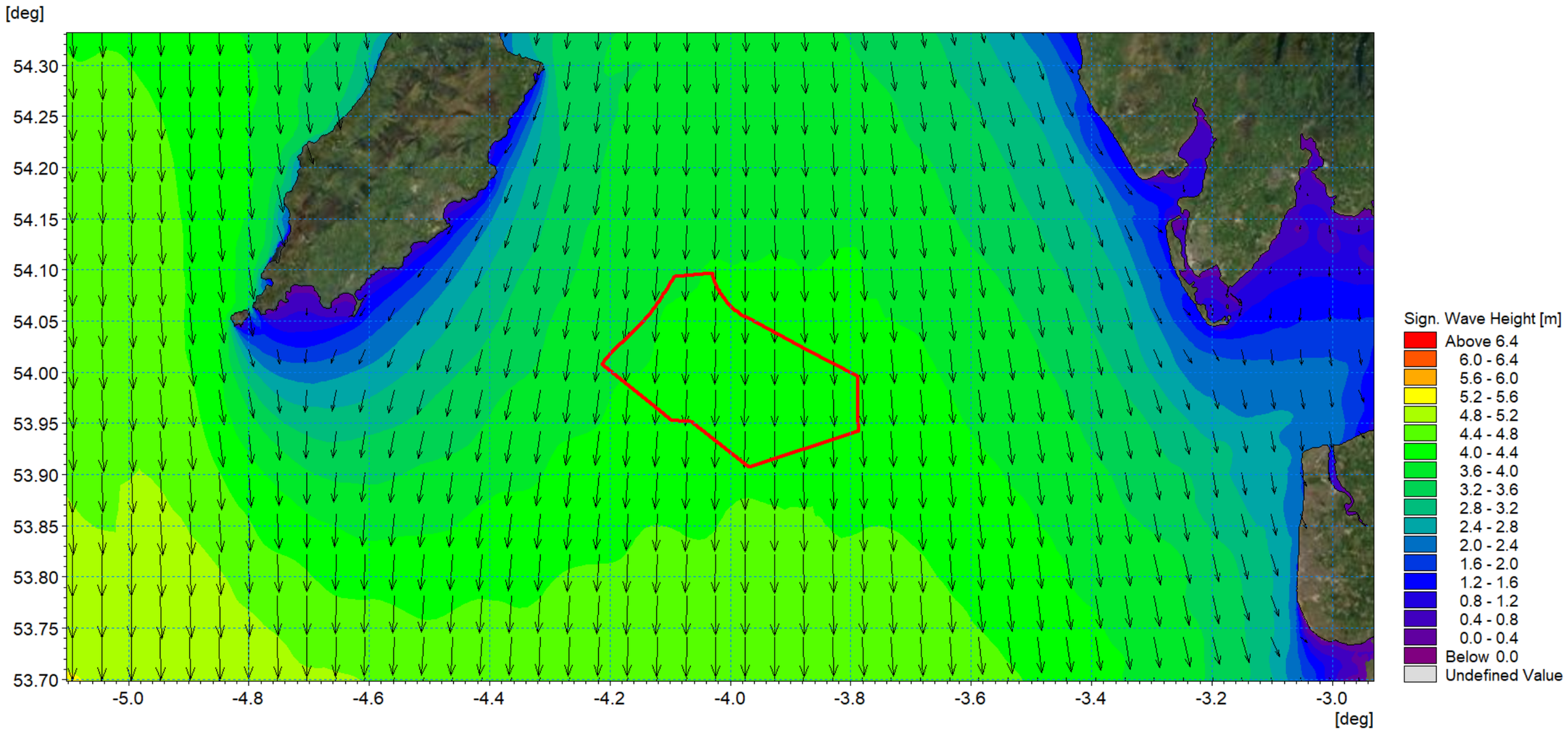

Figure 1.74: Post-construction wave climate 1in20 year storm 000° MHW.

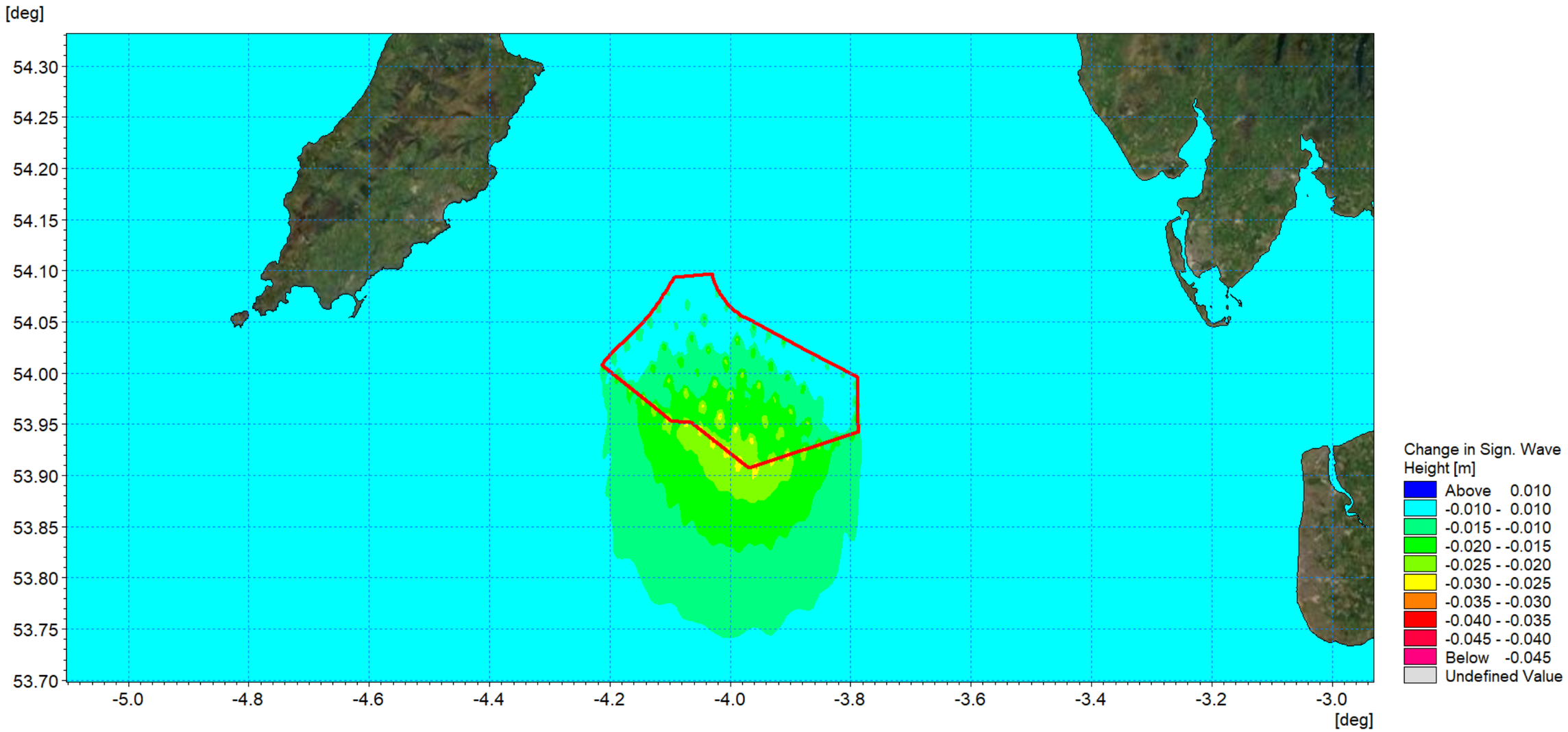

Figure 1.75: Change in wave climate 1in20 year storm 000° MHW (post-construction minus baseline).

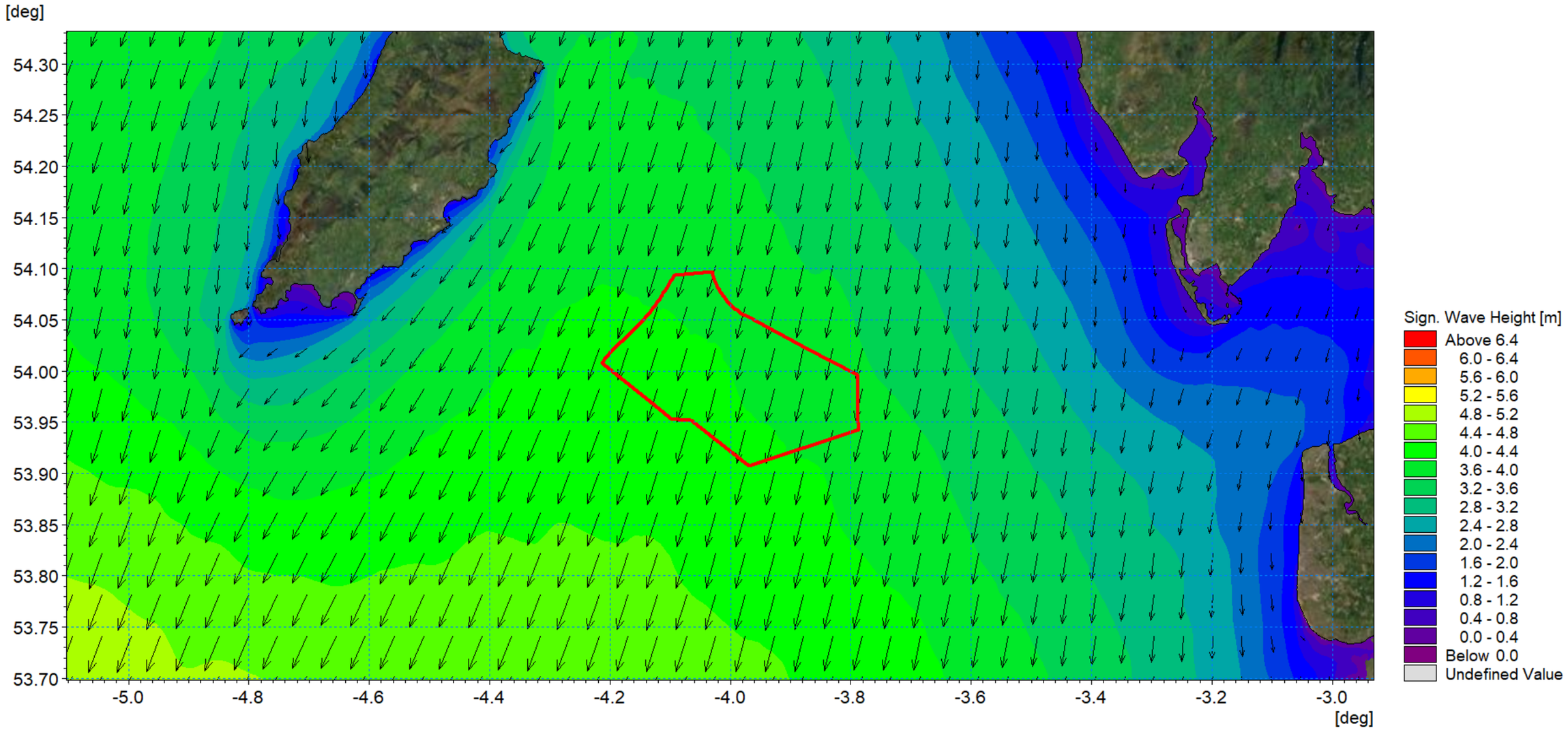

Figure 1.76: Post-construction wave climate 1in20 year storm 030° MHW.

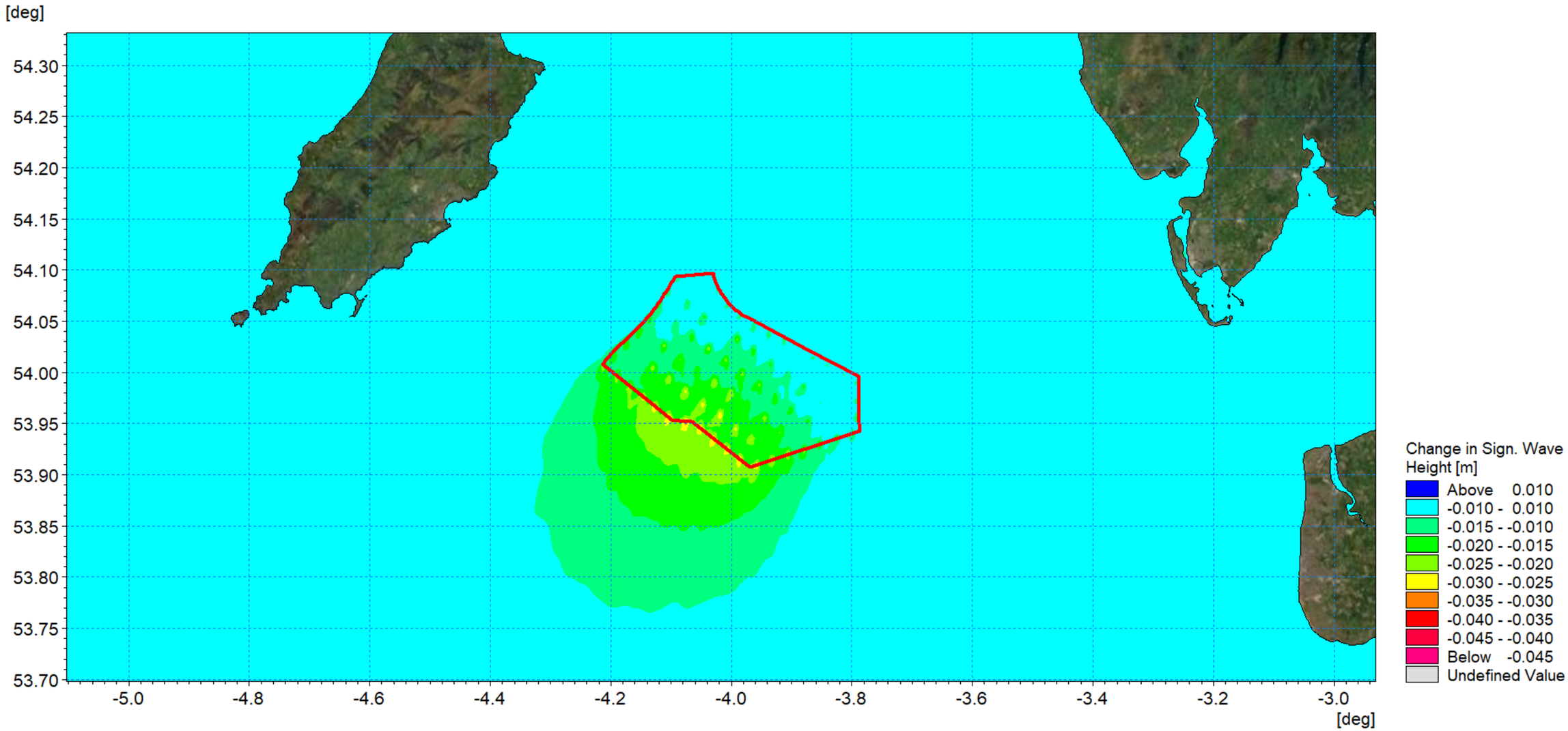

Figure 1.77: Change in wave climate 1in20 year storm 030° MHW (post-construction minus baseline).

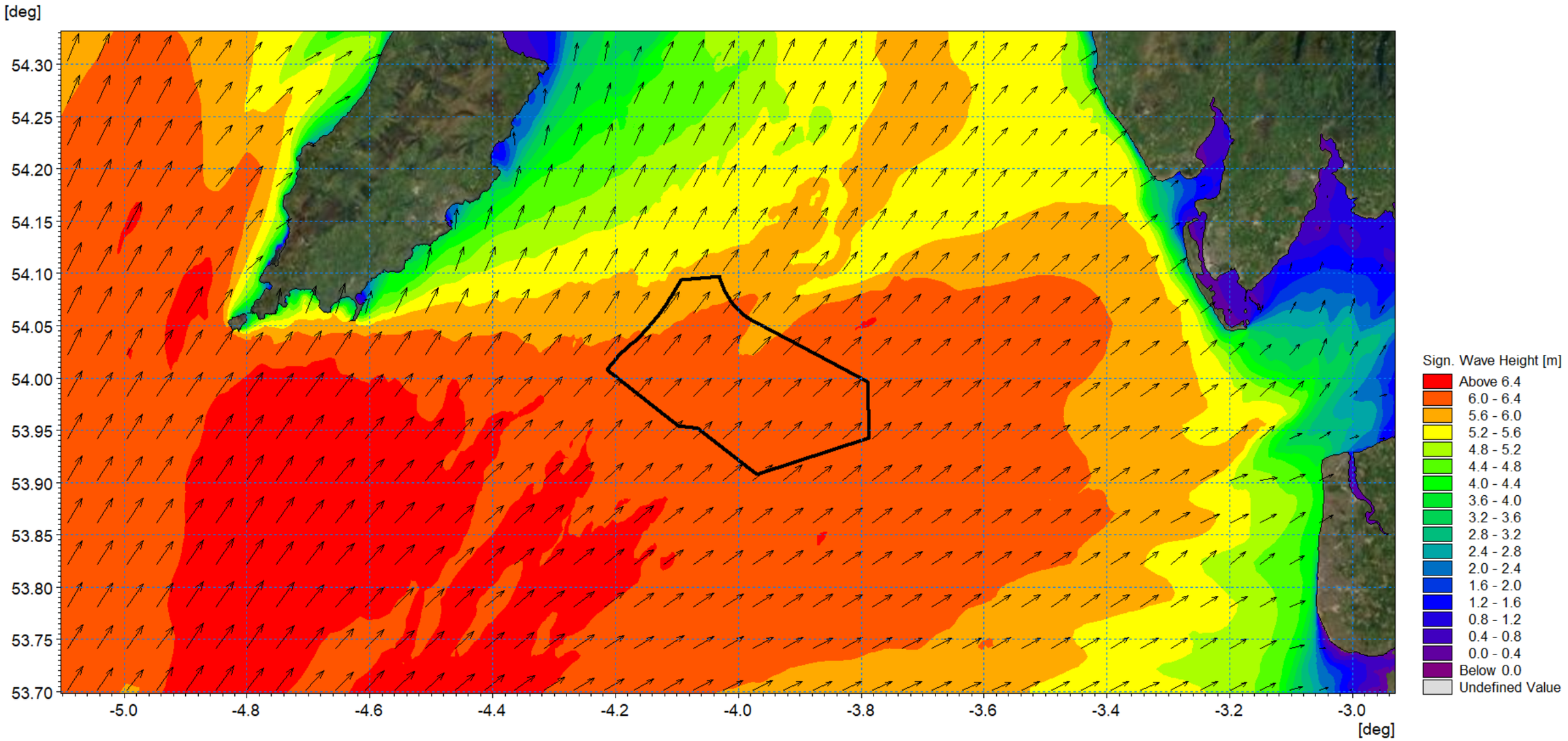

Figure 1.78: Post-construction wave climate 1in20 year storm 240° MHW.

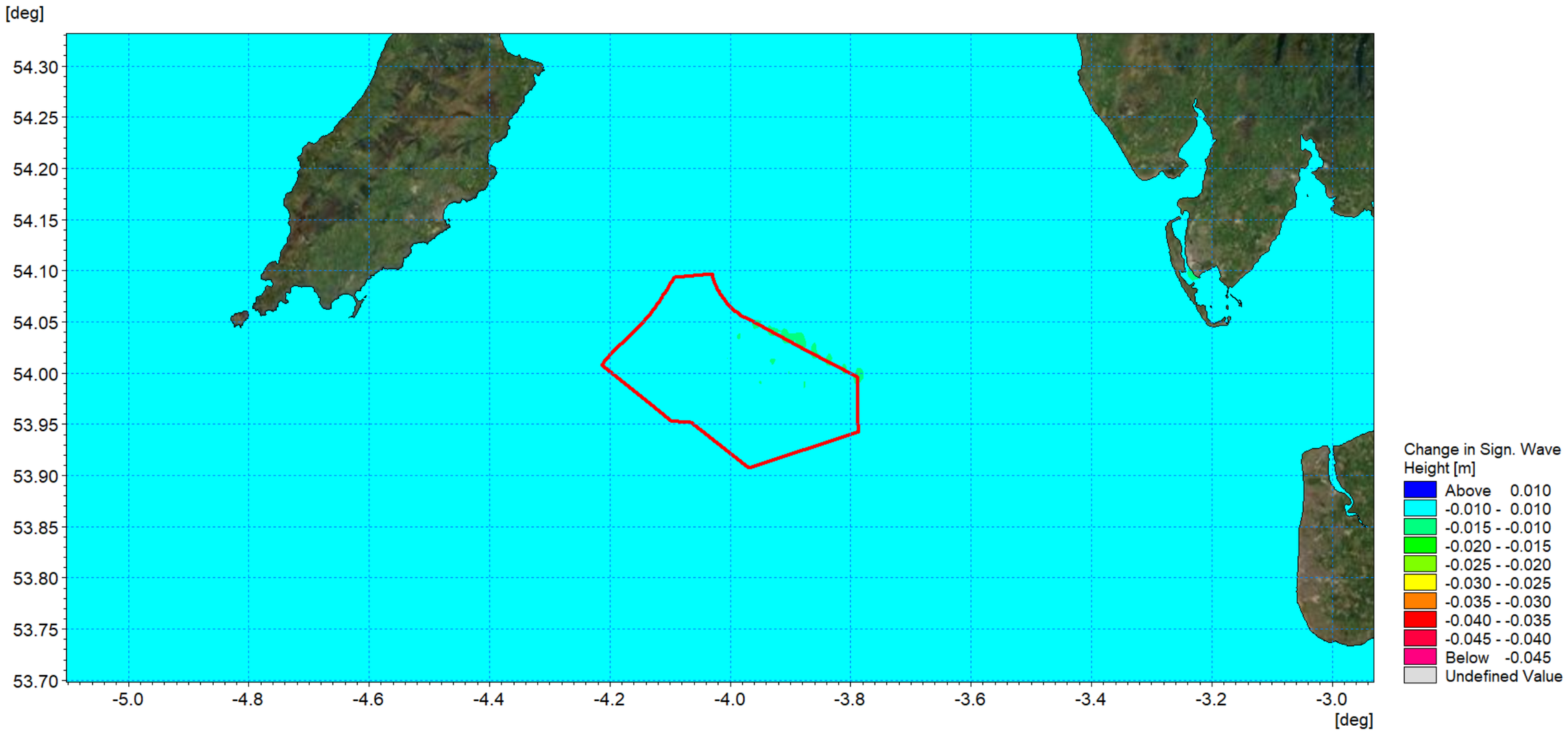

Figure 1.79: Change in wave climate 1in20 year storm 240° MHW (post-construction minus baseline).

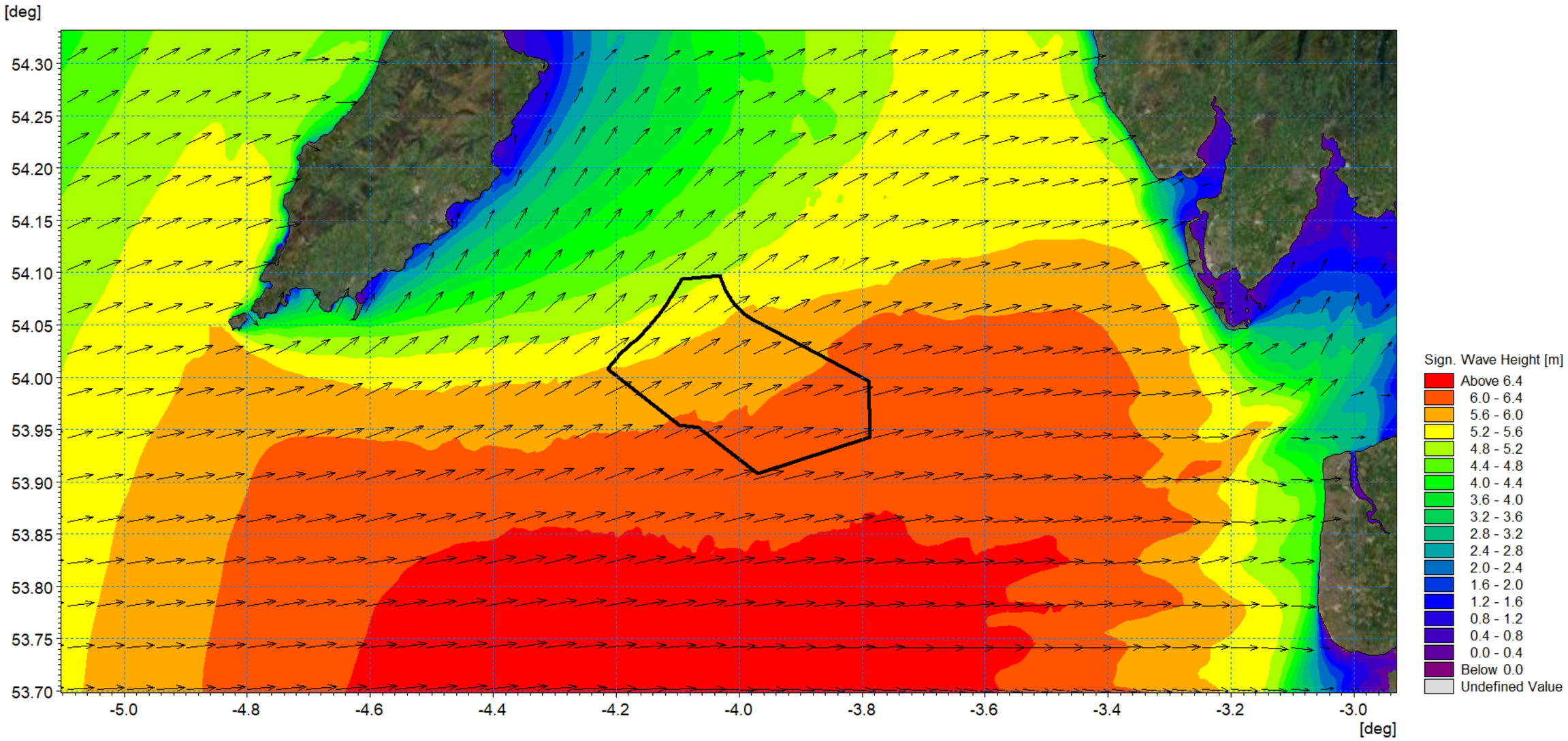

Figure 1.80: Post-construction wave climate 1in20 year storm 270° MHW.

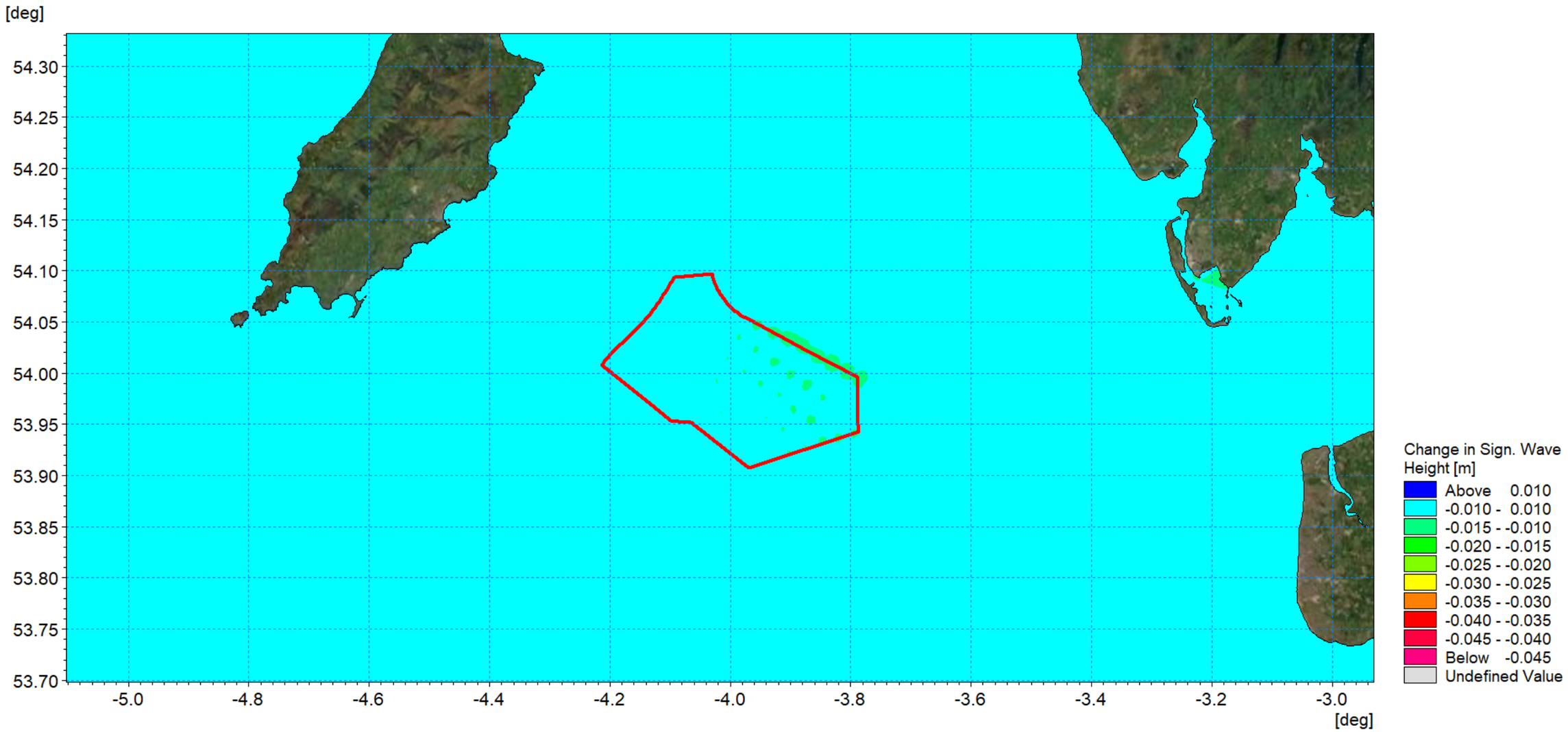

Figure 1.81: Change in wave climate 1in20 year storm 270° MHW (post-construction minus baseline).

Littoral currents

1.7.2.8 The previous sections established the magnitude of the changes in tidal currents and wave conditions individually, however sediment transport regimes are driven by a combination of these factors. Although the modelling has demonstrated that the Morgan Generation Assets results in minor localised changes for each aspect, for the sake of completeness, the influence on littoral currents was examined.

1.7.2.9 The modelling was extended to include the post-construction scenario for the 1in1 year storm from 210°. The baseline littoral currents for mid ebb and mid flood were presented in Figure 1.54 and Figure 1.55 respectively. The corresponding post-construction littoral currents are shown in Figure 1.82 and Figure 1.85 for the ebb and flood tides.

1.7.2.10 As with the previous difference in current speed post construction, a log plotting scale was necessary to present the changes due to their localised nature. The changes for the flood tide are presented in Figure 1.83 a more detailed plot in Figure 1.84 whilst for the ebb tide Figure 1.86 and Figure 1.87 show the corresponding information.

1.7.2.11 During the flood tide the influence of the wave climate is in concert with the tidal current and during the ebb tide, the tidal flow is in opposition to the wave climate and the resultant littoral current is reduced in magnitude. The presence of the structures was seen to have a limited influence on the wave climate and there is little difference between changes in littoral current magnitude and the tidal flows alone due to the installation during the flood tide, Figure 1.68. The extent of the change is larger for the ebb tide condition particularly at the locations where the alignment of the array is in concert with both the tidal flow and wave direction, although it should be noted that these are still <1% of baseline tidal flow. Overall, the magnitude of these changes remains limited to ±6% of the baseline currents at 300m and reduces significantly with increased distance from each structure.

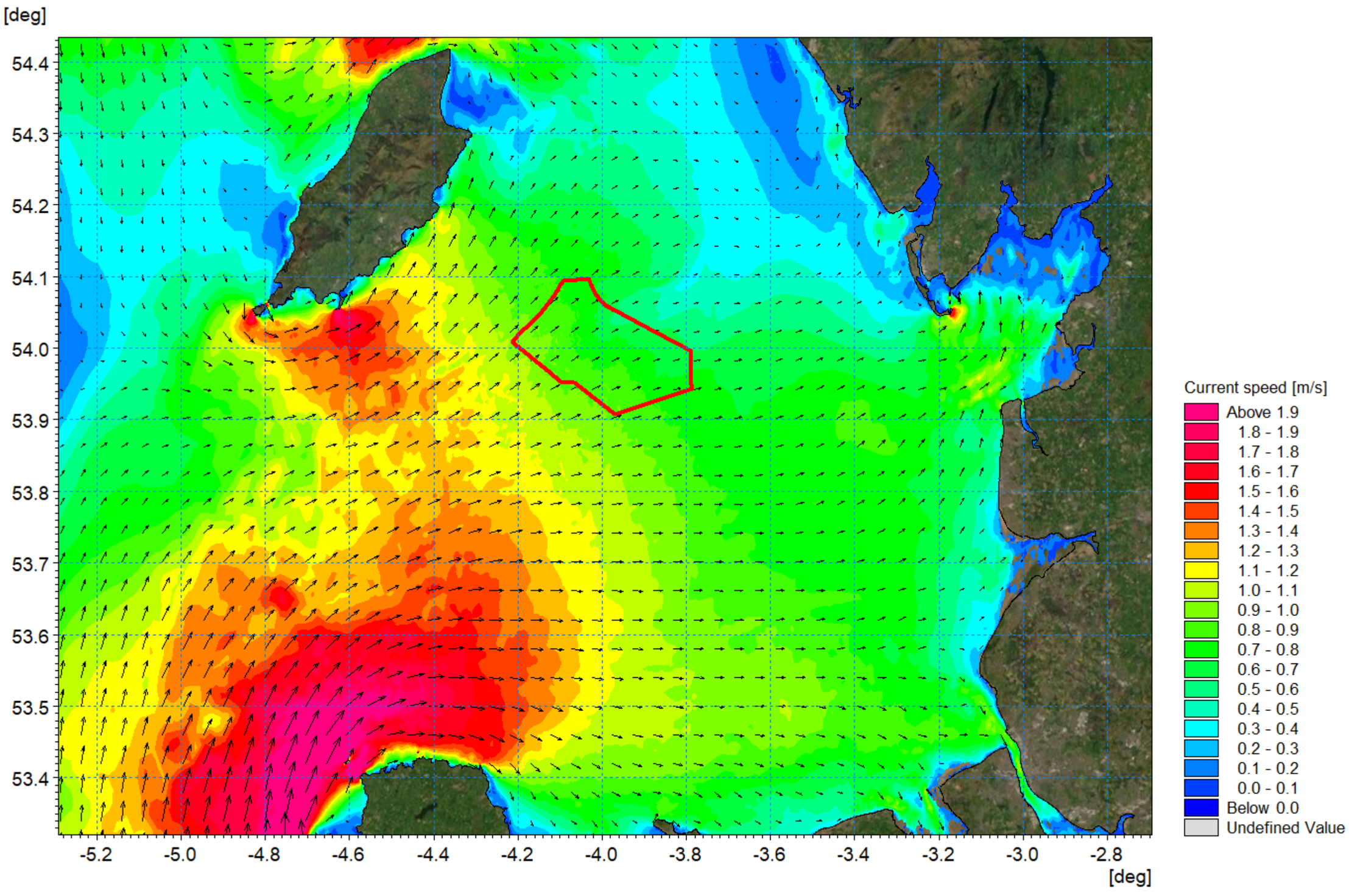

Figure 1.82: Post-construction littoral current 1in1 year storm from 210° - Flood Tide.

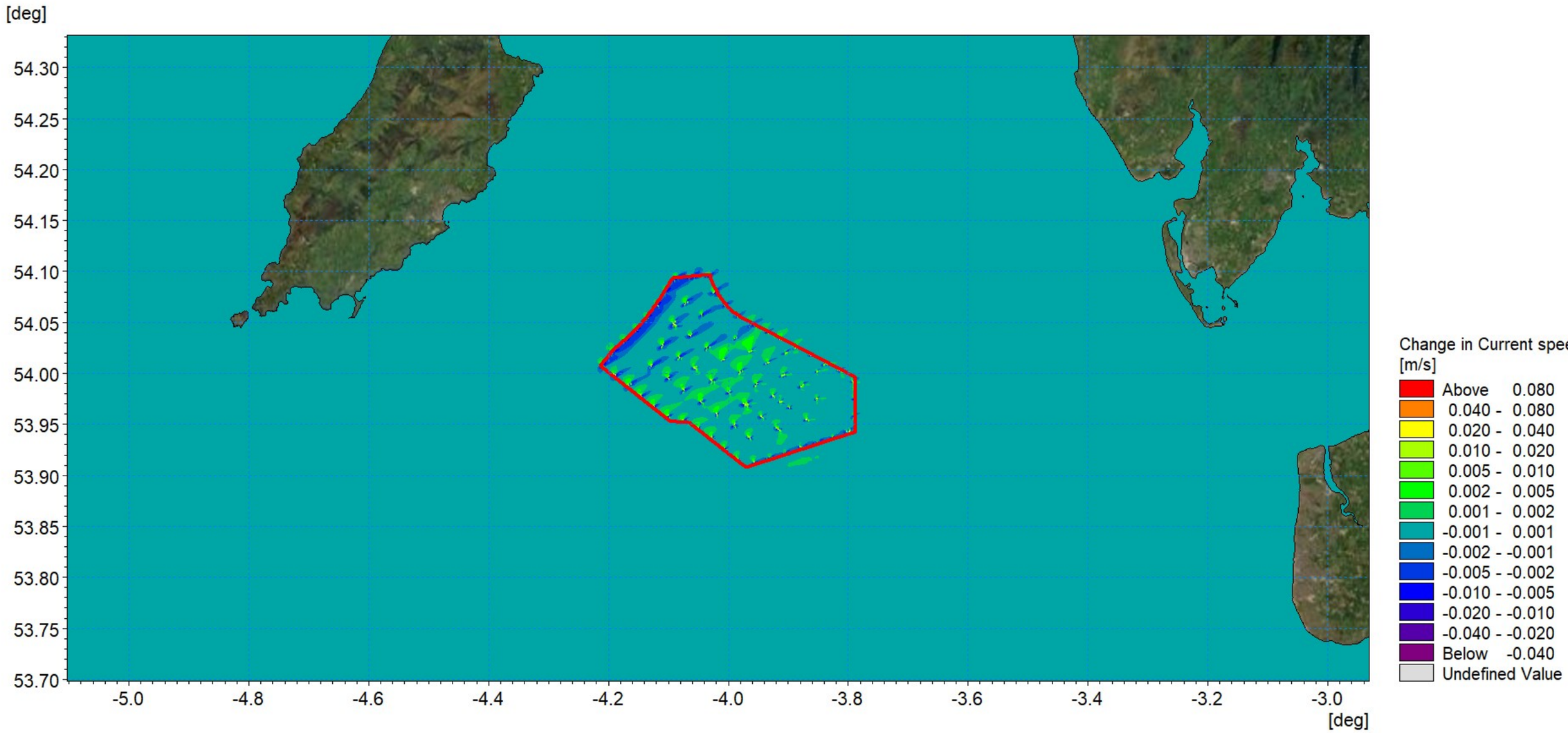

Figure 1.83: Change in littoral current 1in1 year storm from 210° - flood tide (post-construction minus baseline).

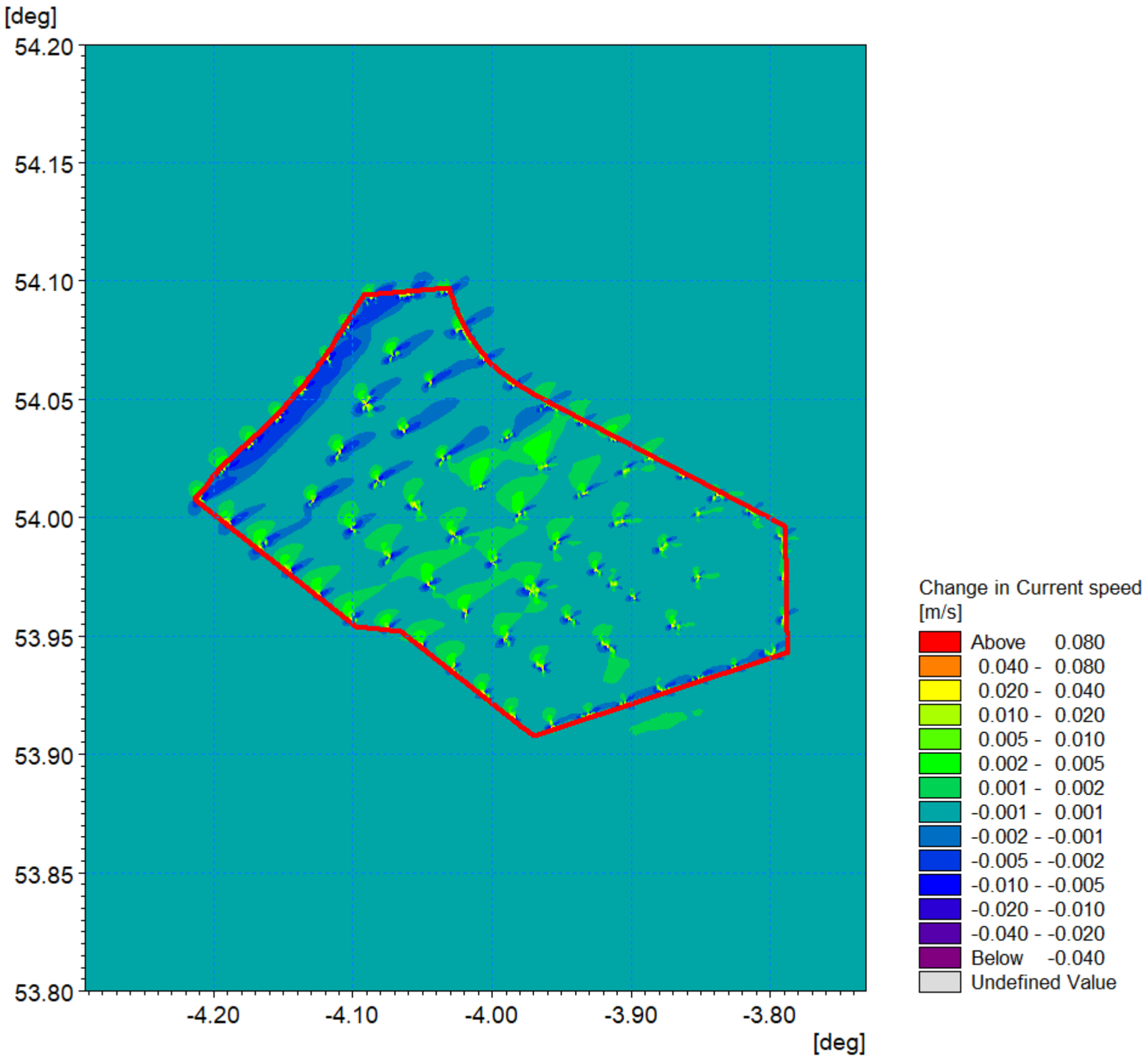

Figure 1.84: Change in littoral current 1in1 year storm from 210° - flood tide (post-construction minus baseline) detailed view.

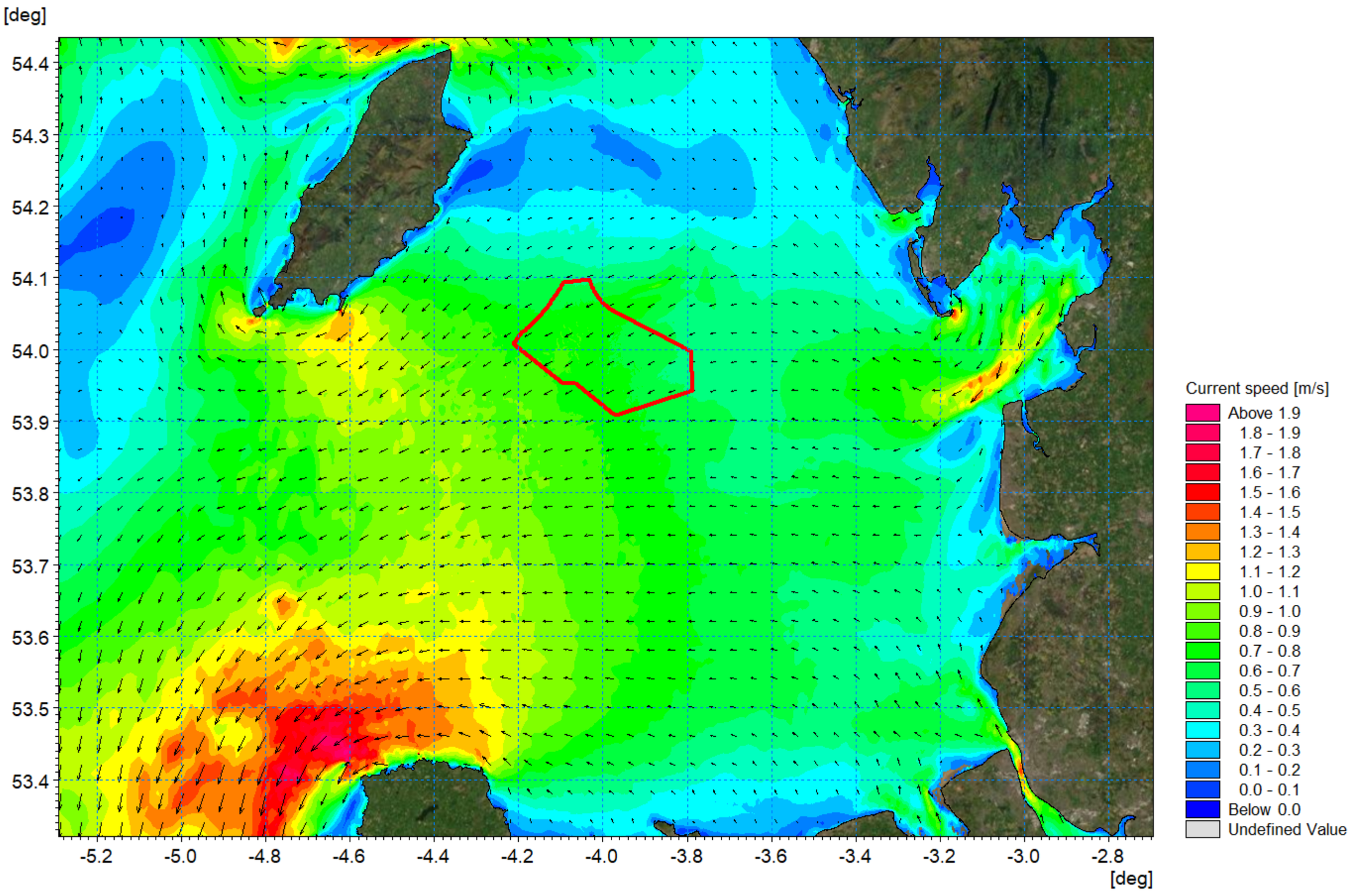

Figure 1.85: Post-construction littoral current 1in1 year storm from 210° - ebb tide.

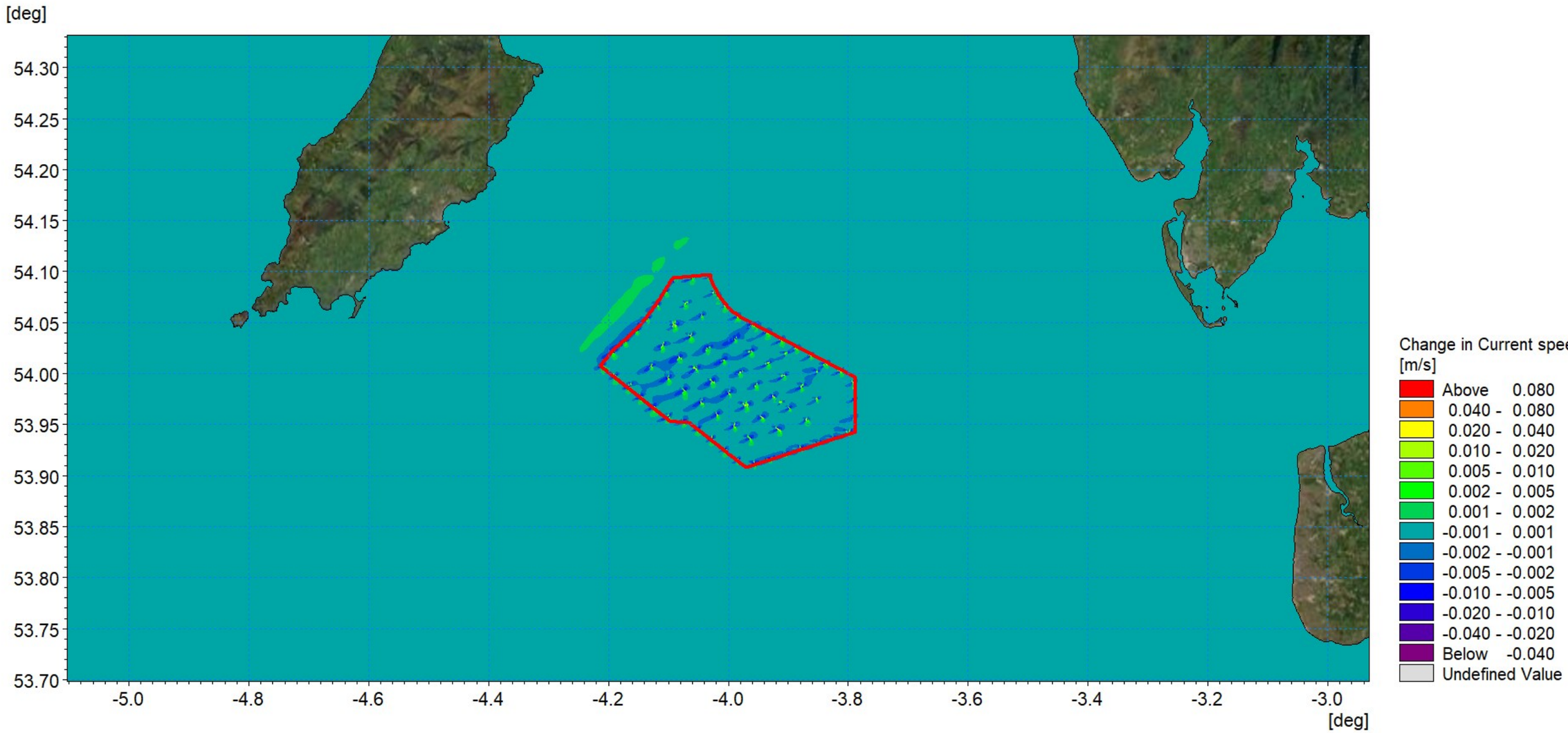

Figure 1.86: Change in littoral current 1in1 year storm from 210° - ebb tide (post-construction minus baseline).

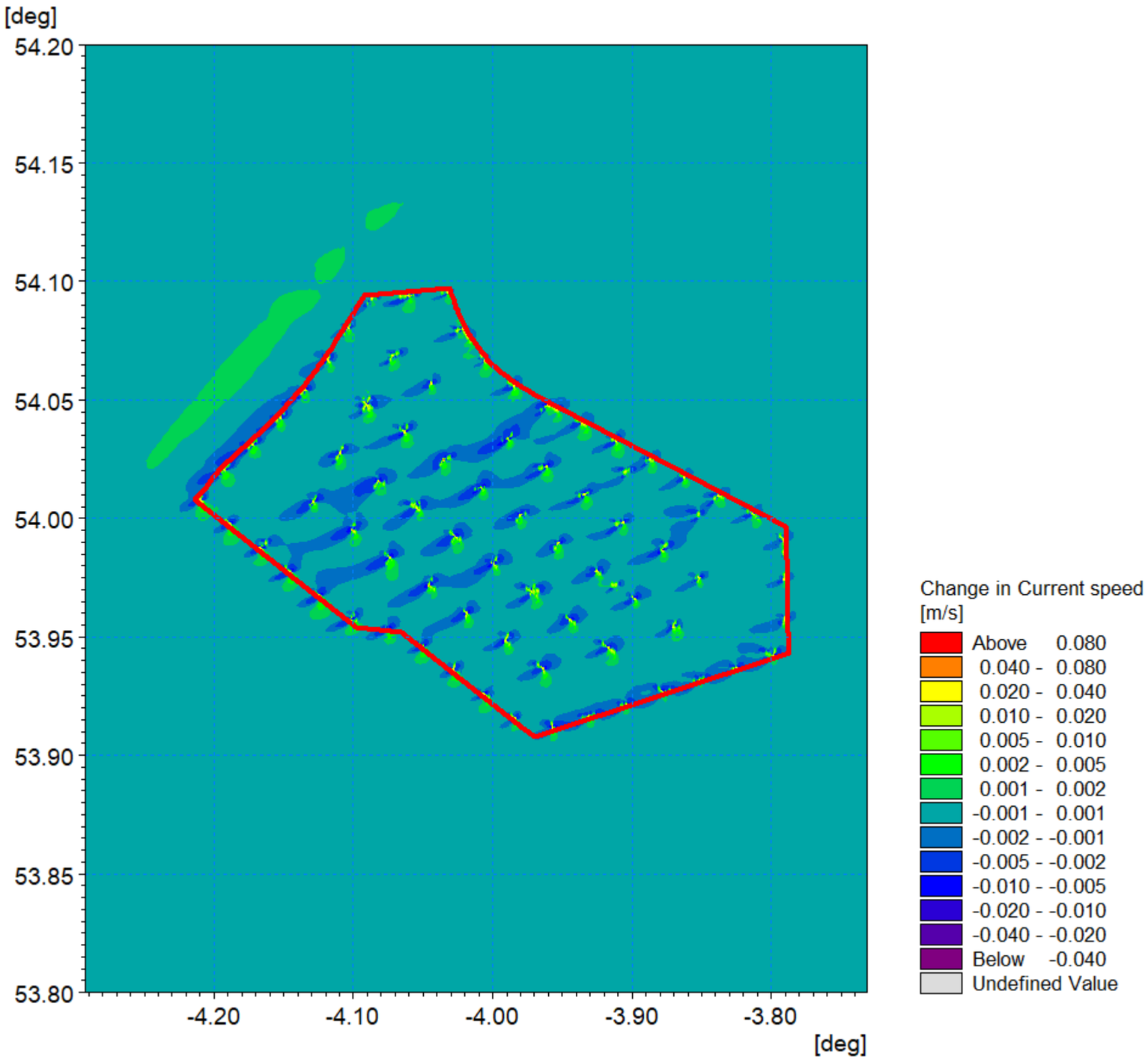

Figure 1.87: Change in littoral current 1in1 year storm from 210° - ebb tide (post-construction minus baseline) detailed view.

1.7.3 Post-construction sedimentology

Sediment transport

1.7.3.1 The numerical modelling methodology for sediment transport was described in section 1.6.6, which indicated how the baseline information was discretised to form the basis of the modelled scenarios. For the post-construction scenario, in addition to the Morgan Generation Assets structures being included in the tide and wave models, the bed material map was edited to represent the areas of scour protection where sediment supply is restricted. In each case an area of fixed bed was applied overlain with a thin layer of sand to initialise the model and avoid instabilities. The scour protection was defined as 56m diameter for each wind turbine structure leg and 49m diameter for each OSP leg. The models were then re-run for a spring tide under calm conditions.

1.7.3.2 There are a number of approaches for quantifying potential sediment transport, given that transport rates vary both across the area and due to tidal state and climate conditions. For this analysis, the residual current was calculated over the course of two tidal cycles (one day) with the structures in place and compared with that for the baseline (Figure 1.58) for the calm condition as this is effectively the driver for sediment transport. The post-construction residual current and changes are shown in Figure 1.88 and Figure 1.89 respectively. As with previous results a more detailed plot is presented in Figure 1.90.

1.7.3.3 The corresponding sediment transport was simulated over the course of one day where the equivalent baseline daily sediment transport rate was shown in Figure 1.59. The post-construction daily sediment transport rate and differences are shown in Figure 1.91 and Figure 1.92 respectively. It should be noted that both the sediment transport and difference plots use a log palette as there is a large range in sediment transport potential across the domain.

1.7.3.4 This analysis shows that although there are changes as a result of the installation of the Morgan Generation Assets structures and associated scour and cable protection, the extent and magnitude is limited. As anticipated, in areas of reduced residual current in the lee of structures the sediment transport rate is also reduced and vice versa. Generally residual currents are low within the Morgan Generation Assets and within the context of this comparative study there is a maximum change in residual current of circa ±10% which is largely sited within very close proximity to the wind turbine foundation structures (less than 100m elongated in the direction of principle tidal currents). It is noted that areas of reduced residual current and sediment transport are often accompanied by a similar increase in close proximity. This indicates that the residual current and resulting sediment transport paths are adjusted to accommodate the structures rather than transport pathways being cut off.

1.7.3.5 This process was repeated for the 1in1 year storm. The baseline residual current (Figure 1.62) was compared with the equivalent post-construction residual current pattern as shown in Figure 1.93; with the difference in Figure 1.94 and in more detail in Figure 1.95. The pattern of changes is similar to the previous scenario but with a wider area of influence. It should however be noted that although the absolute values of these changes are increased from the purely tidal condition the underlying baseline residual currents are of greater magnitude under storm conditions and are proportionately smaller than those exhibited under calm conditions.

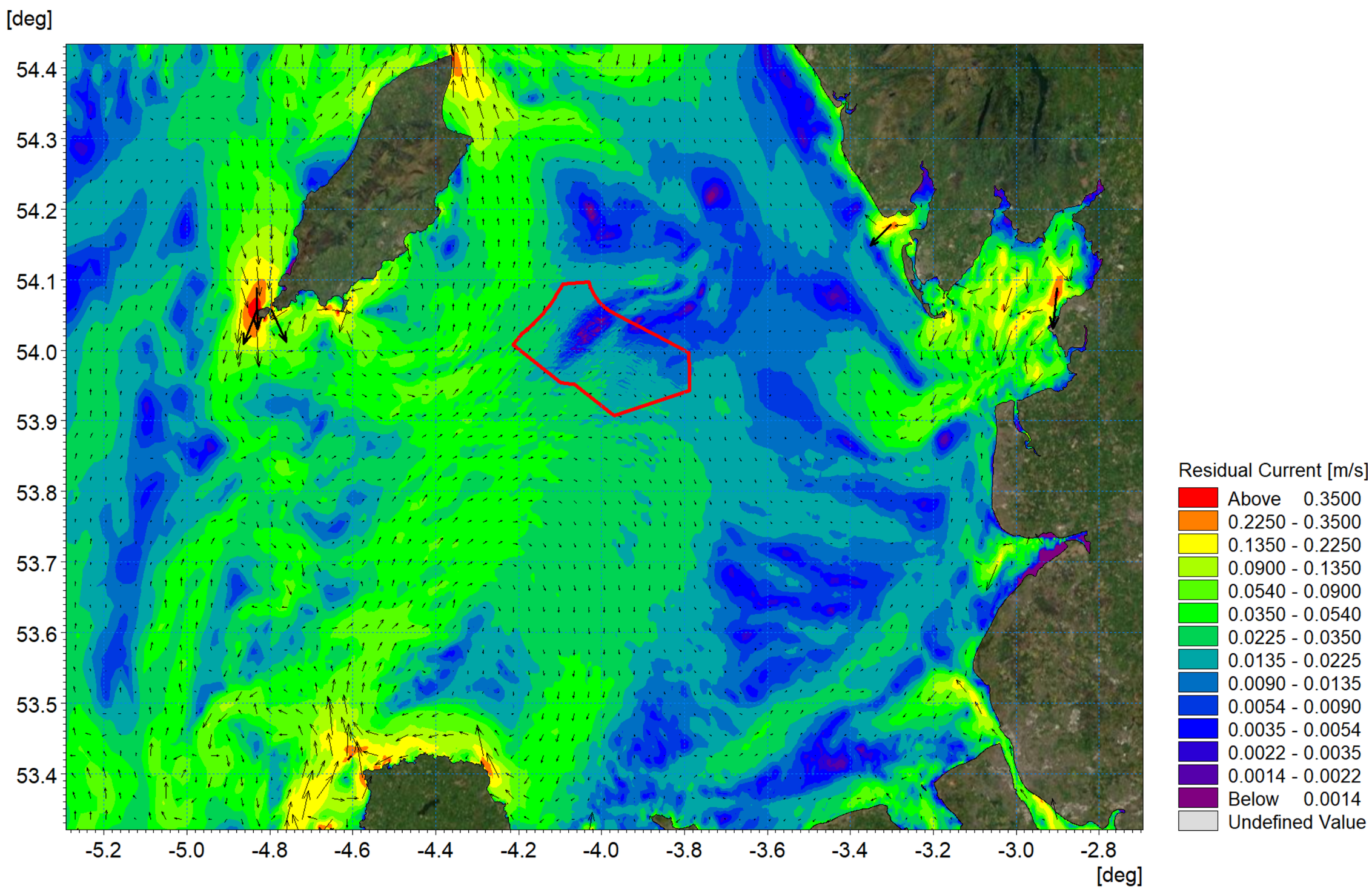

Figure 1.88: Post-construction residual current spring tide.

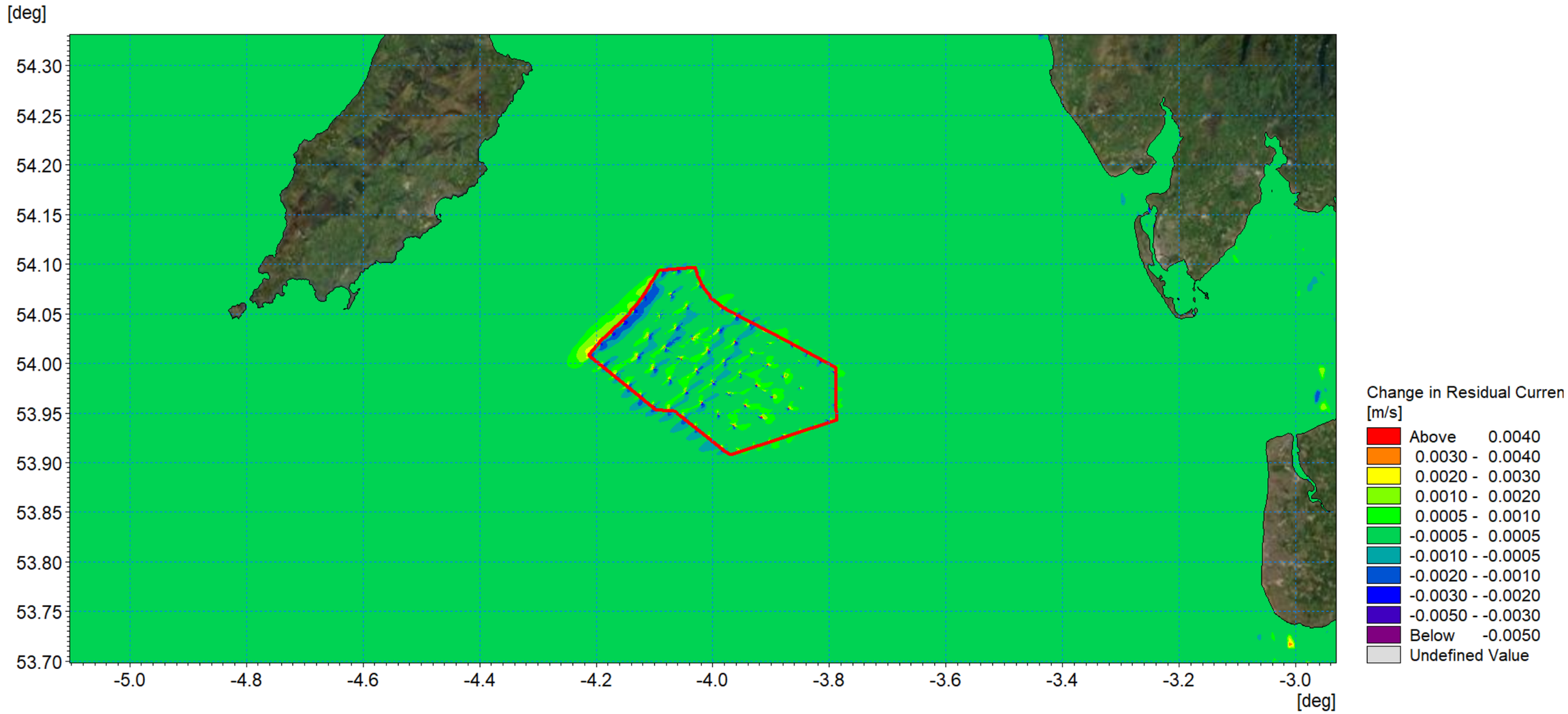

Figure 1.89: Change in residual current spring tide (post-construction minus baseline).

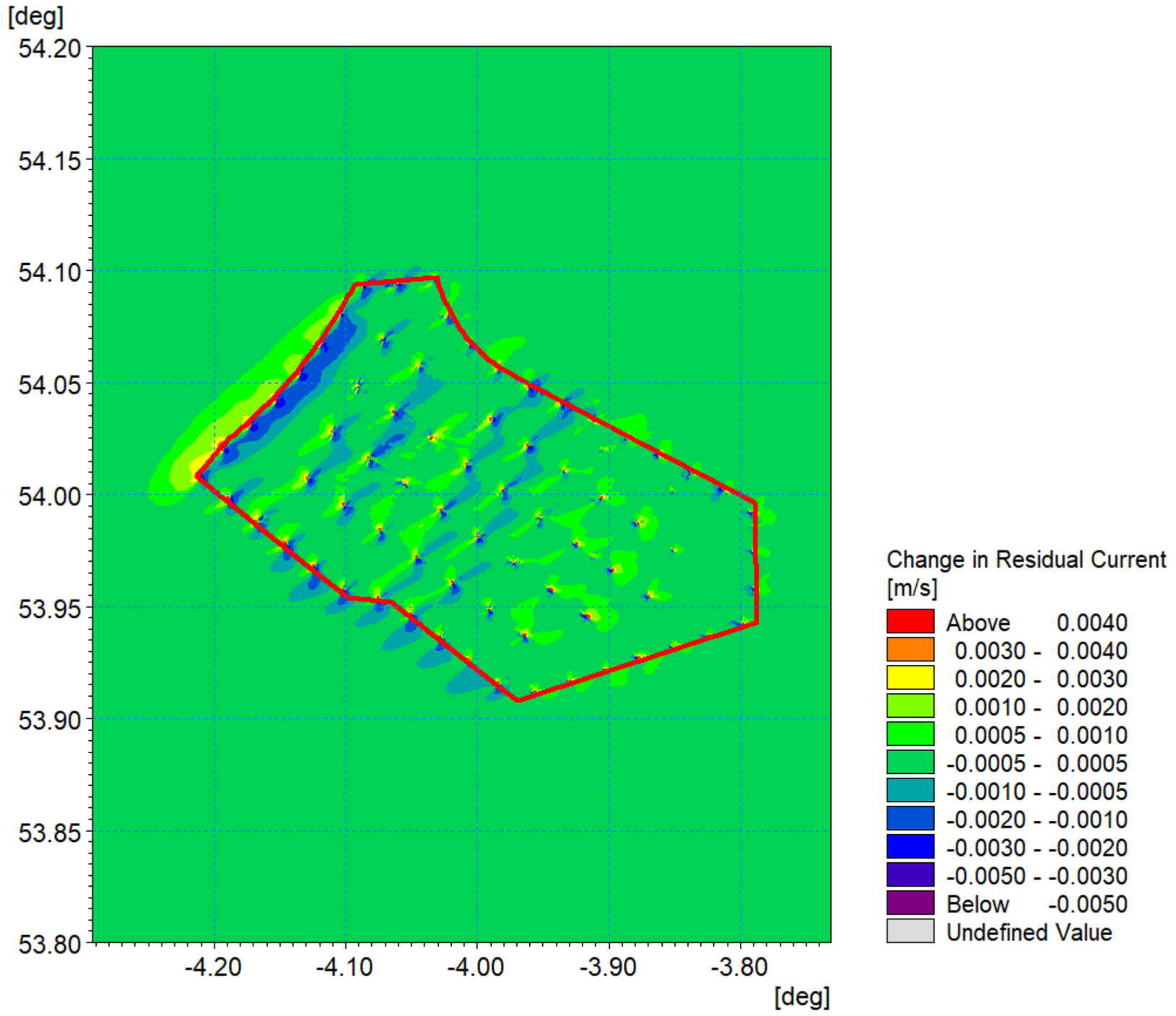

Figure 1.90: Change in residual current spring tide (post-construction minus baseline) Morgan Generation Assets detailed view.

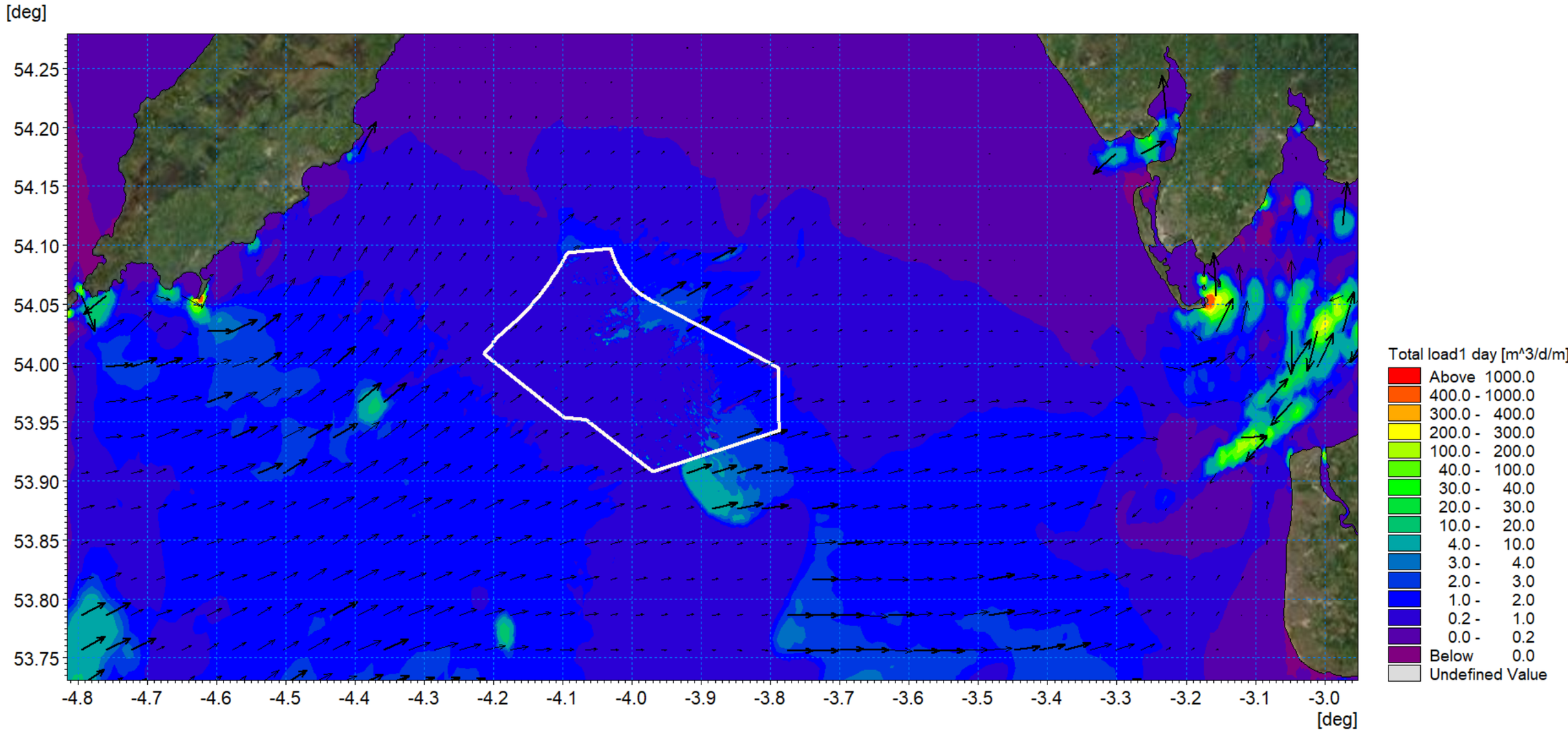

Figure 1.91: Post-construction potential sediment over the course of 1day (two tide cycles).

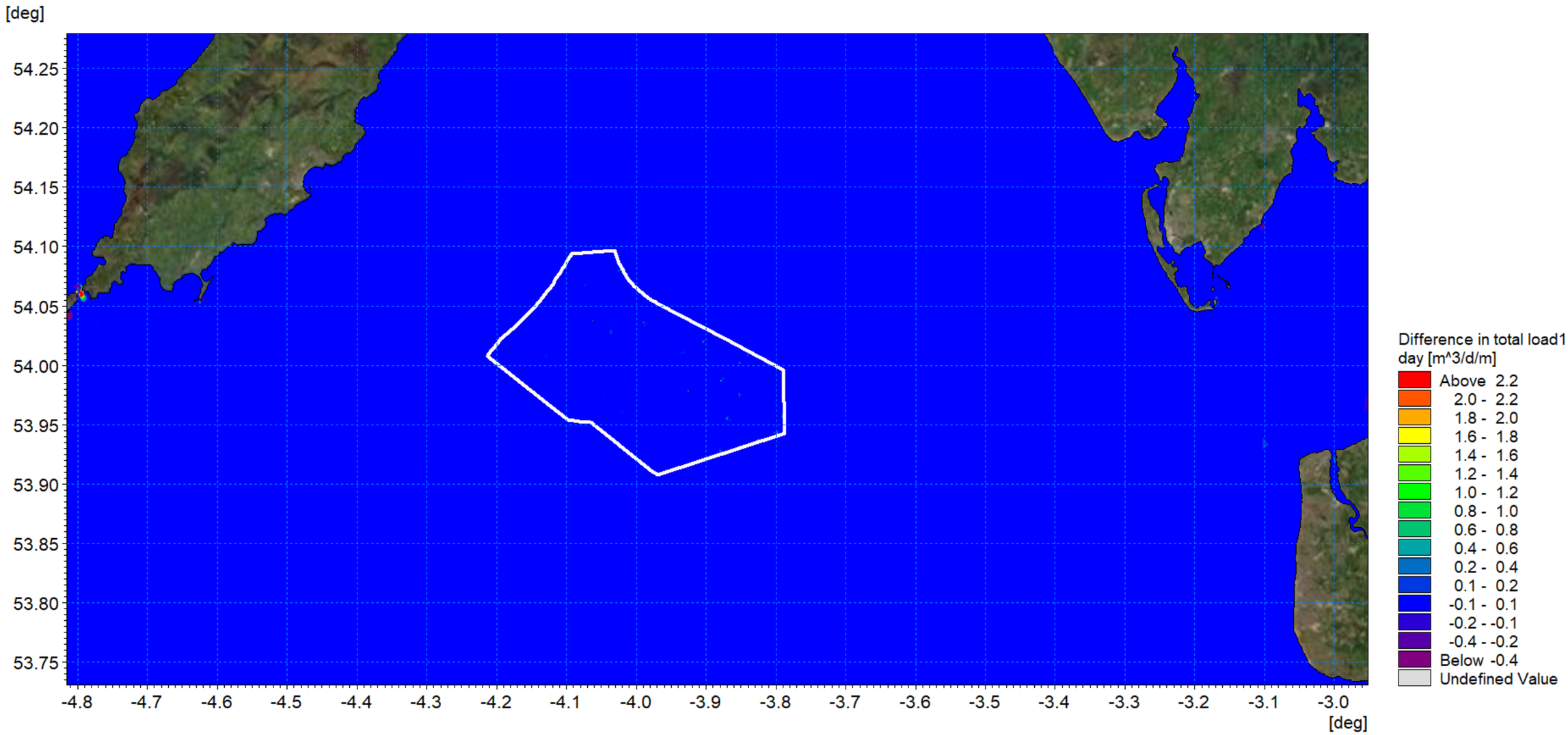

Figure 1.92: Difference in potential sediment transport over the course of 1day (post-construction minus baseline).

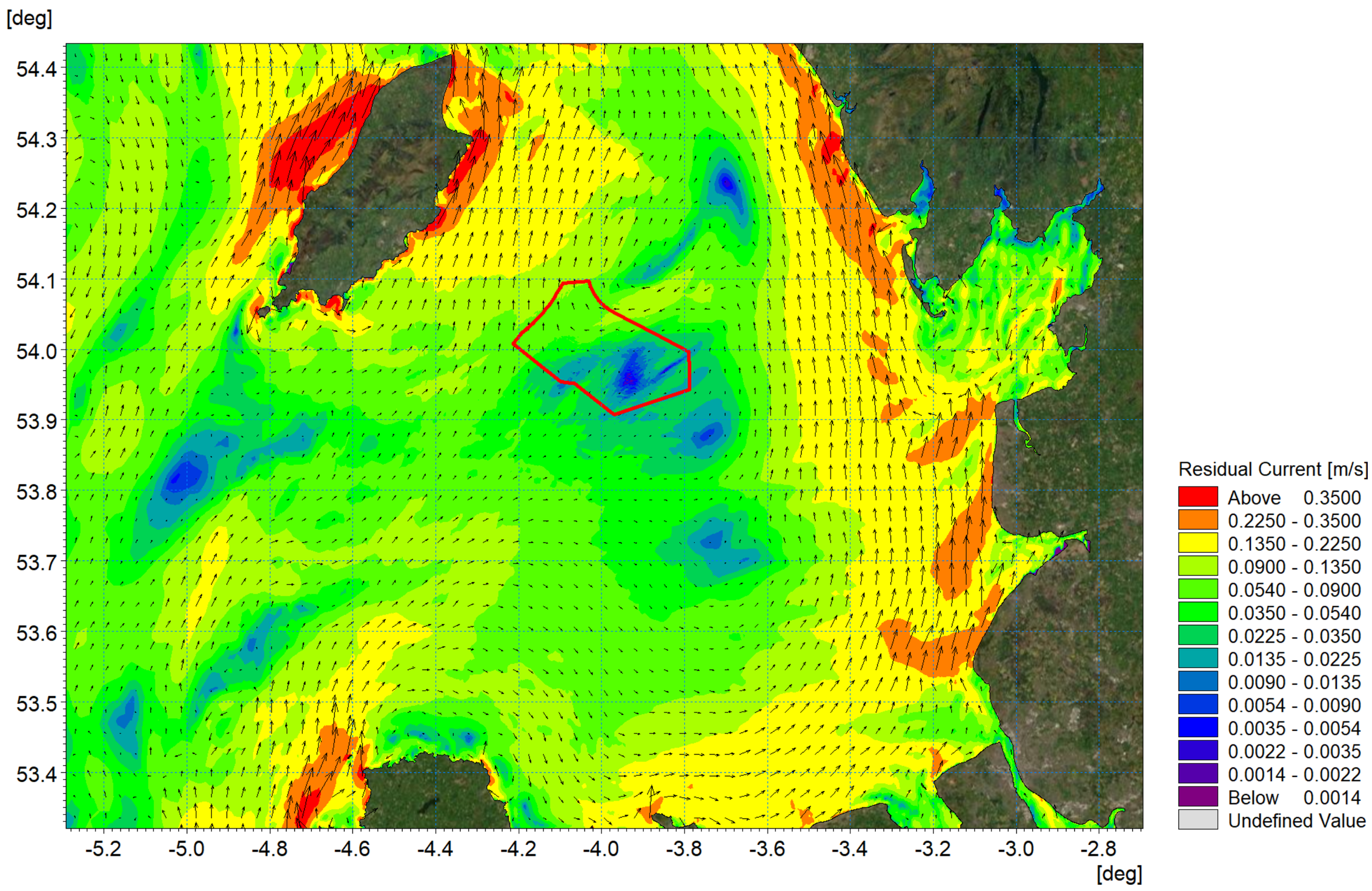

Figure 1.93: Post-construction residual current 1in1 year storm from 270° spring tide.

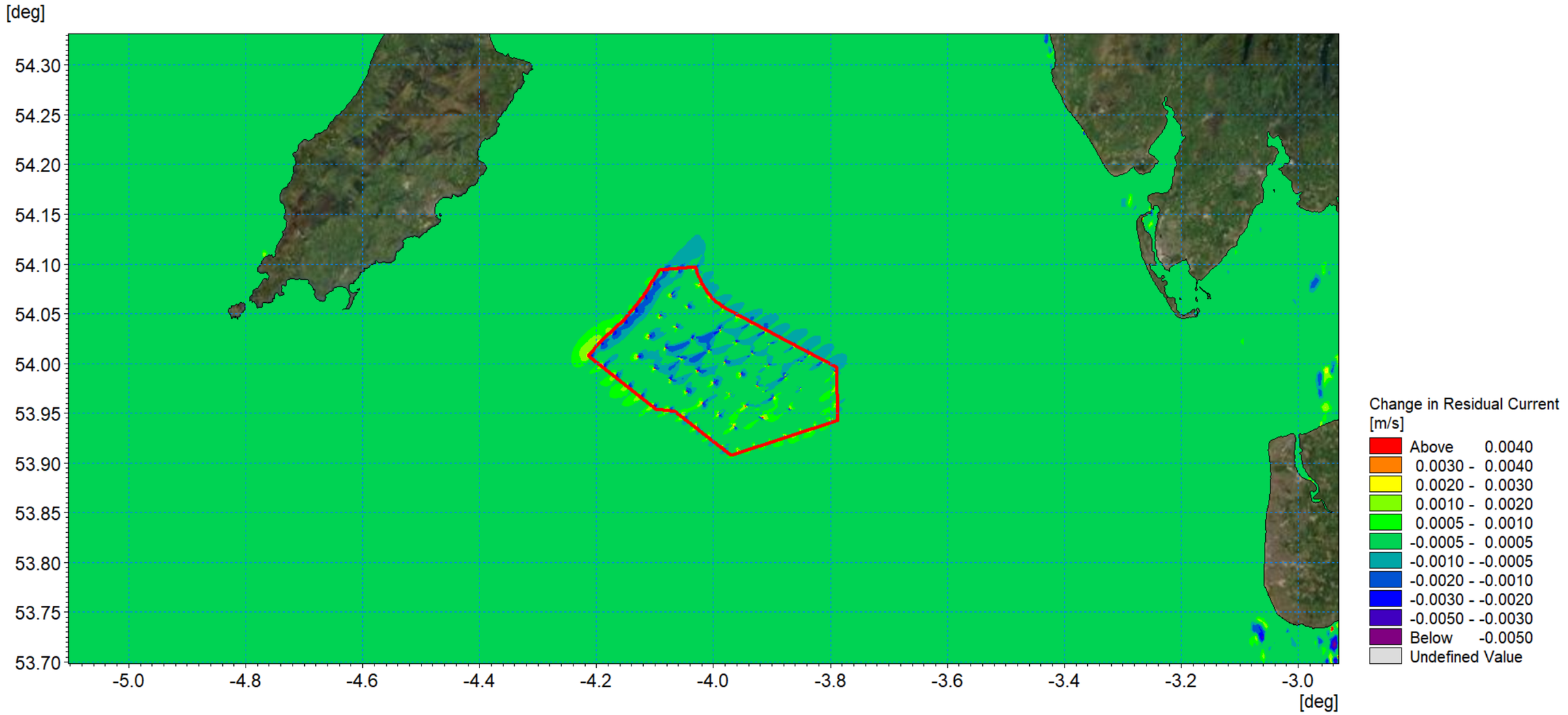

Figure 1.94: Change in residual current 1in1 year storm from 270° spring tide (post-construction minus baseline).

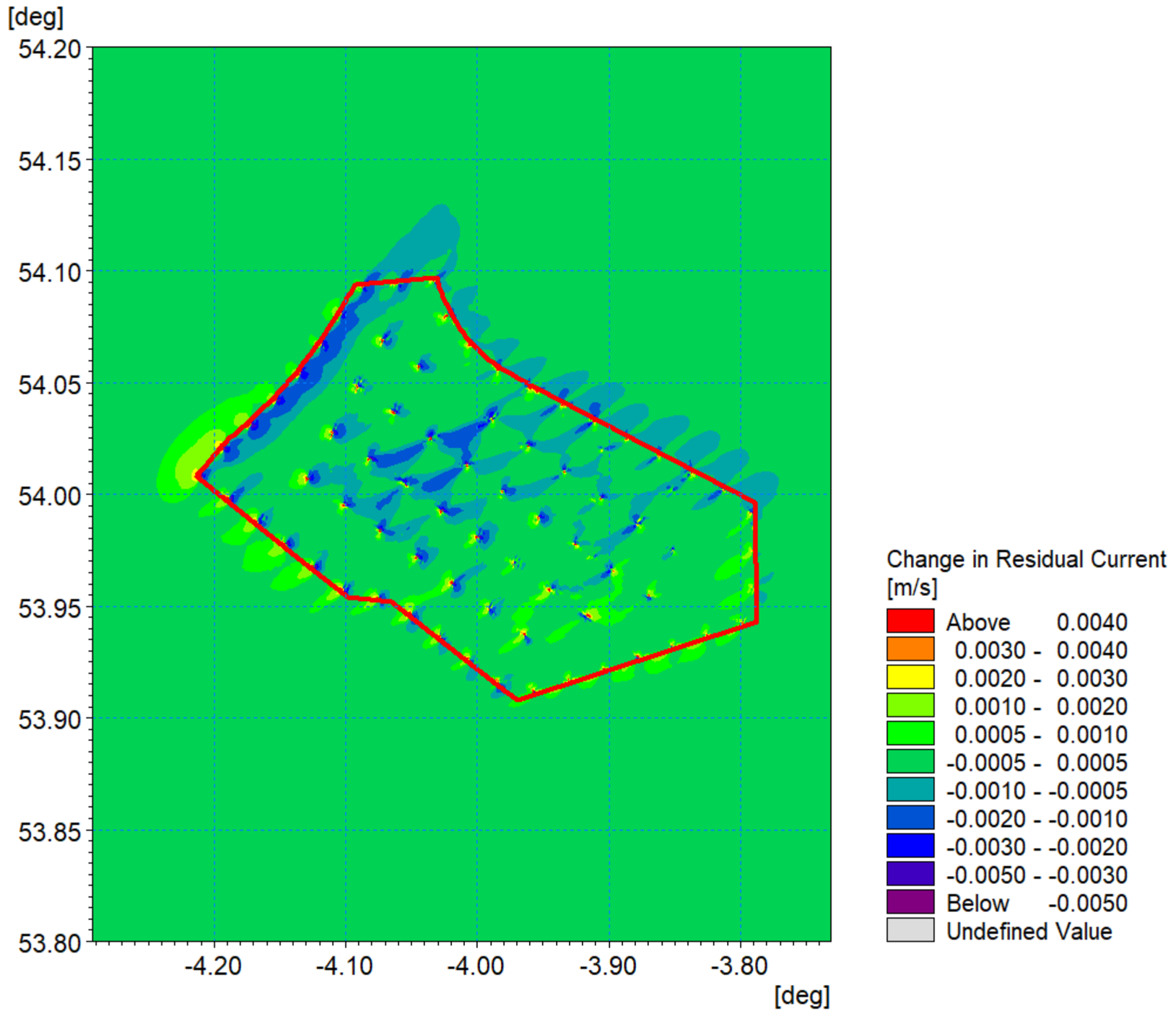

Figure 1.95: Change in residual current 1in1 year storm from 270° spring tide (post-construction minus baseline) detailed view.

1.8 Potential changes during construction

1.8.1.1 In addition to the changes in physical process resulting from the presence of the Morgan Generation Assets, the construction phase influences were quantified. The principal construction elements relate to the transport and fate of sediment brought into suspension due to seabed preparation, the installation of the foundation structures and the laying of inter-array and interconnector cables between the wind turbines and OSPs. An overview of the modelling techniques implemented is provide in Table 1.1.

1.8.1.2 As with the post-construction aspects, the approach was to examine the construction technique which represents the MDS in terms of coastal processes. In practice, these changes are therefore likely to be of lesser magnitude. In each scenario the modelling examined excess SSC arising from the proposed activities (i.e. ambient SSC were not included). Baseline studies outlined in Section 1.6.7 indicate that turbidity levels vary greatly across the domain and throughout the year, being relatively low in deep water areas compared with active sediment transport mechanisms within the estuaries. Therefore, the excess SSC data presented would be applicable independent of the season in which the operations are undertaken.

1.8.1.3 The baseline residual currents and sediment transport modelling has corroborated the knowledge that the east Irish Sea is a sediment sink with active sediment transport processes. Sedimented material arising from the construction phase activities would therefore be amalgamated into the sediment transport regime. The numerical modelling provides DA SSC values and do not therefore differentiate between bed load and water column suspended sediment.

1.8.1.4 During each phase of the assessment the transport of suspended sediment was modelled by undertaking simulations which released sediment at a rate and location appropriate to each type of construction. The sediment released was defined according to the characteristics derived from the BGS data at each specific location. Where a number of locations were encountered, such as a dredging path, then a representative grading was used. The sediment sample locations are presented in Figure 1.56.

1.8.2 Seabed preparation

1.8.2.1 Due to the nature of the seabed in the Morgan Array Area, the cable installation is likely to require seabed preparation in the form of seabed features clearance. The Project Design Envelope (PDE) presented by the project description outlined in volume 1, chapter 3: Project description of the PEIR indicates that sand waves may be cleared for the inter-array and interconnector cabling along up to a 104m wide corridor. Clearance activities may extend along 50% of the inter-array cable route and 60% of interconnector route with an average clearance depth up to 5.1m.

1.8.2.2 The modelling undertaken to quantify the potential increases in SSC and sedimentation simulated the use of a suction hopper dredger to remove material from the crest of sandwaves and deposit material in the adjacent trough area. In practice plough dredging may be undertaken however this type of operation would have less impact in terms of both SSCs and sedimentation footprint.

1.8.2.3 A representative clearance operation was assessed for the inter-array cables which has the same characteristics as clearance for the inter-connector cables. The geophysical survey data was used to identify areas of sandwaves where the operations are most likely to be required. Figure 1.96 indicates the sand areas by yellow shading and the clearance route modelled is specified in green. The clearance was undertaken in a north to south direction with a dredging rate of 10,000m^3/h with a spill of 3%.

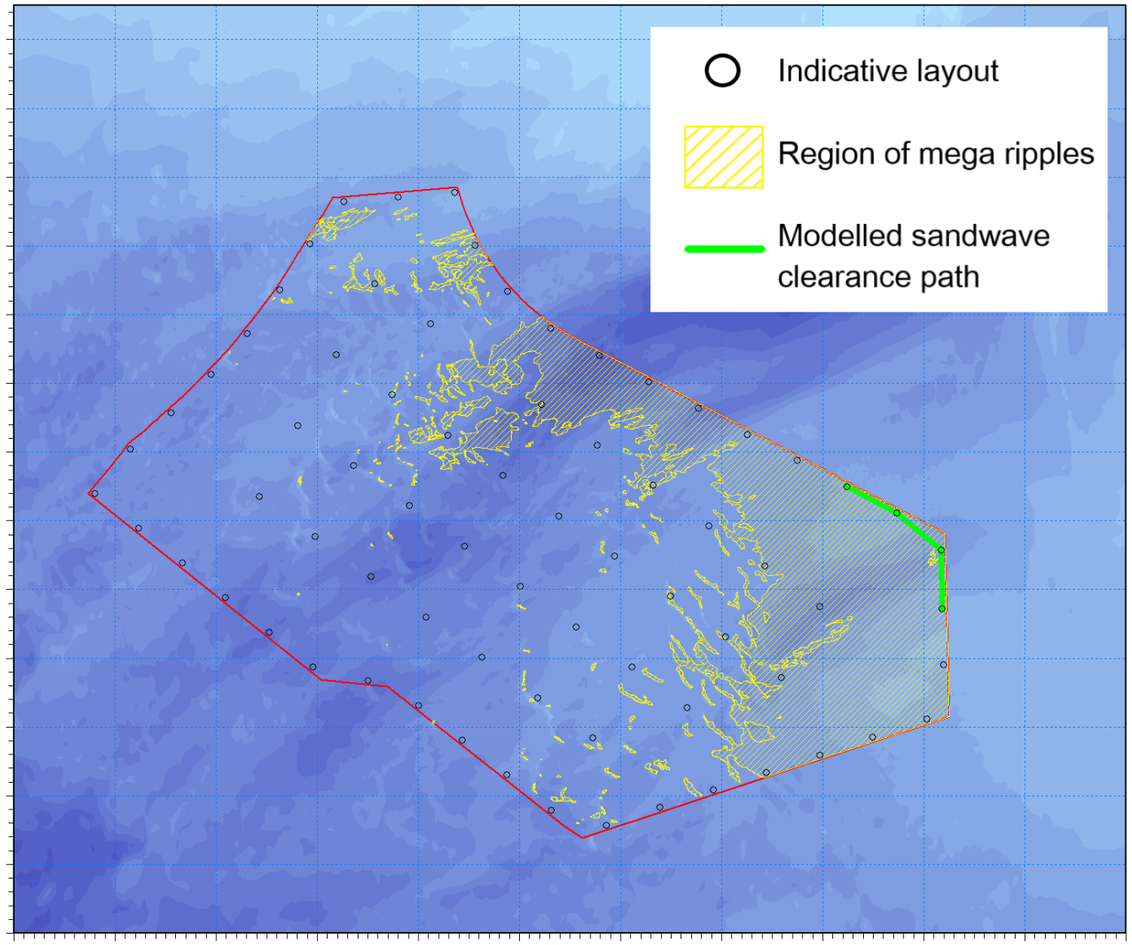

Figure 1.96: Sand wave clearance path modelled.

Inter-array cable sandwave clearance

1.8.2.4 The inter-array cable route was cleared at 100m/h along the 104m wide route for a period of four hours, in line with the dredging rate and removal depth. The material was then deposited over a 45minute period from the hopper with the 5.6km modelled route taking just over two days to prepare with mean tidal conditions. The redistributed material was classified using the properties identified from the sampling undertaken along the route simulated.

- Coarse sand: 28.6%
- Medium sand: 0.5%
- Fine sand: 6.1%
- Very fine sand: 60.2%
- Mud: 4.6%.

1.8.2.5 The SSCs vary greatly during the course of the operation. During the dredging phase, when 3% of the material is spilled at the seabed, the sediment plumes exhibit much lower concentrations. These are typically <50mg/l along the clearance route as shown in Figure 1.97. Similarly, the release phase plume extent is slightly larger than the dredging plume with concentrations reaching 3000mg/l at the dumping site, Figure 1.98. At this site the greatest area of increased SSC, extending a tidal excursion circa 20km from the site, is also associated with re-mobilisation of the deposited material on subsequent tides with concentrations of 500 – 1000mg/l whilst average levels <500mg/l as illustrated in Figure 1.99 and Figure 1.100 respectively.

1.8.2.6 The average sedimentation depth, shown in Figure 1.101 and in detail in Figure 1.102, is up to 0.5mm. The sedimentation one day following the cessation of the clearance operation is presented in Figure 1.103 and Figure 1.104 and shows deposited material at the site of release with depth 0.3mm whilst in the locality lower depths, typically <0.01mm, are present at circa 100m distance from the release with the formation of sandwaves being visible.

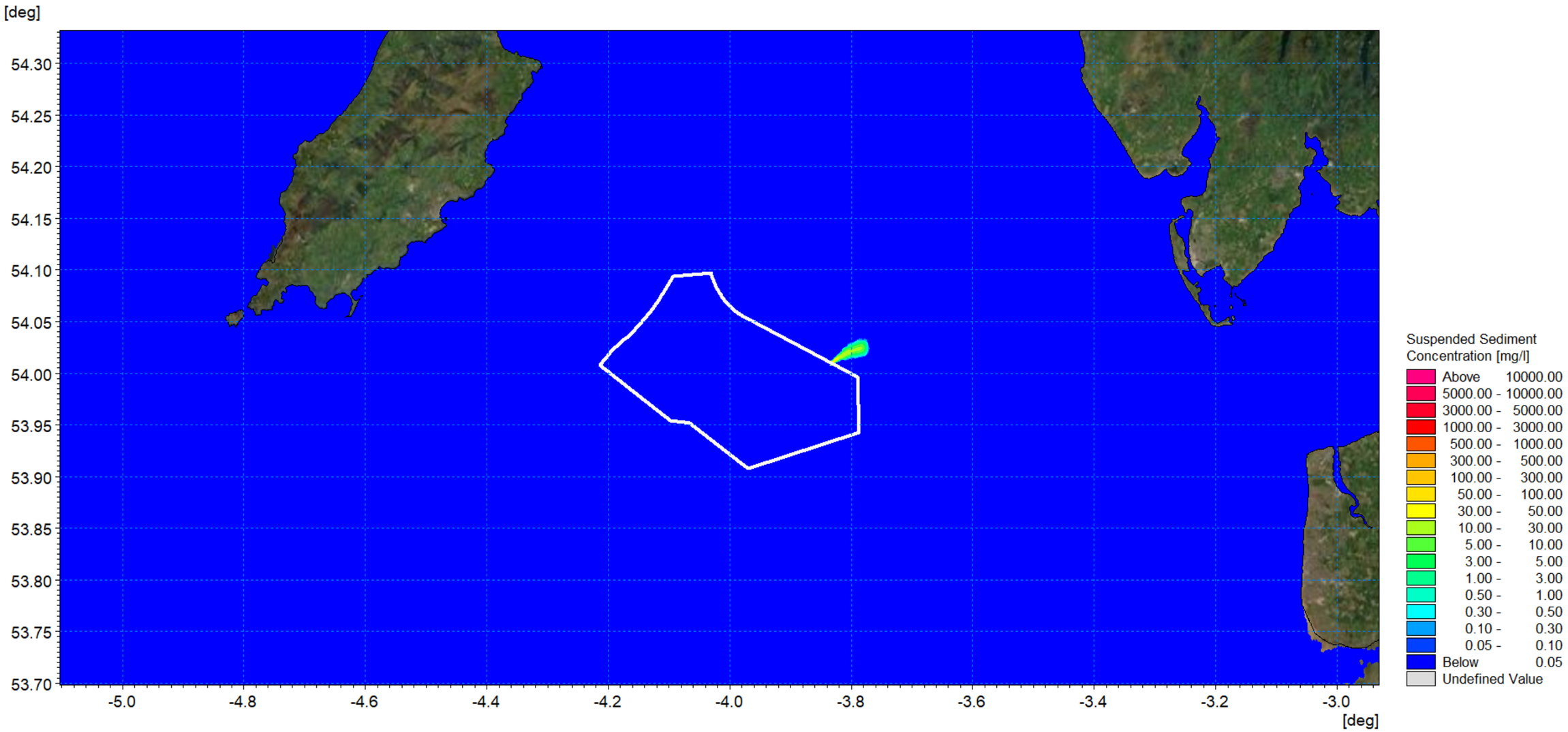

Figure 1.97: SSC during dredging phase– inter-array cable path.

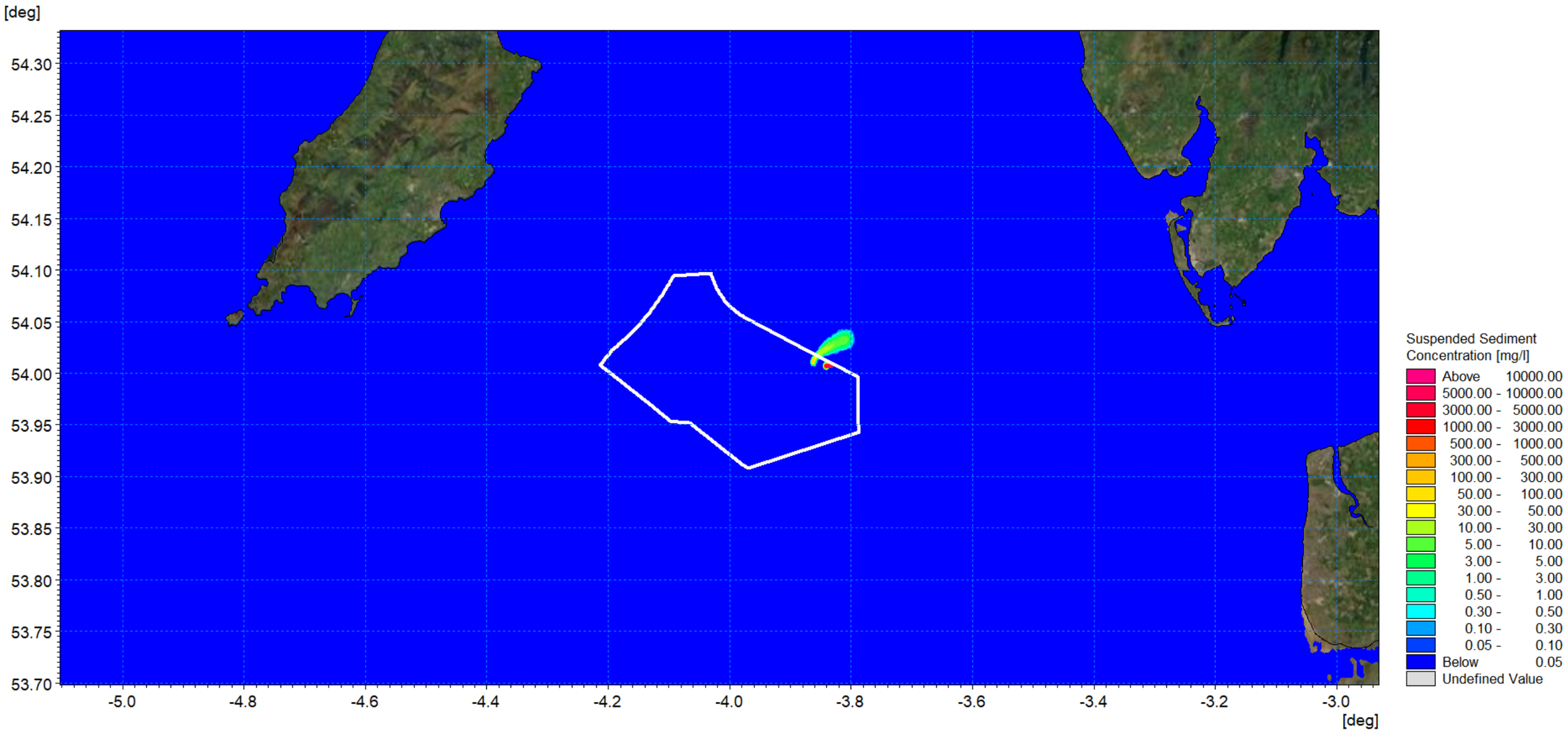

Figure 1.98: SSC during dumping phase– inter-array cable path.

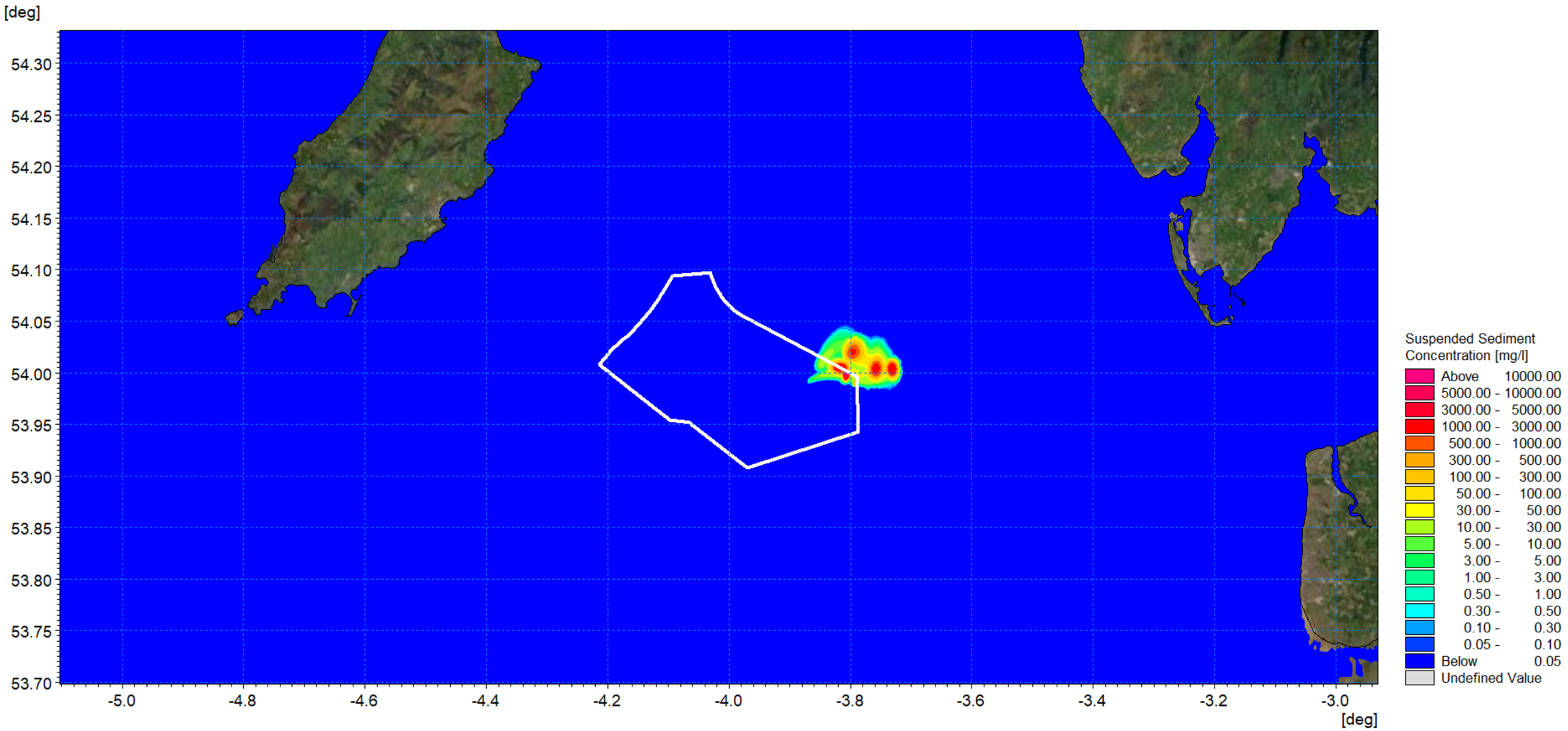

Figure 1.99: SSC with sediment re-mobilisation – inter-array cable path.

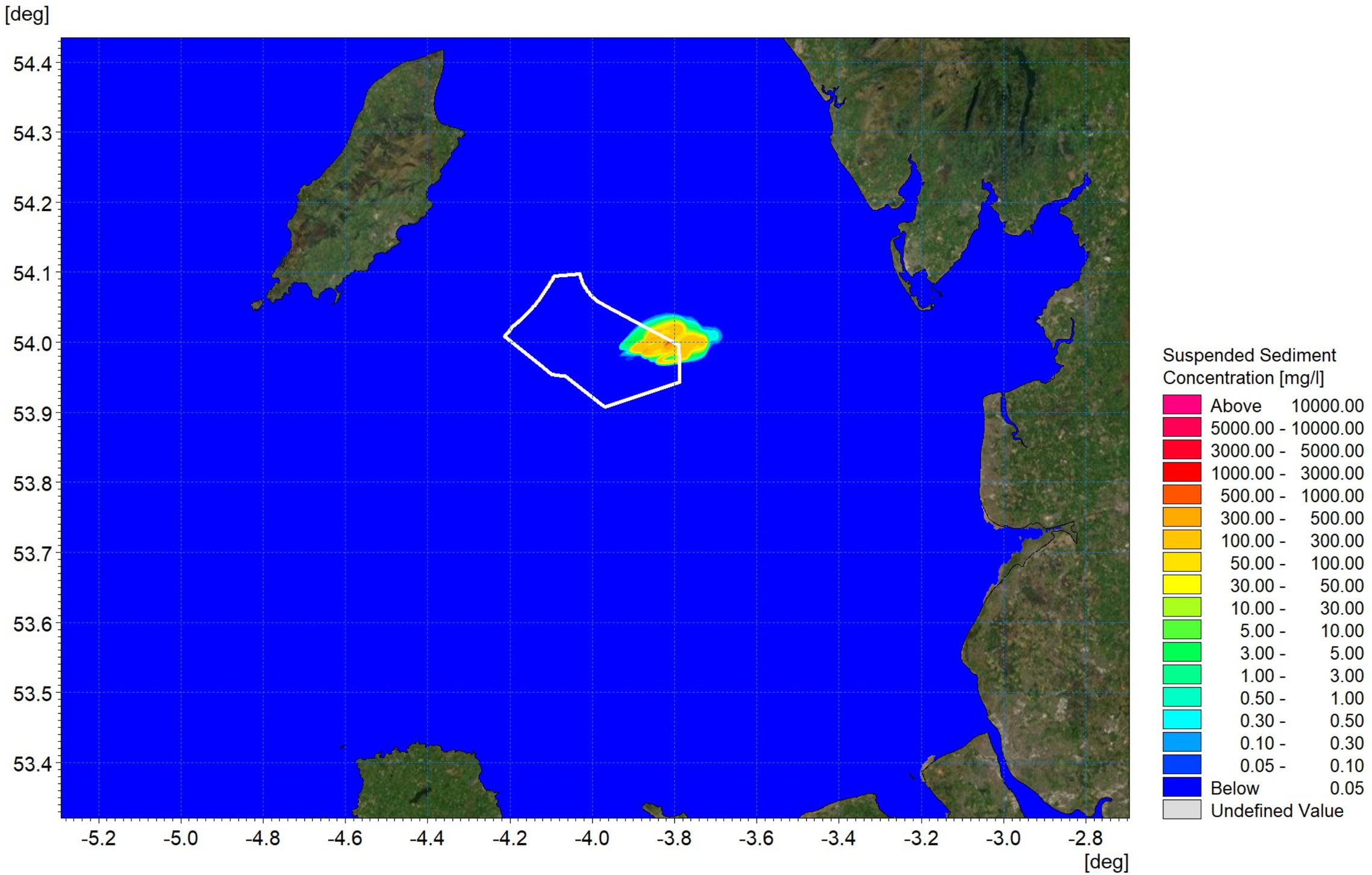

Figure 1.100: Average SSC during operation – inter-array cable path.

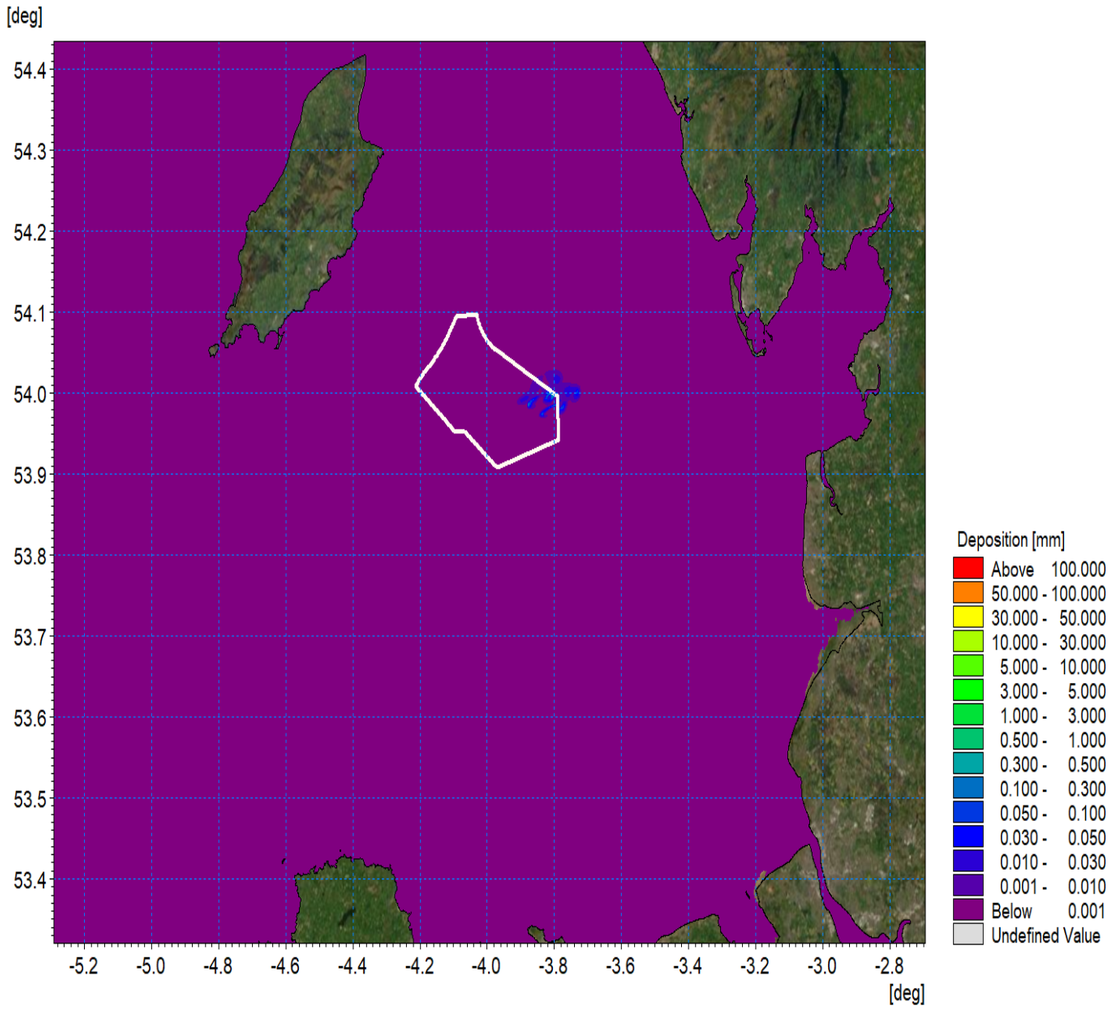

Figure 1.101: Average sedimentation during operation – inter-array cable path.

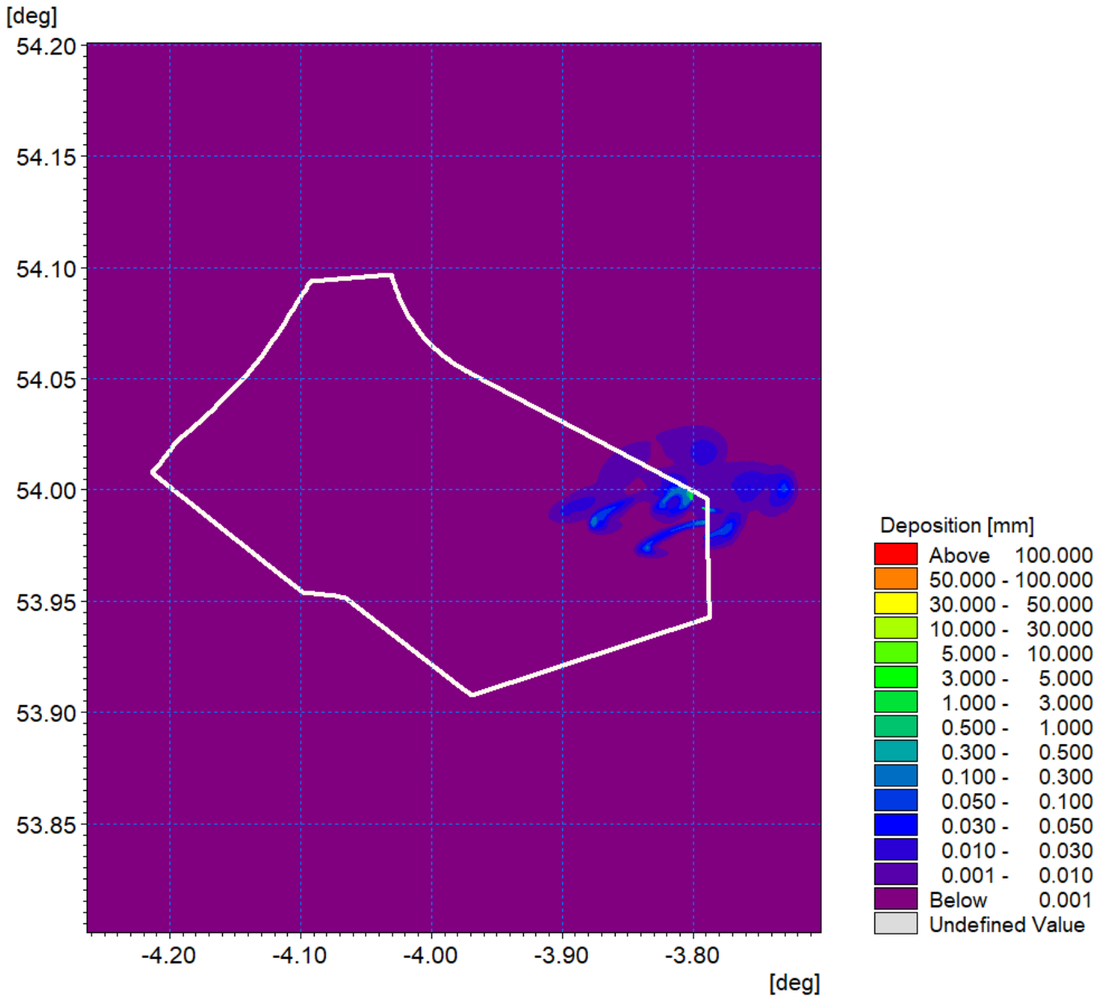

Figure 1.102: Average sedimentation during operation – inter-array cable path detailed view.

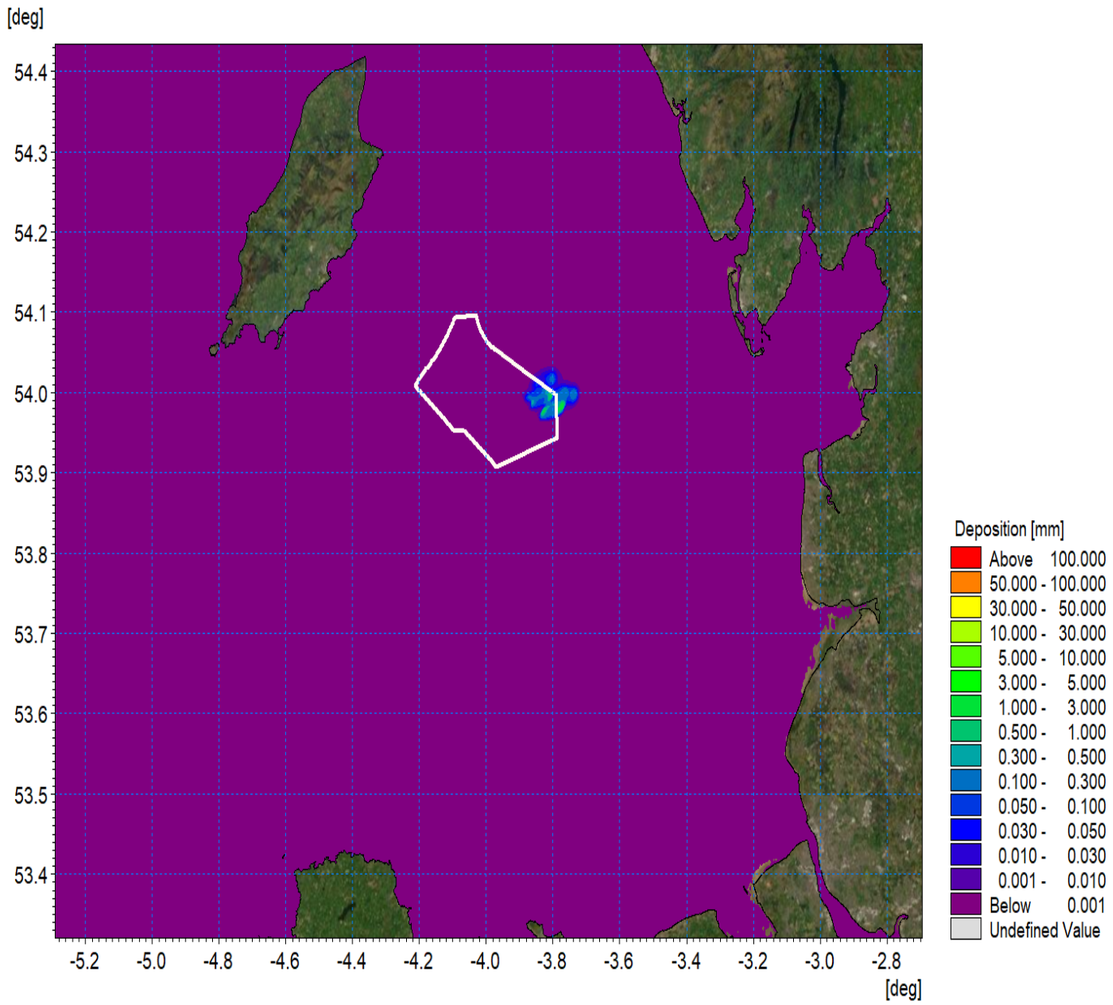

Figure 1.103: Sedimentation 1day following cessation of operation – inter-array cable path.

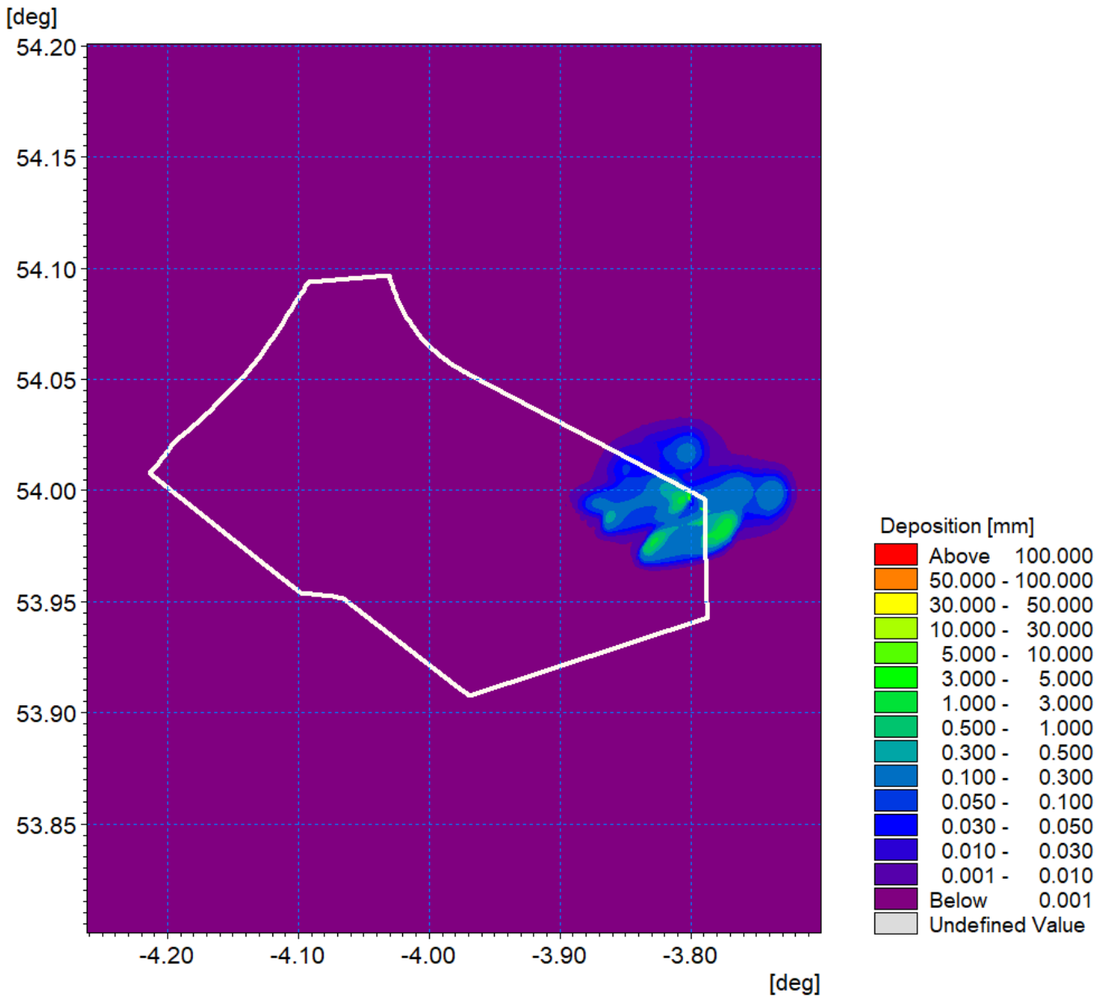

Figure 1.104: Sedimentation 1day following cessation of operation – inter-array cable path detail view.

1.8.3 Foundation installation

1.8.3.1 The project design envelope presented in volume 1, chapter 3: Project description of the PEIR includes a number of potential foundation types including piled and suction caissons foundations. The caissons were applied in the hydrographic assessments as they created the largest potential obstruction to tidal flow and sediment transport however the installation produces much less seabed disturbance than installation of piled foundations. Therefore, the piled structures were assessed in terms of potential increases in SSCs.

1.8.3.2 The largest potential release would be from augured (drilled) piles, where the material would be jetted and released to the water column as a plume. It is anticipated that all piles across the site may require drilling up to the full pile depth. The modelling assumed that at each site the material which is released has a similar composition to the sampled sediment. In reality, to require drilling (rather than driving) the sediments are generally less granular and augured material would be less easily brought into suspension therefore the modelled scenario provides a conservative assessment in terms of SSC.

1.8.3.3 A sample of three representative Pile Installation Scenarios were simulated to cover the range of conditions in terms of water depth, tidal currents and sediment grading. It also took account of the proximity of piling where two concurrent events may take place. The modelling was undertaken using the MIKE MT module which allows the modelling of erosion, transport and deposition of cohesive and non-cohesive/granular sediments. This model is suited to sediment releases in the water column and allows sediment sources which may vary spatially and temporally. In this case, the cohesive functions were not utilised as the material released comprised of sand. The sediment grading was defined for each location and assumed two concurrent drilling operations located at adjacent wind turbine or offshore platform locations to provide the largest augmented sediment plume concentration.

1.8.3.4 At each location it was assumed that the auguring was required to the 60m pile depth for an assumed 16m diameter pile with 0.9m casing as a worst-case scenario (i.e. 13,460m^3 per pile). The drilling rate was taken as 0.89m/h which was both prescribed in the project description presented in volume 1, chapter 3: Project description of the PEIR and allowed the release to cover the full range of tidal conditions. The auguring was undertaken continuously over a 67hour period with material released throughout the water column.

1.8.3.5 For each location a set of results are presented. Firstly, the average suspended sediment plume during the course of the installation is shown. Due to the variation in suspended sediment levels, instantaneous plots of the sediment plumes are also presented during peak flood and ebb tides on two installation days. It should be noted that all the plots require the use of a log scale to cover this range of values whilst providing clarity and during slack water SSCs decrease significantly to values in the order of background levels.

1.8.3.6 The final set of plots relates to sedimentation. Due to the fine sandy nature of the material, it is clear that the sediment will be dispersed. It will be transported mid-tide, settle on slack water and be re-suspended and further dispersed on the resumption of tidal flow. For all simulations, sediment levels after the cessation of construction are presented, using the same contour palette for both the wider extent and detailed figures. The piling activities do not remove any material from the immediate vicinity of the site and the released material returns the native sediment back into the existing sediment transport regime.

Piling scenario A

1.8.3.7 The two piles locations are illustrated in Figure 1.105. The sediment release was modelled over successive neap tidal cycles and at the location coarser material is present with the following composition being implemented within the simulation.

- Gravel: 17%
- Coarse sand: 10.6%
- Medium sand: 63.8%
- Fine sand: 5.2%
- Very fine sand: 3.4%.

1.8.3.8 This location exhibits slightly coarser graded material than at other locations and current speeds are lower during neap tides therefore this presents a scenario with a reduced plume envelope and higher SSC for the range of potential operations. The average suspended sediment plot shown in Figure 1.106 illustrates the effect of the dominant flood tide with the plume envelope extending further to the east. Average concentrations are typically <30mg/l at the sites and reduce rapidly with distance from the two discharge locations. Where the plumes converge concentrations are <1mg/l.

1.8.3.9 Figure 1.107 and Figure 1.108 illustrate the instantaneous concentrations on the flood and ebb tide of the first day of the drilling whilst Figure 1.109 and Figure 1.110 correspond with the same information for the third day. Areas of increased suspended sediment are evident on the latter plots where material has been deposited on slack tide and subsequently re-suspended. Typically, the plume concentration is <50mg/l, and reduces with the distance from the site as the sediment is dispersed.

1.8.3.10 Figure 1.111 and Figure 1.112 show the average sedimentation, with the latter providing a more detailed view. It is evident that sedimentation depths are particularly low with sedimentation values of <0.1mm. This corresponds with the immediate settlement of coarser material fractions, the lower neap current speed and also for the portion of work undertaken on slack tide. Figure 1.113 and Figure 1.114 present sedimentation one day following cessation of the drilling operation. The resulting sedimentation depths are typically <0.1mm one day following the end of drilling demonstrates that the settlement of sediment would be imperceptible to background sediment transport levels.

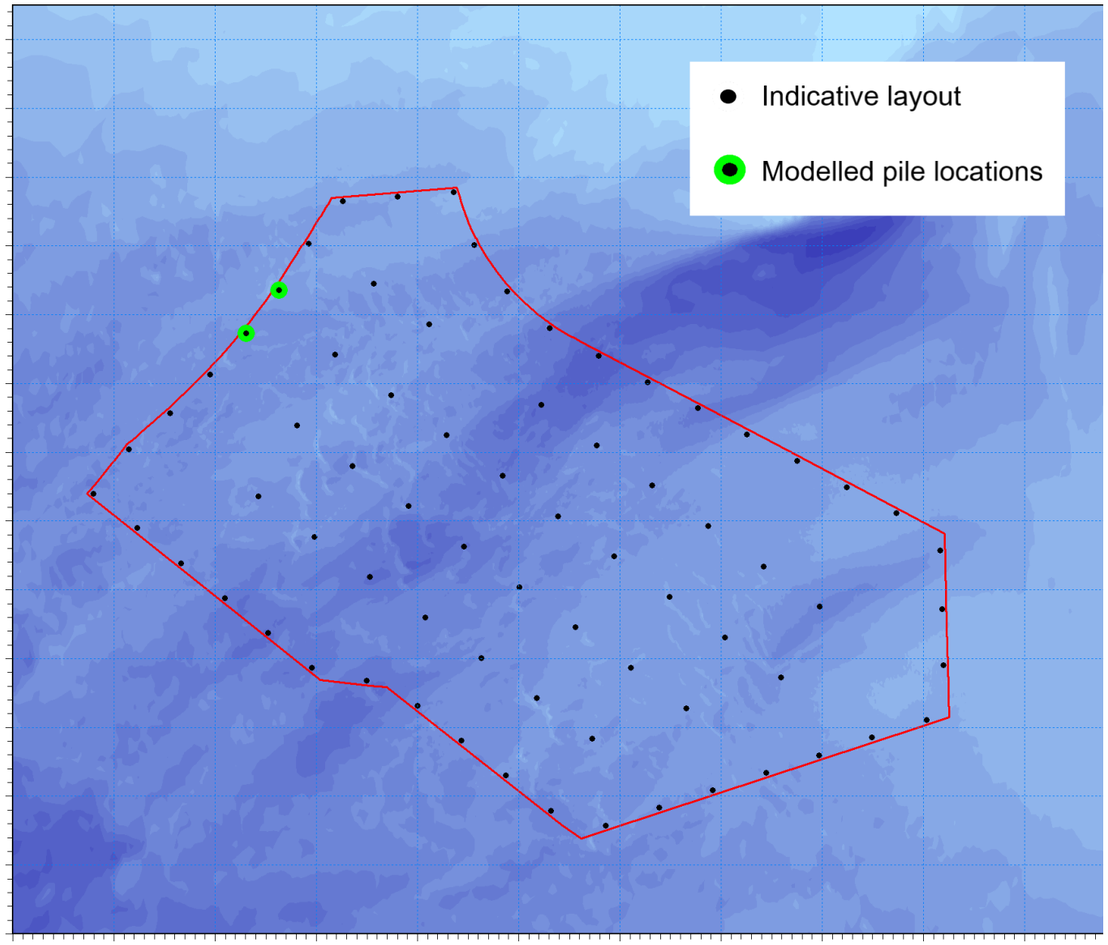

Figure 1.105: Location of modelled piled installation for piling - Scenario A.

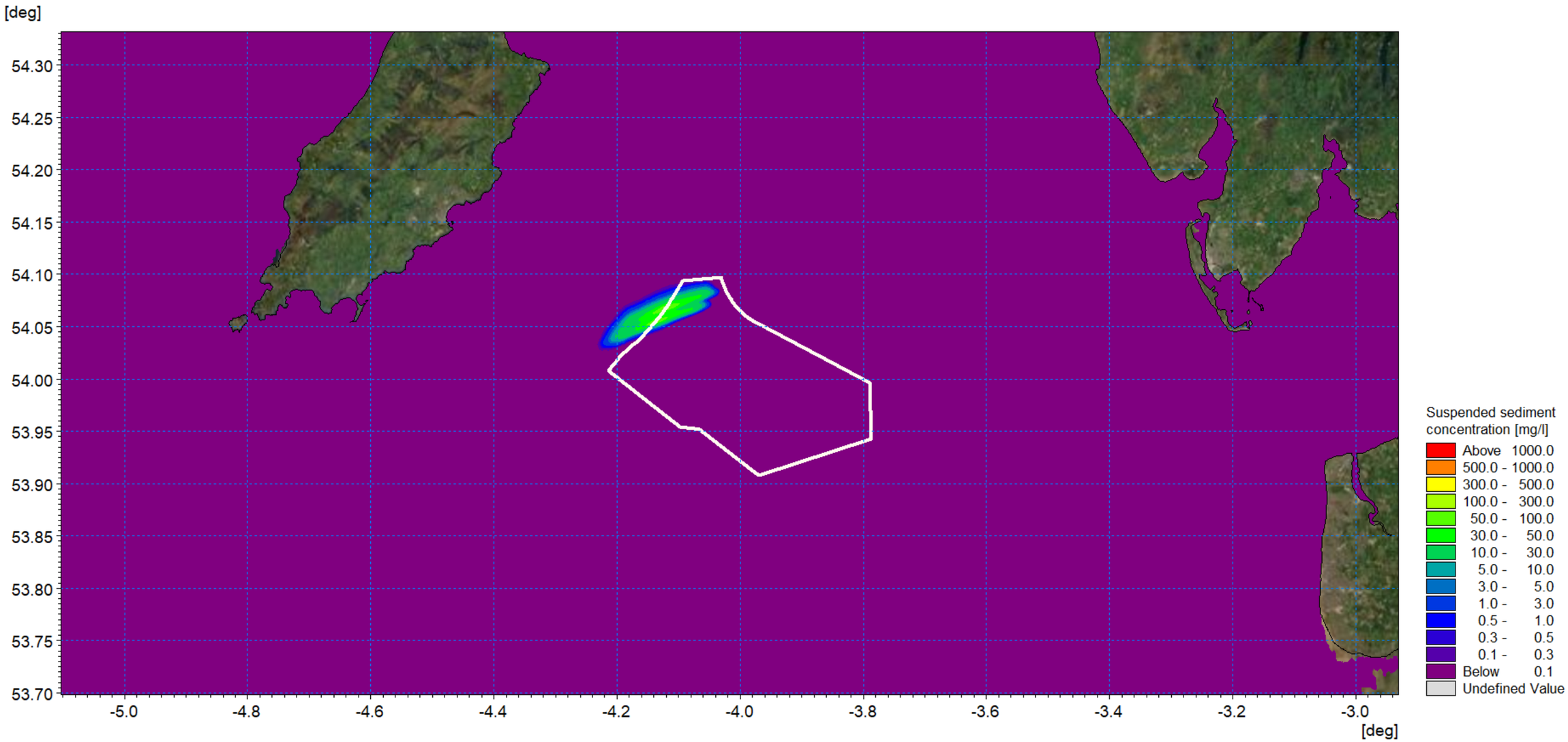

Figure 1.106: Average SSC – Pile Installation Scenario A.

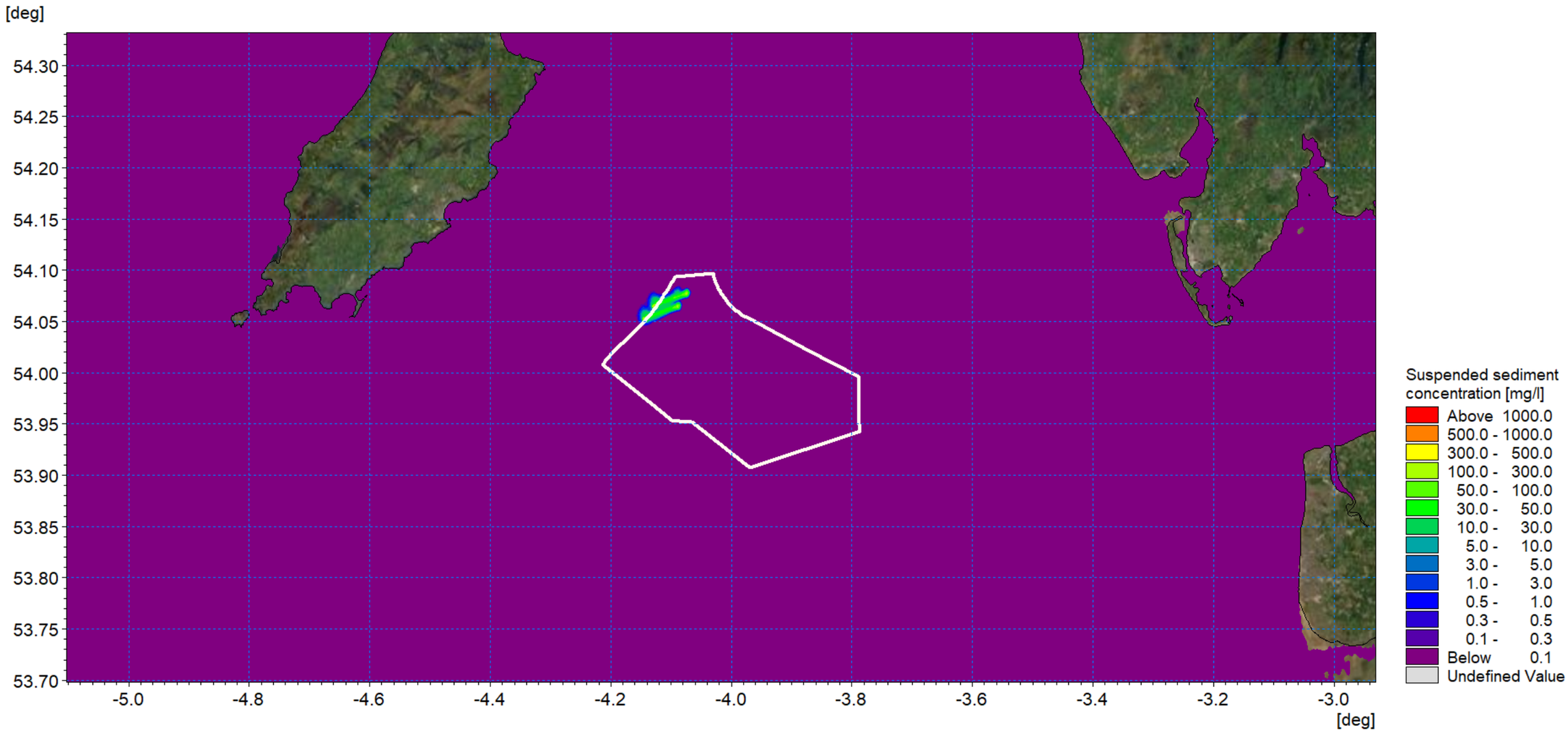

Figure 1.107: SSC day 1 flood - Pile Installation Scenario A.

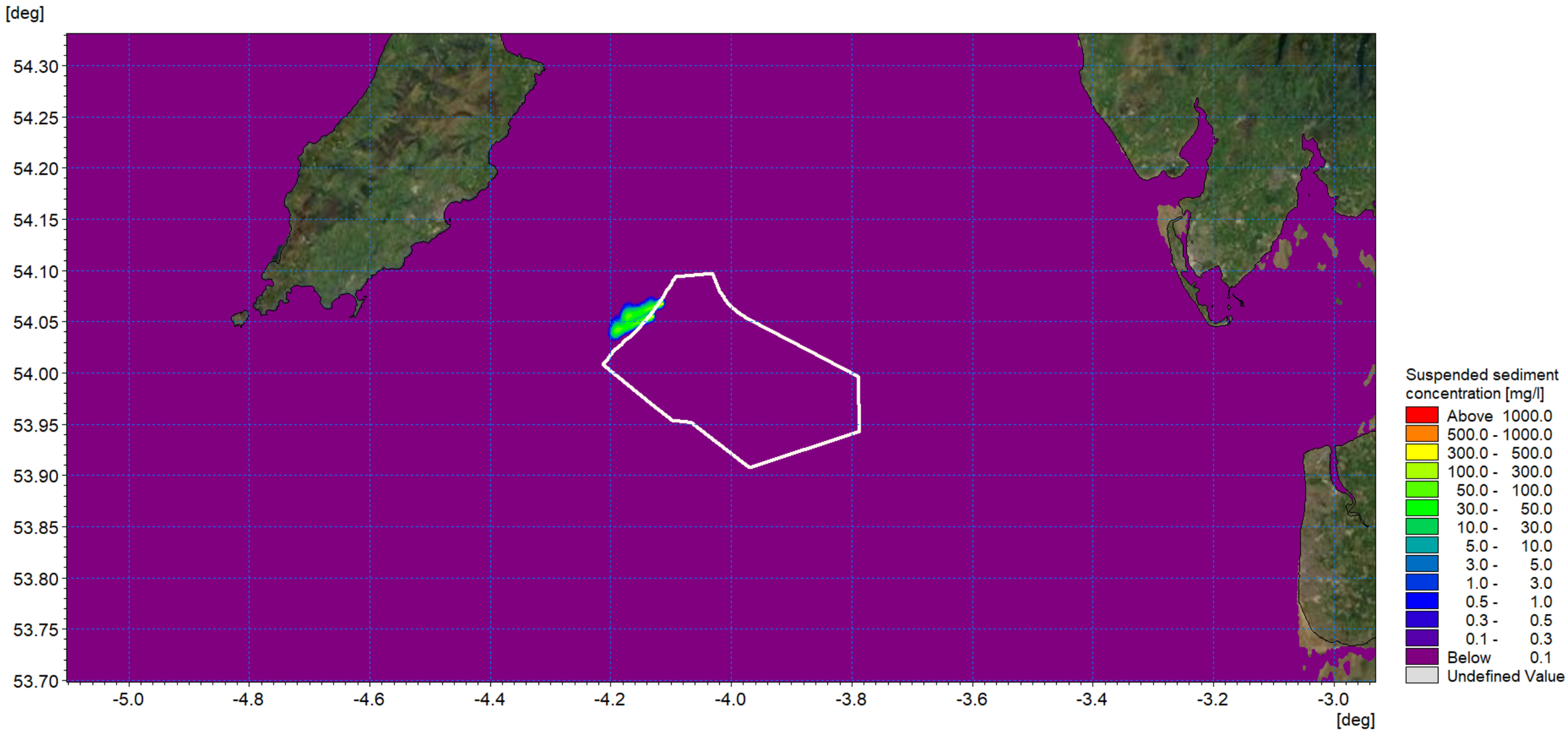

Figure 1.108: SSC day 1 ebb - Pile Installation Scenario A.

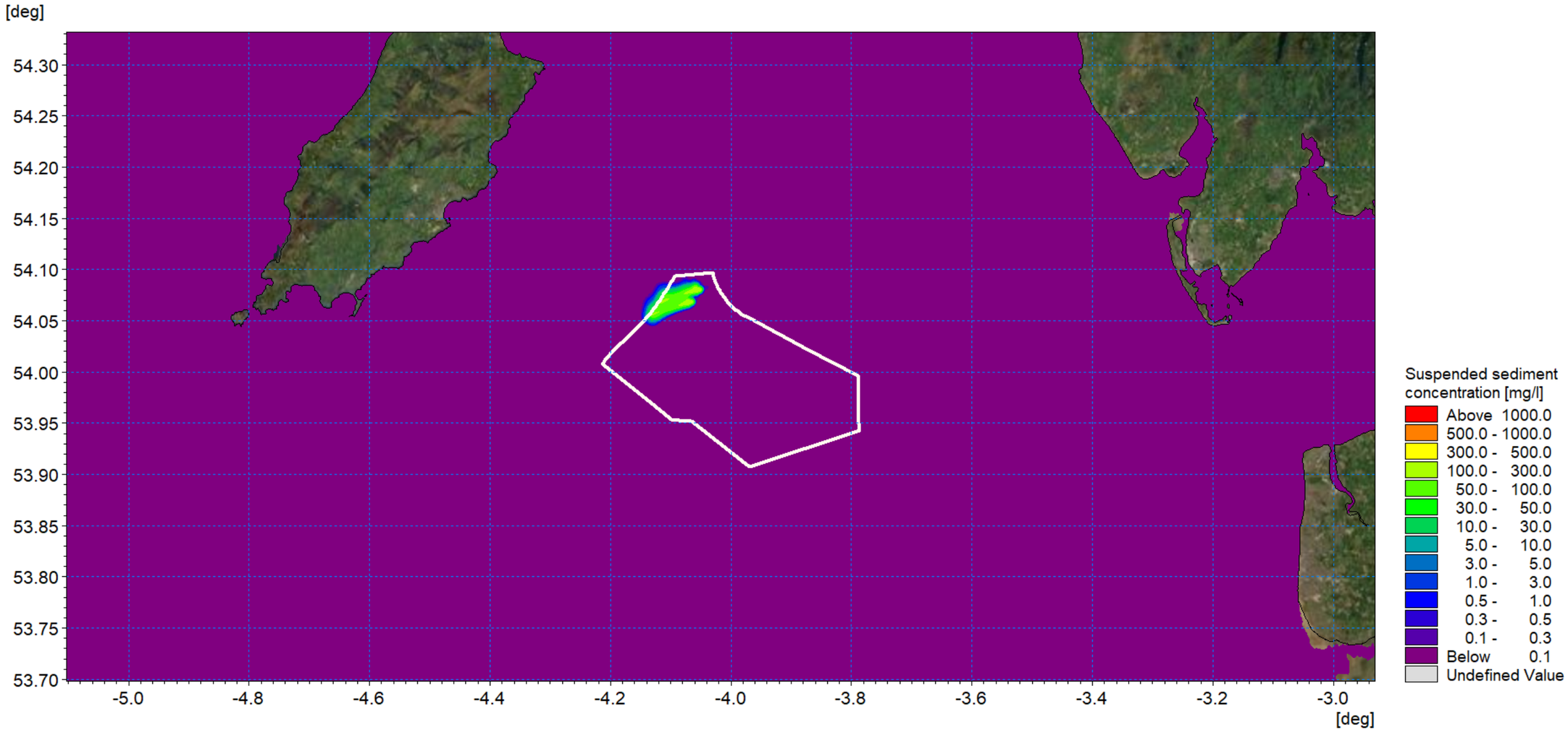

Figure 1.109: SSC day 3 flood - Pile Installation Scenario A.

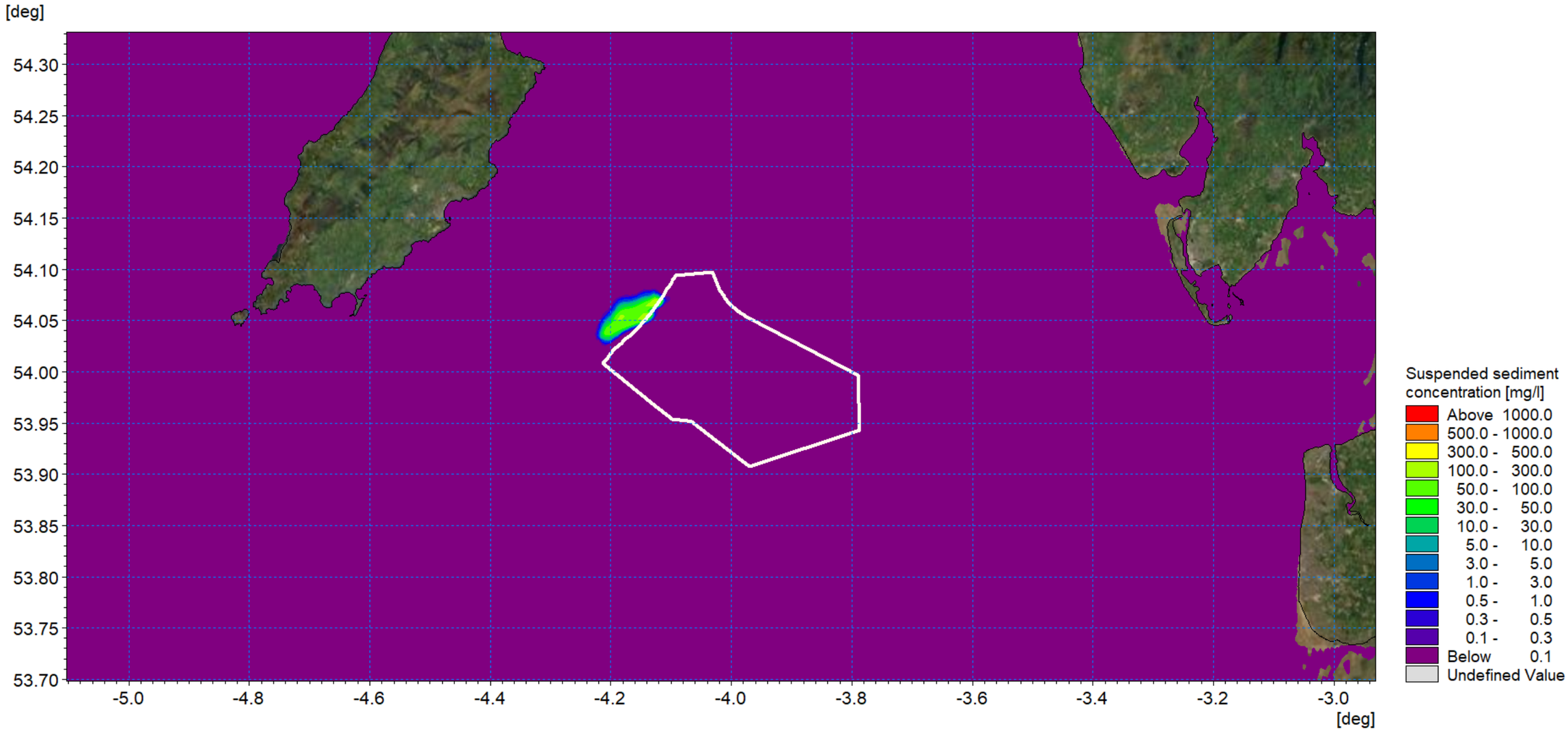

Figure 1.110: SSC day 3 ebb- Pile Installation Scenario A.

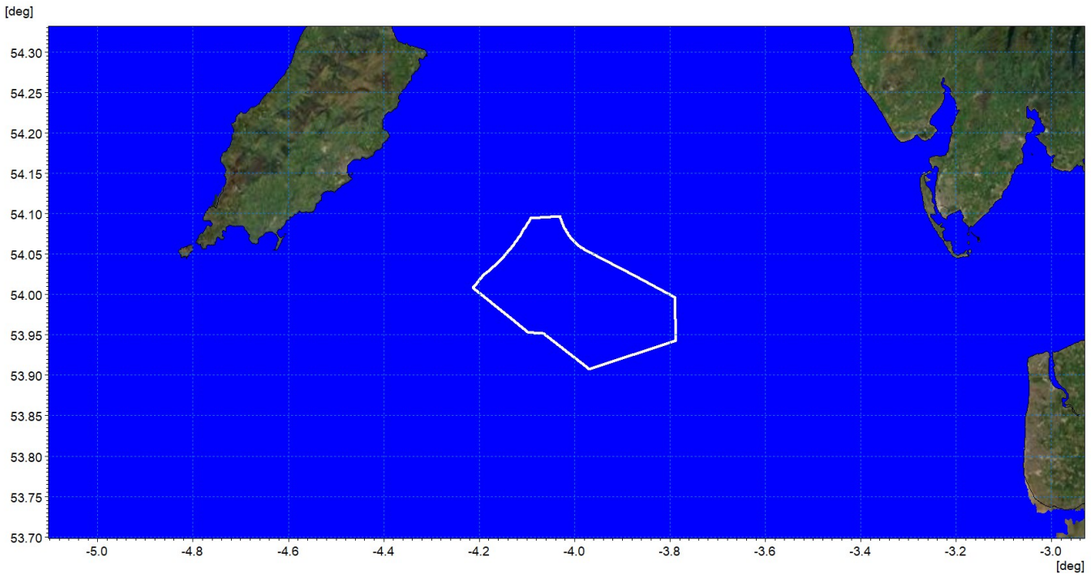

Figure 1.111: Average sedimentation during pile installation – Scenario A.

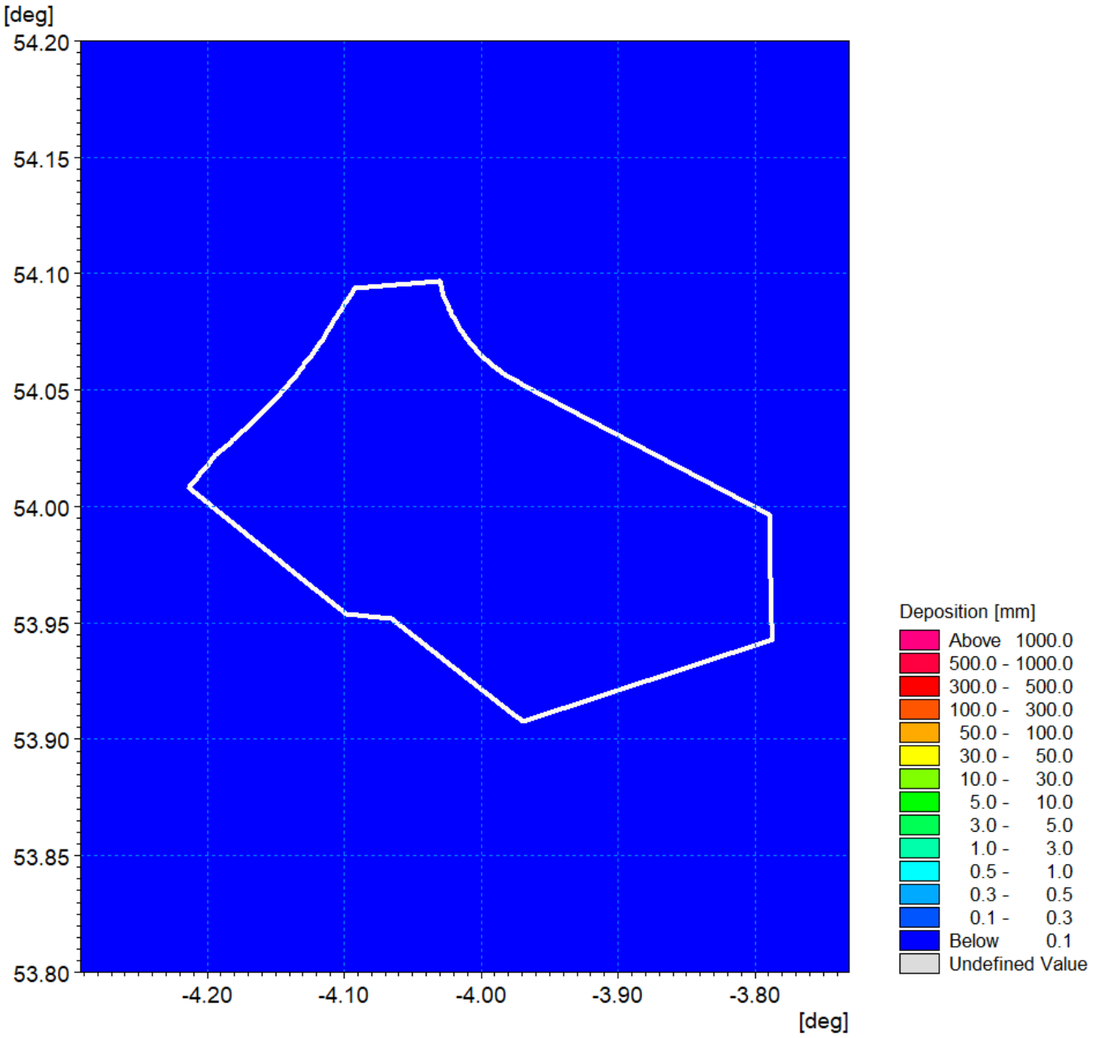

Figure 1.112: Average sedimentation during pile installation – Scenario A detail view.

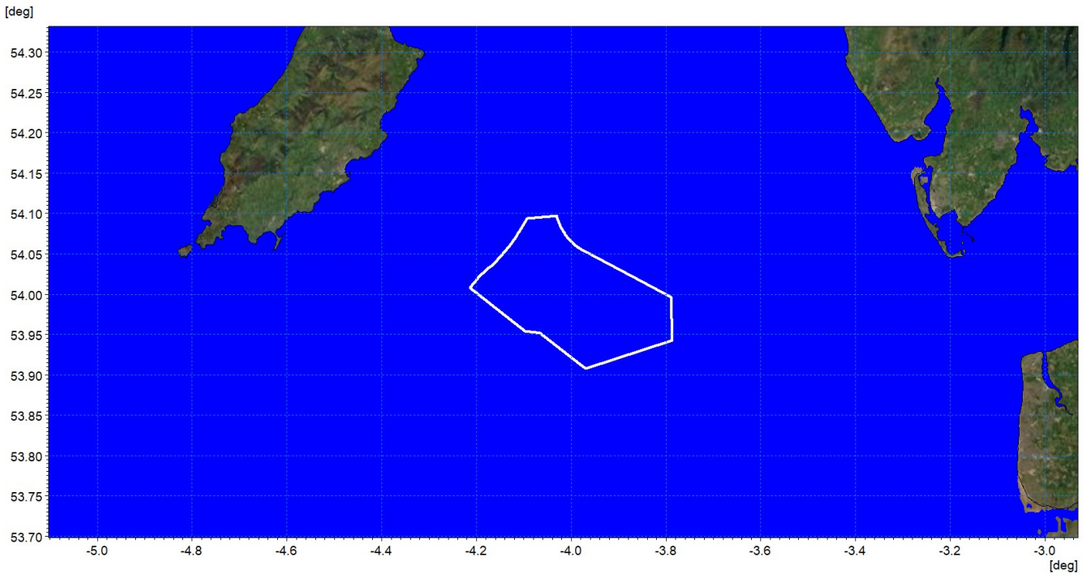

Figure 1.113: Sedimentation 1day following cessation of pile installation – Pile Scenario A.

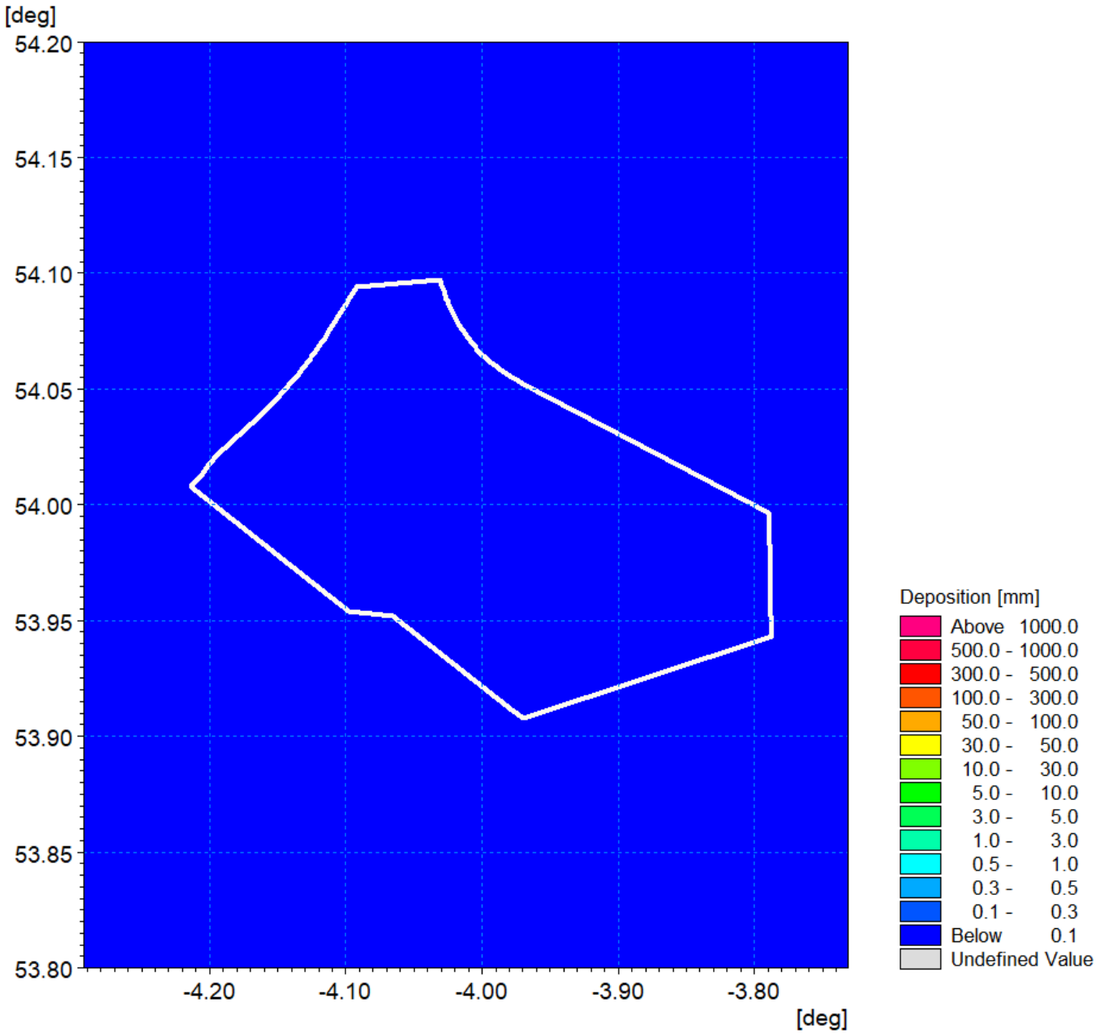

Figure 1.114: Sedimentation 1day following cessation of pile installation – Pile Scenario A detail view.

Piling scenario B

1.8.3.11 The piling locations are sited in the centre of the Morgan Array Area at the north boundary as shown in Figure 1.115. The simulation was undertaken during spring tides and at this location finer sediment and sandwaves are present. The following composition was implemented within the modelling.

- Coarse sand: 28.6%
- Medium sand: 0.5%
- Fine sand: 6.1%
- Very fine sand: 60.2%
- Mud: 4.6%.

1.8.3.12 The average suspended sediment plume envelope is shown in Figure 1.116. As anticipated the extent of the envelope is greater than that for the previous scenario as it was undertaken during spring tides when peak currents are typically double that of neap tides. It may be expected that the subsequent concentrations would be lower as the water depths are similar at the two locations however the stronger currents and finer material means that a greater proportion of the material is in suspension. The instantaneous figures for day one and three, ebb and flood tides are presented in Figure 1.117 to Figure 1.120, where peak concentrations are circa 50mg/l and average values are typically less than one fifth of this magnitude. At this location the transport cycle is also evident with material settling out on slack tides and becoming re-suspended with increasing current speeds.

1.8.3.13 The highly dispersive nature of spring tidal currents coupled with a portion of work undertaken on slack tide and the finer material located at this site results in average sedimentation levels <0.1mm as illustrated in Figure 1.121 and Figure 1.122. The resulting sedimentation depths after one day following cessation of the two drilling operations is shown in Figure 1.123 and Figure 1.124 and are typically less than 0.1mm and demonstrate that this settlement would be imperceptible from the background sediment transport activity.

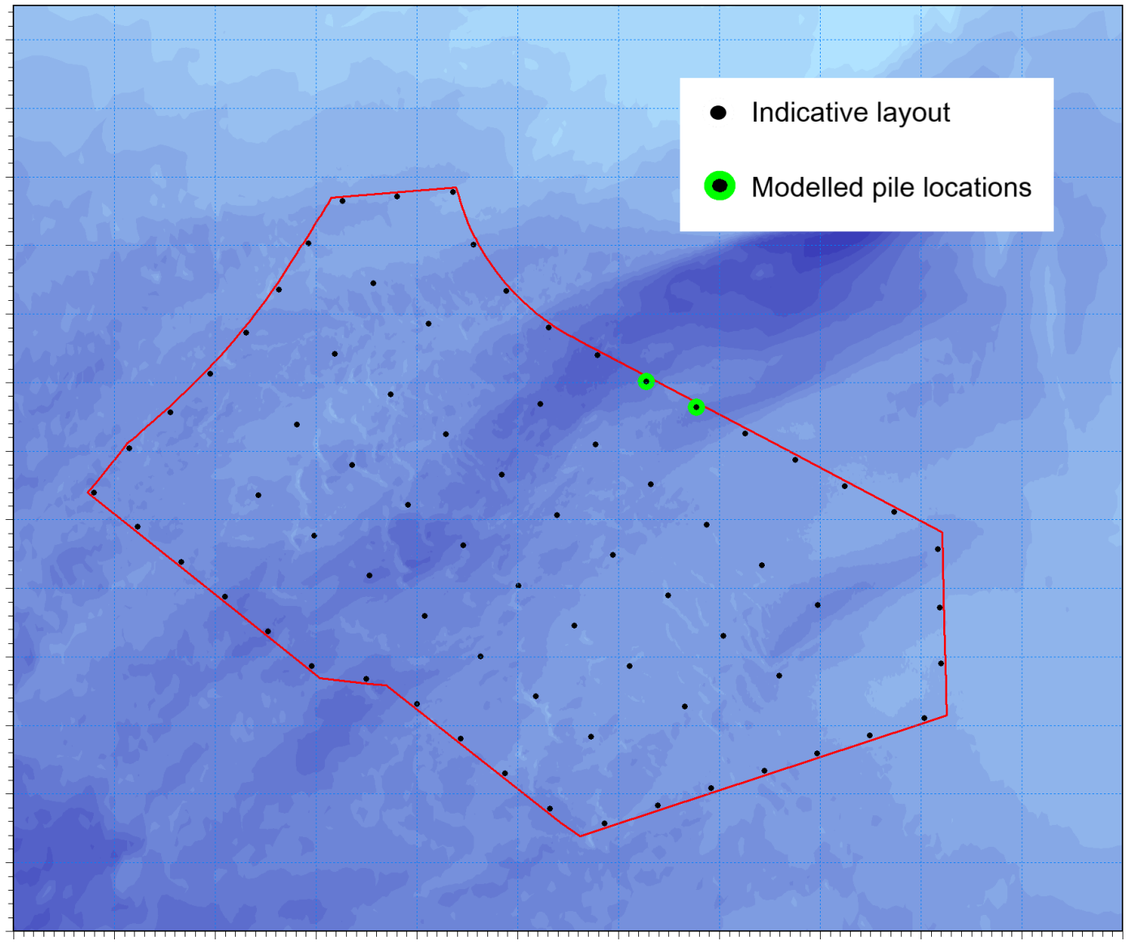

Figure 1.115: Location of modelled piled installation for piling Scenario B.

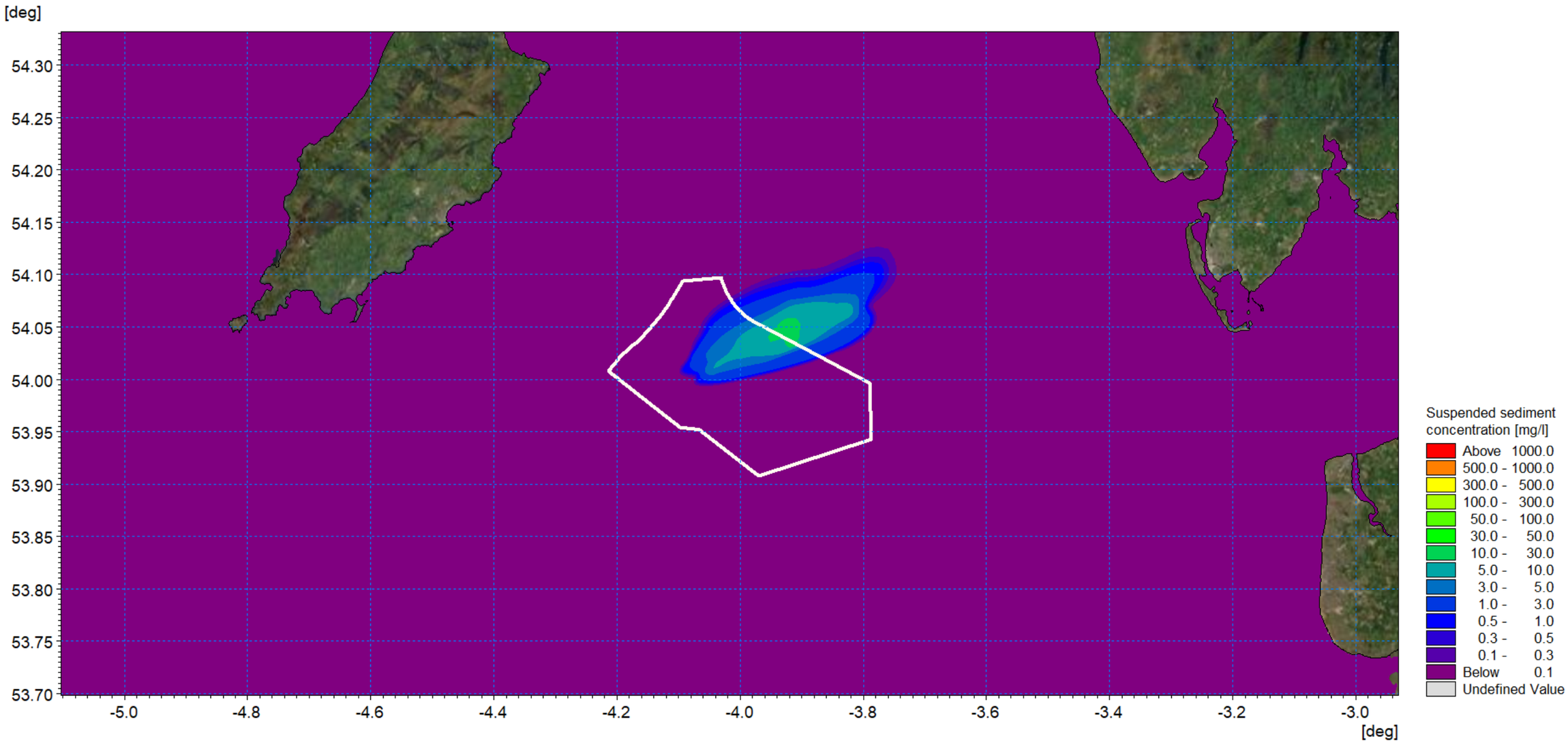

Figure 1.116: Average SSC – Pile Installation Scenario B.

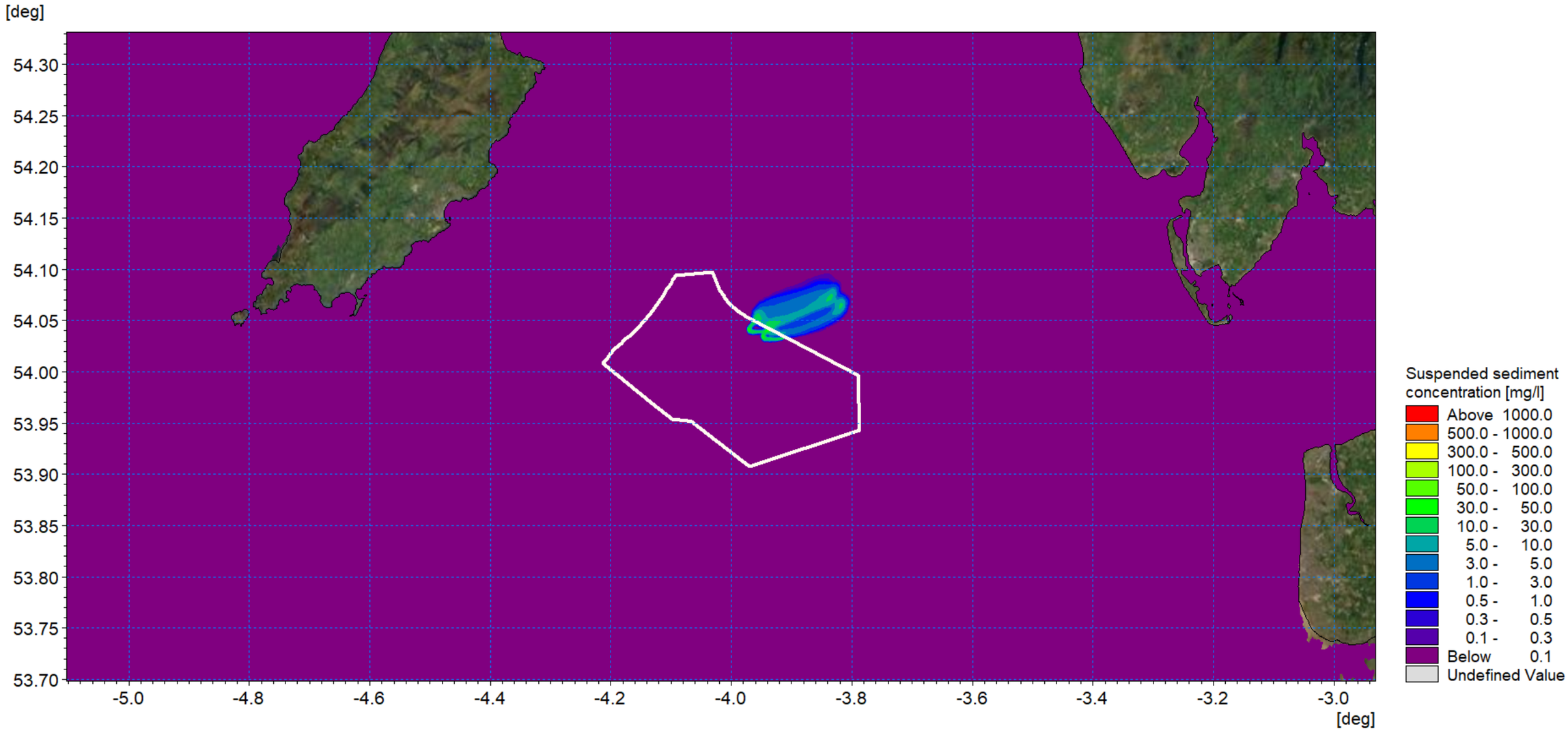

Figure 1.117: SSC day 1 flood- Pile Installation Scenario B.

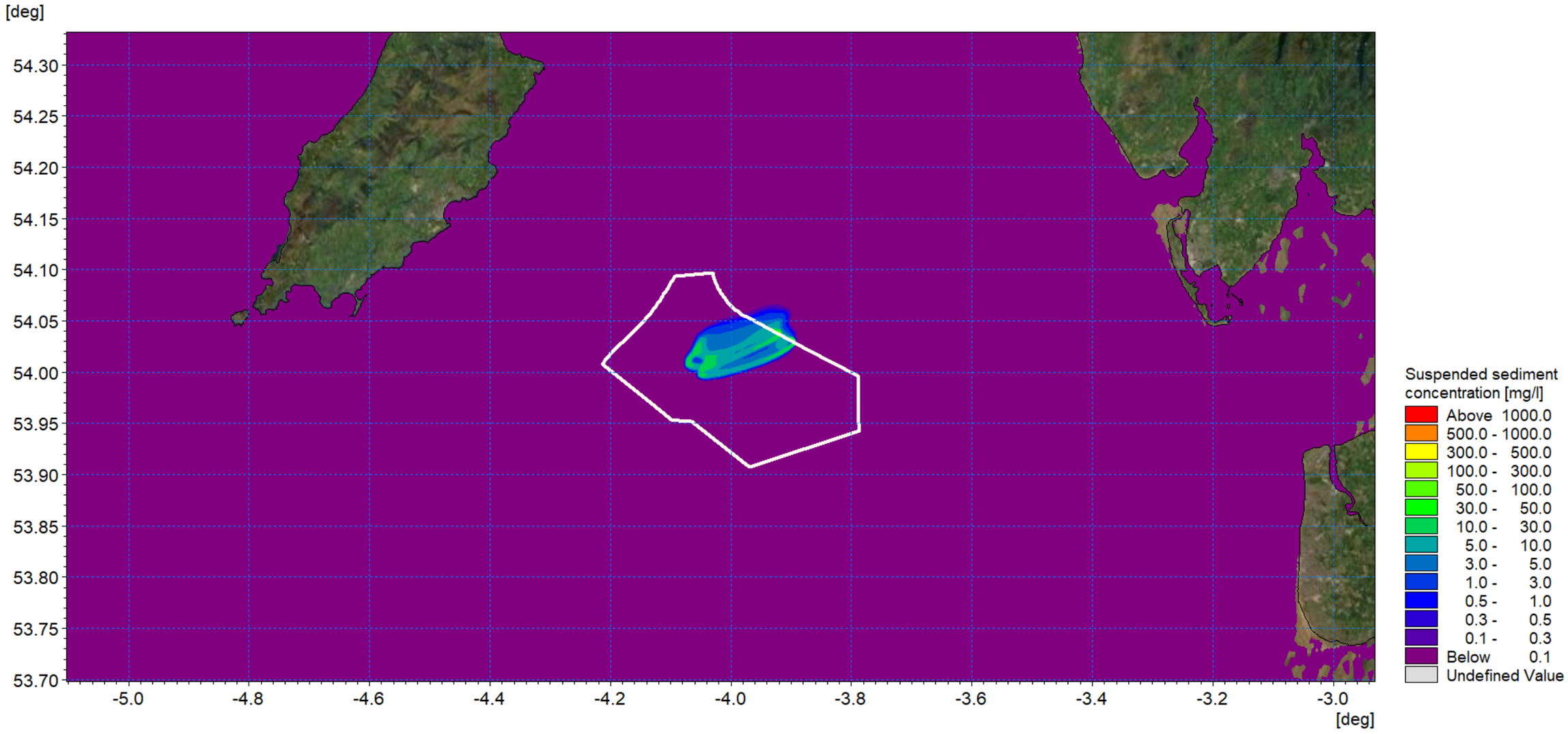

Figure 1.118: SSC day 1 ebb- Pile Installation Scenario B.

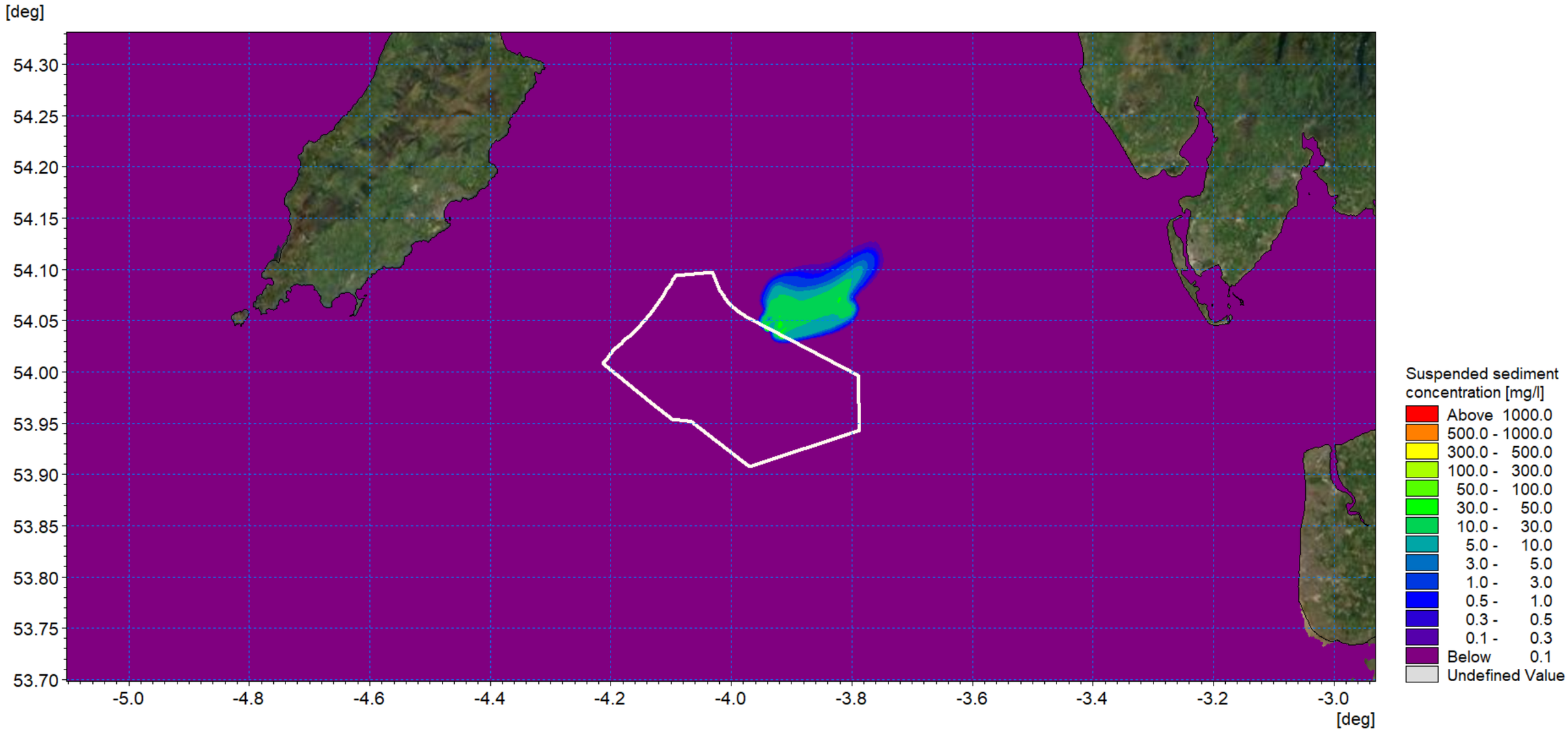

Figure 1.119: SSC day 3 flood- Pile Installation Scenario B.

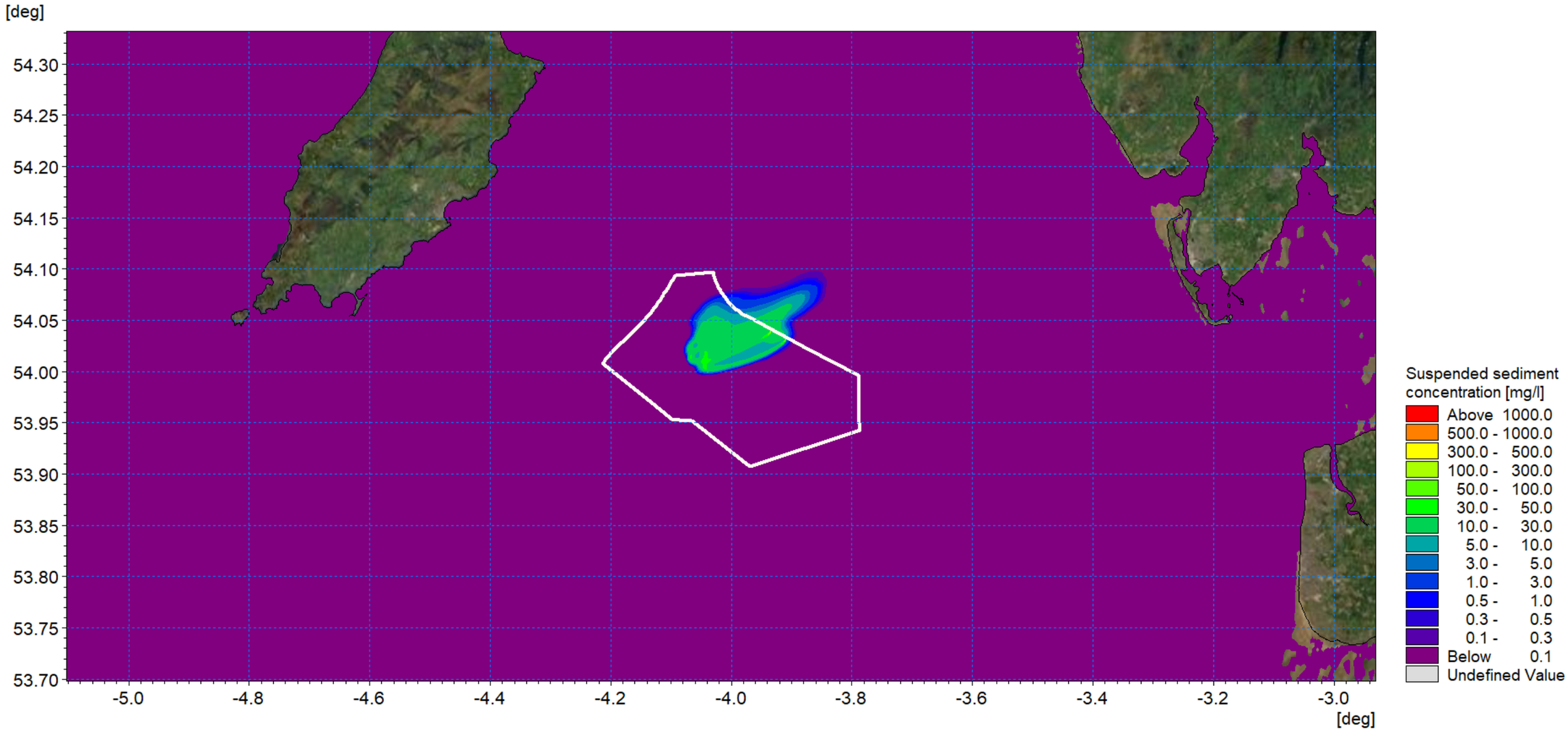

Figure 1.120: SSC day 3 ebb- Pile Installation Scenario B.

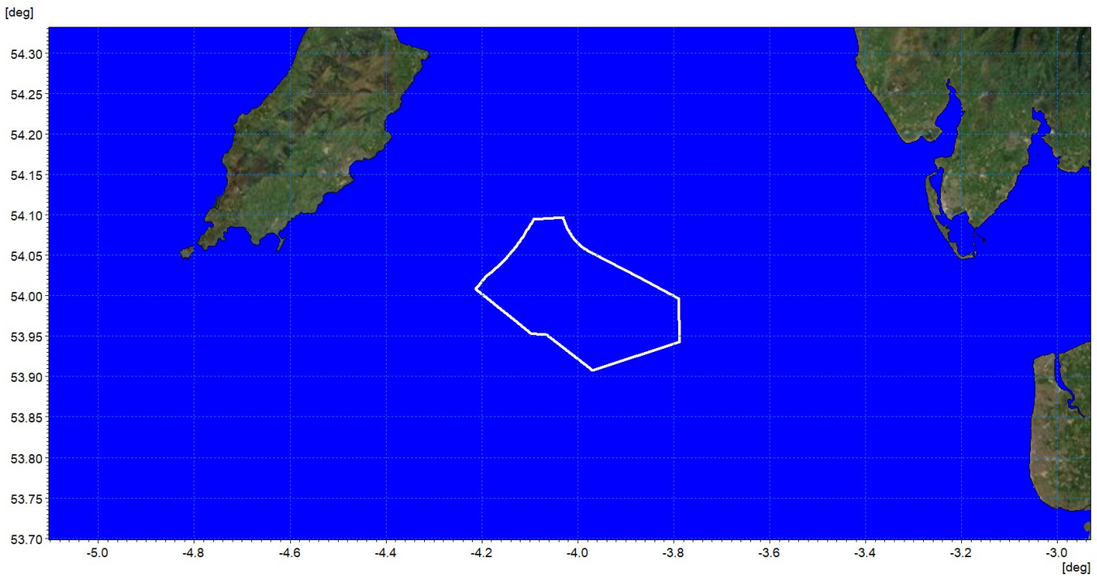

Figure 1.121: Average sedimentation during pile installation – Scenario B.

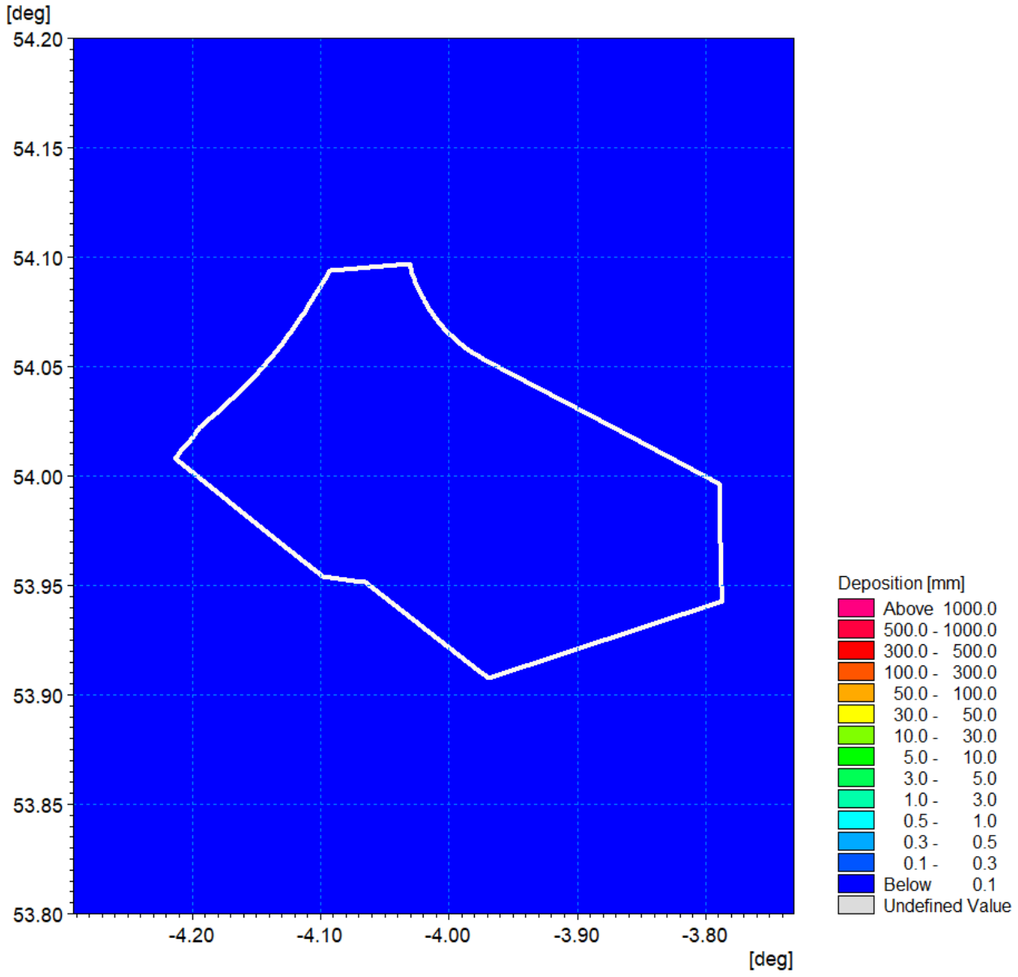

Figure 1.122: Average sedimentation during pile installation – Scenario B detail view.

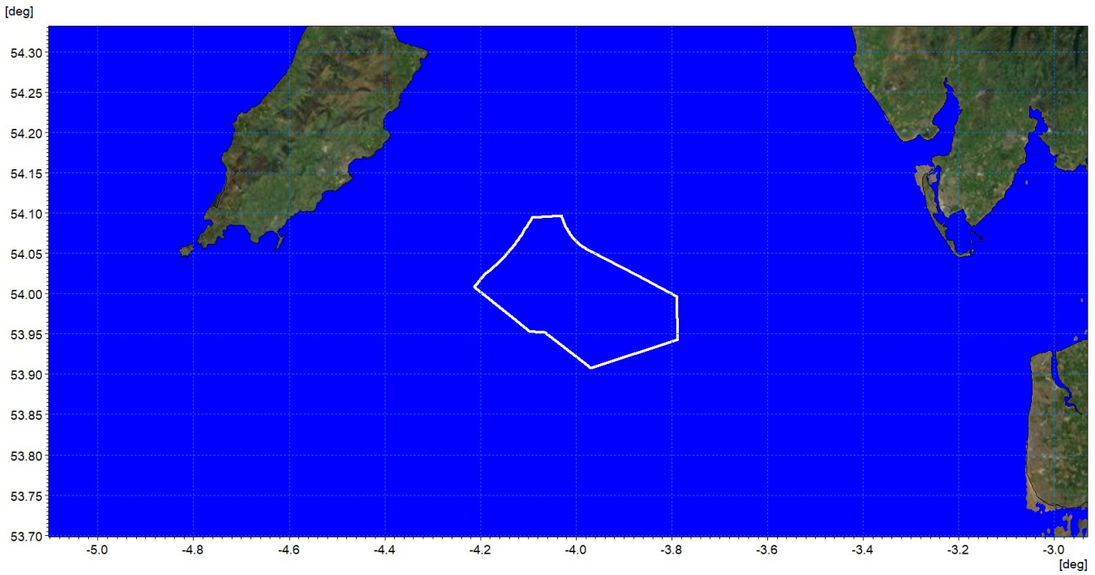

Figure 1.123: Sedimentation 1day following cessation of pile installation – Pile Scenario B.

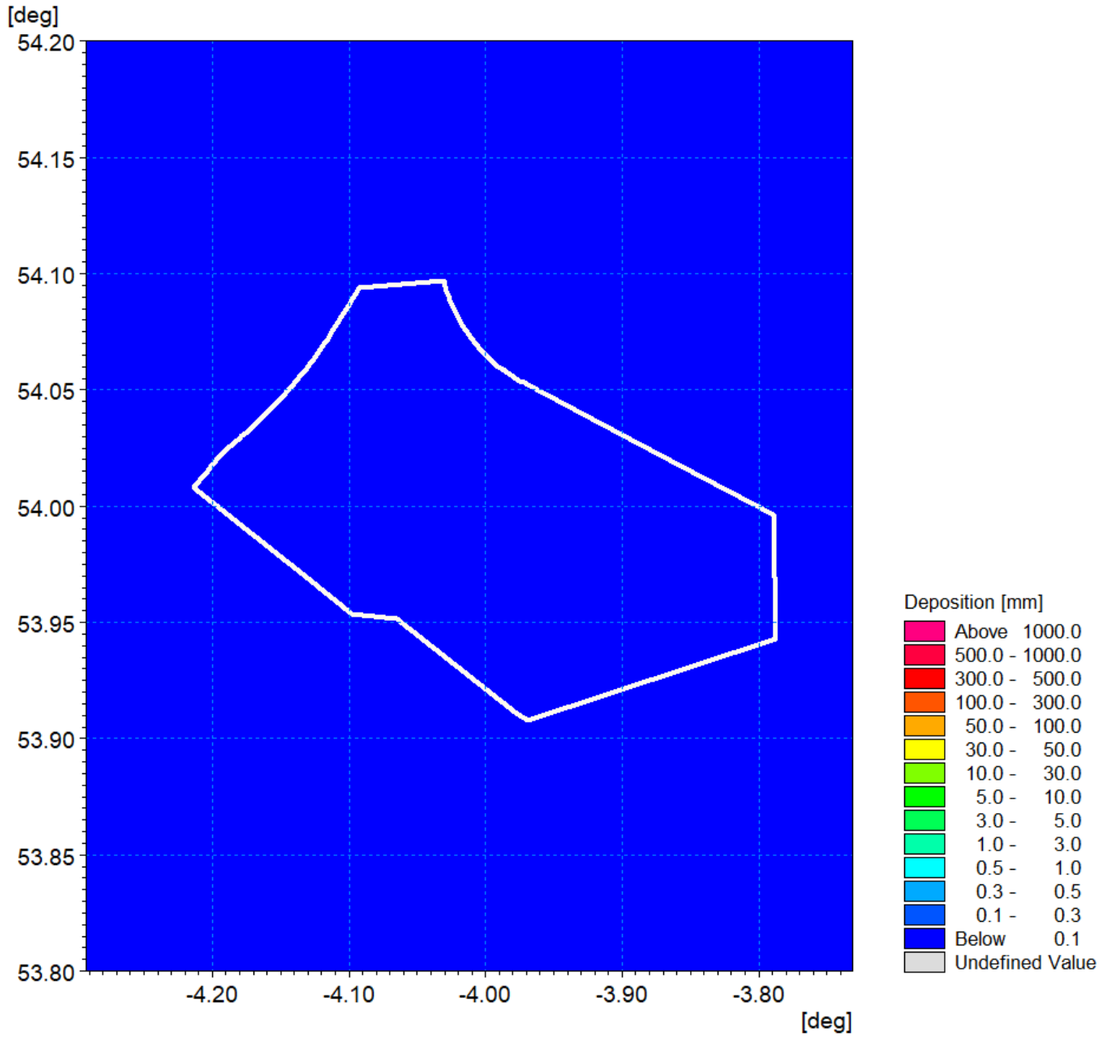

Figure 1.124: Sedimentation 1day following cessation of pile Installation – Pile Scenario B detail view.

Piling scenario C

1.8.3.14 The piling locations are illustrated in Figure 1.125 and they are orientated in alignment with the tidal current to provide an augmented plume scenario under mean tidal currents. The sediment composition at this location comprised sandy sediments similar to those at scenario B as follows.

- Coarse sand: 28.6%
- Medium sand: 0.5%
- Fine sand: 6.1%
- Very fine sand: 60.2%
- Mud: 4.6%.

1.8.3.15 The average plume envelope shown in Figure 1.126 has a similar extent to the circa 25km shown in the spring tide scenario B; this is accounted for by the average tidal range coupled with the orientation of the releases. Average concentrations of circa 50mg/l are evident where the plumes coalesce. This is similar to the unmerged values as the plumes are travelling in concert with the tide (and not towards one another) and at the point that the plume reaches the adjacent discharge it is highly dispersed.

1.8.3.16 The suspended sediments for peak flood and ebb tides on the first day are shown in Figure 1.127 and Figure 1.128 respectively. At the centre of the plume envelope peak values are circa 50mg/l. The plots for day three tides (Figure 1.129 and Figure 1.130) have been selected to illustrate the settlement and mobilisation patterns. With decreased current speed, sediment concentrations reduce as material settles and, as current speed increase through the tidal cycle, settled material is mobilised and concentration increase once again.. Under these circumstances peak concentrations are circa 50mg/l and average values are typically one tenth of this value, with the peaks centred on areas of remobilised material.

1.8.3.17 The accumulated deposition from the two operations is not evident in the sedimentation plots Figure 1.131 to Figure 1.134 due to the low levels of sedimentation <0.1mm. Similar to the piling scenarios A and B, native material from the sediment cell would be entrained into the baseline sediment transport patterns.

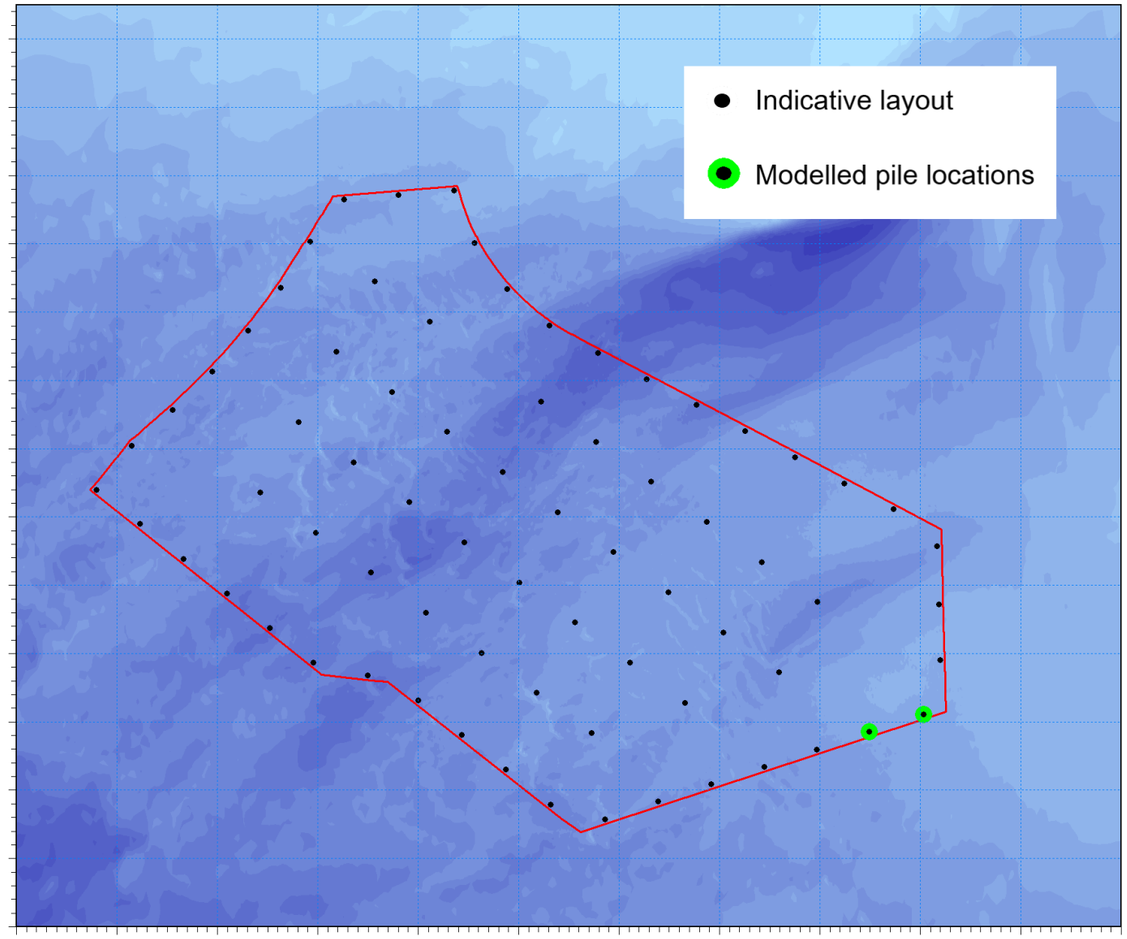

Figure 1.125: Location of modelled piled installation for Piling Scenario C.

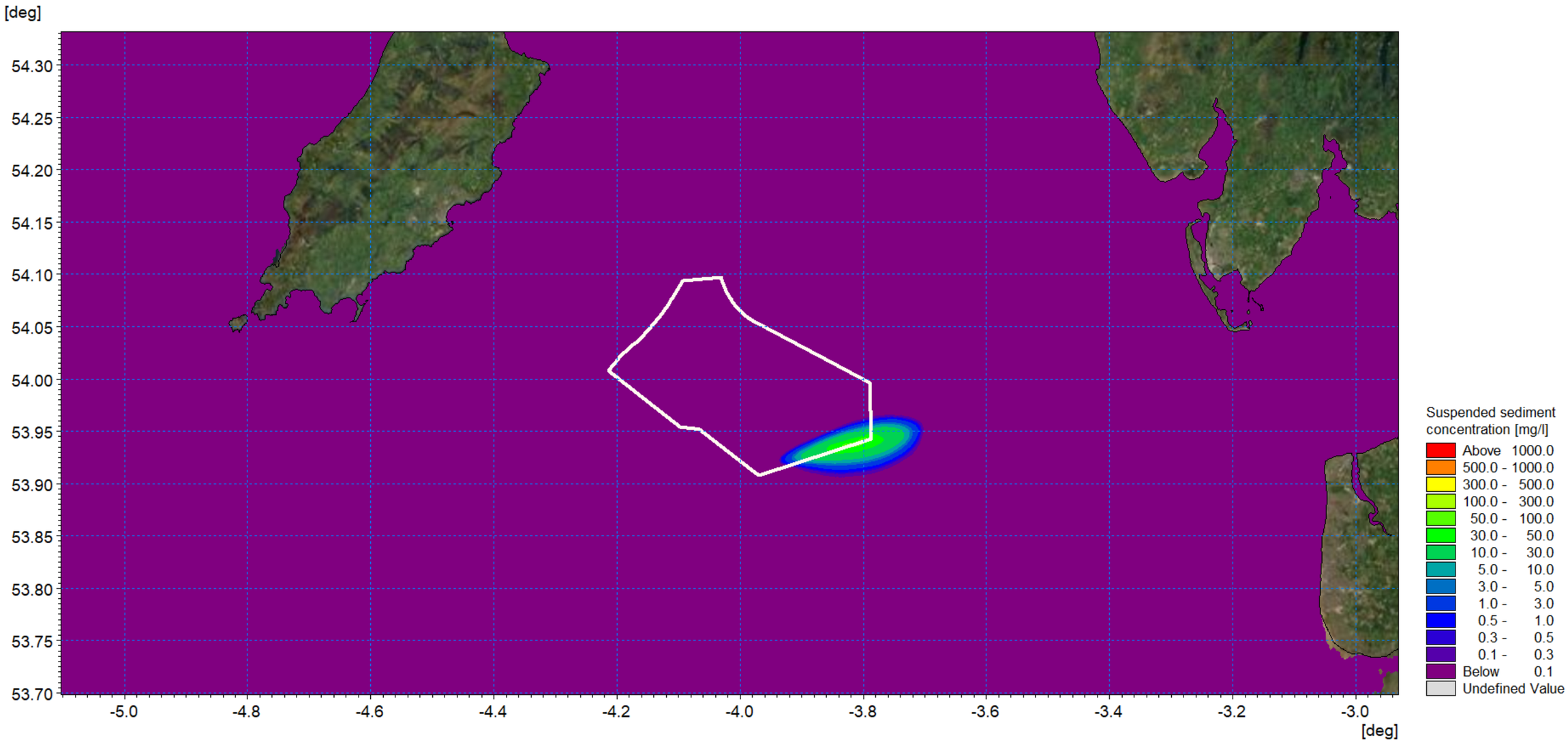

Figure 1.126: Average SSC – Pile Installation Scenario C.

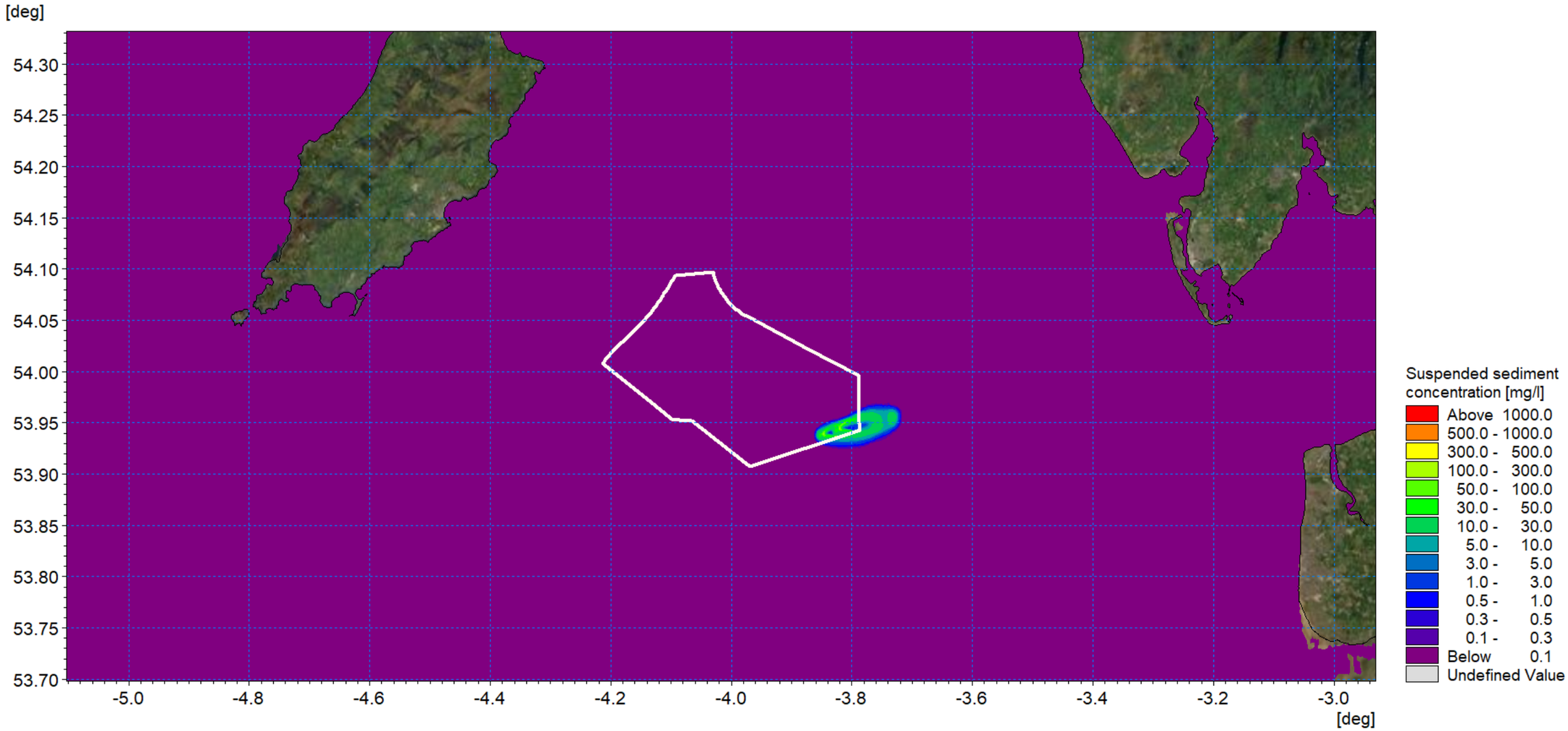

Figure 1.127: SSC day 1 flood- Pile Installation Scenario C.

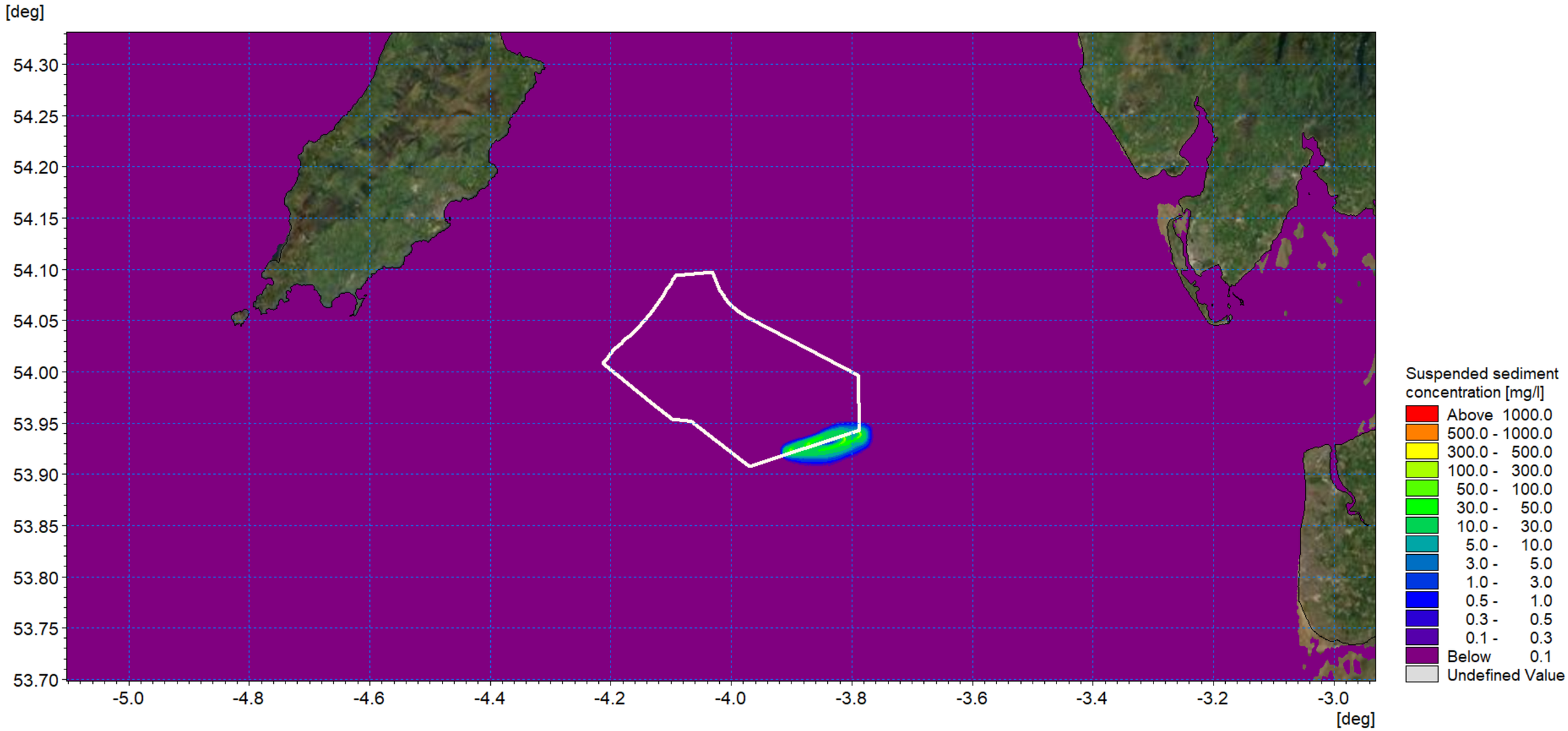

Figure 1.128: SSC day 1 ebb- Pile Installation Scenario C.

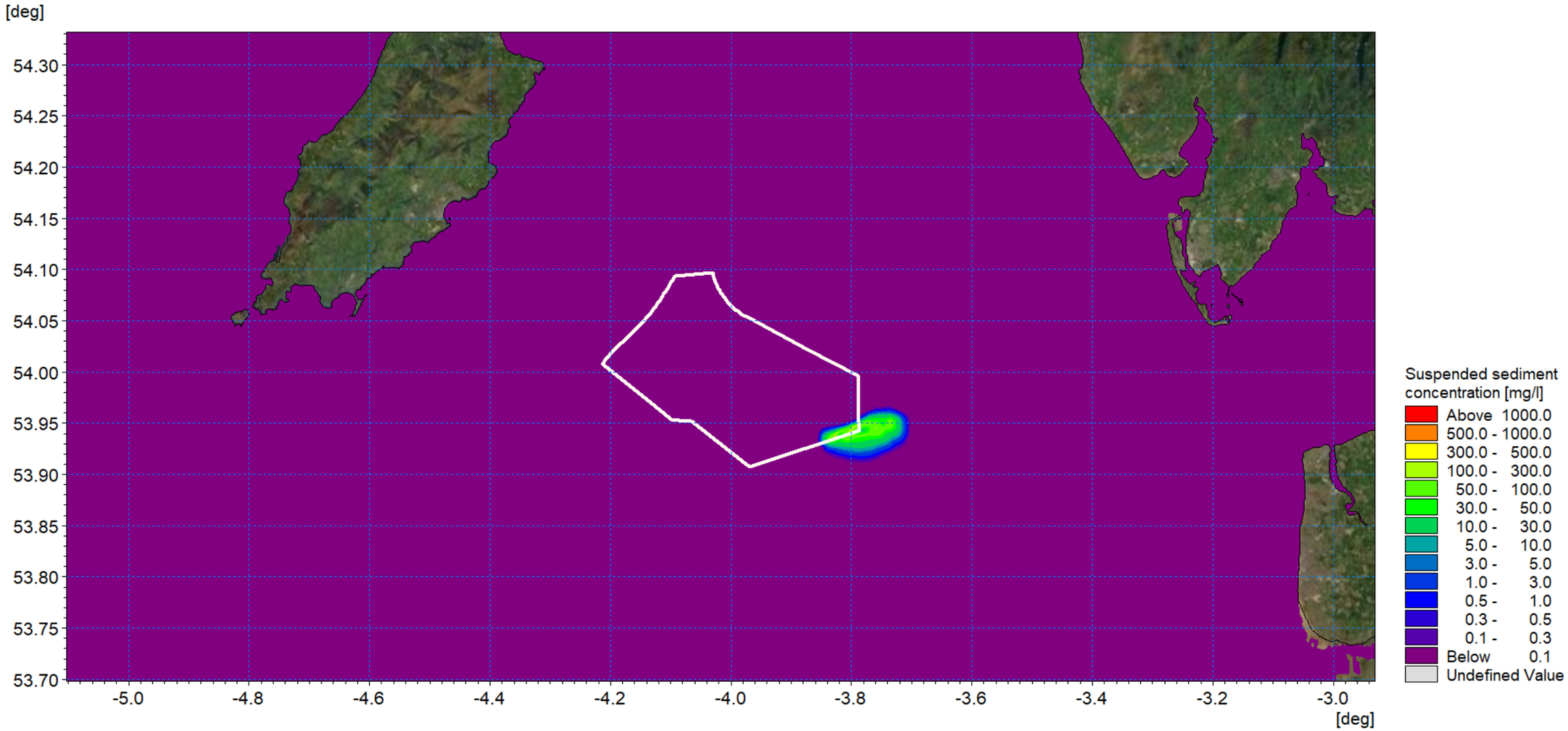

Figure 1.129: SSC day 3 flood- Pile Installation Scenario C.

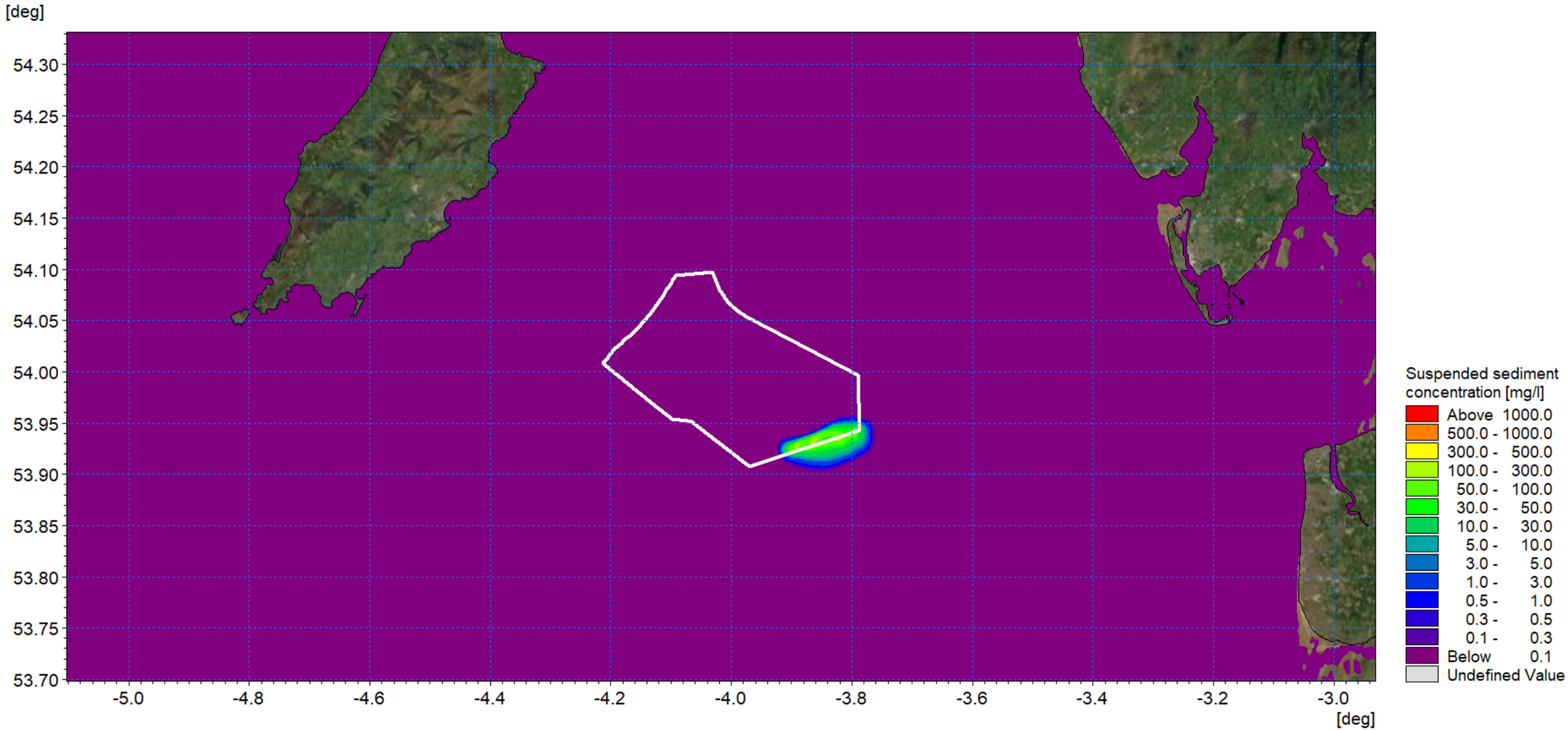

Figure 1.130: SSC day 3 ebb- Pile Installation Scenario C.

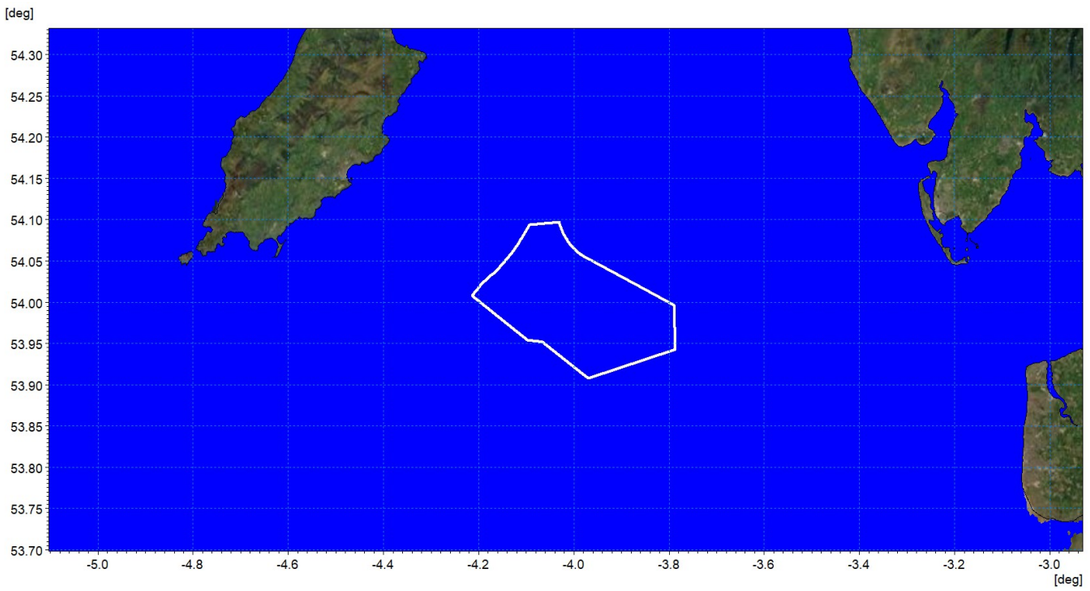

Figure 1.131: Average sedimentation during pile installation – Scenario C.

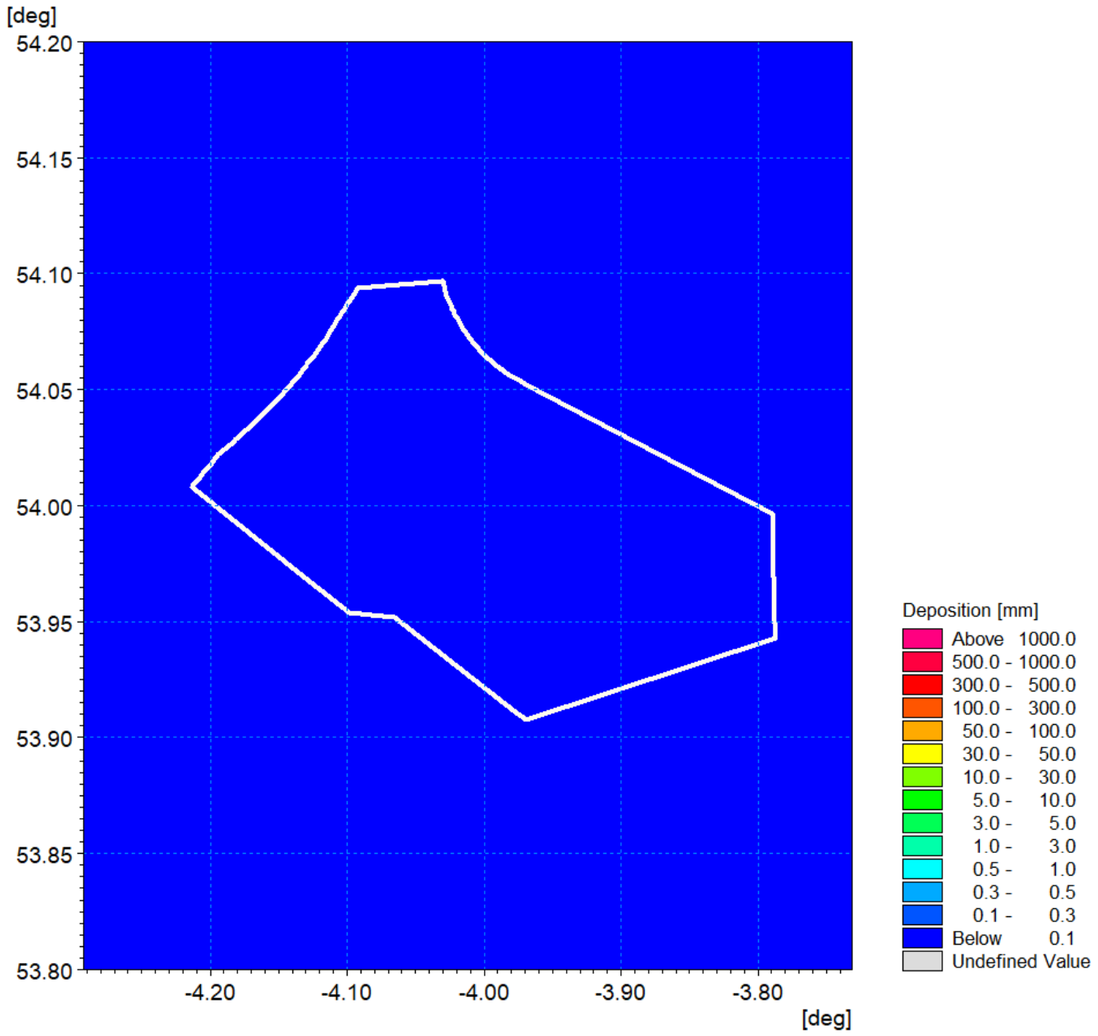

Figure 1.132: Average sedimentation during pile installation – Scenario C detail view.

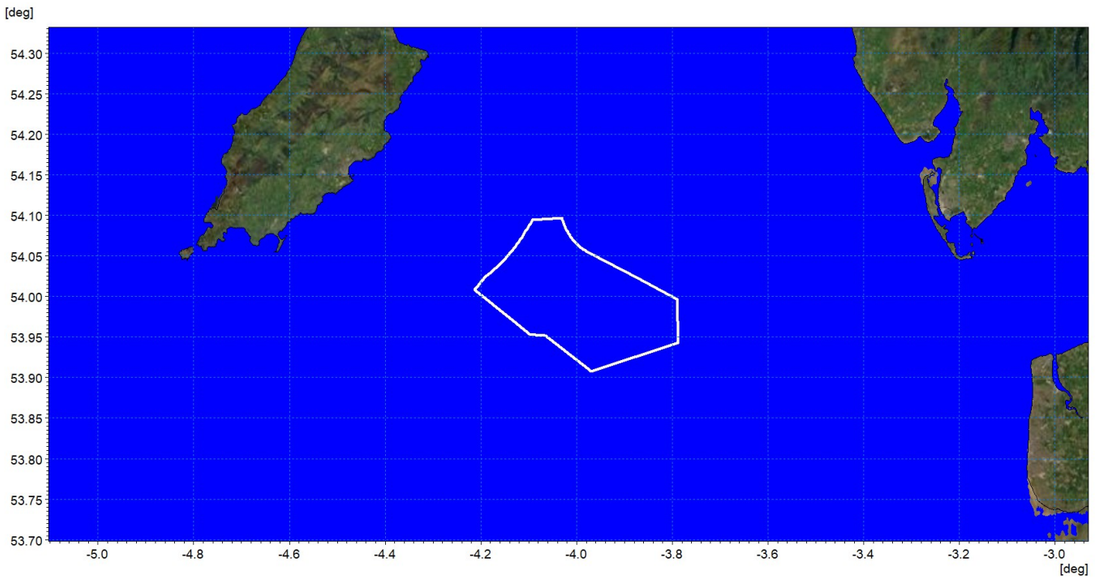

Figure 1.133: Sedimentation 1day following cessation of pile installation – Pile Scenario C.

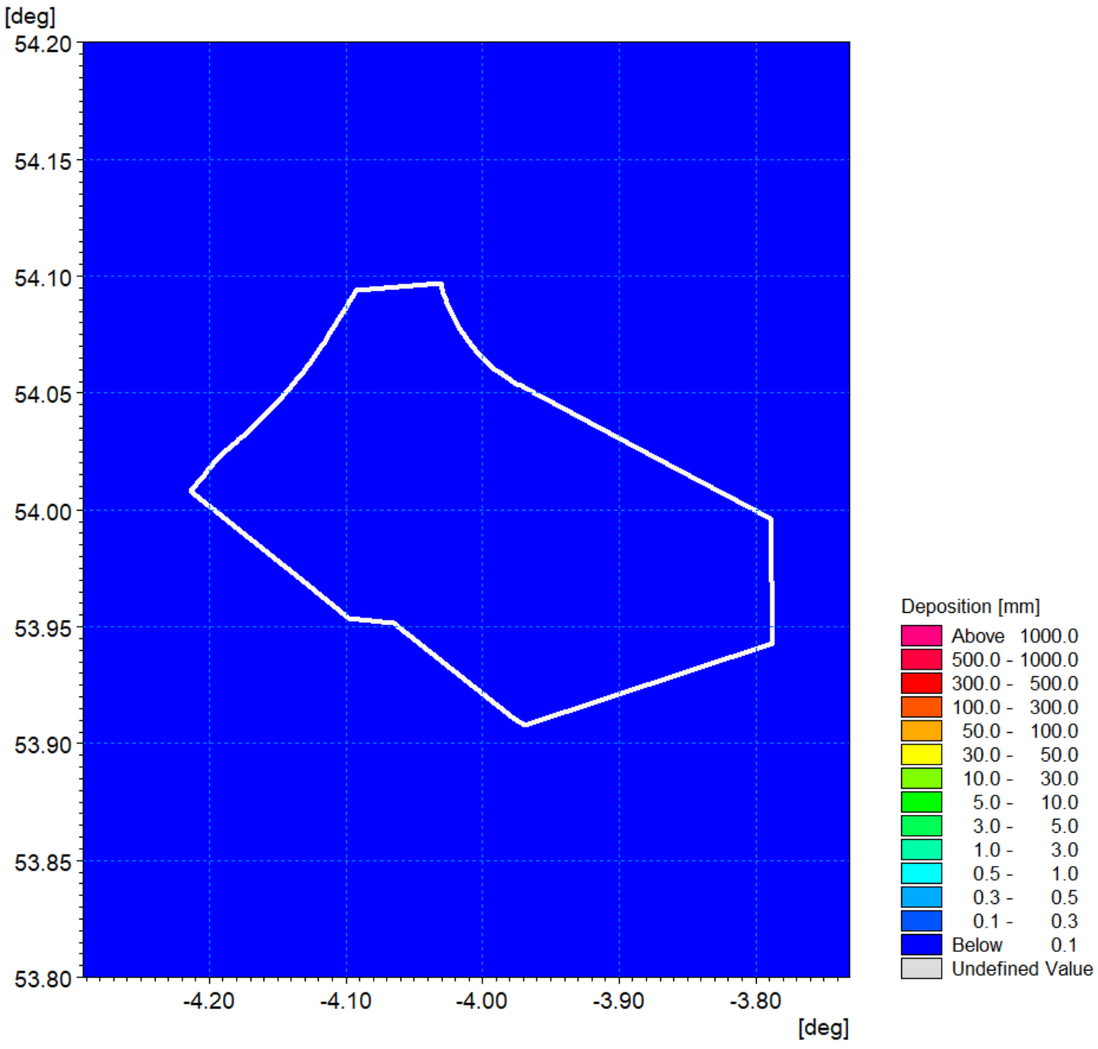

Figure 1.134: Sedimentation 1day following cessation of pile installation – Pile Scenario C detail view.

1.8.4 Cable installation

1.8.4.1 The third aspect of the construction phase is cable installation, including the inter-array cables and interconnector cables. For the MDS in terms of release of sediment into the water column, cables were assumed to be trenched. A number of trenching techniques may be suited to the ground conditions; however it was assumed within the modelling that a trench of material of the maximum depth presented in the project description outlined in volume 1, chapter 3: Project description of the PEIR was mobilised into the lower water column as a result of the burial process, in line with the Business Enterprise and Regulatory Reform (BERR) guidelines (BERR, 2008). In reality the final installation technique may result in less sediment being mobilised and the maximum depth may not always be achieved with a corresponding reduction in the amount of material disturbed.

1.8.4.2 Similar to the pile installation, the model simulations used the sediment grading determined from BGS sediment sampling data. However, the modelling was undertaken using the MIKE PT module. This module was implemented as it had the advantage that it could be used to describe the transport of material released in a specific part of the water column. In this way, the dispersion would not be over-estimated or the corresponding sedimentation under-estimated by the application of a current profile through the water column.

1.8.4.3 Trenching rates can vary widely depending on the bed material and equipment used; typically, rates are between 25m/h and 780m/h. For the simulation, a relatively high rate of 450m/h was used over an extensive sample route ensuring that material was released at all tidal states over a number of tides and ensuring initial concentrations were not underestimated.

Inter-array cables

1.8.4.4 Inter-array and interconnector cable installation will be undertaken along a number of paths which connect groups of wind turbines to a local hub (i.e. an OSP) or which connect two OSPs to each other. Each route would be undertaken as a separate operation and thus a single example has been selected to quantify the potential suspended sediment levels during the installation. Figure 1.135 shows an indicative wind turbine layout with the modelled inter-array cable route shown in green. This route was run from the north of the site, perpendicular to the tidal flow, then in line with tidal flows in an easterly direction. This ensured that the full extent of the site and neap tidal conditions were incorporated into the simulation.

1.8.4.5 The inter-array cabling was undertaken along the indicated route with a trench 3m wide at the bed and 3m in depth with a triangular cross-section in accordance with a trenching plough. Thus circa 98,400m^3 of material was mobilised during the 2day simulation along the 21.9km route. The sediment grading characteristics were derived from sediment sampling along the route and defined by the following sand fractions.

- Gravel: 17%
- Coarse sand: 10.6%
- Medium sand: 63.8%
- Fine sand: 5.2%
- Very fine sand: 3.4%.

1.8.4.6 The model results presented follow the same format as those for the piled foundation installation described in the previous section. Figure 1.136 shows the average SSC over the course of the trenching phase. It is clear that the sediment is dispersed on subsequent tides as the plume envelope illustrates the flood and ebb tidal excursions with peak values of 300-500mg/l.

1.8.4.7 Figure 1.137 to Figure 1.142 show the suspended sediment patterns over the course of this operation, day two, three and four mid flood and ebb tides respectively. The volume of material mobilised is relatively large, and elevated tidal currents disperse the material giving rise to concentrations of up to 500mg/l. As was evident in the previous operations, the material settles during slack water and then is re-suspended to form a secondary plume which becomes amalgamated. This is further illustrated in Figure 1.143 and Figure 1.144 which show the average sedimentation and the sedimentation one day following cessation at slack water. The sedimentation is greatest at the location of the trenching and may be up to 50mm in depth where the coarser material has settled within close proximity, circa 100m. The depths reduce significantly with distance to <0.5mm which is indicated by the use of a log scale in all figures. Although the material is dispersed, it remains within the sediment cell and is therefore retained within the transport system.

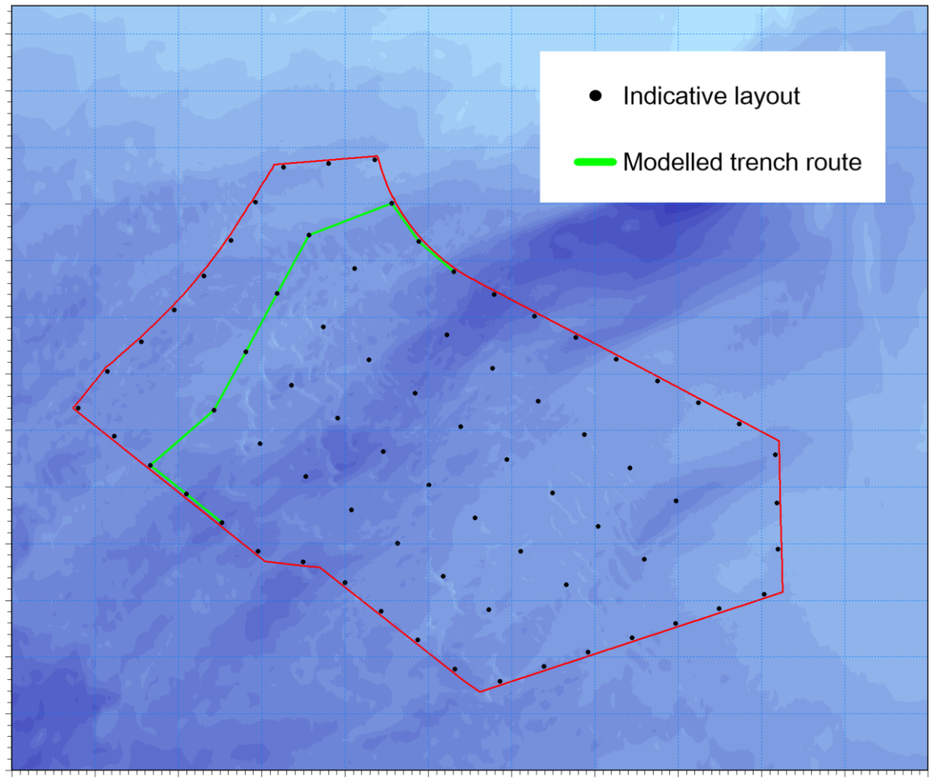

Figure 1.135: Modelled inter-array cable route.

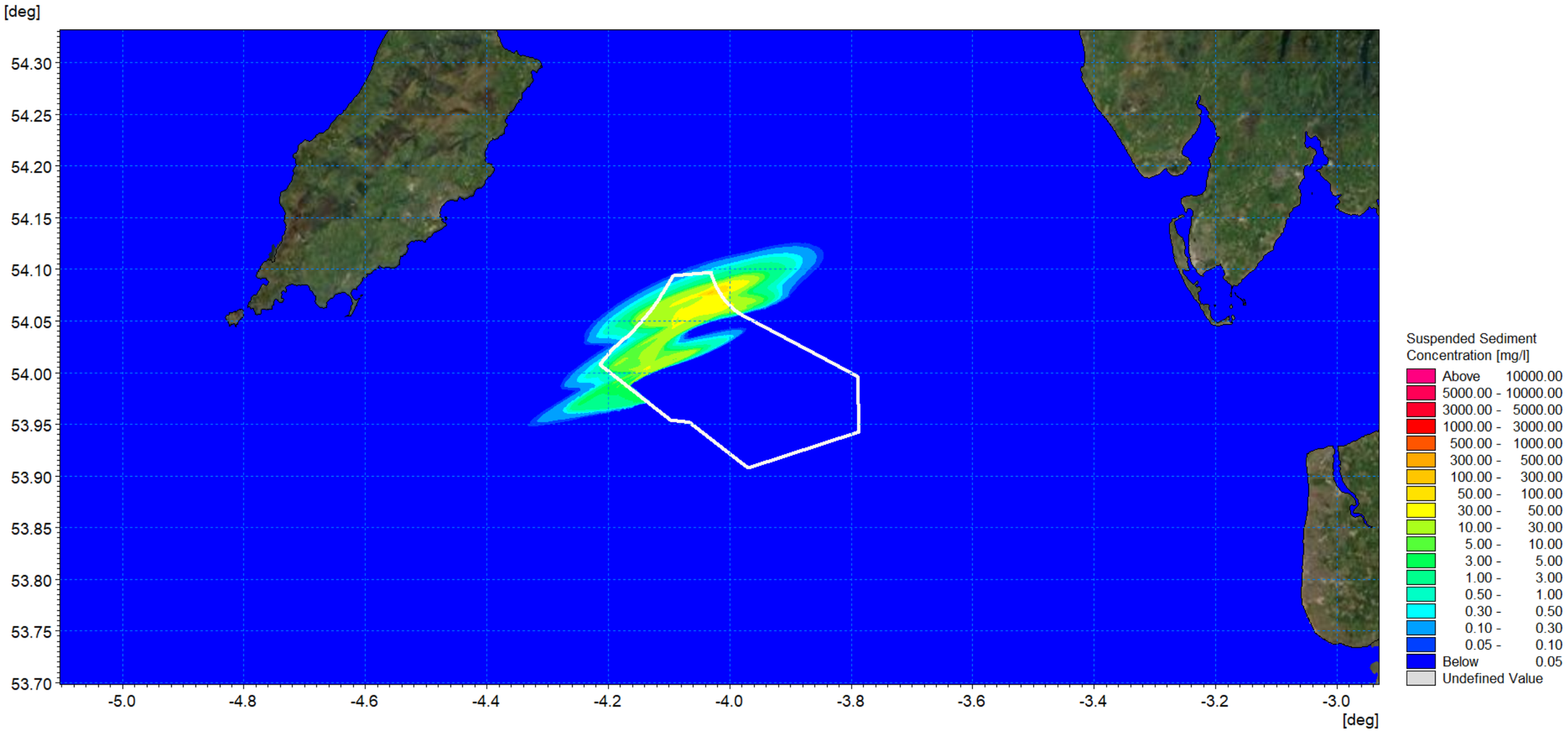

Figure 1.136: Average SSC during inter-array cable trenching.

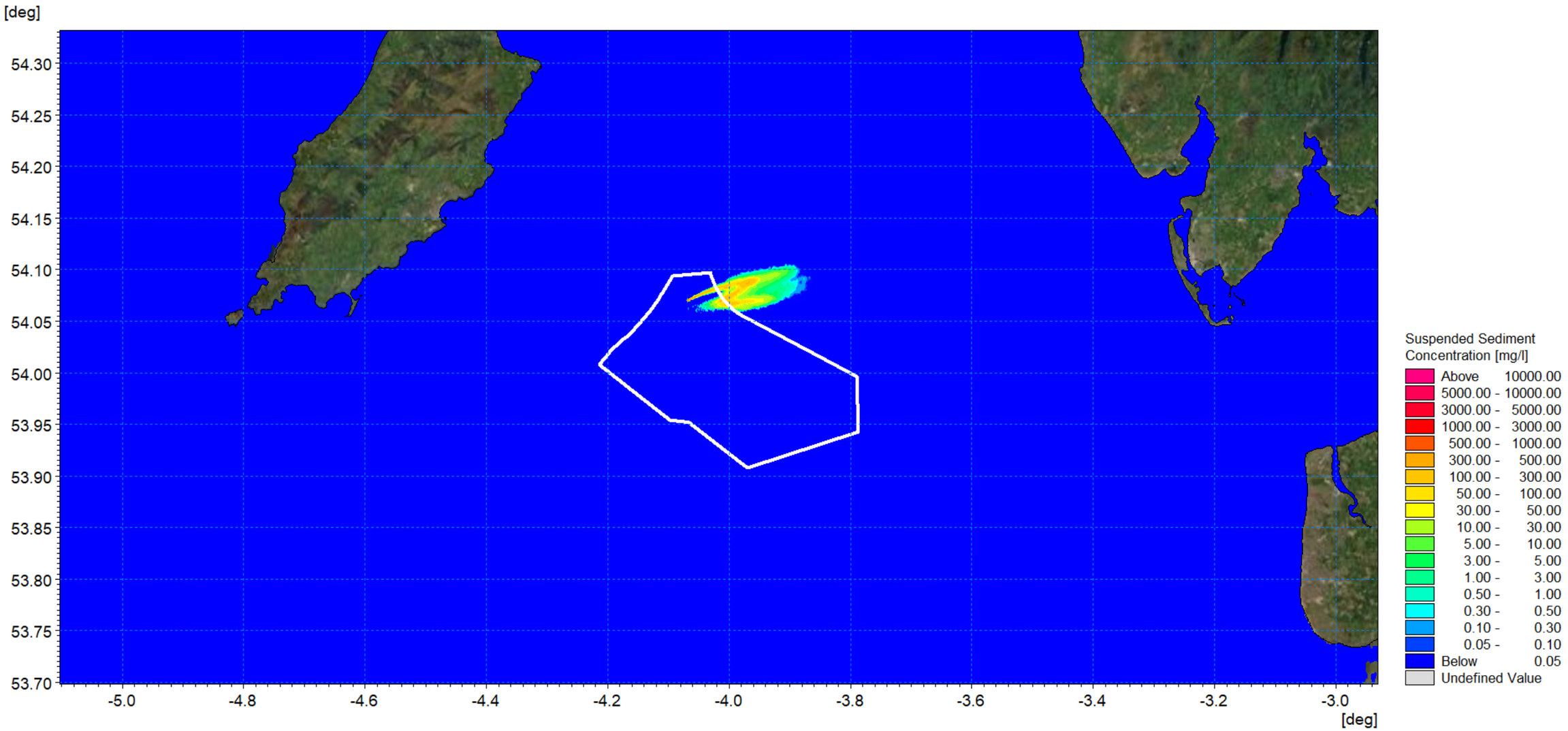

Figure 1.137: SSC day 2 flood – inter-array cable installation.

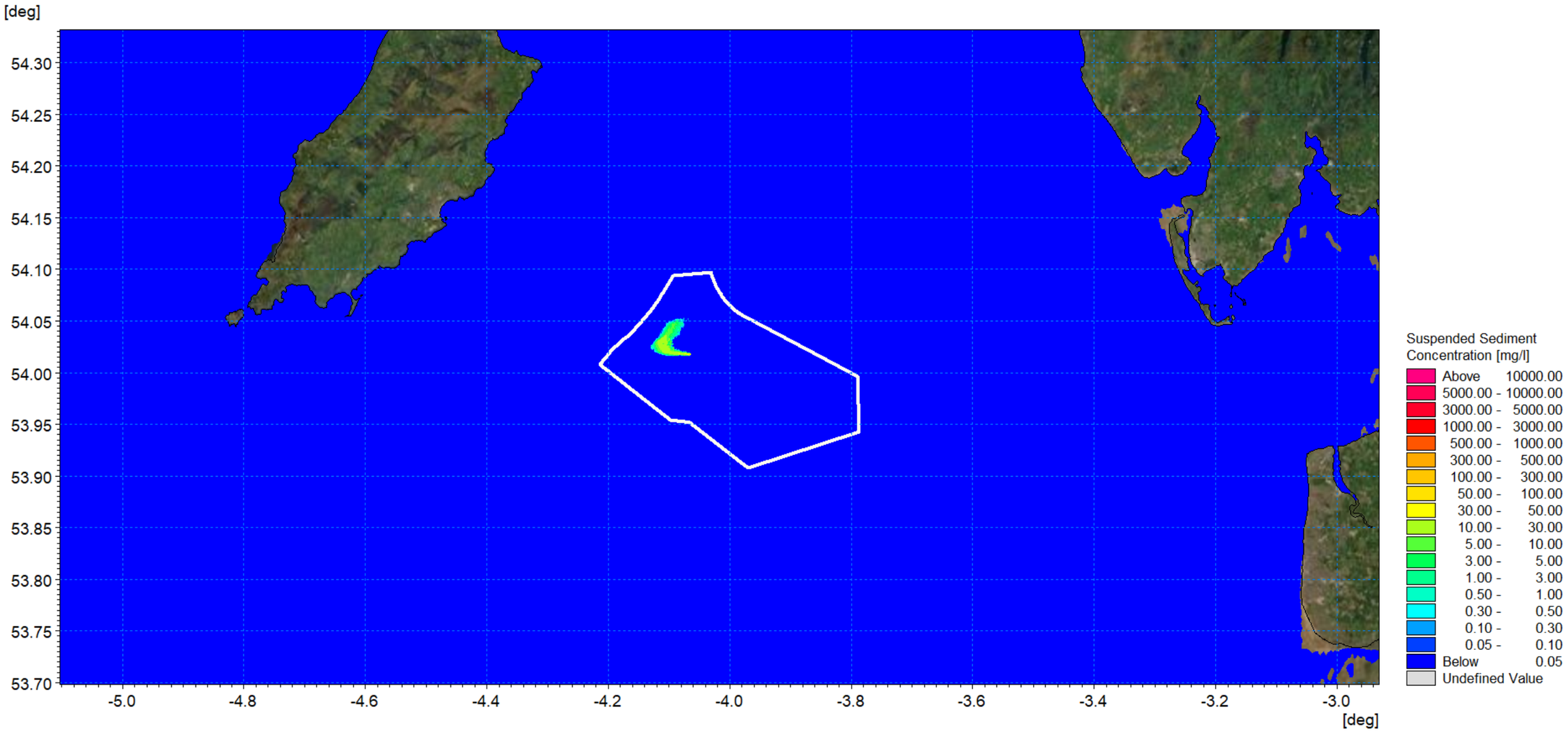

Figure 1.138: SSC day 2 ebb – inter-array cable installation.

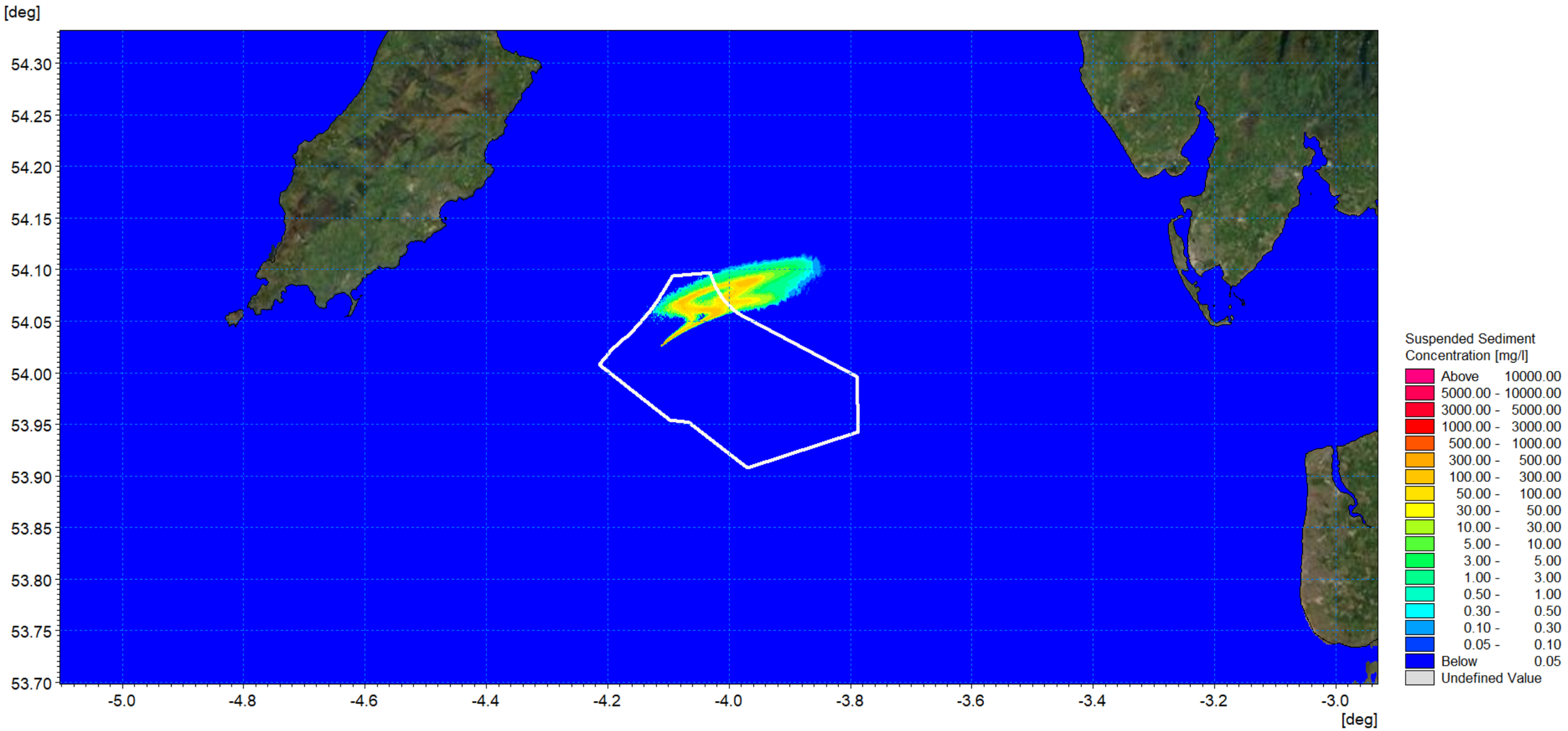

Figure 1.139: SSC day 3 flood – inter-array cable installation.

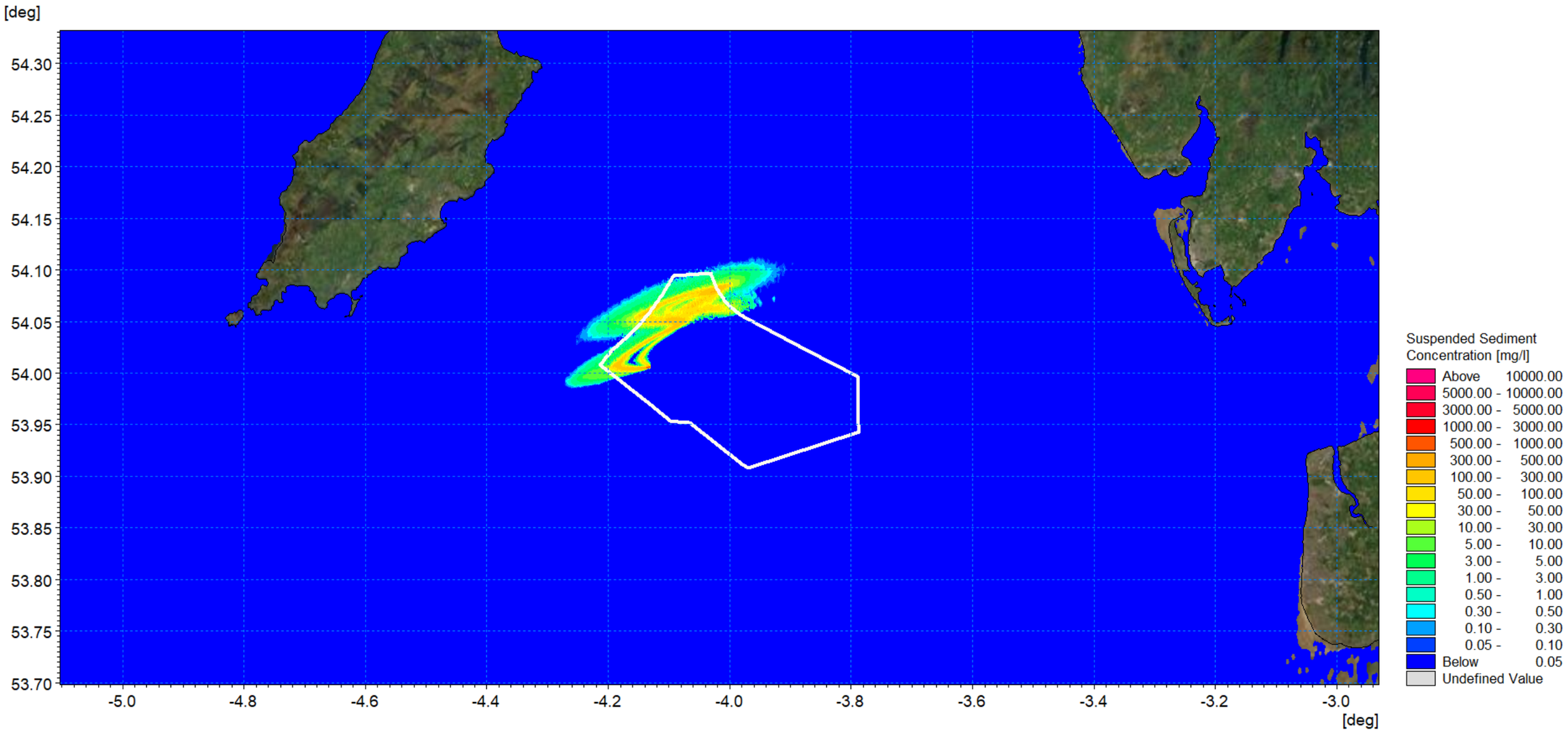

Figure 1.140: SSC day 3 ebb – inter-array cable installation.

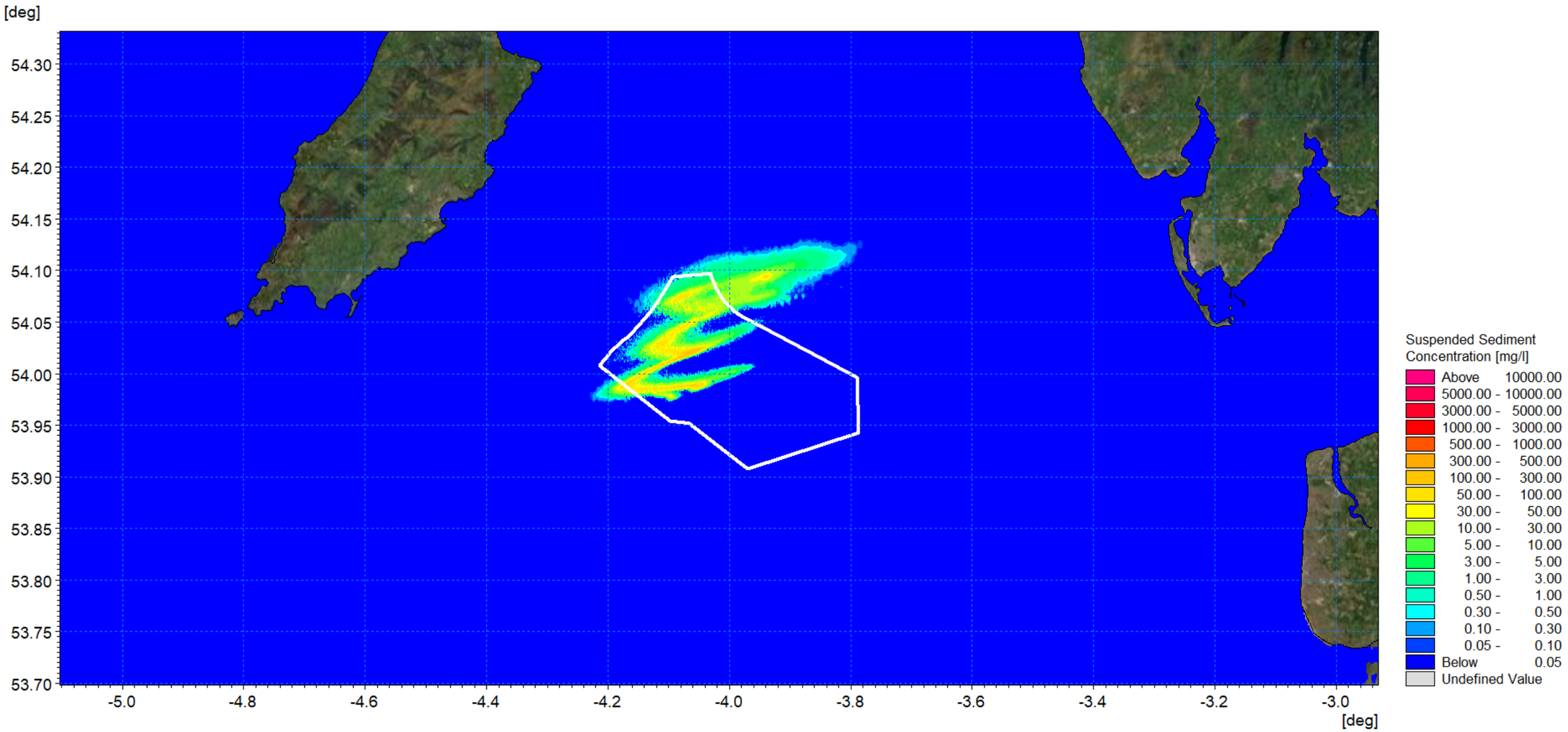

Figure 1.141: SSC day 4 flood – inter-array cable installation.

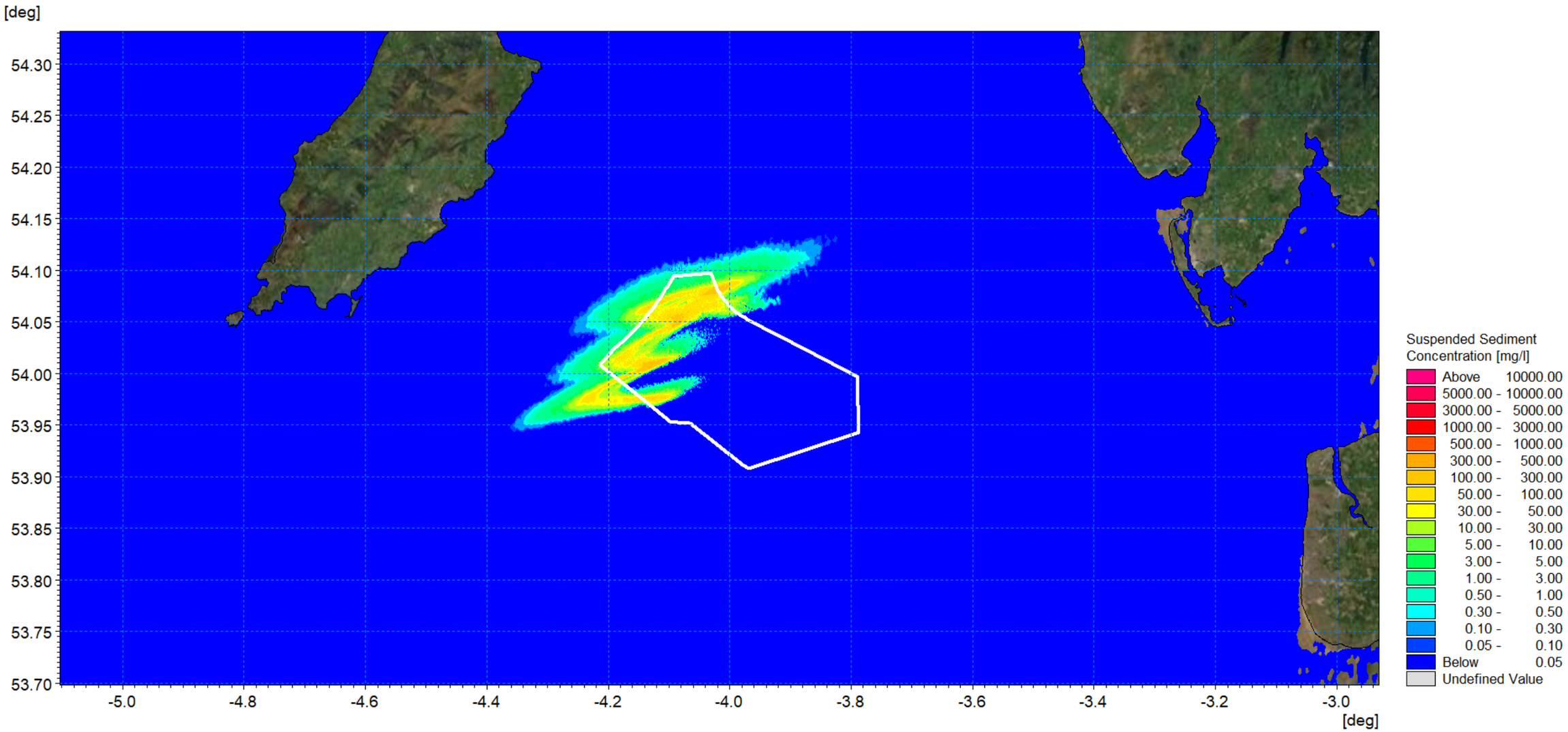

Figure 1.142: SSC day 4 ebb – inter-array cable installation.

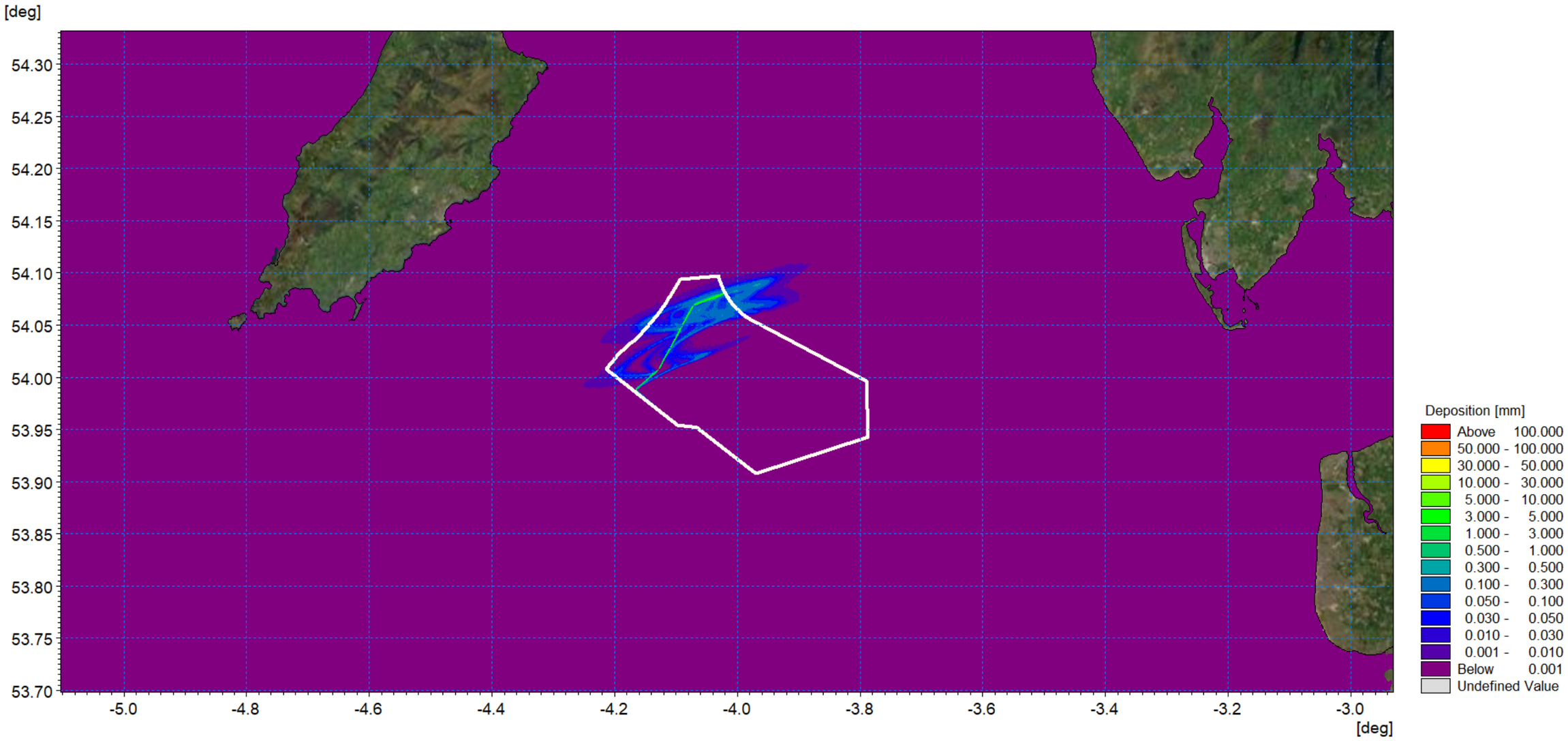

Figure 1.143: Average sedimentation during inter-array cable installation.

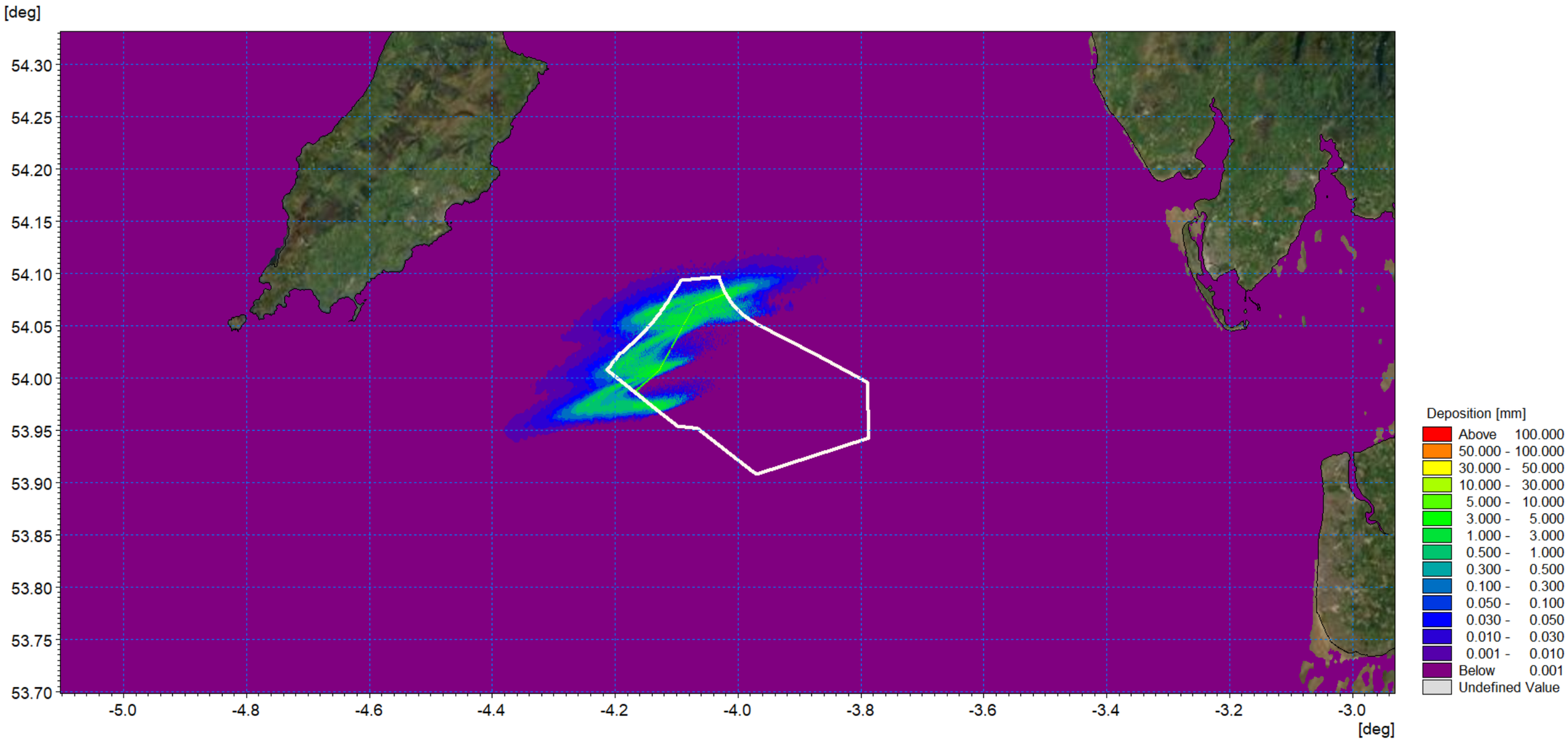

Figure 1.144: Sedimentation 1day following cessation of inter-array cable installation.

Interconnector cables

1.8.4.8 The Morgan Generation Assets interconnector cable route was examined using numerical modelling. The simulation assumed the same trenching rate as with the inter-array cables (i.e. 450m/h), and that installation began from north and continued southeast of the modelled route. Each trench was 3m at the surface extending to a depth of 3m (i.e. the greatest burial depth proposed), with a triangular profile. The operation took approximately 1day to complete encompassing a range of tidal conditions and mobilised 54,570m^3 of material. The composition was determined from the sampling data and was similar the inter-array route material.

- Gravel: 17%
- Coarse sand: 10.6%
- Medium sand: 63.8%
- Fine sand: 5.2%
- Very fine sand: 3.4%.

1.8.4.9 The trenching route modelled is illustrated by the green trace in Figure 1.145 and the average suspended sediment plume during the course of the operation is shown in Figure 1.146. The figure shows how the plume travels east and west on the tide as the release progresses along the route perpendicular to the tidal flow. This gives rise to average SSCs <50mg/l offshore.

1.8.4.10 The instantaneous SSCs for mid flood and ebb tides are presented for day two, day three and day four in Figure 1.147 to Figure 1.152 respectively. They show increases where sediment is released at the cable location but also at the extent of each tidal cycle as material is re-suspended. The plume travels east and west on the tide as the release progresses along the route perpendicular to the tidal flow and sediment concentrations reduce to background levels on slack tides. SSCs along the route range between 50 and 1000mg/l where the greatest levels are located at the source of the sediment release.

1.8.4.11 Finally, Figure 1.153 shows the average sedimentation whilst Figure 1.154 illustrates sedimentation levels one day following cessation of the sediment release. Tidal patterns indicate that although the released material migrates both east and west by settling and being re-suspended on successive tides, the sedimentation level is small typically <0.5mm and the greatest levels of deposition occur along the trenching route as coarser material settles. Although the material is widely dispersed, sediment remains within the cell and would be drawn into the baseline transport regime with small increases in bed sediment levels.

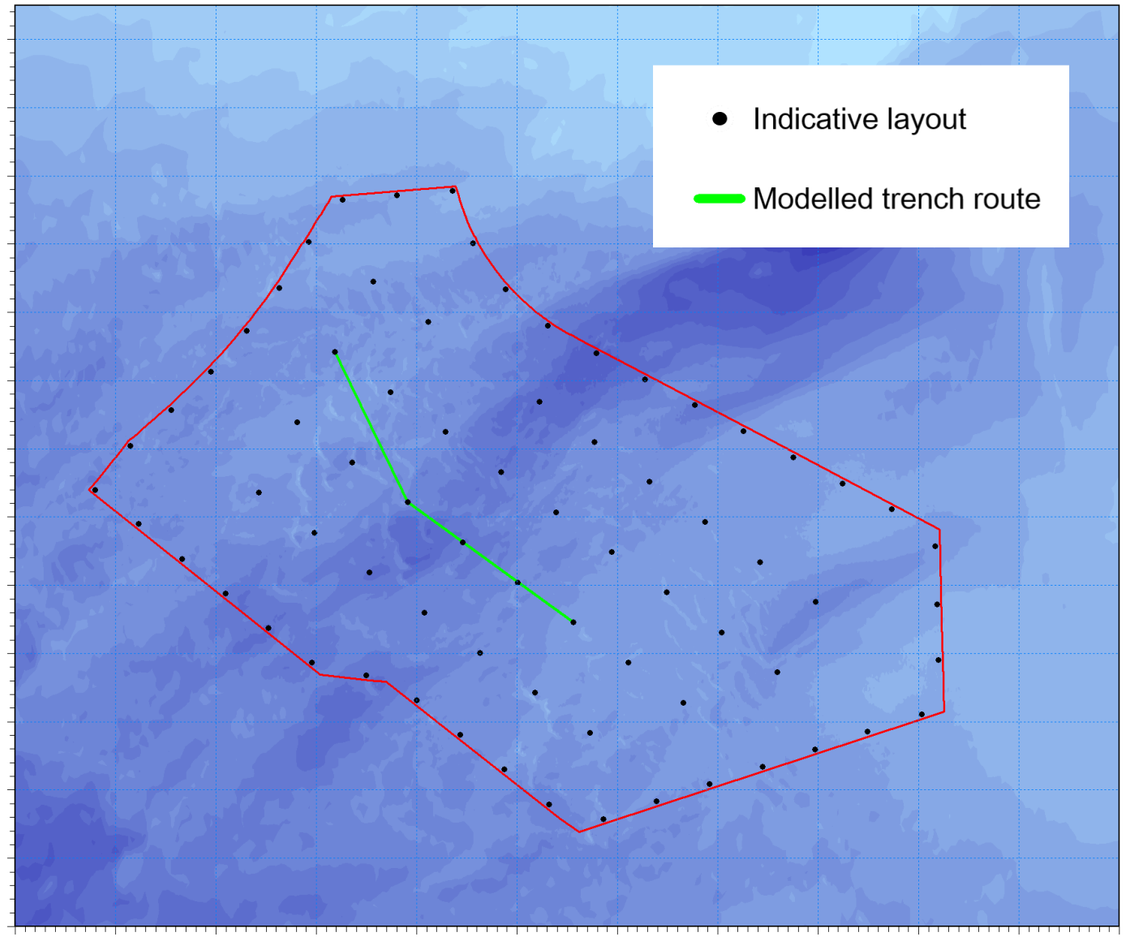

Figure 1.145: Modelled export cable route.

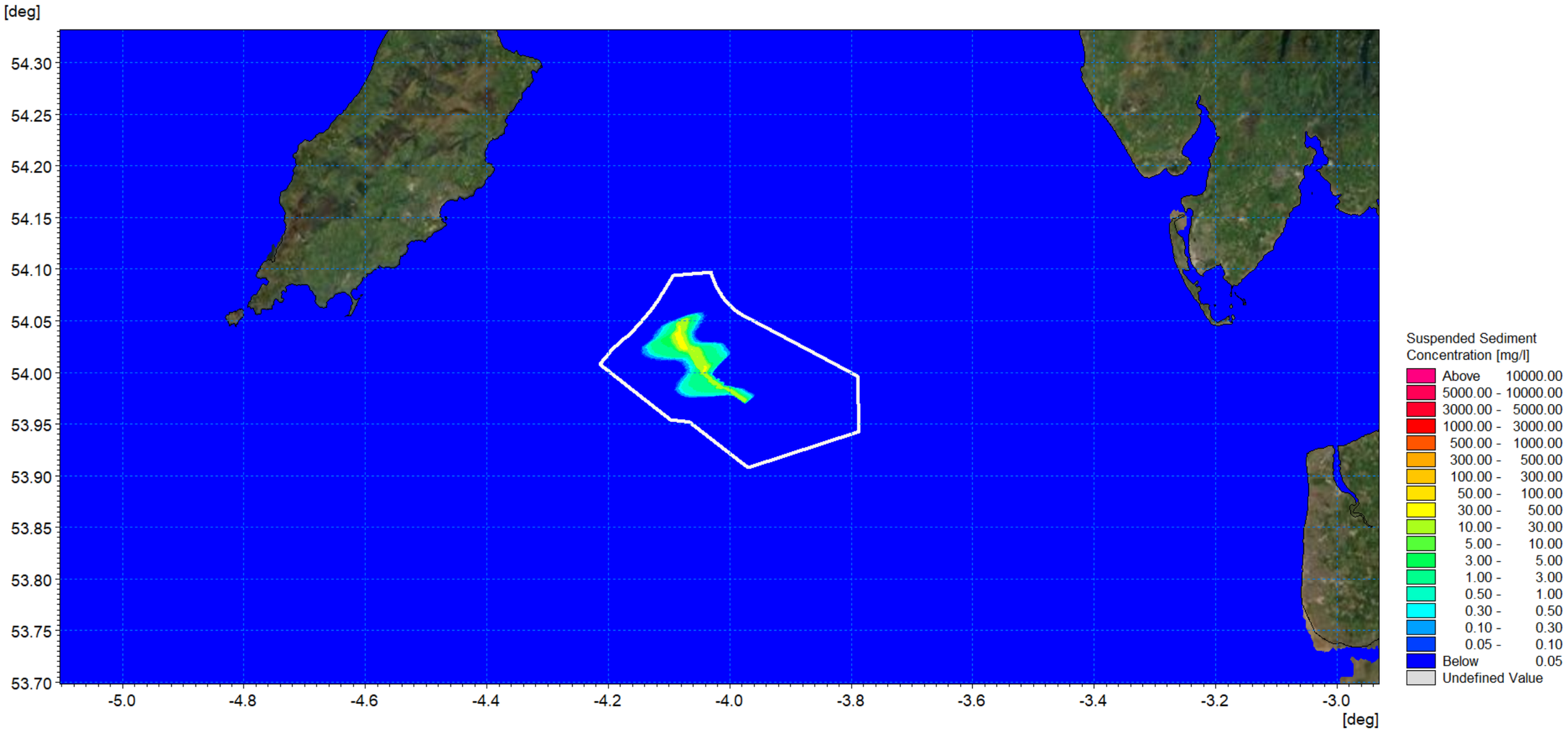

Figure 1.146: Average SSC during interconnector cable trenching.

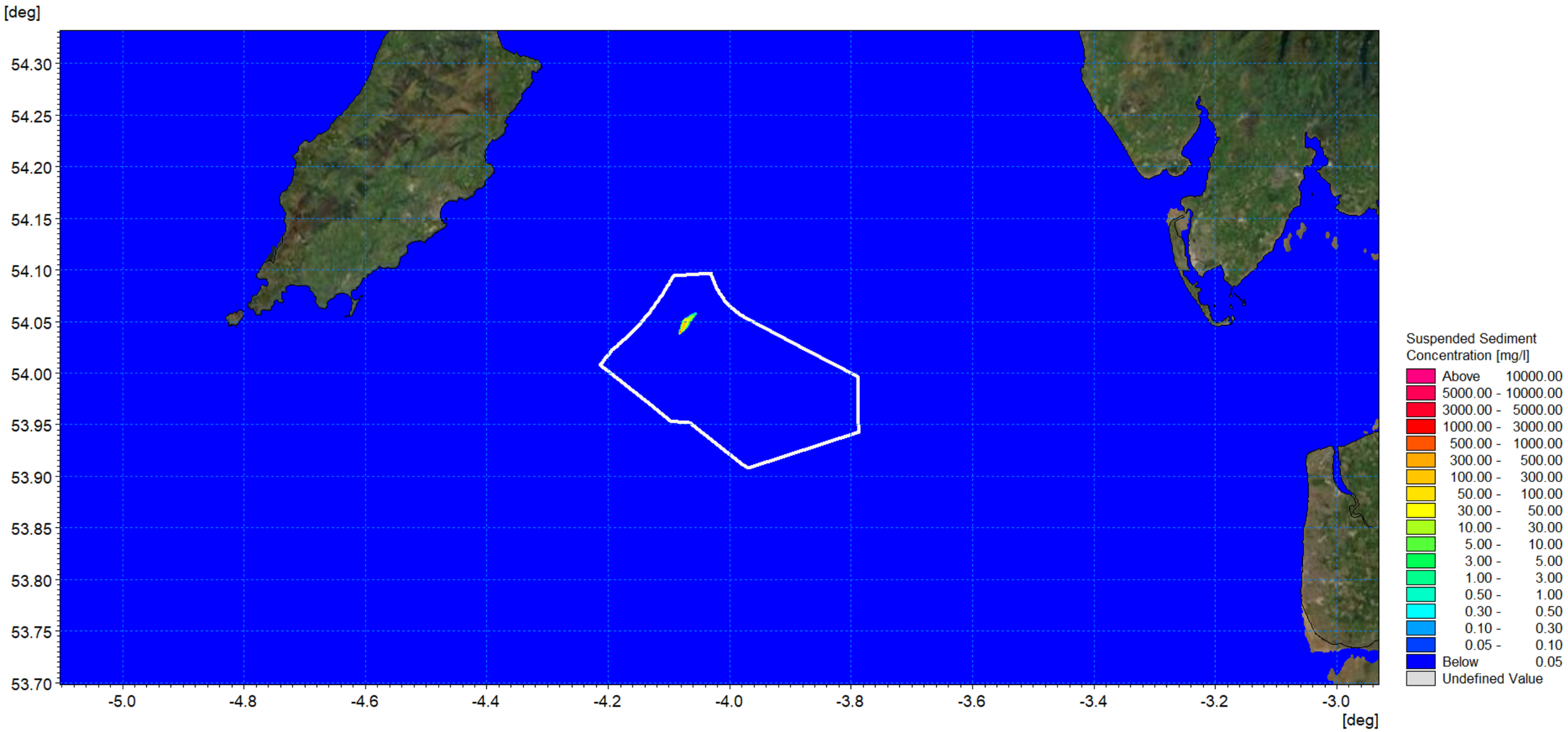

Figure 1.147: SSC day 2 peak flood – interconnector cable installation.

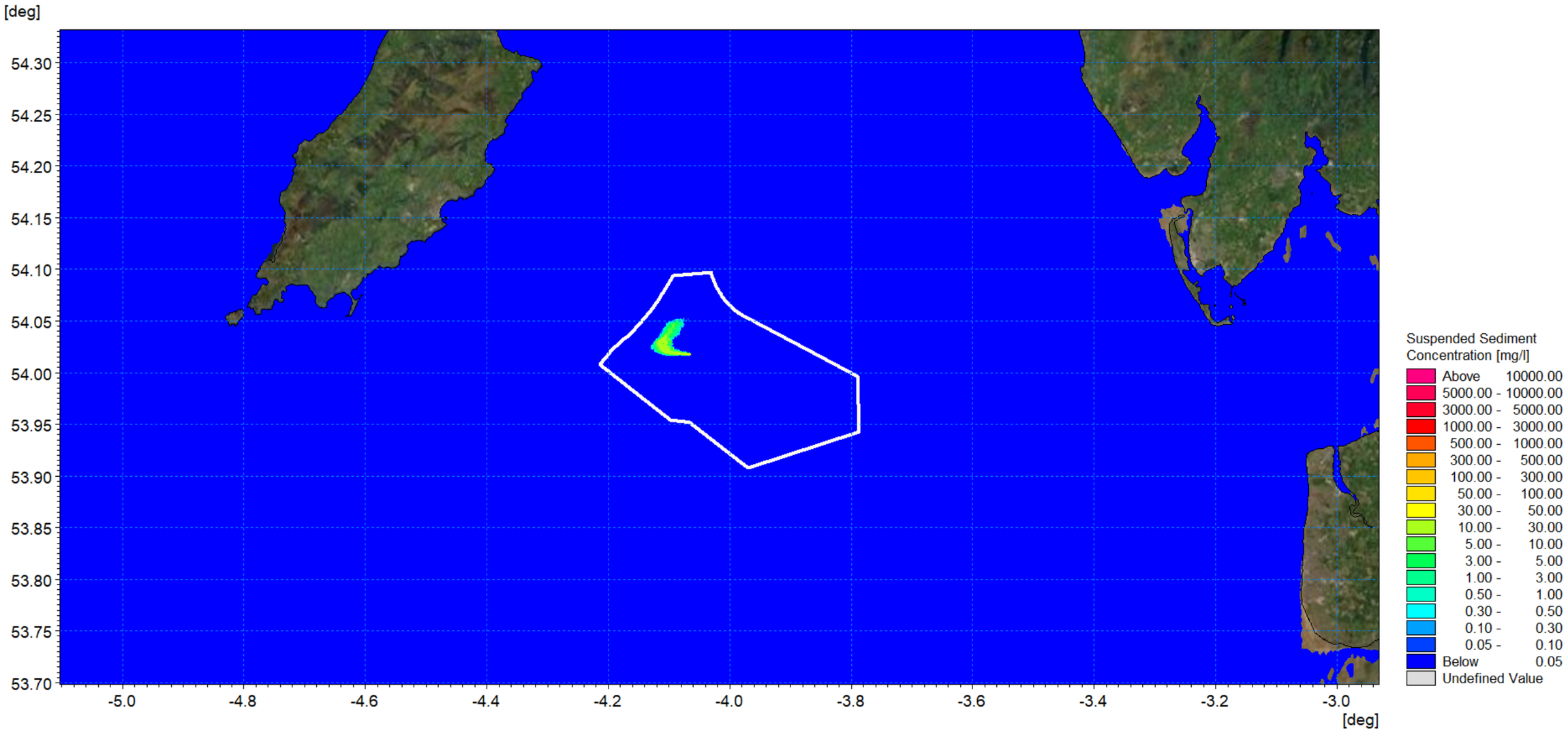

Figure 1.148: SSC day 2 peak ebb – interconnector cable installation.

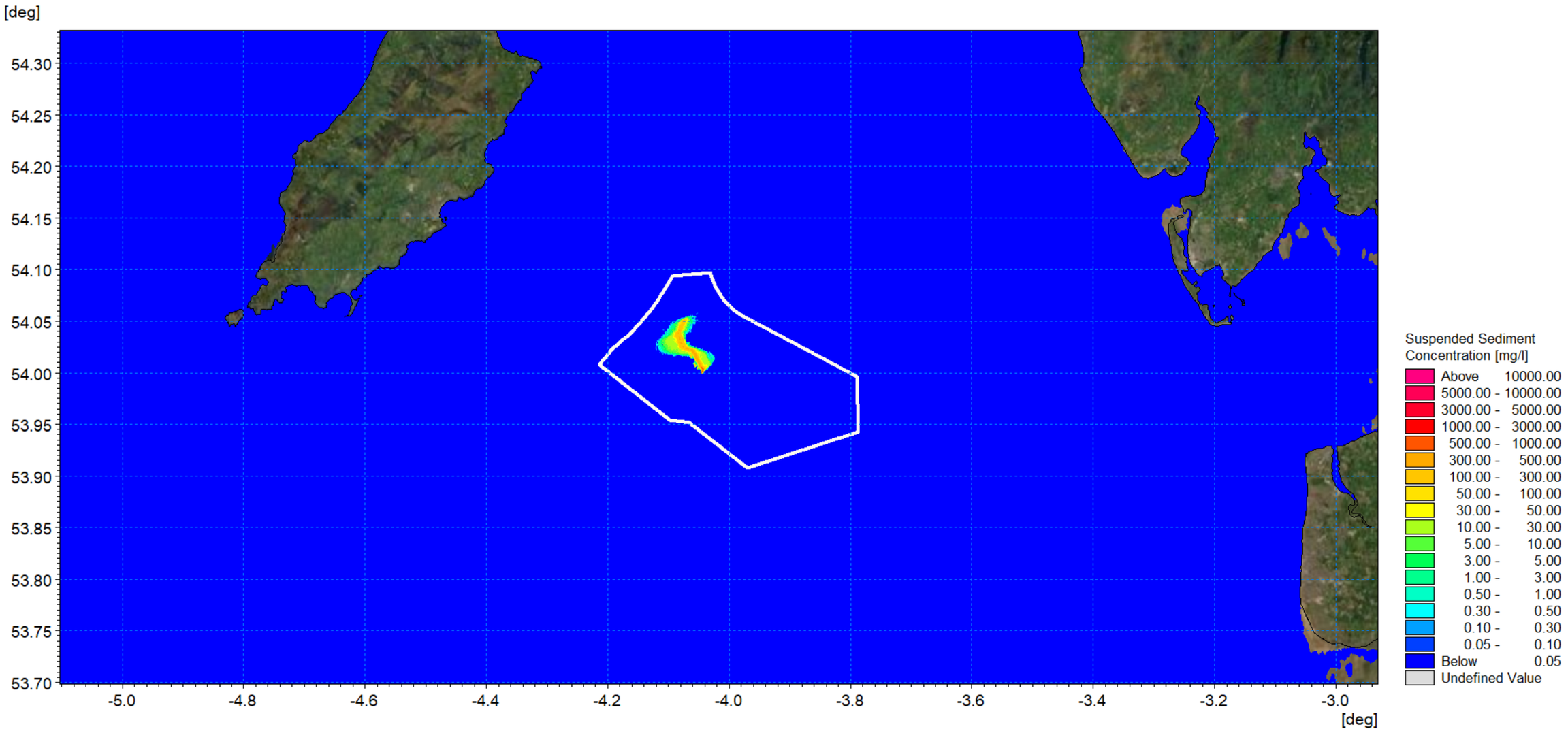

Figure 1.149: SSC day 3 peak flood – interconnector cable installation.

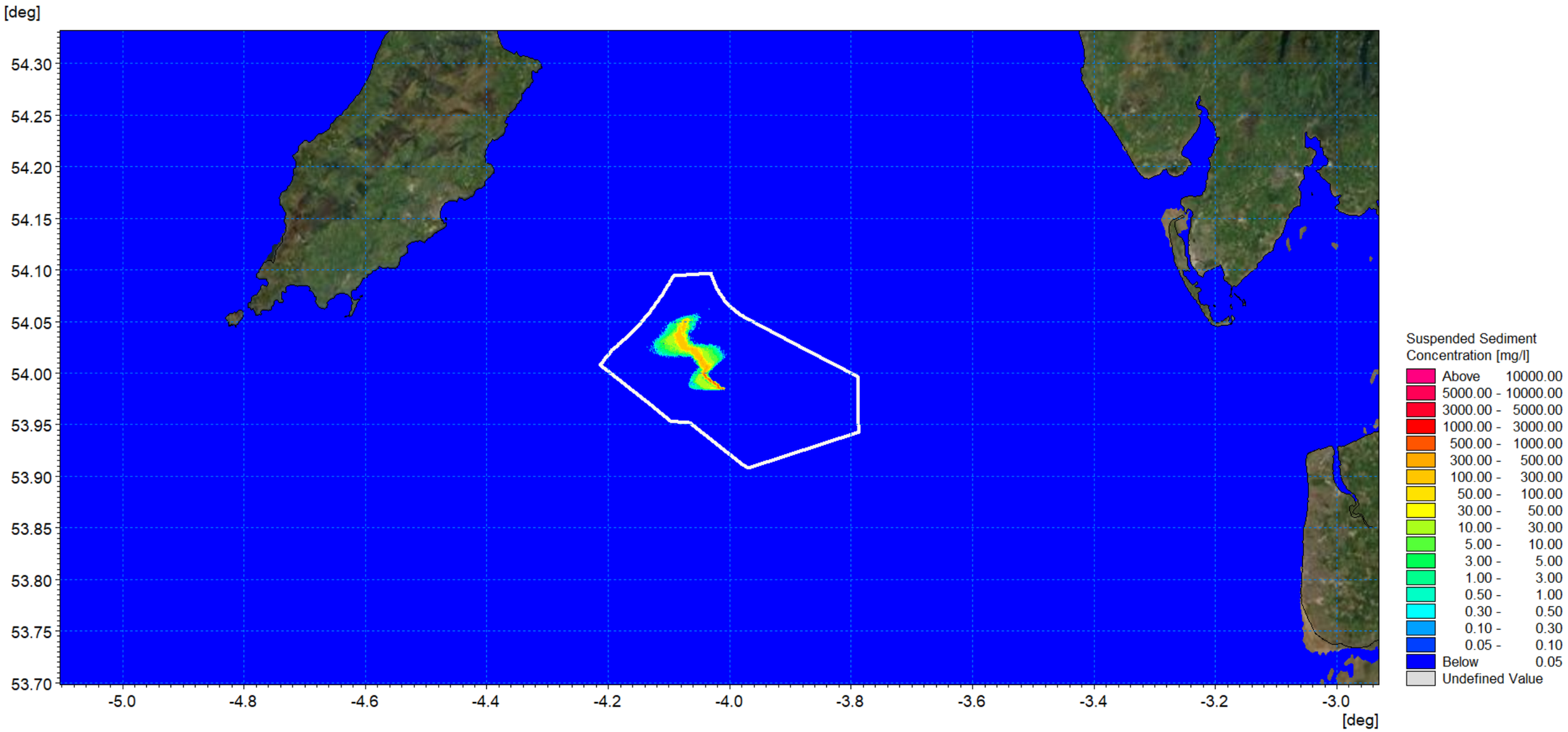

Figure 1.150: SSC day 3 peak ebb – interconnector cable installation.

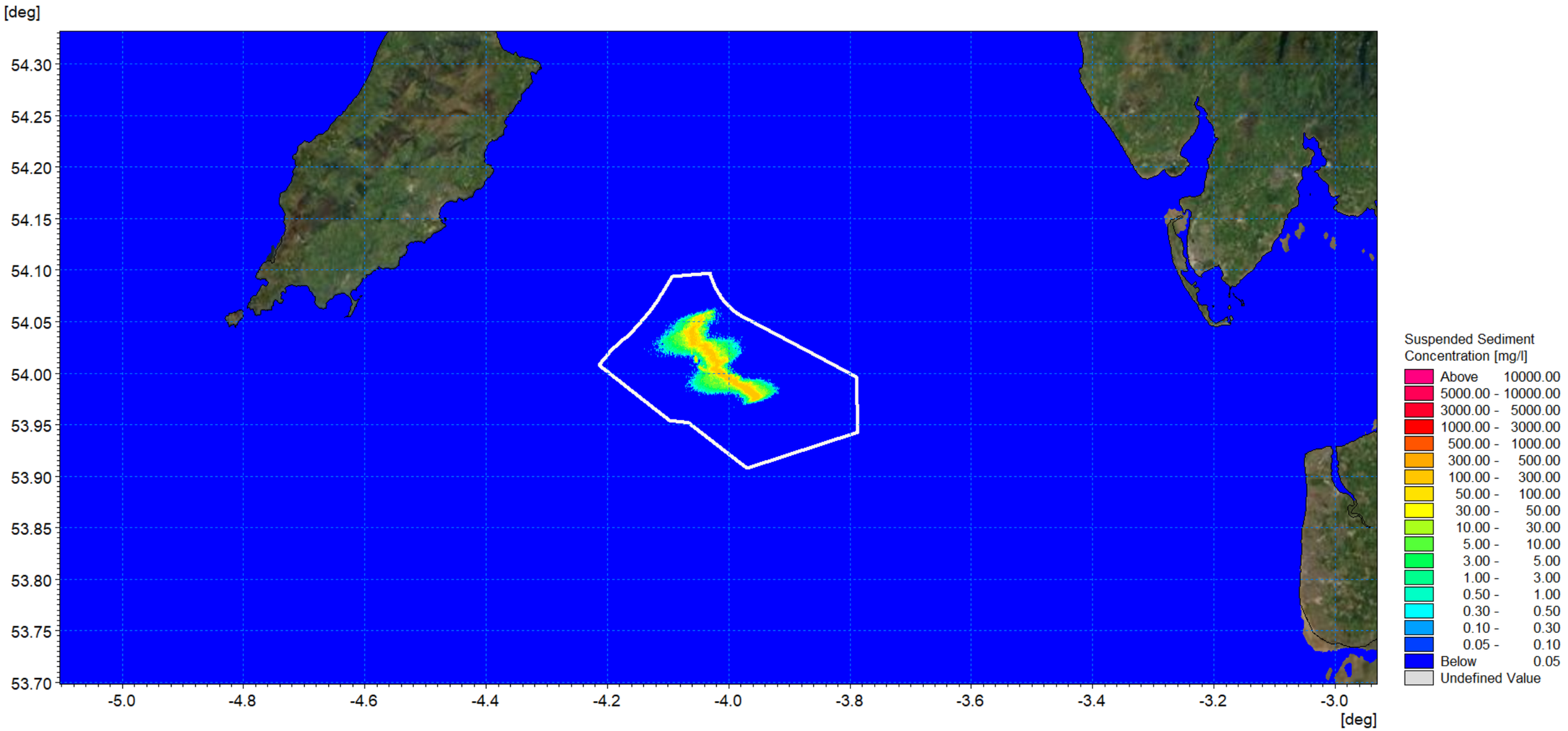

Figure 1.151: SSC day 4 peak flood – interconnector cable installation.

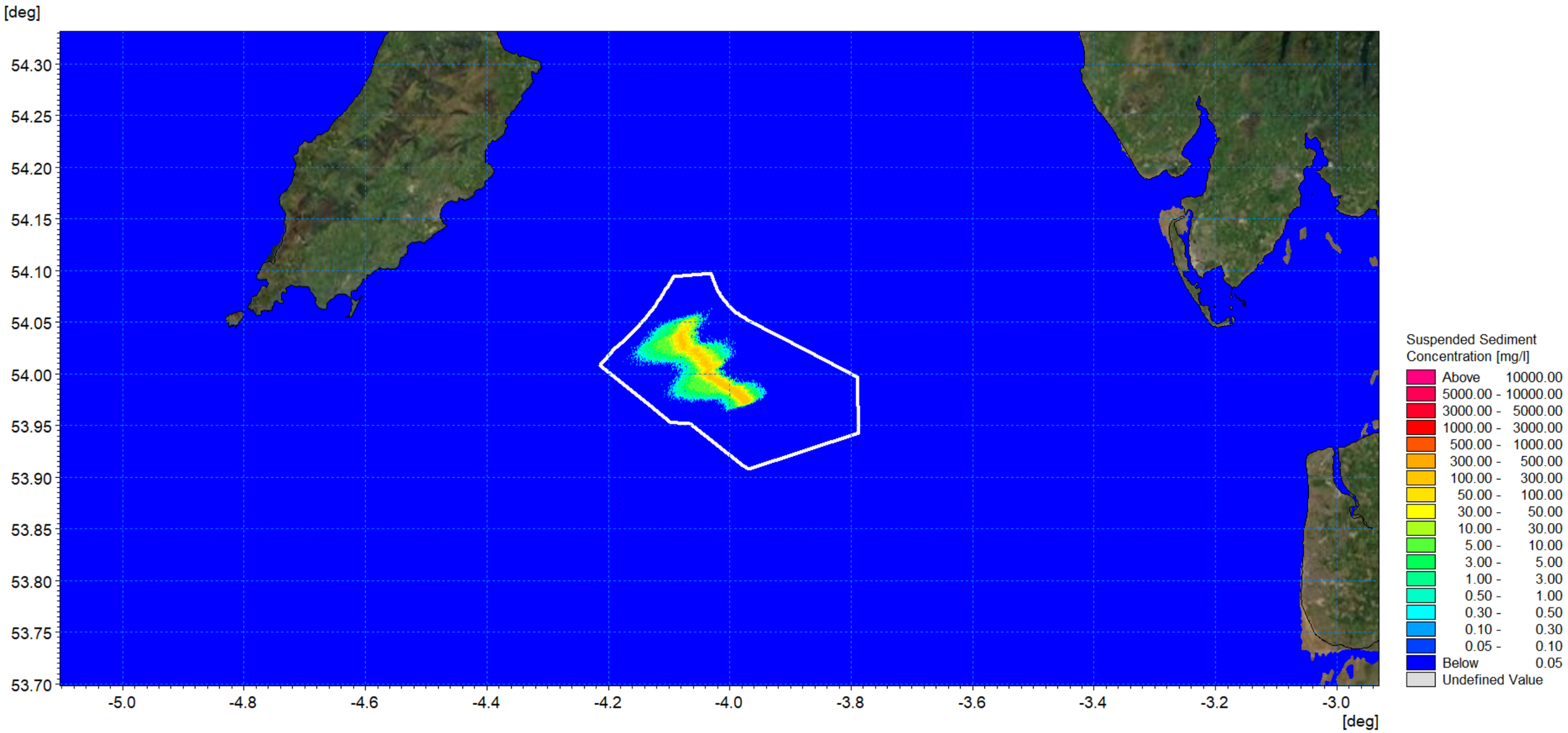

Figure 1.152: SSC day 4 peak ebb – interconnector cable installation.

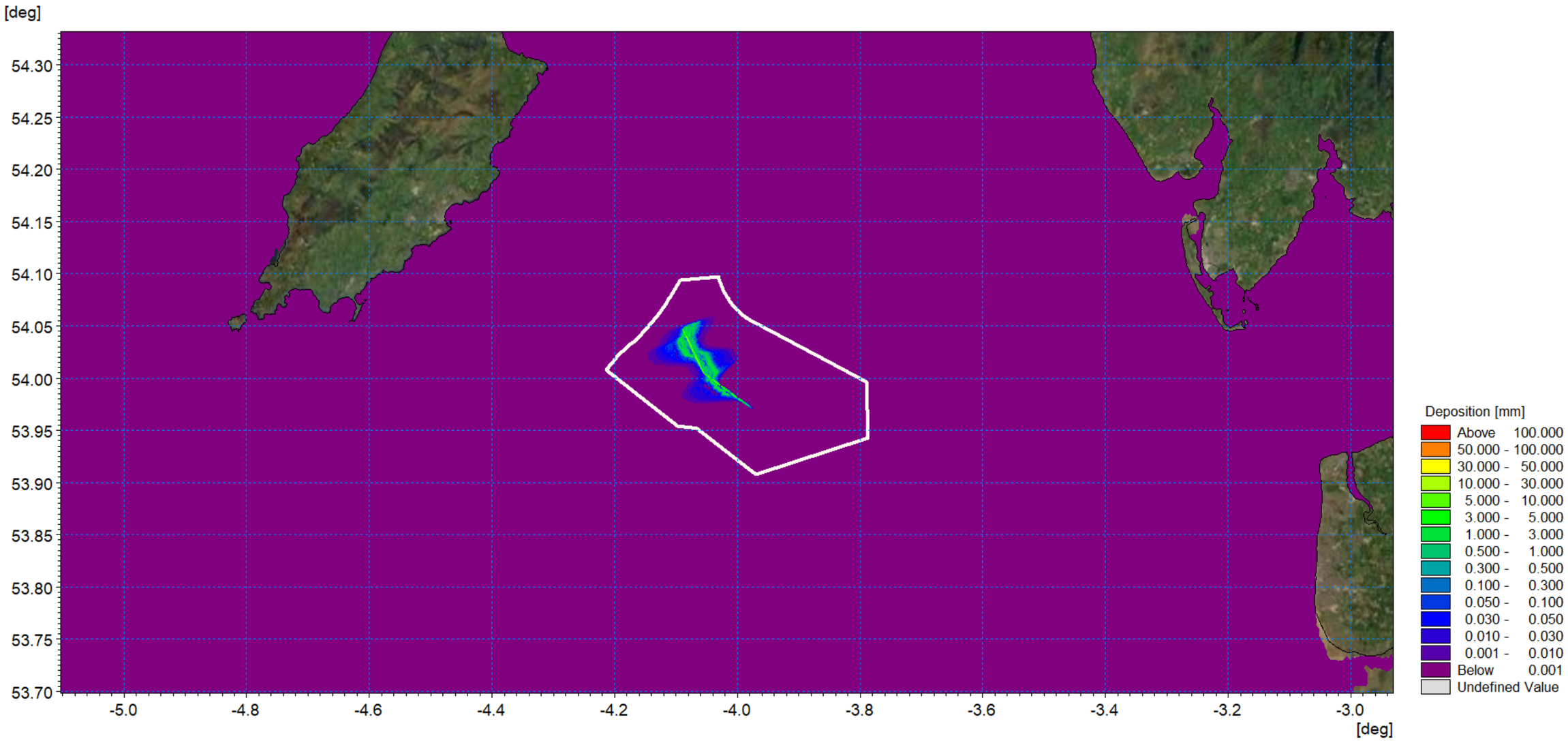

Figure 1.153: Average sedimentation during interconnector cable installation.

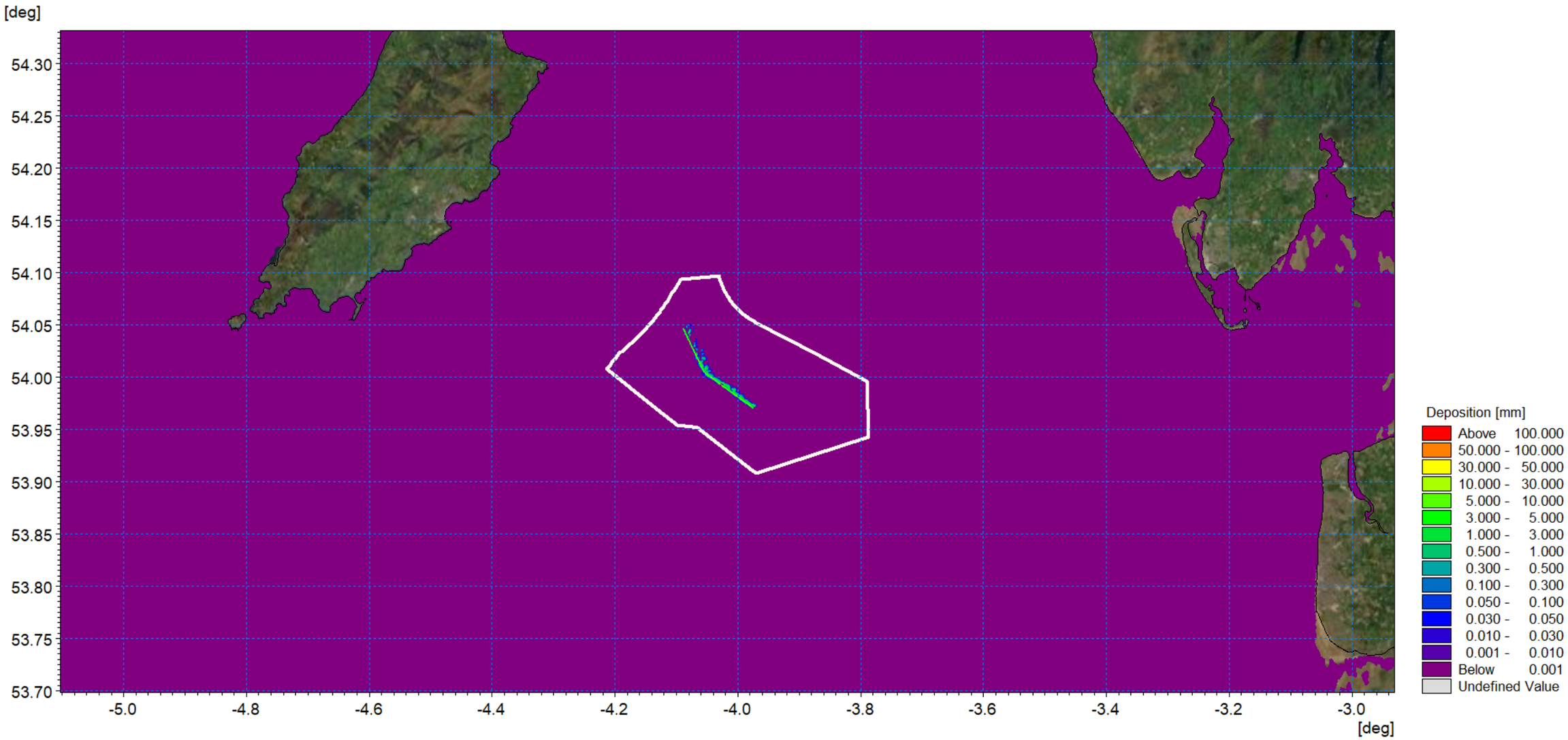

Figure 1.154: Sedimentation 1day following cessation of interconnector cable installation.

1.9 Summary

1.9.1.1 A numerical modelling study was undertaken to inform and qualify the potential impacts of the Morgan Generation Assets on physical processes. This report has outlined the baseline characteristics of the region in terms of physical processes. This includes tidal current, wave climate and sediment transport under both calm and storm conditions. Numerical modelling has been used to quantify the changes in physical processes due to the installation of the Morgan Generation Assets. The presence of the wind turbine foundations redirects both waves and tidal flow and although some changes in sediment transport were revealed, these were limited in magnitude and represented an adjustment in the transport path alignment.

1.9.1.2 The installation of the Morgan Generation Assets was seen to marginally reduce wave heights in the lee of the structures whilst a marginal increase was noted at the periphery, however during larger storm events these effects were less marked. Any significant changes in tidal currents and wave climate would not extend to the coastline and there would be no change in coastal processes in this area.

1.9.1.3 Finally, suspended sediment plumes for construction activities were quantified. In all cases, the material released was native to the bed sediments and, although there are periods of increased turbidity, the material was retained in the sediment cell and would be subsequently assimilated into the existing sediment transport regime.

1.10 References

ABPmer (2008) WebVision Atlas of UK Marine Renewable Energy Resources. Available: https://www.renewables-atlas.info/explore-the-atlas/. Accessed June 2022.

ABPmer (2018) Data Explorer. Available: https://www.seastates.net/explore-data/ Accessed June 2022.

BERR (2008) Review of Cabling Techniques and Environmental Effects applicable to the Offshore Windfarm Industry. Technical Report, Department for Business Enterprise and Regulatory Reform (BERR), in association with Defra, 164pp.

British Geological Survey (2022) Sediment sample data. Available: https://www.bgs.ac.uk/information-hub/bgs-maps-portal/. Accessed May 2022.

British Oceanographic Data Centre (BODC) (2021) UK tide gauge network. Available at: https://www.bodc.ac.uk/data/hosted_data_systems/sea_level/uk_tide_gauge_network/. Accessed 24 June 2022.

Centre for Environment, Fisheries and Aquaculture Science (Cefas) (2016) Suspended Sediment Climatologies around the UK, CEFAS.

Centre for Environment, Fisheries and Aquaculture Science (Cefas) (2022) Wave data. Available: https://wavenet.cefas.co.uk/map. Accessed June 2022.

Department for Environment Food and Rural Affairs (2022). Bathymetry and SSSI information. Available: https://environment.data.gov.uk/DefraDataDownload. Accessed 15 June 2022.

European Centre for Medium-range Weather Forecast (ECMWF) (2022) Long term wind and wave datasets. Available: https://www.ecmwf.int/en/forecasts/datasets. Accessed June 2022.

EMODnet (2020) Bathymetry. Available: https://www.emodnet-bathymetry.eu/. Accessed May 2022.

EMODnet (2022b) EODnet Geology. Available: https://www.emodnet-geology.eu/. Accessed June 2022.

EMODnet (2022c) EODnet Geology. Available: https://www.emodnet-physics.eu/. Accessed June 2022.

EMU (2013) Irish Sea Zone, Hydrodynamic measurement campaign October 2010- October 2012. Report issued to Centrica Energy Renewable Investments.

Furgro (2022) Metocean Data Report, Morgan and Mona Offshore Wind Projects. Ref: 210674_190291-MDR-01 02

Gardline Ltd (2022) Integrated Offshore Wind Farm Site Survey. Document number: 11602.

GEMS (2011) Metocean data collection, Ormonde wind farm project. Report prepared for: Offshore Design Engineering Ltd Document number: GSL10108-FIN-001-01.

Howarth M.J. (2005) Hydrography of the Irish Sea, SEA6 Technical Report, POL Internal document 174.

Integrated Mapping for the Sustainable Developments of Ireland's Marine Resource (INFOMAR) (2022) Seabed mapping data Geological Survey Ireland (GSI) and Marine Institute. Available at http://www.infomar.ie/. Accessed Feb 2022.

Marine Environmental Data Information Network (MEDIN) (2021) Bathymetry data. Available: https://data.admiralty.co.uk/portal/apps/sites/#/marine-data-portal. Accessed March 2021.

Mellett, C, Long, D, Carter, G, Chiverell, R and Van Landeghem, K. (2015) Geology of the seabed and shallow subsurface: The Irish Sea. British Geological Survey Commissioned Report, CR/15/057 52pp.

National Network of Regional Coastal Monitoring Programmes (2022) Metocean data. Available: https://coastalmonitoring.org/cco/. Accessed June 2022.

National Oceanic and Atmospheric Administration (NOAA) (2022) Metocean data. Available: https://www.dhigroup.com/data-portals/metocean-data-portal. Accessed April 2022.

RPS (2018) Tide and Storm Surge Forecast (TSSF) model of Irish coastal waters.

The Environment Agency National LiDAR Programme (2022) LiDAR data. Available: data.gov.uk. Accessed May 2022.

UKHO (2022) Admiralty Tide Tables – Volume 1B.

Whitehouse, R.J.S., Sutherland, J. and O'Brien, D. (2006) Seabed scour assessment for offshore windfarm. Proceedings Third International Conference on Scour and Erosion, November 1-3, CURNET, Gouda, The Netherland.

XOCEAN Ltd (2022) 00275-BPX-UKX-WIND bp Elizabeth Project Processing Report.